THE JOURNAL
OF
CHEMICAL PHYSICS

VOLUME 19, NUMBER 8 AUGUST, 1951

Rotational Isomerism in Oxalyl Chloride (ClOC−COCl)

B. D. SAKSENA AND R. E. KAGARISE
Department of Physics, Pennsylvania State College, State College, Pennsylvania
(Received February 8, 1951)

The Raman spectrum of liquid and the infrared absorption spectrum of liquid and gaseous oxalyl chloride have been investigated. The effects of dilution in benzene and of temperature upon the spectra were also studied. A tentative assignment has been made of all fundamental frequencies. From temperature intensity measurements in the Raman effect, the value of ΔH for the reaction C_{2h} oxalyl chloride—C_{2v} oxalyl chloride was found to be 2.8 kcal/mole. It is suggested that the high value of the depolarization factor for Rayleigh scattering indicates planar structure.

1. INTRODUCTION

THE question of *cis*- and *trans*-isomerism in oxalyl chloride has not been fully studied. The molecule contains two COCl groups joined by a C−C bond which indicates the likelihood of a rotation about the C−C bond. The electron diffraction studies have been made by Wierl[1] and Schomaker. According to the latter, the C−C distance is 1.5A, the C−Cl distance 1.72A, C=O distance 1.2A, and the C−C−O and the Cl−C−O angles are each 123°. The full paper on this work is not available, and the above data have been taken from a report by Sutton and Allen.[2] According to Wierl,[1] the electron diffraction studies indicate the existence of molecules with varying Cl−Cl distances.

The dipole moment of oxalyl chloride has been measured by Martin and Partington[3] in benzene solutions, and according to them the value of 0.92 *D* agrees well with that to be expected on the basis of free or restricted rotation about the C−C bond. These authors have also discussed the unsymmetrical molecule

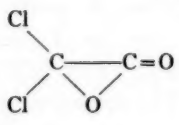

suggested by Heuberger, Maier, and Fröschl,[4] but they find that the small value of the moment agrees better with the symmetrical form.

From the Raman effect studies Saksena[5] stated that the molecule may possess a small rotation about the stable *trans*-form. Kohlrausch and Wittek[6] and Ziomek, Cleveland, and Meister[7] also suggest that the molecule has probably a stable *trans*-form with restricted rotation about the C−C bond.

For the closely allied molecule of glyoxal OHC−CHO which has two CHO groups linked together by a C−C bond, LuValle and Schomaker[8] find that the molecule is planar with the C−C distance equal to 1.47A, the C=O distance 1.2A, the C−H distance 1.09A, and the C−C−O angle 123°. According to these authors, this molecule is predominantly *trans*-, the *trans*-form being 6.9 kcal more stable than the *cis*-form, and it is considered likely that there is a potential barrier of 12 kcal per mole. Since the C−C bond in glyoxal is shorter than that in oxalyl chloride, the former has a greater double bond character than the latter. We may therefore expect a greater tendency of rotation about the C−C bond in oxalyl chloride than in glyoxal. This is suggested by the electron diffraction results of Wierl[1] and by the temperature variation of the intensities of the Raman lines. In this connection it may be interesting

[1] R. Wierl, Physik Z. **31**, 366 (1930).
[2] L. E. Sutton and P. W. Allen, Acta Cryst. **3**, 46 (1950).
[3] G. T. O. Martin and J. R. Partington, J. Chem. Soc. **82**, 1178 (1936).
[4] Heuberger, Maier, and Fröschl, Monatsh. **59**, 256 (1932).
[5] B. D. Saksena, Proc. Indian Acad. Sci. **12**, 416 (1940).
[6] K. W. F. Kohlrausch and H. Wittek, Z. Physik. Chem. **B48**, 177 (1941).
[7] Ziomek, Cleveland, and Meister, J. Chem. Phys. **17**, 669 (1949).
[8] J. E. LuValle and V. Schomaker, J. Am. Chem. Soc. **61**, 3520 (1939).

TABLE I.—Raman spectra.

Kohlrausch and Wittek	Ziomek, Cleveland, and Meister	This work	Pol	$\frac{I_0}{I_{86}}$	Mode of vibration	Assignment *Trans*	Assignment *Cis*
		175(12)	*P*		COCl in plane rocking		$\nu_5(a_1)$
189(5) (0.84)	193(5) (0.88)						
		201(8)	*D*		COCl rocking out of plane		$\nu_7(a_2)$
260(4*s*) 277(4*sb*)	261 279 (33)						
(0.41)	(0.37)	276(39) br.	*P*	2.2	COCl rocking in plane	$\nu_5(a_g)$	
346(1) 367(1) (*p*?)	354(3) (0.96)?	350(6)	*D*	1.5	COCl deformation or rocking in plane	$\nu_8(b_g)$	$\nu_3(a_1)$
396(2)		400(0)	*P*				2×201
450(4*sb*) (0.44) 471(4) (0.44) 488(4) (0.44)	443(21) (0.51) 465(28) (0.48) 483(30) (0.50)	465(50) v. br. band	*P*	1.35	COCl deformation in plane	$\nu_3(a_g)$	$\nu_9(b_1)$
512(6) (*P*)	522(7) (*P*)	519(8)	*P*				350+175
533(3*b*) (*P*)	533(12) (*P*)	533(20)	*P*	0.75	C−Cl valence		$\nu_4(a_1)$
620(12*b*) (0.14)	620(100) (0.17)	619(92)	*P*	2.5	C−Cl valence	$\nu_4(a_g)$	
672(0)							
704(1/2)	709(1)	707(2)	*P*			$2\nu_8$, $\nu_3+\nu_9$, $\nu_1-\nu_2$	$\nu_4+\nu_5$
818(0, Bd)	802(V.W.)	809(1) v. br	*D*			$\nu_8+\nu_3$	likely coincidence with broad infrared band at 795 $\nu_{11}(b_1)$
1078(4*b*) (0.40)	1081(5) (0.32)	1078(14)	*P*	1.8	C−C valence	$\nu_2(a_g)$	likely coincidence with infrared band at 1077$\cdots\nu_2(a_1)$
		1230(0)				$2\nu_4$	
1411(00)	1416(V.W.)	1417(1) 1530(0)	*P*			$\nu_2+\nu_4-\nu_5$, $2\nu_{12}$ $\nu_2+\nu_9$, $2\nu_{11}$	
1780(10) (0.66)	1781(57) (0.79)	1778(67)	*P*	1.8	C=O valence	$\nu_1(a_g)$	high value of "ρ" suggests $\nu_1(a_1)$

to note the formation of cyclic ureide called oxalyl urea from oxalyl chloride and urea.[9]

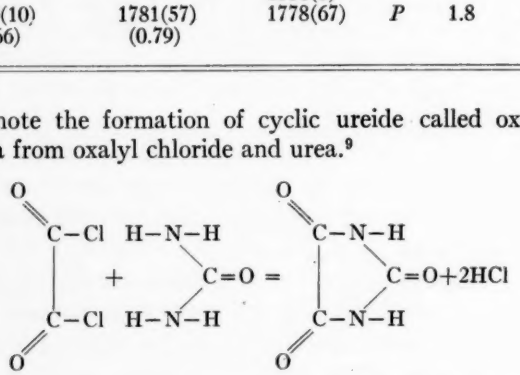

The reaction takes place at 110°C. While this reaction by itself cannot be regarded as an evidence for the structure of the molecule, it appears possible that at higher temperatures there is a greater preponderance of molecules in the *cis*-form; and so the formation of a closed compound like oxalyl urea is favored.

Apart from the above considerations, the infrared spectrum in the vapor has not been studied, and no analysis of the vibrations has been made. In the present investigation, we have studied the Raman and infrared spectra of oxalyl chloride, the effect of temperature and of dilution in benzene upon the Raman and infrared frequencies, and have used these results to show the existence of rotational isomers at higher temperatures and for the assignment of frequencies to the normal modes of the *trans*- and *cis*-forms of the molecule.

[9] J. B. Conant, *Chemistry of Organic Compounds*, Macmillan Company, New York 1947 p. 259.

2. EXPERIMENTAL

Oxalyl chloride used in this investigation was obtained from the Eastman Kodak Company, and was fractionally distilled before being used. The Raman spectrum of this sample is almost identical with the one obtained earlier by one of us.[5] The Raman and infrared spectra have been obtained with the help of the instruments which have been described in earlier communications from this laboratory, and polarization measurements were made by the method first used by Douglas and Rank.[10] The intensity of the Raman lines as well as the variation of intensity with temperature were determined with the photoelectric spectrograph described previously.[11] The effect was also studied photographically. The recorded intensity of a Raman line is its peak value above the background intensity which was not appreciably different in the exposures taken at 85°C and 0°C (Fig. 2). The ratio of the peak

[10] A. E. Douglas and D. H. Rank, J. Opt. Soc. Am. **38**, 281 (1948).

[11] D. H. Rank and R. V. Wiegand, J. Opt. Soc. Am. **30**, 325 (1946).

intensities at these two temperatures is given as I_0/I_{85} in Table I.

(a) Raman Spectrum

The Raman spectrum recorded here differs in some important respects from those of earlier workers: (1) In place of the frequency at 189 cm^{-1} we recorded two frequencies, one at 175 cm^{-1} and the other at 201 cm^{-1}. These two frequencies may be seen in the spectrograms (b), (d), (e), (f) reproduced in Fig. 1. Furthermore, the frequency 201 shows a larger variation in intensity with temperature. (Spectrograms (f), (g).) (2) The frequencies 276 and 465 appear as single broad bands. Kohlrausch and Wittek[6] and also Ziomek, Cleveland, and Meister[7] have reported the first band as two frequencies of equal intensity and the latter as three of equal intensity. This region has been examined by a grating spectrograph, and there is no separation into distinct bands as reported by these authors. In a photograph taken earlier by one of us,[5] both these frequencies appeared as broad bands. (3) Two very weak lines are observed at 1230 and 1530 cm^{-1} in our pictures, Fig. 1(c). The very weak frequency at 707 and the broad weak band at 809 cm^{-1} are also recorded with good intensity. (4) The frequencies 1778, 350, 201, and 175 have a high value of "ρ," if 1778 is considered as polarized, 201 and 350 appear depolarized and 175 polarized.

(b) Effect of Temperature on the Raman Lines

The intensities of the Raman lines in arbitrary units were measured on a photoelectric spectrograph. The frequencies 175 and 201 were not observed, while 519 and 533 are not resolved. The frequency 519–533 cm^{-1} increases in intensity as the temperature is raised, while all the other frequencies are diminished in intensity. This diminution is the largest for the frequencies 619 and 276, smallest for the frequencies 465 and 350 cm^{-1}, and has an intermediate value for the frequencies 1078 and 1778 cm^{-1}. A record of the photoelectric spectrograph showing the frequencies 619, 533, and 465 at temperatures of 85°C and 0°C is reproduced in Fig. 2. It may be seen that the frequency 465 becomes broader at lower temperatures than at higher ones and further there is an increase in frequency of 8 cm^{-1} in passing from the lower to the higher temperature.

The Raman spectra taken at 85°C, 25°C, and −10°C with a camera lens of aperture $F/2$ are reproduced in Fig. 1 (f), (g), (h). Besides the change in the frequency 465 mentioned above, we also notice that the frequencies 175, 201, and 519–533 appear strongly at 85°C, at 25°C both the frequencies 519–533 as well as 201 are weak, and at −10°C, 175 and 201 almost disappear, while 519–533 becomes weaker. Furthermore, the frequency 1078 appears to gain in intensity at the lower temperature. In the solid only three frequencies 619, 1078, and 1778 were obtained; and here the frequency 1078 appears of comparable intensity with the other two.

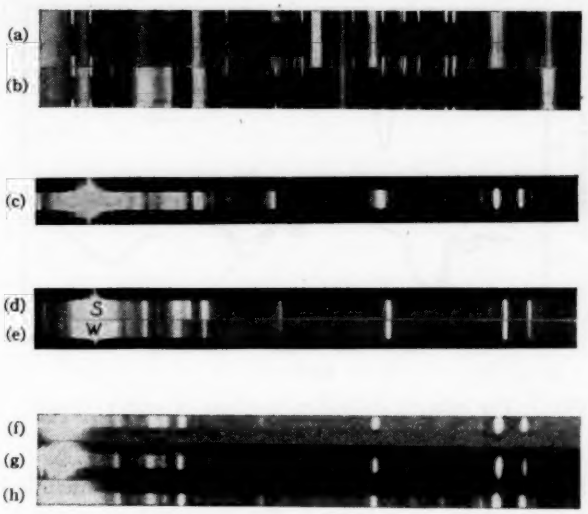

FIG. 1. Reproductions of Raman spectra. (a) Oxalyl chloride in benzene; (b) and (c) oxalyl chloride; (d) and (e) polarization measurements, S—strong component, W—weak component; temperature effect, (f) high, (85°C), (g) room, (h) low temperature (−10°C).

(c) Raman Spectrum of Oxalyl Chloride in Benzene Solutions

The spectra of oxalyl chloride in benzene solution (3 parts of benzene to one part of oxalyl chloride) and of oxalyl chloride are reproduced in Figs. 1(a) and (b). The frequencies in the benzene solution are the same as those in the pure liquid. But there appears to be a significant change in the intensity of the frequency 1078. This frequency is much weaker than any of the frequencies 1778, 619, 533, 465, and 276 in the spectrum of the pure liquid, but in benzene solution it is stronger than the frequency 533, and comparable in intensity to others.

The Raman spectra are recorded in Table I. The fre-

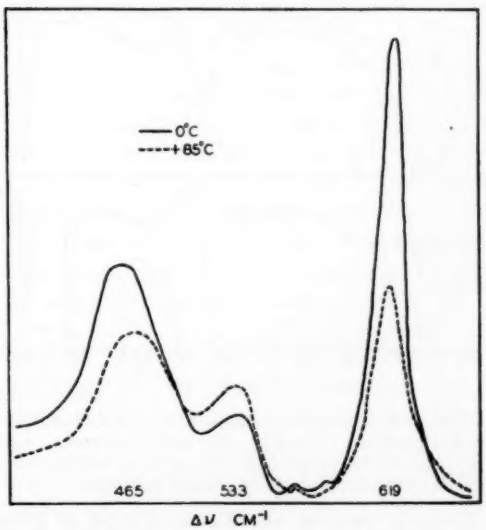

FIG. 2. Photoelectric traces of Raman spectra of oxalyl chloride.

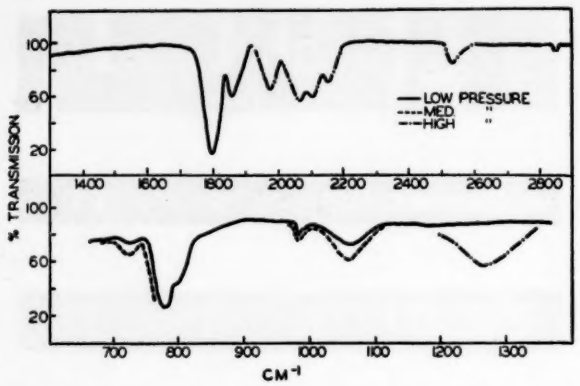

FIG. 3. The infrared absorption spectrum of oxalyl chloride, 10-cm gas cell.

quencies recorded by earlier workers are also included for comparison. In column 5, the mean ratios (mean of two independent observations) of the intensities of Raman lines at 0°C and 85°C as measured by a photoelectric spectrograph are stated, while in columns 6 and 7 we have given the assignments of the frequencies to the various normal modes of vibration of the *cis*- or *trans*-molecule. The notation of Herzberg[12] for the molecule $C_2H_2Cl_2$ (both *cis*- and *trans*-) has been adopted.

(d) Infrared Spectrum

The infrared spectrum of the pure substance has been measured in the liquid and gas phases. In the liquid, the infrared bands appearing in the vapor at 777–795 and at 1060–1077 are very broad; and so it is not possible to locate the position of the peak frequencies. It is noticed, however, that the frequencies 1790 and 1852 of the vapor appear at 1750 and 1824 in the liquid. It is possible that the 777 band of the vapor shifts to 752 in the liquid, since Ziomek, Cleveland, and Meister consider the middle of this very broad band at 752 in the liquid.

The spectrum of the vapor is recorded in Fig. 3. The characteristic feature of the spectrum is the presence of doublet frequencies (980, 988), (1060, 1077), and (777, 795). The vapor spectrum was investigated with a sodium chloride prism using a 10-cm gas cell. The pressure was suitably adjusted to bring out the peak absorptions and the combination bands.

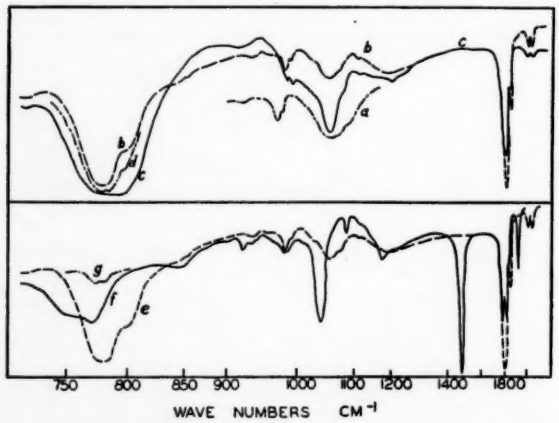

FIG. 4. Infrared absorption spectrum of oxalyl chloride: vapor at room temperature, (a) high, (b) lower pressure; vapor at 150°C, (c) high, (d) lower pressure; (e) vapor at reduced pressures; (f) diluted in benzene solution; (g) liquid benzene.

[12] G. Herzberg, *Infrared and Raman Spectra of Polyatomic Molecules* (D. Van Nostrand Company, Inc., New York, 1945), p. 331.

(e) Effect of Increase of Temperature on the Infrared Bands

To obtain higher temperatures, the gas cell was heated externally. The effect of the increase of temperature on the infrared bands is shown in Figs. 4(b), (c), (d). The following points may be noted. (1) The contour of the 777–795 band changes at higher temperatures. In the spectrum taken at 150°C there are three bands, the frequencies being 774, 781, and 795 (see Fig. 4(d)). Further, the 795 band gains in intensity relative to its companion band at 777. (2) The band at 1060 also gains in intensity relative to the band at 1077. (3) If the intensities of 777–795 band and the 1790 band are compared at the room temperature and 150°C, it is noticed that whereas the band at 1790 is weaker in intensity at the higher temperature than at the room temperature, the 777–795 band shows an opposite behavior (see Fig. 4(b) and Fig. 4(c)).

(f) Effect of Dilution in Benzene on the Infrared Bands

The spectra were investigated by liquid cells having 0.03-and 0.04-mm spacers. The benzene-oxalyl chloride solution was very dilute (about 50 parts of benzene to 1 part of oxalyl chloride) the dilution being adjusted so as to bring sharp and well defined contours of the 771 C−Cl and also of the 1777 C=O bands. The spectra are reproduced in Figs. 4(e) and 4(f). It is noticed that there is a change in the position of the C=O frequency in benzene solution, the frequency dropping from 1790 in the vapor to 1777 in benzene solutions. The 777–795 band now occurs at 757–771, and there is a relative change in the intensity of the two bands. It may be noted, however, that there is no shift in any of the frequencies of oxalyl-chloride in the Raman spectrum of the solution of oxalyl chloride in benzene.

The infrared spectra are recorded in Table II.

3. EVIDENCE FOR THE EXISTENCE OF ROTATIONAL ISOMERS

Three isomeric forms appear to be possible for the molecule, a *trans*-form of symmetry C_{2h}, a *cis*-form of symmetry C_{2v}, and a staggered form of symmetry C_2. In the last case we may regard one of the COCl groups lying in the plane of the paper and the other perpendicular to the plane.

TABLE II. Infrared spectra.

Ziomek, Cleveland, and Meister Liquid	This work Liquid	This work Vapor 25°C	This work Vapor 150°C	This work Benzene solution	Mode of vibration	Assignment *Trans*	Assignment *Cis*
488(st)					COCl deformation in plane	$\nu_{10}(b_u)$	
532(st)					C—Cl		Raman line at 533 $\nu_4(a_1)$
594(st)							
		724(w, br)			COCl out of plane	$\nu_{12}(b_u)$?	
	Very intense	777(br. and V.V.S.)	774	757	C—Cl	$\nu_{11}(b_u)$	
752 V.V.S.	absorption		781				
		795(br. and V.V.S.)	795	771	C—Cl		Raman line at 809 $\nu_{10}(b_1)$
942 st	932(w, br.)				···	$\nu_{10}+\nu_3$	
	986(w, br.)	980(m.st)	980	980	···	$\nu_6(a_u)$	
		988(m. st)	988				
1058 V.V.S.	Very intense absorption	1060(st. br.)	1060	1060	···		2×533 or Fermi resonance of 2×533 with 1077
		1077(m.st, br)	1077		···		Raman line at 1078, $\nu_2(a_1)$
			1262*		···	$\nu_3+\nu_{11}$	$\nu_2+\nu_7$
1310 V.S.	1286(v.w)?		(w, br)				
1388 st							
1754 V.V.S.	1750(br)V.S.	1790(V.S.)	1794	1777	C=O	$\nu_9(b_u)$	$\nu_8(b_1)$
1826 V.V.S.	1824(st)	1852(st)				$\nu_2+\nu_{11}$	
	1964(m.s.)	1970(m.st)*				$2\nu_4+\nu_{11}$	2×988
		2060(m.st)*				$\nu_9+\nu_5$	
		2100(m.st)*				$\nu_2+\nu_5+\nu_{11}$	2×1060
		2160(m.st)*				$\nu_2+\nu_4+\nu_{10}$	2×1077
2510 st	2480(m)	2530(m)				$\nu_1+\nu_{11}$	
2830 V.S.	2828(m)	2855(m)				$\nu_2+\nu_9$	
3740 V.S.						$\nu_1+\nu_5+\nu_9$	
5140 w						$2\nu_1+\nu_9$	

*Were recorded strongly at 150°C with a high vapor pressure: (v.w) very weak, (w) weak, (m) medium, (m.st) medium strong, (st) strong, (V.S) very strong, (V.V.S) very very strong, (br) broad.

For the *trans*-form: (1) The strong Raman frequencies do not coincide with the strong infrared bands which shows the presence of a molecule with a center of symmetry. (2) There are only two depolarized Raman lines in the spectrum which favors a *trans*-structure because we require only one depolarized Raman line for the latter. For the *cis*-form we require seven depolarized lines and for the staggered form five. (3) There is only one C=O frequency in the Raman effect or infrared. For both the *cis*- and the staggered forms we require two C=O frequencies, one polarized and the other depolarized, both active in the infrared.

For the *cis*- and the staggered forms: (1) There is a larger number of Raman lines than can be accounted for on the basis of the *trans*-structure for which we require only six Raman lines. (2) The frequencies 201 and 533 increase in intensity at the higher temperature. The latter frequency also appears in the infrared spectrum of the liquid according to the measurements of Ziomek, Cleveland, and Meister. (3) Most of the Raman lines show considerable variation in intensity with temperature as is seen from the results of measurements with the photoelectric spectrograph. (4) Some of the strong Raman frequencies appear weakly in the infrared and also some of the strong infrared bands appear weakly in the Raman effect. (5) Since the method of Douglas and Rank does not give the values of the depolarization factors "ρ" of Raman lines, it is not possible for us to say whether the frequency 1778 is polarized or depolarized. There is no doubt, however, that it has a high value of "ρ" as may be seen from spectrograms (d) and (e), Fig. 1. Kohlrausch and Wittek[6] and also Ziomek, Cleveland, and Meister[7] consider it to be polarized, their values being 0.66 and 0.79. We may therefore consider it a polarized frequency with a high value of "ρ." For the *trans*-molecule we can have only one C=O frequency in the Raman effect, since besides the five polarized vibrations the only other Raman active vibration belongs to the class B_g and should be of low frequency. The C=O frequency should therefore be highly polarized. For both the *cis*- and the staggered forms, we need two C=O frequencies, one polarized and the other depolarized, both active in the Raman effect and infrared. If the two frequencies are very close to each other, the value of "ρ" for the C=O frequency would be high. (6) The 795 band, corresponding to which we have a very broad Raman band at 809, appears to gain in intensity corresponding to 777 band at high temperatures. (7) The combination frequencies 1970, 2100, and 2160 can all be expressed as overtones of the infrared active frequencies which is not permitted for the *trans*-form.

It would appear from the preceding paragraph that the spectroscopic results indicate the existence of rotational isomers at higher temperatures. It appears difficult to say from the observed Raman data whether the higher temperature isomer is the *cis*-form or the staggered form. We require five polarized and seven depolarized lines for the *cis*-form and seven polarized and five depolarized lines for the staggered form. According to our data, the total number of polarized lines is 11, and since we require only five for the *trans*-form, the remaining number can be made to fit both the *cis*- and the staggered forms equally well. The following points however suggest that the *cis*-form may be more probable: (1) Comparing the *trans*- and the staggered forms we note that the seven vibrations forming the classes A_g[5] and A_u[2] of the *trans*-form combine to produce the polarized class A[7] of the staggered form. Since the torsion mode falls in class A_u of the *trans*-form, it will appear as a polarized vibration for the staggered form and as a depolarized vibration for the *cis*-form. In the next section we have considered the frequency 201 as the torsion mode on account of the low value of the frequency and its behavior with temperature, and it is seen to be depolarized. (2) The C—C bond in oxalyl-chloride has partly a double-bond character because the C—C distance is 1.5A, and there are conjugated single and double bonds in the molecule which have a tendency to make it planar. The analogous molecule of glyoxal is known to be planar from the electron diffraction data. (3) The formation of oxalyl urea at higher temperatures discussed earlier in this paper, and the formation of a complex with benzene in benzene-oxalyl chloride solutions described in a later communication[13] both suggest the existence of a *cis*-form of the molecule.

4. ASSIGNMENT OF FREQUENCIES TO THE NORMAL MODES OF THE *CIS*- AND *TRANS*-MOLECULES

For the *trans*-molecule the frequencies are distributed into four classes A_g,[5] A_u,[2] B_g,[1] and B_u.[4] A_g and B_g are Raman active, and A_u and B_u are infrared active. The assignment is fairly straightforward for all classes except A_u. The frequencies 1778, 1078, 619, 465, and 276 have been assigned to class A_g and 350 to class B_g. The frequency 1778 shows an anomalous polarization, and the frequency 1078 has a corresponding infrared absorption, but since the former is a C=O and the latter a C—C frequency, the above assignment seems to be correct. In fact, it is very likely that these frequencies are common to both *cis*- and *trans*-forms. This is also seen from the temperature behavior of these frequencies. For both these frequencies the ratio I_0/I_{85} is 1.8; i.e., the diminution of intensity between 0°C and 85°C is the same for these lines. Since both are valence frequencies, they should behave similarly if they belong to the same molecule. But this diminution of intensity is not so large as is found in the case of the frequencies 276, 619, for which I_0/I_{85} is 2.5. The frequency 533, on the other hand, increases in intensity at the higher temperatures. These results become consistent if we assume that 533 belongs to the *cis*-form only, 276, 619 to the *trans*-form only, and 1778 and 1078 to both *cis*- and *trans*-forms. Since the frequencies of the *cis*-form gain in intensity at higher temperatures, those of purely *trans*-form will show a maximum diminution of intensity, and those belonging to both forms will show a lesser diminution.

The assignment of the frequency 350 to the out-of plane $\nu_8(B_g)$ vibration appears to be satisfactory, since this frequency is depolarized and is a low frequency. One may like to explain 350 as 619–276 or 2×175, but this assignment does not appear to be correct, because the combination 619–276 or the overtone 2×175 would be polarized, while 350 is depolarized.

Considering now the B_u frequencies, the assignments of 488 (COCl), 777 (C—Cl), 1790 (C=O) are straightforward since these are the strongest bands in the infrared. We have assigned 777 to $\nu_{11}(B_u)$ of *trans*-form and 795 to $\nu_{10}(B_1)$ of *cis* for reasons stated in Sec. 3. Their values also are of the right order for in *trans*-and *cis*-$C_2H_2Cl_2$ the former occurs at 820 and the latter at 857. There is some difficulty in choosing the in-plane bending frequency $\nu_{12}(B_u)$. For *trans*-$C_2H_2Cl_2$, Herzberg[14] takes it as 917, but Bernstein[15] considers it to be as low as 265 cm^{-1}. In glyoxal, Thompson[16] takes it as 550. We have provisionally put it at 724, but the assignment is doubtful. It is possible that the Raman frequency 1416 is an overtone of this band. We have not assigned ν_{12} to the strong band at 1060, because the latter increases in intensity at higher temperatures and may be a *cis*-frequency or may have arisen due to Fermi-resonance of 2×533 with 1078.

The position is still more difficult with regard to the two A_u frequencies. In *trans*-$C_2H_2Cl_2$ one of them $\nu_6(A_u)$ has a high value 895 cm^{-1} and is a strong infrared band. We may therefore associate it with the frequency 980 cm^{-1} which does not show an appreciable increase in intensity with the rise of temperature. The other frequency would be a low frequency and is a torsion mode which should be largely responsible for the *cis*- and *trans*-isomerism. It is forbidden in the Raman effect for the *trans*-form but should appear in the *cis*-form as a depolarized line and should be very sensitive to temperature. Frequency 201 satisfies these requirements well and we may consider it as a torsion mode $\nu_7(A_2)$. Since this frequency may have a large anharmonicity, its overtone is also likely to appear and the frequency 400 may be 2×201.

The frequencies of the *cis*-form belonging to class A_1 may be taken as 1778, 1077, 533, 350, 175. We have already discussed the assignment of the first three.

[13] B. D. Saksena and R. E. Kagarise J. Chem. Phys. **19**, 994 (1945).

[14] See reference 12, p. 330.

[15] H. J. Bernstein, J. Chem. Phys. **17**, 556 (1949).

[16] H. W. Thompson, Trans. Faraday Soc. **36**, 988 (1940).

The last one is polarized and increases in intensity at higher temperatures, and so is a *cis*-frequency. The frequency 350, however, shows a diminution in intensity at higher temperatures which is much smaller than that for the frequency 619 but almost the same as that of 465. It is therefore likely that it belongs to both *cis*- and *trans*-forms, and is a C−O−Cl deformation. Bernstein[17] has given the product rule for *cis*- and *trans*-isomers. The calculated and observed ratios are found to be 2.5 and 2.44, respectively.

The frequencies belonging to class B_1 of *cis*-form may be taken 795 (C−Cl) and probably 1790 (C=O) and 465 (C=O−Cl).

5. ENERGY DIFFERENCE BETWEEN *CIS*- AND *TRANS*-ISOMERS

We have assigned 619 as ν_4 C−Cl (A_g) for the *trans*-molecule and 533 as ν_4 C−Cl (A_1) for *cis*. Following Bernstein[18] we can estimate the energy difference between the *cis*- and *trans*-isomers. If N_a and N_b are the numbers of the *cis*- and *trans*-molecules, respectively, at temperature t_1, and N_a' and N_b' are the corresponding numbers at temperature t_2, and if I_{t_1} and I_{t_2} are the intensities of the *cis*-bands, and I_{t_1}' and I_{t_2}' of the *trans*-bands at temperatures t_1 and t_2, then it can be shown that

$$\frac{I_{t_1}}{I_{t_1}'}\times\frac{I_{t_2}'}{I_{t_2}}=\frac{N_a}{N_b}\times\frac{N_b'}{N_a'}=\exp\left[\frac{-\Delta H}{R}\left(\frac{1}{T_1}-\frac{1}{T_2}\right)\right],$$

where ΔH is the energy of the reaction $b\rightarrow a$ and R is the gas constant. We find $\Delta H=2.8$ kcal per mole. The value is of the same order of magnitude as that found for substituted ethanes which are known to exhibit rotational isomerism.

6. POSSIBILITY OF ASSOCIATION IN OXALYL CHLORIDE

The existence of a broad Raman band at 465, and of the very broad infrared band at 777,[2] the shift of the C=O and C−Cl infrared frequencies from 1790 and 777 in the vapor to 1750 and 752 in the liquid and to 1777 and 757 in very dilute benzene-oxalyl chloride solutions and[3] the narrowing of the 465 band on heating may be regarded as evidence in favor of association. Against this view we have the following arguments: (1) The frequency shifts are small and may be explained in terms of dielectric effects. (2) In the Raman effect the low frequencies are increased in intensity on heating. If they were due to association, they should be weakened. (3) In the Raman effect, frequency 1078 appears stronger in benzene solutions than in the spectrum of the pure liquid. If it be assumed that its increased intensity is due to dissociation into more monomers, then since it is the C−C frequency, other frequencies C=O, C−Cl should behave similarly. (4) The association is brought about largely through the oxygens, and so the C=O frequency should diminish in magnitude. Further, in the infrared we should get two C=O frequencies, one of lower frequency for the associated molecule and the other of higher frequency for the unassociated one, which is not observed. (5) There will be far less symmetry in the associated molecule, so that most Raman lines will be infrared active.

On the whole, it appears justifiable to assume that there is no association in the molecule, but only dielectric effects due to the presence of highly polarizable ions of oxygen and chlorine.

7. DEPOLARIZATION OF RAYLEIGH SCATTERING IN OXALYL CHLORIDE

Rank[19] has pointed out a correlation between the depolarization of Rayleigh scattering (ρ) and the geometrical structure of the molecule. For planar molecules "ρ" will have a high value (about 0.5), while for associated molecules having a three-dimensional network, as in methyl hydrazine,"ρ" would tend to be small. The liquid used in the present investigation was carefully vacuum distilled and was free from dust particles. This may be judged from Fig. 1 (spectrograms (d) and (e)), where the mercury lines close to 4916 appear very weakly in spite of long exposures. It may be seen that the mercury line 4980 does not show a low value of "ρ" which indicates a planar structure of the molecule.

ACKNOWLEDGMENT

We have to thank Dr. D. H. Rank for going through the paper and for several useful suggestions.

[17] H. J. Bernstein, J. Chem. Phys. **17**, 256 (1949).
[18] H. J. Bernstein, J. Chem. Phys. **17**, 258 (1949).
[19] D. H. Rank, J. Chem. Phys. **19**, 511 (1951).

Formation of Complexes in Benzene-Oxalyl Chloride Solutions*

B. D. SAKSENA AND R. E. KAGARISE
Department of Physics, Pennsylvania State College, State College, Pennsylvania
(Received February 8, 1951)

Extinction coefficients have been obtained for solutions of oxalyl chloride diluted with benzene, *n*-heptane, and *me*-cyclohexane; and for solutions of diacetyl, acetyl bromide, acetyl chloride, α-methyl acrolein, and crotonaldehyde diluted with benzene and *n*-heptane. It has been possible to correlate the observed data in the infrared, Raman, and ultraviolet spectra of oxalyl chloride-benzene solutions by postulating a complex formation of the type $Ar^+[COCl]_3^-$.

INTRODUCTION

IN an earlier communication[1] we have investigated the Raman and infrared spectra of oxalyl chloride in the liquid and vapor states and in benzene solutions. The main features of the spectra are the following:

(1) There is a very broad Raman line at 465 cm^{-1} and a very broad infrared band at 777–795 cm^{-1}.

(2) In the infrared, the C=O frequency occurs at 1790 cm^{-1} in the vapor and at 1750 cm^{-1} in the liquid, whereas in the Raman effect its value is 1778 cm^{-1} for the liquid.

(3) The 777–795 cm^{-1} infrared band is shifted to 752 cm^{-1} in the liquid state.

(4) In benzene-oxalyl chloride solutions, the infrared bands appearing at 1790 and 777–795 in the vapor, are shifted approximately 20 cm^{-1} to 1777 and 757–771 cm^{-1}. No such displacemen of frequencies is observed in the Raman effect, but the 1078 cm^{-1} line shows a considerable change of intensity. For the pure liquid it is weaker than even the 533 cm^{-1} line but in benzene solution it is stronger than 533 and becomes comparable in intensity with the other frequencies.

Since several resonance structures are possible for acid chlorides it is likely that the spectral changes observed in the liquid state or upon dilution may be due to ionic binding between the molecules. For this reason we have investigated the ultraviolet spectra of oxalyl chloride and several other molecules of similar structure in benzene and *n*-heptane solutions.

We have obtained the following results which are of considerable interest in connection with the behavior of the spectra in the Raman effect and infrared.

(1) Solutions of oxalyl chloride in *me*-cyclohexane and in *n*-heptane are transparent in the 380–280 mμ region (the extinction coefficient is about 25 at 280 mμ), while solutions of oxalyl chloride in benzene exhibit large extinction coefficients of approximately 800 in this region.

(2) No such large scale changes are observed in the ultraviolet spectra of acetyl chloride and bromide, diacetyl, α-methylacrolein and crotonaldehyde when investigated in benzene solutions.

We have attempted to interpret these results on the basis of a complex formation following the work of Benesi and Hildebrand.[2] According to these authors the phenomenon of a complex formation can be represented by a chemical equilibrium of the type $A+B \rightleftharpoons AB$ where A represents benzene, B oxalyl chloride, and AB the complex formation. If K is the equilibrium constant for the reaction, then by definition,

$$K=\frac{[C]}{\{[B]-[C]\}\{[A]-[C]\}},$$

where $[C]$ is the molar concentration of the complex AB $[B]-[C]$ the molar concentration of free oxalyl chloride and $[A]-[C]$ the molar concentration of free benzene. Assuming that the intense absorption in the ultraviolet is due to the presence of the complex, they find that

$$B/D=1/KE_c\cdot 1/[A]+1/E_c,$$

where E_c is the true molar extinction coefficient, B the concentration of oxalyl chloride in solution, and D the optical density. We have used this equation to estimate K and E_c, assuming that there is a 1:1 complex formation.

EXPERIMENTAL

The oxalyl chloride used in this investigation was supplied to us by Mr. Ziomek of DePaul University and was carefully purified by him. All other chemicals were fractionally distilled, the middle fraction being used. The benzene and *n*-heptane were Merck products.

Using a 10-mm cell, *n*-heptane was found to be transparent to 210 mμ and benzene to 276 mμ. The extinction coefficients were measured with a Beckman quartz spectrophotometer, using quartz cells of 10-mm thickness for all liquids. The results are listed in Tables I and II.

To investigate the extinction coefficients of oxalyl chloride dissolved in benzene, the following solutions were prepared.

I. 0.1 cc of oxalyl chloride in 50 cc of benzene.
I(a). 10 cc of solution I in 20 cc of benzene.
II. 10 cc of solution I(a) diluted with 5 cc of heptane.
III. 10 cc. of solution I(a) diluted with 10 cc of heptane.
IV. 10 cc of solution I diluted with 20 cc of heptane.
V. 5 cc of solution I diluted with 20 cc of heptane.
VI. 5 cc of solution I diluted with 25 cc of heptane.

Since oxalyl chloride is highly volatile, all solutions were used immediately after preparation.

Table I shows the extinction coefficient of the various solutions at the designated wavelengths.

* This research was carried out on Contract N6 onr-269 Task V of the ONR.

[1] B. D. Saksena and R. E. Kagarise, J. Chem. Phys. **19**, 987 (1951).

[2] H. A. Benesi and J. H. Hildebrand, J. Am. Chem. Soc. **70**, 2382 (1948); **71**, 2703 (1949).

TABLE I.

Solution	I	II	III	IV	V	VI	VII	VIII
	Benzene and oxalyl chloride in heptane						Solutions in	
Molar* concentration	1	1/1.303	1/1.606	1/2.212	1/3.424	1/4.03	*m*-C_6H_{12}†	*n*-heptane
Concentration of oxalyl chloride	0.02345 mole/liter	0.00521	0.00391	0.00782	0.00469	0.00391	0.02345	0.02345
280 mμ	792	565	448	318	237	204	62.5	28.7
290	720	470	363	270	192	167	53.0	24.6
300	560	353	272	199	139	122	50.1	22.0
310	407	243	185	134	92.6	81.7	47.7	21.8
320	260	150	114	83	60.2	54.5	47.0	24.6
330	154	87	66	48.8	38.3	34.5	39.5	22.5
340	83.6	47.5	35.6	28.1	23.9	22.5	30.3	17.7
350	49.2	28.8	23.4	19.6	18.6	17.4	25.0	15.5
360	21.0	12.5	10.6	9.1	8.5	8.3	13.2	7.3

* Molar fraction of benzene in heptane solutions.
† It is possible that *m*-cyclohexane has a slight benzene impurity. This is apparent from the spectrum of oxalyl chloride in cyclohexane and of benzene. (Fig. 1).

TABLE II.

Substance	Diluted with *n*-heptane	Diluted with benzene
Diacetyl Conc: 0.0382 mole/liter	Band maxima (mμ) 445 421 285 270 230 (*E*) 22.5 22.6 15 18 22 The spectrum shows three broad absorption regions; the first between 470 and 340 mμ, the second in the 320–230 mμ region, and the third lying beyond 230 mμ with weak maxima listed above. The extinction coefficient increases after 230 mμ and is 80 at 210 mμ.	A perceptible change occurs between 300 and 275 mμ. The extinction coefficient starts increasing at 300 mμ and is 35 at 276 mμ as compared to 18 at 276 mμ in *n*-heptane.
Acetyl chloride 0.06211 mole/liter	Band maxima (mμ) 240 (*E*) 34.5 The absorption extends from 210 mμ to 320 mμ; the coefficient of extinction at 211 mμ is 12.6, and is 0 at about 300 mμ.	No appreciable change in *E* in the region below 276 mμ.
Acetyl bromide 0.05435 mole/liter	Band maxima (mμ) 250 (*E*) 93 Absorption begins at 320 mμ and increases to 93 at 250 mμ where curve shows a flat maximum. From this point *E* increases to 443 at 212 mμ.	No change in *E* below 276 mμ.
α-methyl acrolein 0.09434 mole/liter	Band maxima (mμ) 214 330 360 370 (*E*) 8800 25.8 13.6 6.6 The absorption curve shows two distinct bands, the one at 214 being quite large. The extinction coefficient falls rapidly to 1.1 at 260 mμ and then rises again. Besides the maximum at 330 mμ, there are maxima at 360 and 370 mμ which appear as shoulders of the main band. The extinction coefficient diminishes to 0.1 at 390 mμ.	From 390 to 276 mμ the two curves are quite similar except for the disappearance of the two shoulder maxima. The extinction coefficient of the 330 mμ maxmum increases from 25.6 to 29.
Crotonaldehyde 0.06116 mole/liter	Band maxima (mμ) 213 330 360 370 (*E*) 11,500 25.8 13.4 6.6 As in α-methyl acrolein there are two distinct bands, but the shoulders are much less pronounced.	Only change is the shift in the maximum at 330 mμ in heptane to 326 mμ.

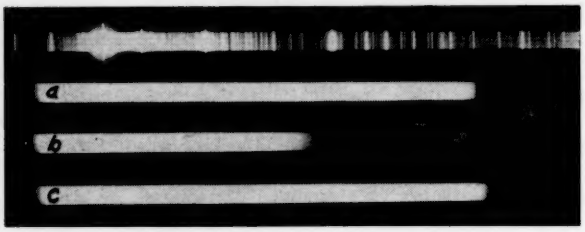

FIG. 1. Reproductions of ultraviolet spectra of (a) oxalyl chloride in *me*-cyclohexane; (b) oxalyl chloride in benzene; (c) benzene.

The aforementioned compounds have been previously studied in *n*-hexane solutions. References to these investigations are listed in review articles by Sponer and Teller[3] and Platt and Klevens.[4]

DISCUSSION

It is apparent from the results described above that the extinction coefficients of solutions of oxalyl chloride in benzene are much larger than those of oxalyl chloride in heptane or cyclohexane. From the spectrogram reproduced in Fig. 1, it is seen that whereas benzene and the solution of oxalyl chloride in cyclohexane are transparent up to 270 mμ, the solution of oxalyl chloride in benzene becomes opaque at 313 mμ. If the phenomena is considered to be a molecular association then one can represent it by an equation of the type $B+A \rightleftharpoons BA$ and determine the equilibrium constant. From the results given for solutions III and VI in Table I, it is seen that although the concentration of oxalyl chloride is the same for both solutions, the molar fraction of benzene and the extinction coefficients for solution VI are less than half of those for solution III. This is to be expected if the phenomena is represented by a molecular equation of the type stated above since the formation of the complex BA would depend not only upon the concentration of B but also upon that of A. We have therefore used Benesi and Hildebrand's method to plot the values of B/D agains $1/[A]$ where $[A]$ is the molar fraction of benzene in solutions of benzene and oxalyl chloride in *n*-heptane. The values of B/D are reciprocals of the extinction coefficients (E) listed in Table I. In Fig. 2(a) we have plotted E against the wavelength (λ) for vari-

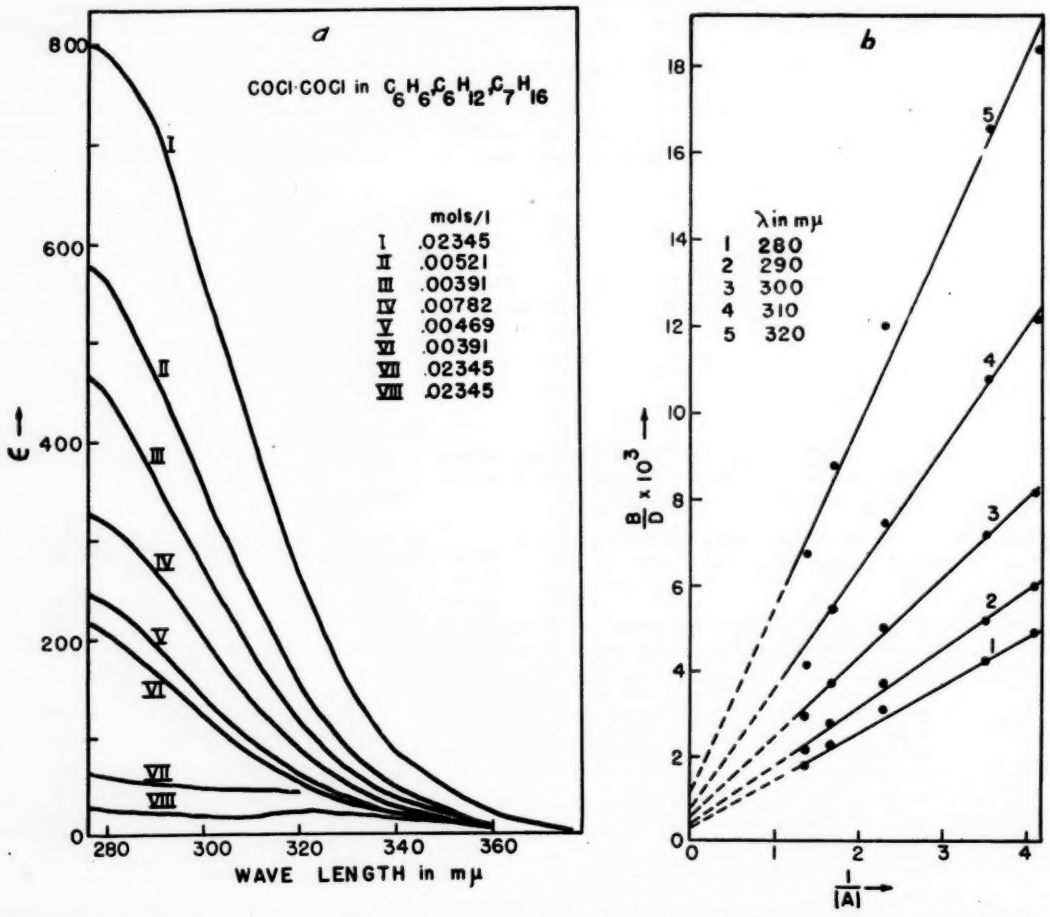

FIG. 2. (a) Extinction coefficients of oxalyl chloride in various solvents; (I, II, III, IV, V, VI) in benzene-heptane solutions; VII in *me*-cyclohexane; VIII in *n*-heptane. (b) A plot of $1/[A]$ against B/D where $[A]$ is the molar fraction of benzene, and D/B extinction coefficients.

[3] H. Sponer and E. Teller, Revs. Modern Phys. **13**, 76 (1941).
[4] J. R. Platt and H. B. Klevens, Revs. Modern Phys. **16**, 182 (1944).

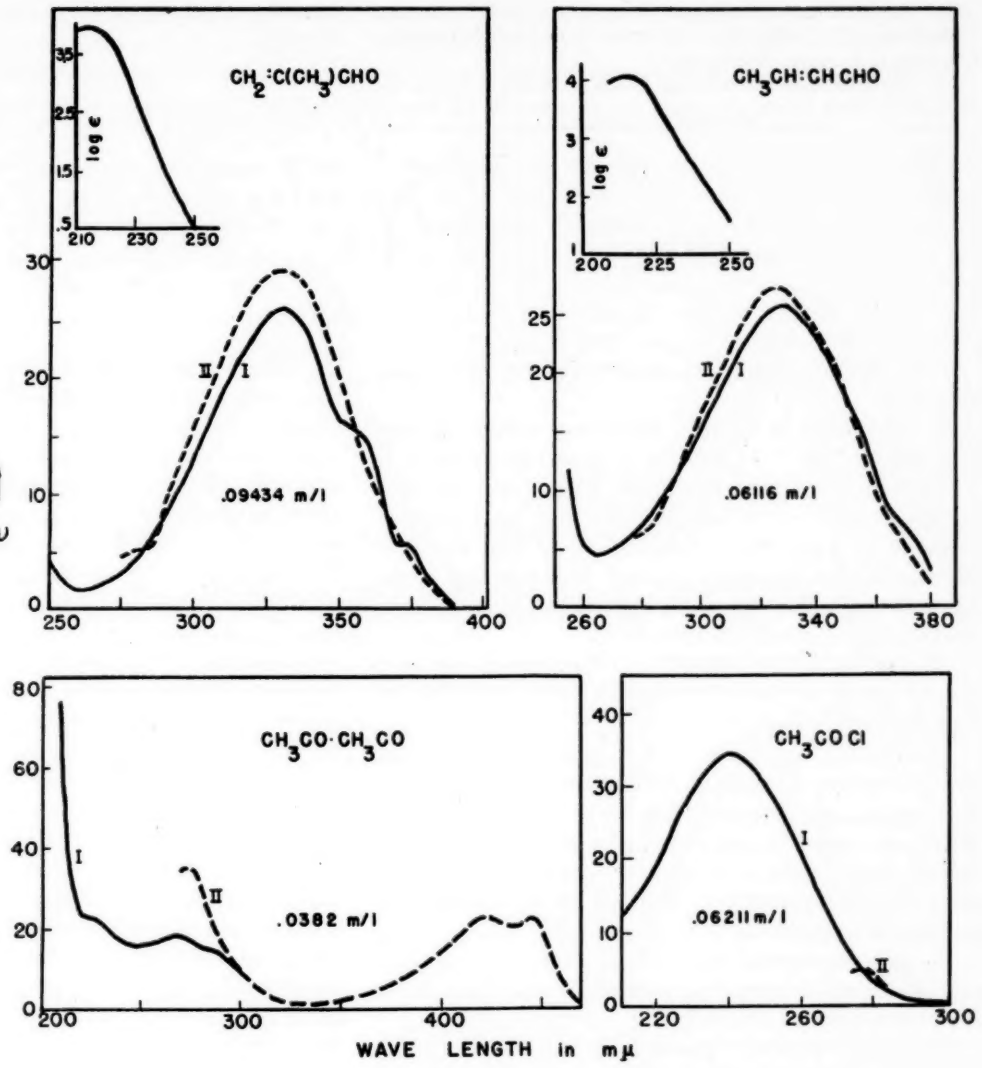

FIG. 3. Extinction coefficients of solutions of designated compounds in I-heptane and II-benzene.

ous solutions and it is seen that the curves have the same general form for all solutions. In Fig. 2(b) we have plotted values of $1/[A]$ against B/D. These points lie roughly on straight lines. To estimate K and E_c, the equilibrium constant and extinction coefficient of the complex, respectively, we have extended these straight lines to the vertical axis. The intercept on the B/D axis is $1/E_c$, from which K can be computed. The results are given below in Table III.

We have neglected the extinction coefficient of oxalyl chloride in comparison to that of the complex for these wavelengths. The mean value of K is 0.27, which indicates that in benzene-oxalyl chloride solutions the ratio of the concentration of the complex to that of oxalyl chloride is 0.21.

MECHANISM OF COMPLEX FORMATION

In order to ascertain the nature of complex formation we have investigated the various compounds listed in Table II diluted with benzene. Acetyl chloride and bromide contain a C=O and a COCl or COBr group, crotonaldehyde and α-methyl acrolein a C=C−C=O group, and diacetyl a O=C−C=O group. The purpose was to determine which group produces large extinction coefficients such as those observed in oxalyl chloride-benzene solutions. As previously mentioned, the only significant change occurs in diacetyl, and even here the effect is small.

According to Benesi and Hildebrand the complexes formed by iodine and benzene result from an acid-base interaction in the electron donor sense in which iodine acts as an acid or an electron acceptor. Mulliken[5] has treated the problem of the formation of complexes between benzene and halogens from a theoretical standpoint. His main conclusions are as follows:

(1) There is only a small change in the electronic structure of iodine present in aromatic complexes.

(2) The proximity of iodine in some orientations destroys the hexagonal symmetry so that the forbidden 2600λ transition of benzene becomes strongly allowed.

[5] R. S. Mulliken, J. Am. Chem. Soc. **72**, 600 (1950).

(3) There are appreciable quantities of resonance structures of the type $A_r^+I_2^-$, where A_r is the aromatic molecule in the wave functions of aromatic complexes.

(4) The interatomic distance in I_2(2.67A) closely matches the distance (2.78A) between opposite carbon atoms in the ring so that the model has the proper symmetry to break down the 2600λ transition.

For benzene and oxalyl chloride we can postulate a complex formation of a similar nature as shown below.

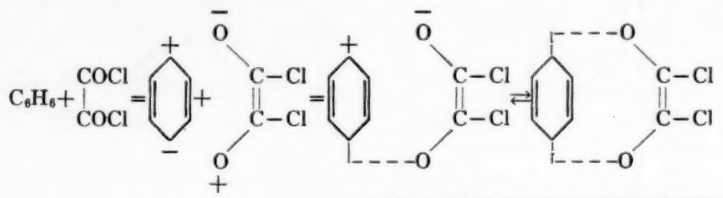

The following arguments support the above complex structure.

(1) According to electron diffraction studies (Sutton and Allen[6]) the C−Cl distance in oxalyl chloride is 1.72A, the C−C distance 1.5A, the C=O distance 1.2A, and the C−C=O angle 123°. The O−O distance is therefore 2.8A which compares quite well with the distance (2.78A) between opposite carbon atoms in the benzene ring. Thus the molecules could become closely packed due to intermolecular forces.

(2) Oxygen, like halogens, is electronegative and should act as an electron acceptor, while the aromatic molecule acts as a donor.

(3) The $(COCl)_2$ molecule can lie in the same plane as the aromatic compound, or in a parallel plane above it, or in a plane perpendicular to it. The distance between the atoms is very nearly the sum of the radii of carbon and oxygen atoms. In each case the hexagonal symmetry is destroyed so that the λ2600 transition of benzene is permitted.

(4) In a conjugated molecule like O=C−C=O, the end atoms alone may be expected to take part in an acid base reaction. (Branch and Calvin.[7])

(5) On the basis of argument (1) it is possible to see why a complex formation may occur in diacetyl but not in acetyl chloride, crotonaldehyde, or α-methyl acrolein. In the latter case the distance between the extreme C and O atoms of the C=C−C=O group is (3.5A) which is much greater than the distance (2.78A) between opposite carbon atoms of benzene, whereas in acetyl chloride this distance is much too small. Furthermore, in all of these compounds the oxygen atom is linked to hydrogen atoms of the CH or aldehyde group by means of either a chelation or an enol formation. This greatly reduces the possibility of the formation of the complex and explains why in diacetyl the extinction coefficient changes only slightly upon dilution with benzene. (18 to 40.)

(6) Since the binding between the carbon and oxygen atoms in the proposed complex structure is ionic the resulting phenomena will be strong in the infrared, but may be too weak for observation in the Raman effect. This structure implies a weakening of the C=O frequency and possibly of the C−Cl frequency also. This is actually observed since the C=O frequency at 1790 cm^{-1} and the C−Cl vibration at 777 cm^{-1} in the infrared spectrum of the vapor shifts to 1777 and 757 cm^{-1} in benzene solutions. In the Raman effect no shifts of frequencies are observed but the 1078 cm^{-1} line, which is a C−C frequency, becomes much stronger upon dilution. This is to be expected on the basis of the proposed structure, since the C−C bond now has a higher polarizability due to increased bond order.

(7) The structure proposed implies a *cis*-form of the molecule at room temperature. The frequency 533 cm^{-1}, which we have identified as a *cis*-frequency at room temperature supports this implication. Since the *cis*-form becomes more abundant at higher temperature, the extinction coefficient of oxalyl chloride-benzene solutions should increase with temperature if the proposed structure represents the actual complex formation.

According to McMurry and Mulliken,[8] the C=O group has two transitions denoted by $N \rightarrow A$, which is forbidden, and by $N \rightarrow B$, which is allowed. The latter has large values of extinction coefficients while the former transition has small values, since they are only partially allowed by vibration effects. In crotonaldehyde and α-methyl acrolein the allowed transition occurs at 214 mμ (11,000), while the $N \rightarrow A$ transition appears at 240 mμ in acetyl chloride and bromide, at 330 in crotonaldehyde and acrolein, and at 285–270 mμ in both diacetyl and oxalyl chloride. Thus we see that the forbidden $N \rightarrow A$ transitions in both diacetyl and oxalyl chloride, which form complexes with benzene, fall in the same region as the forbidden transition of benzene.

The same is true for iodine which has a forbidden transition at 2760A. For the other molecules already

TABLE III.

λ	E_c	$1/K$
280	3333	3.8
290	2500	3.75
300	1852	3.7
310	1250	3.75
320	830	3.61

[6] L. E. Sutton and P. W. Allen, Acta Cryst. **3**, 46 (1950).

[7] G. E. K. Branch and M. Calvin, *Theory of Organic Chemistry* (Prentice Hall Inc., New York, New York, 1941), p. 467.

[8] H. L. McMurry and R. S. Mulliken, Proc. Natl. Acad. Sci. **26**, 312 (1940).

mentioned which do not form complexes with benzene, the $N \rightarrow A$ transitions are far removed from the forbidden transition of benzene.

DIPOLE MOMENT OF OXALYL CHLORIDE

Martin and Partington[9] have found the value of the dipole moment of oxalyl chloride in benzene solutions to be 0.92D. From the evidence produced by this investigation it appears that oxalyl chloride forms a complex with benzene which, since it is due to an ionic binding, will possess a dipole moment. It would be interesting to measure the dipole moment in other nonpolar solvents in order to determine whether or not oxalyl chloride possesses a definite moment.

[9] G. T. O. Martin and J. R. Partington, J. Chem. Soc. **82**, 1178 (1936).

ACKNOWLEDGEMNT

The work was done by one of us (B.D.S.) during his visit to the University of Chicago. We have to thank Professor R. S. Mulliken for the facilities provided for the investigation, and the first author is also deeply grateful for the great kindness shown to him in being allowed to work in the laboratory. Thanks are also due to Mr. Ziomek for the supply of some oxalyl chloride purified by him.

THE JOURNAL OF CHEMICAL PHYSICS VOLUME 19, NUMBER 8 AUGUST, 1951

The Ultraviolet Spectrum of Oxalyl Chloride*

B. D. Saksena and R. E. Kagarise
Department of Physics, Pennsylvania State College, State College, Pennsylvania

(Received February 8, 1951)

The ultraviolet spectrum of oxalyl chloride in the liquid and vapor phases has been investigated in the region 380–280 mμ. The spectrum of the vapor shows considerable structure and progressions of 70, 390, 940, 1380, and 1420 cm^{-1} are observed. The liquid spectrum in this region shows several maxima having small extinction coefficients. Beyond 280 mμ the extinction coefficient increases rapidly.

1. INTRODUCTION

THE ultraviolet spectrum of oxalyl chloride in hexane solution has been studied by Herold,[1] who reports an absorption at 28,150 cm^{-1}. No other investigation of the ultraviolet spectrum of oxalyl chloride appears to have been made. We have investigated the spectrum in the 3800 to 2000A region for both liquid and vapor phases. This investigation was undertaken in continuation of our work on rotational isomerism in oxalyl chloride and the effect of dilution in benzene on the Raman, infrared, and ultraviolet spectra.

2. EXPERIMENTAL

The ultraviolet spectrum of liquid oxalyl chloride in *n*-heptane solutions was studied by means of a Beckman quartz spectrograph. The extinction coefficients for various wavelengths are recorded in Table I and have been plotted in Fig. 1.

In addition there are very broad bands at λ=287 (24.5) and 276 (32) mμ.

The spectrum of the vapor was investigated with a medium quartz spectrograph and quartz tubes 5 cm and 100 cm long. The spectrum was also obtained at a higher temperature (60°C), using the 100 cm absorption tube. Considerable structure is visible in the spectra as shown in Fig. 2. Measurements of these bands are listed below in Table II, with an accuracy of 0.5A.

With the 5-cm tube and at room temperature, only the more prominent bands appear. These bands are 27,196 (s); 27,582 (w); 28,641 (s); 29,032 (w); 30,067 (s); and 31,482 (s). In addition to these there are broad bands between λ=2694 and 2752, 2925 and 2840, and 2803 and 2890.

3. DISCUSSION

The structure of the carboxyl group in its normal and excited electronic states has been discussed by McMurry and Mulliken[2] and by McMurry.[3] The normal configura-

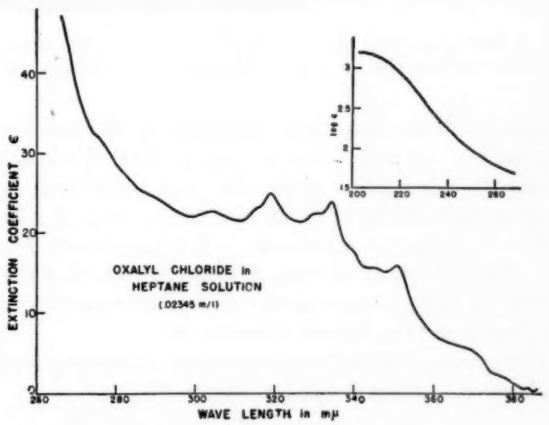

FIG. 1. Extinction coefficients of oxalyl chloride in *n*-heptane solution for various wavelengths.

* This research was carried out on Contract N6 ONR-269. Task V of the ONR.

[1] W. Herold, Z. physik. Chem. **B18**, 265 (1932).

[2] H. L. McMurry and R. S. Mulliken, Proc. Natl. Acad. Sci. U.S. **26**, 312 (1940).

[3] H. L. McMurry, J. Chem. Phys. **9**, 242 (1941).

TABLE I. Extinction coefficients of oxalyl chloride in *n*-heptane (0.02345 mole/liter).

$\lambda(m\mu)$	210	220	230	240	250	260	270	280	290	300	305	310	
	1404	864	393	170.4	98.0	62	38.4	28.7	24.6	22.0	22.8	21.8	
$\lambda(m\mu)$	315	320	325	330	335	340	349	351	360	370	380	390	400
	23.0	24.6	21.5	22.5	23.3	17.7	15.1	16.0	7.3	5.5	1.33	0.6	0.3
The absorption increases continuously from 380 to 210 $m\mu$ and has the following maxima:													
$\lambda(m\mu)$	384.0	369.0		351.0	346.5	340.0	334.5		330.0	319.5	315.5	306.0	
		5.5		16	15.7	17.5	23.5		22.5	25	23.5	22.8	
$\nu \cdot cm^{-1}$	26034	27093		28482	28852	29403	29887		30294	31290	31686	32670	
	v.w.	w. and broad		St. and sharp	broad		St. and sharp		m. St. and sharp	St. and sharp	broad	St. and broad	

tion, designated as N, is $(zt)^2(xx)^2(yo)^2$; where the letters x, y, z denote the $2p$ A.O. with axes along the direction perpendicular to C=O(x), in the plane and perpendicular to C=O(y), and along C=O(z). In addition, t is a trigonal carbon atomic orbital. For the excited states there are two important possibilities, $(zt)^2(xx)^2yo(x\bar{x})$ and $(zt)^2(xx)^2yo(z\bar{t})$, called singlet states A and B, respectively.

The transition $N-B$ is allowed, while the transition $N-A$ is forbidden. However, owing to electronic vibrational coupling, the latter transition may appear weakly. In conjugated aldehydes and ketones this weaker absorption occurs in the 2900A region.

Thus the transition proposed to explain the weaker absorption by unconjugated C=O group involves the

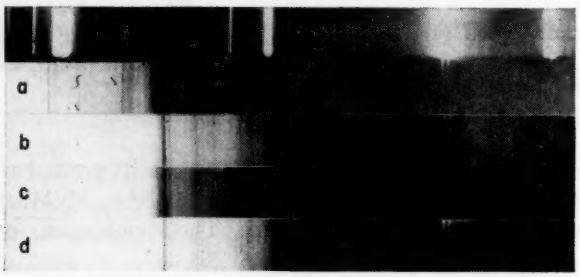

FIG. 2. The ultraviolet spectrum of the vapor with one meter absorbing path length: (a, b) at room temperature, (c, d) at 60°.

excitation of an essentially nonbonding electron localized on the oxygen to the excited x M.O. of the C=O group. In conjugated molecules also transitions from similar nonbonding M.O. to each of the excited x M.O. are to be expected. However, when two C=O are at the ends of a chain of two or more carbon atoms, this transition is no longer forbidden by the selection rules and we have two allowed transitions.

The ground state of molecules such as oxalyl chloride, diacetyl, and glyoxal can be represented by

$$N_2 \cdots x_1^2x_2^2y_1^2y_2^2 \begin{matrix} b_1a_2a_1b_2 \ cis\text{-} \\ a_ub_ga_gb_u \ trans\text{-}. \end{matrix}$$

The two y atomic orbitals interact to produce the M.O. orbitals y_1 and y_2 whose wave functions are symmetric, and antisymmetric combinations of the y atomic orbitals of each C=O group, respectively. Similarly, x_1 and x_2 are symmetric and antisymmetric combinations of the x A.O. The representations of x_1, x_2, y_1, and y_2 are shown in the margin for the *cis*- and *trans*-forms of the molecule. The excited states involving transitions to x molecular orbitals are

(i) $x_1^2x_2^2y_1\,y_2^2\bar{x}_1$,

(ii) $x_1^2x_2^2y_1^2y_2\,\bar{x}_1$,

(iii) $x_1^2x_2^2y_1\,y_2^2\bar{x}_2$,

(iv) $x_1^2x_2^2y_1^2y_2\,\bar{x}_2$.

For both *cis*- and *trans*-forms only (i) and (iv) are allowed, the electric moment being along $x(a_u)$ for the *trans*- and along $x(b_1)$ for the *cis*-form, while (ii) and (iii) are forbidden according to the selection rules. According to McMurry,[3] the intensity gained in this way should be small.

This feature of the spectrum is observed in the spectrum of diacetyl, glyoxal, and oxalyl chloride.

Diacetyl	4700–3400 (22)	3400–2300 (18)
Glyoxal[4]	4780–3400	3200–2300
Oxalyl chloride	3800–3000 (22)	2800–2400 (60)

In all three cases the second band system is broad and diffuse and is weak in intensity, while the first system shows a structure. It appears, therefore, that they arise from the same type of transitions. The extinction coefficients for these two systems in both oxalyl chloride and diacetyl are small so that it appears quite likely that they arise from transitions of the type discussed above.

It is likely, as suggested by Herold,[1] that the shift in the absorption region in oxalyl chloride towards shorter wavelengths is perhaps due to the substitution of negatively charged chlorine atoms for a positively charged H or CH_3 group. This shift is most pronounced in the first band.

As can be seen from Figs. 1 and 2 the band in the 3800–3000A region exhibits considerable structure. At the present time it is not possible to interpret the spec-

[4] H. W. Thomson, Trans. Faraday Soc. **36**, 988 (1940).

TABLE II.

λ(A)	ν(cm⁻¹)		λ(A)	ν(cm⁻¹)	
3747.0	26,681	w.	3417.0	29,257	w.
3736.0	26,759	v.w.	3393.0	29,464	v.v.w.
3707.5	26,965	v.w.	3385.0	29,534	v.w.
3689.0	27,100	m.st.	3379.5	29,582	m.st.
3683.0	27,144	v.w.	3371.0	29,656	w.
3676.0	27,196	v.st.I	3366.0	29,700	w.
3672.5	27,222	v.w.	3356.5	29,784	w.
3667.0	27,263	m.st.	3346.5	29,873	w.
3659.0	27,322	w.	3336.5	29,963	m.st.br.
3640.0	27,465	v.v.w.	3330.0	30,021	m.st.
3635.5	27,499	v.v.w.	3325.0	30,067	v.st.III
3630.0	27,540	v.v.w.	3316.5	30,144	m.st.
3624.5	27,582	m.st.	3308.0	30,221	v.w.
3615.0	27,655	w.	3303.5	30,262	v.w.
3606.0	27,724	v.v.w.	3295.5	30,336	m.st.
3590.0	27,847	v.v.w.	3286.5	30,419	w.
3580.0	27,925	v.v.w.	3281.0	30,470	w.
3571.0	27,995	v.w.	3275.0	30,526	w.
3552.0	28,145	m.st.	3266.5	30,605	w.
3543.0	28,217	w.	3258.0	30,685	w.
3539.0	28,249	w.	3216.0	31,086?	
3527.0	28,344	v.w. diff.	3212.5	31,119?	
3517.0	28,425	v.w. diff.	3179.5	31,442	m.st.
3508.5	28,494	st.	3175.5	31,482	v.st.IV
3498.0	28,580	st.	3167.5	31,561	m.st.
3490.5	28,641	v.st.II	3149.0	31,747	w.
3482.0	28,711	m.st.	3039.5	32,891	v.st.V
3467.0	28,835	v.w.			
3457.5	28,914	w.			
3449.0	28,986	w.			
3443.5	29,032	m.st.			
3439.0	29,112	w.			
3425.0	29,189	v.w.			

trum, but progressions of the very strong and medium strong bands by 1380 and 1420 cm^{-1} are observed. It is possible that this may be the C=O frequency in the excited state, since there is no frequency, other than the C=O, which is higher than 1077 cm^{-1} in the Raman and infrared spectra. The appearance of two frequencies in this region is of considerable interest with respect to the question of rotational isomerism, but further work appears to be necessary in order to prove this point.

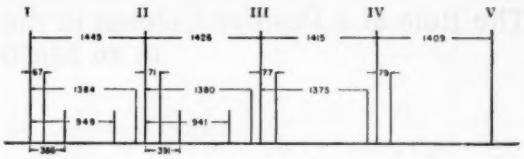

FIG. 3. General form of stronger bands showing progressions of 1380 and 1420 cm^{-1}.

There are also other progressions of about 70, 390, and 940 cm^{-1}. The general form of the stronger bands is shown in Fig. 3.

In Fig. 2 two spectra are shown, one at 25°C, the other at 60°C. There does not appear to be any appreciable change in the spectrum.

In the liquid phase the wavelengths of the main absorption bands are slightly shifted towards longer wavelengths, and frequency differences of 1400 and 380 cm^{-1} are observed.

ACKNOWLEDGMENT

The work was done by one of us (BDS) during his visit to the University of Chicago. We have to thank Professor R. S. Mulliken for the facilities provided for the investigation.

The Role of a Positive Column in the Reduction of Current Due to External Light in an Electrodeless Discharge

V. V. AGASHE
Physics Department, The Institute of Science, Bombay, India
(Received December 13, 1950)

The discharge current in a cylindrical tube (45 mm in diameter and 45 mm in length) with external electrodes decreases on exposure to external light. An attempt has been made to determine the contribution to the reduction in current, by the different regions of the discharge tube, by exposing equal volumes of the discharge tube, one after another, from one electrode to the other. In the studies of Hg vapor discharge, the intensity and the source of the irradiation are changed and the pressure of Hg vapor is kept constant, while in the studies of Cl_2 discharge, the intensity and the frequency of irradiation are kept constant and the pressure of Cl_2 is changed from 3 mm to 70 mm of Hg. The results show that the reduction in current is maximum when the positive column of the discharge tube is exposed to external light. It has been suggested that a few more electrons in the positive column are lost by the formation of negative ions under the influence of external light. This reduces the average velocity of negatively charged particles and is probably responsible for the observed decrease in current.

IN 1940, Joshi[1] observed that the discharge current in a glass ozonizer filled with Cl_2 at a pressure of about 10 cm of Hg decreases on exposure to external visible light, so that the current is restored to its original value after the external light is shut off. The discharge tube was excited by a 50-cycle ac potential. Later, this reduction[2] was observed in gases such as Cl_2, O_2, N_2, H_2 and in vapors such as bromine, iodine, and mercury. The reduction in current increases with intensity, reaching a saturation value, and it also increases with the frequency of the external light.[3,4] Penning[5] had already observed a reduction in current in a corona discharge tube filled with neon contaminated with argon, when exposed to a neon source. That is, Penning observes a decrease in current with light of resonance frequency, while Joshi observes it with all frequencies.

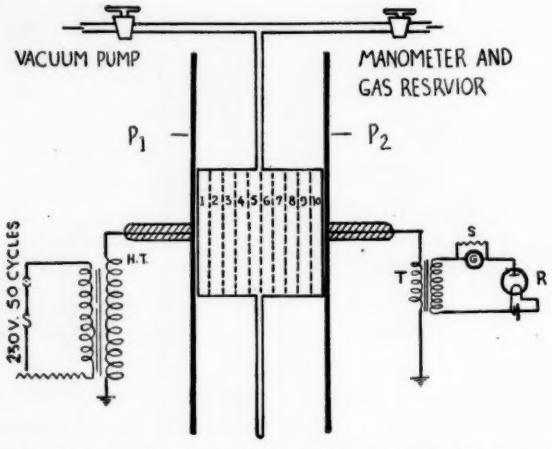

FIG. 1. A is the discharge tube. P_1 and P_2 are metal plates acting as electrodes. H.T. is the high tension transformer (2 kw). T is the coupling transformer. G is the moving coil mirror galvanometer. S is the galvanometer shunt. R is rectifier (30 used as a diode). V is a voltmeter which measures the primary voltage of the H.T. Numbers (1, 2, ···10) represent the portions of the discharge tube exposed separately to the external beam of light.

In the work done so far on the decrease in current on exposure to external light by Joshi and others, the discharge tubes used were either of the ozonizer type, (i.e., two glass cylinders coaxially sealed as virtual electrodes) or of the semi-ozonizer type (i.e., a central wire in a glass cylinder which acts as the virtual electrode). Furthermore, in the studies made so far, the entire discharge tube has been exposed to external light.

The current in a discharge tube is determined by the number of charged particles arriving at the electrodes per unit time[6,7] and is given by $i=\Sigma nekX$ (the symbols carry the usual meaning). A change in "i" thus indicates a change in some or all the factors on the right-hand side of the above equation.

The field distribution and the ion and electron concentrations are different in the different regions of a discharge tube; it could, therefore, be reasonably expected that the changes of the current produced by changes in n, k, or X would vary with the region of the discharge tube exposed to light. The differences in the changes produced in the different regions can be brought out clearly, not by exposing the entire discharge simultaneously to an external beam of light, but by exposing equal volumes of the discharge tube situated in different portions, one after another.

In the ozonizer or semi-ozonizer type of discharge tube, it is very difficult to isolate the different regions, irradiate them separately, and study their differential contribution to the reduction in current, because the distance between the electrodes is very small (of the order of a few mm) and the interelectrode space is

[1] S. S. Joshi and V. Narasimhan, Current Sci. (India) **9**, 536 (1940).
[2] S. S. Joshi, Presidential address, Chemistry Section of the Indian Science Congress (1943).
[3] P. G. Deo, Indian J. Phys. **18**, 83 (1944).
[4] N. R. Tawde and K. Gopalkrishnan, Proc. Indian Acad. Sci. **29**, 171 (1949).
[5] F. M. Penning, Physica (old series) **8**, 137 (1928); **12**, 65 (1932).
[6] K. R. Dixit, J. Chem. Phys. **16**, 742 (1948).
[7] J. J. Thomson and G. P. Thomson, *Conduction of Electricity through Gases* (Cambridge University Press, London, 1933), Vol. II, p. 361.

annular, bounded by two coaxial cylinders. In order to be able to ascertain the relative contribution of the different portions in a discharge to the reduction of current by scanning (i.e., by irradiating equal and restricted volumes of the discharge tube from one electrode to the other electrode), we chose a tube of cylindrical cross section (45 mm in diameter) with flat ends (Fig. 1). The tube was prepared from Pyrex glass, and the flat ends were 45 mm apart. Two circular metal plates (P_1, and P_2) of about 16 cm diameter and parallel to each other were placed outside and close to the flat ends of the tube, and a 50-cycle ac potential from a H.T. transformer (2 kw) was applied to these metal plates. As the diameter of these metal plates was three times the diameter of the discharge tube, the field was always fairly uniform throughout the discharge tube.

The discharge current is measured with the help of a transformer coupling (T). The primary of the coupling transformer (T) is in series with the discharge tube, and the potential induced across its secondary is fed to the plate of the rectifying valve (R). The plate current, which is thus proportional to the discharge current, is measured by a mirror galvanometer (G), by a lamp and scale arrangement. The discharge current[8,9] contains high frequency components besides the 50-cycle component and its harmonics, and the reduction in current is more predominant in H.F. part. The transformer coupling will magnify these different components to different extents and, hence, may not be satisfactory when absolute values of the discharge current are to be measured.[10] Our object in this work is to locate the region which shows the maximum reduction in current. We are therefore more interested in the relative changes in current than in their absolute values, and we chose the transformer coupling which magnifies the high frequency component preferentially and hence is more sensitive to the reduction in current.

SCANNING OF THE DISCHARGE TUBE

The ideal arrangement for scanning consists of a parallel beam of light which is made as narrow as possible. There is, however, a practical limit to the width of the slit used. A too-narrow slit reduces the total amount of light (number of photons which are incident on the gas in the discharge) to such an extent as to make the total reduction in current smaller than the fluctuations of the galvanometer. Such a slit therefore is not desirable in the interest of accuracy of observations, and it was observed that the narrowest beam which could be used was about 4.5 mm. This enables us to scan our tube in ten different parts. Naturally, this width will depend on the nature of the gas in the tube, the nature and frequency of the light, and the absolute amount of light (photons) incident on the tube.

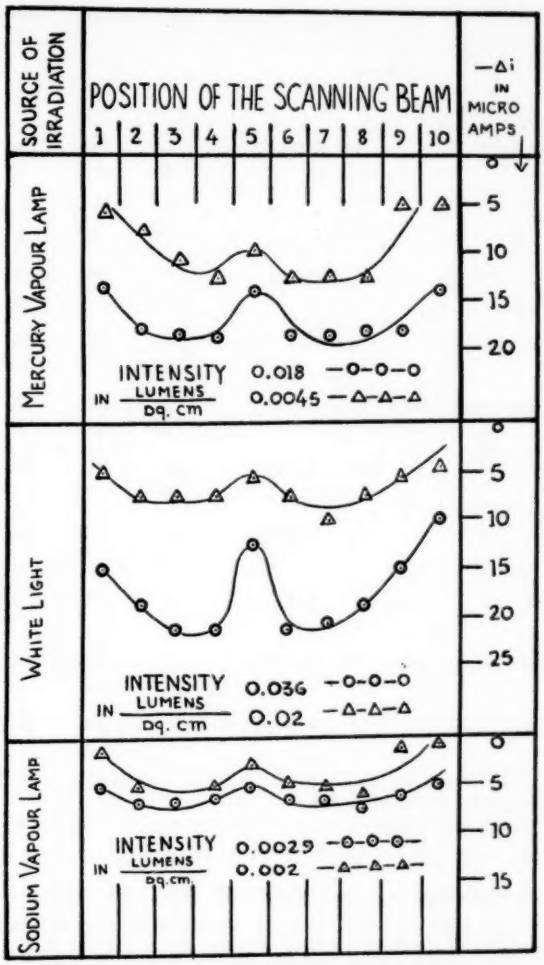

FIG. 2. The variation in $(-\Delta i)$ as a function of the position of the scanning beam at two selected intensities for three different sources in mercury vapor discharge at $X=433$ volts/cm and $i_D=203$ microamperes. ("Dq." should read "Sq.")

A beam of white light from an epidiascope was projected on the discharge tube, and a slit was introduced in the path of the beam. The discharge tube was placed in a wooden box made light-tight but with an opening for the slit on one side. On the wall of the light-tight box, opposite to the opening, a paper scale was pasted. By moving the slit, different portions of the discharge tube could be irradiated from one electrode to the other in succession. The position of the exposed portion could be noted by the beam of light on the scale. The divergence of the beam, which was made as small as possible, was noted, and the slit was shifted from one position to the next position in such a way that there was no overlapping along the axis of the discharge tube.

EXPERIMENTS WITH MERCURY

In this work the discharge tube contained mercury vapor at room temperature, and the intensity of the white light used for irradiation was changed by using

[8] S. S. Joshi, Nature **154**, 147 (1944); Current Sci. (India) **14**, 67 (1945).
[9] S. R. Mohanti, J. Indian Chem. Soc. **27**, 218 (1950).
[10] V. V. Agashe, "Effect of irradiation on the mobility of negative ions in an ozonizer discharge," (to be published).

TABLE I. Mercury vapor discharge; field strength $X=500$ volts/cm; $i_D=209$ microamperes.

Irradiation Source	Intensity lumens/sq cm		Position of the scanning beam H.T. side 1	2	3	4	5	6	7	8	9	L.T. side 10
White light	0.057	i_L	195	190	185	185	190	185	185	186	188	195
		$-\Delta i$	14	19	24	24	19	24	24	23	21	14
	0.036	i_L	198	195	195	195	197	195	193	195	197	199
		$-\Delta i$	11	14	14	14	12	14	16	14	12	10
	0.026	i_L	202	199	195	195	197	195	194	196	200	204
		$-\Delta i$	7	10	14	14	12	14	15	13	9	5
	0.02	i_L	206	203	199	199	201	199	198	200	205	205
		$-\Delta i$	3	6	10	10	8	10	11	9	4	4
Mercury vapor lamp	0.018	i_L	192	189	186	186	189	184	184	185	187	193
		$-\Delta i$	17	20	23	23	20	25	25	24	22	16
	0.006	i_L	200	200	194	191	195	191	194	196	197	203
		$-\Delta i$	9	9	15	18	14	18	15	13	12	6
	0.0045	i_L	200	200	194	191	196	191	194	196	198	202
		$-\Delta i$	9	9	15	18	13	18	15	13	11	7
	0.004	i_L	206	200	199	197	200	198	196	201	202	207
		$-\Delta i$	3	9	10	12	9	11	13	8	7	2
Sodium vapor lamp	0.0029	i_L	208	206	206	206	208	207.5	206	206	207.5	208
		$-\Delta i$	1	3	3	3	1	1.5	3	3	1.5	1
	0.0016	i_L	209	206	206	206	208.5	208	206	208	208	209
		$-\Delta i$	—	3	3	3	0.5	1	3	1	1	...

i_D = amplified discharge current in microamperes in dark.
i_L = amplified discharge current in microamperes when different portions of the discharge tube are exposed to external light.
$\Delta i = (i_L - i_D)$.

the epidiascope at four different positions relative to discharge tube. Different slits were chosen for different positions of the light source, so that in every case the width of the light beam at the axis of the discharge tube was 4.5 mm. Thus, we could divide the discharge tube in ten equal parts, and irradiate them separately. The reduction in current $(-\Delta i)$ when these different parts are exposed to light was noted for three field strengths greater than the striking field strength. The field strengths (X) were 433, 500, and 583 volts/cm. The actual readings corresponding to some of the intensities of the different sources used are shown graphically for the first field strength in Fig. 2, and all readings corresponding to $X=500$ volts/cm are given in Table I. We have not scanned the discharge tube when the applied electric field is less than the striking field, because the starting of the electrodeless discharge, under these conditions, due to external light is well known.[11,12]

Similar measurements were made by using a mercury vapor lamp and a sodium vapor lamp for irradiation. The intensities of the beam of light at the center of the tube were measured in all cases by a thermopile and a standard lamp.

[11] J. J. Thomson, Proc. Phys. Soc. (London) **11**, 79 (1928).
[12] R. W. Wood, Phys. Rev. **35**, 673 (1930).

EXPERIMENTS WITH CHLORINE

Chlorine was prepared by the electrolysis, with carbon electrodes, of pure concentrated hydrochloric acid. It was dried by passing through $CaCl_2$ traps and allowed to enter the discharge tube at the desired pressure. The pressure was measured by an oil manometer. In these experiments we changed the pressure of Cl_2 from 3 mm to 70 mm of Hg, keeping all other experimental arrangements the same; that is, the same white light, at the same intensity of 0.01 lumen/sq cm, and the same kind of scanning arrangement, namely a scan width of 6.4 mm, enabling the tube to be scanned in seven parts. This arrengement was found to be experimentally convenient. A few experiments were made with 4.5-, 5-, and 5.5-mm scans and compared with a 6.4-mm scan at a pressure of about 50 mm of Hg. The nature of the curves is the same in all cases. A 6.4-mm scan, however, enables us to take quick readings consistent with efficiency and was chosen as most convenient. It should be remembered that chlorine slowly reacts with tap grease, and it is necessary to finish taking readings within that interval of time within which the gas remains reasonably pure.

The reduction in current due to scanning was noted at 12 pressures of chlorine (*viz.*, 70, 63, 55, 48, 40, 34, 28, 22, 15, 9.5, 6, and 3 mm of Hg) and at 4 or 5 field strengths at every pressure. The variation in $(-\Delta i)$ is

TABLE II. Discharge in Cl_2. Source of irradiation is white light of intensity (0.01) lumen/sq cm.

Pressure mm of Hg	Field strength (X) volts/cm	i_D micro-amperes		Position of the scanning beam: H.T. electrode	1	2	3	4	5	6	7	L.T. electrode
70	2816	432	i_L	424	410	390	416	419	424	412	419	424
			$-\Delta i$	8	22	42	16	13	8	20	13	8
	2860	502	i_L	482	481	466	487	487	490	475	487	494
			$-\Delta i$	20	21	36	15	15	12	27	15	8
	3080	550	i_L	534	518	614	530	530	538	518	518	540
			$-\Delta i$	16	32	36	20	20	12	32	32	10
	3300	557	i_L	550	534	528	544	544	544	534	540	550
			$-\Delta i$	7	23	29	13	13	13	23	17	7
6.0	325	169	i_L	160	138	150	154	154	154	138	134	164
			$-\Delta i$	9	31	19	15	15	15	31	35	5
	433	194	i_L	180	169	177	180	180	180	169	169	184
			$-\Delta i$	14	25	17	14	14	14	25	25	10
	542	215	i_L	208	196	202	206	208	208	198	198	208
			$-\Delta i$	7	19	13	9	7	7	17	17	7
	650	227	i_L	218	209	215	215	218	219	213	213	224
			$-\Delta i$	9	18	12	12	9	8	14	14	3
	758	232	i_L	225	222	224	225	225	229	224.5	224	231
			$-\Delta i$	7	10	8	7	7	3	7.5	8	1

similar in all cases, and therefore observations for two pressures only (70 and 6 mm of Hg) are given in Table II. Some of the observations at other pressures are shown graphically in Figs. 3 and 4.

DISCUSSION

The curves (Figs. 2–4) represent the reduction in the discharge current when different portions of the discharge tube are exposed to external light. For both mercury and chlorine, for all the variations introduced, the curves show two minima corresponding to the maximum reduction in the discharge current. We also observe the following: (1) the position of the minima remains unchanged when the potential applied to the discharge tube is changed at constant pressure, but the magnitude of the reduction in the discharge current changes with applied potential (Fig. 3). (2) The position of the minima remains unchanged if the intensity and the source of the irradiation are changed, while the magnitude of the reduction increases with the intensity (Fig. 2). (3) But the position of the minima shows a definite shift when the pressure of the gas in the discharge tube is changed (Fig. 4).

We have also taken a photograph of the mercury vapor discharge showing the positions of the different zones at an applied field of 500 volts/cm. The photograph is reproduced here (Fig. 5), and for comparison, below it, is given the curve representing the corresponding reduction in current, (Obs. No. 1, Table I). This figure appears to indicate that the zone of maximum reduction in the current corresponds with the luminous portion of the discharge. The electrodes do not appear to make a significant contribution to the reduction of the current. The bright and dark zones in the discharge tube show a symmetry about the middle portion of the discharge. Such a symmetry is explained by the assump-

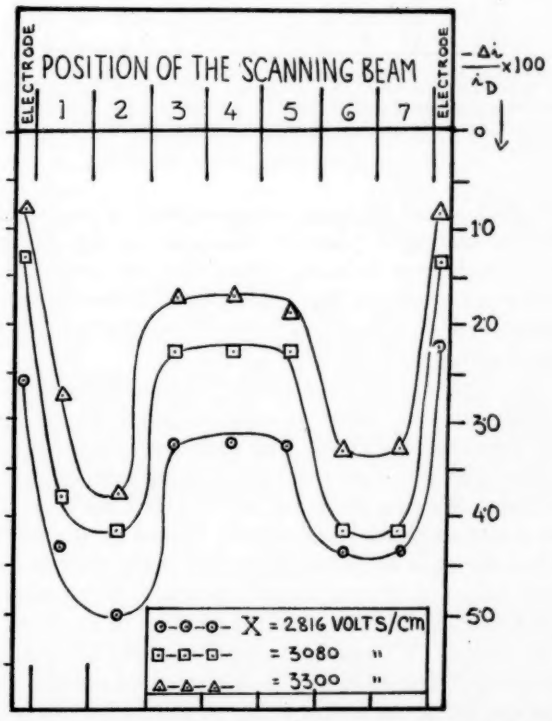

FIG. 3. The variation in $[(-\Delta i/i_D)\times 100]$ as a function of the position of the scanning beam (white light of intensity 0.01 lumen/sq cm) at three field strengths in chlorine discharge at a pressure of 63-mm Hg.

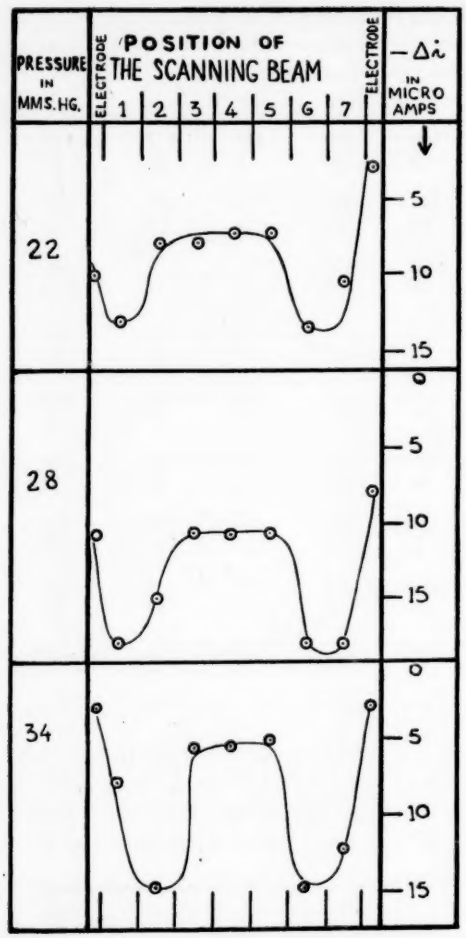

FIG. 4. The variation in $(-\Delta i)$ as a function of the position of the scanning beam (white light of intensity 0.01 lumen/sq cm) at $X=1516$ volts/cm in chlorine discharge at three pressures of chlorine.

tion that an ac discharge is equivalent to two dc discharges having a positive electrode at the center.[13] Our experiments definitely show that the contribution of the electrodes to the reduction in current is insignificant as compared with the contribution of the luminous portion.

The luminous positive column is sometimes uniform and sometimes striated. It contains positive ions, negative ions, and electrons. The mobility of positive and negative ions is, however, small compared to that of electrons. We can, therefore, assume that the current in the positive column is essentially caused by the motion of the electrons under the influence of the electric field. Any change in current could, therefore, be reasonably attributed to the change in the number of electrons.

According to Thomson[14] and Compton, Turner, and McCurdy,[15] the electrons in the positive column of a glow discharge can be lost either by diffusion to the walls or through the formation of negative ions but not by

[13] D. Banerji and R. Ganguli, Phil. Mag. **11**, 410 (1931).
[14] See reference 7, p. 374.
[15] Compton, Turner, and McCurdy, Phys. Rev. **24**, 597 (1924).

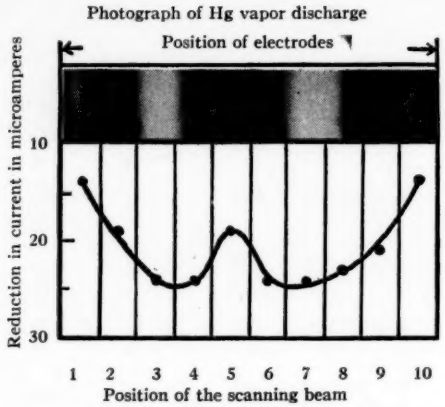

FIG. 5. Change in $(-\Delta i)$ as a function of the position of the scanning beam, compared with the corresponding visual appearance of the discharge.

recombination. In our case we are studying the changes produced by the action of external light. The action of light on diffusion processes, especially when the intensity of light is not sufficient to produce any appreciable change in the temperature of the gas,[10] is not likely to be significant. Thus, we are led to expect that the change of current is due to a decrease in the number of electrons caused by the formation of negative ions.

The magnitude of the decrease in current due to irradiation, if resulting from the formation of few more negative ions, would depend upon the electron affinity. Deshmukh[16] has shown that under identical conditions of the discharge the magnitude of the reduction in current is in the order,

$$H_2 < N_2 < \text{air} < O_2.$$

This order also represents the manner in which the electron affinity for these gases alters. Further, Deshmukh[16] has shown that neon (which has no electron affinity) does not show any reduction in current when exposed to visible light. We can, therefore, reasonably assume that the reduction in current due to irradiation is caused by the formation of a few more negative ions.

In conclusion, we can say that under the action of external light, the number of charged particles does not change appreciably, but their distribution changes by a few electrons attaching themselves to neutral particles to form negative ions. This change in the distribution reduces the average velocity of the negatively charged particles; i.e., the mobility of the negatively charged particles decreases as a result of irradiation. (By using a method similar to that of Chattock, the author[10] has found that a reduction in mobility is associated with the reduction in current due to irradiation in ozonizer discharge.)

The author is thankful to Professor K. R. Dixit, Head of the Physics Department, The Institute of Science, Bombay, for suggesting the problem and for the valuable discussions throughout the work.

[16] G. S. Deshmukh, J. Indian Chem. Soc. **24**, 211 (1947).

The Variation of Atomic Polarizabilities in Molecular Vibrations

FRANK MATOSSI
Naval Ordnance Laboratory, White Oak, Silver Spring, Maryland
(Received April 16, 1951)

The depolarization factor of Raman lines of totally symmetric vibrations can be calculated in agreement with the general concepts of the polarizability theory of the Raman effect and with the concept of mutual interaction of dipoles if it is assumed that the polarizability of an atom depends on the interatomic distances in a molecule. When the totally symmetric species contains more than one vibration, the vibrational patterns, and thus the force constants, are among the factors that determine the depolarization. The results of the theory are evaluated for linear diatomic and triatomic molecules. The utilization of the method for checking force constants and molecular structures is pointed out.

INTRODUCTION

THERE are two well-known general ideas governing the theoretical determination of depolarization factors of Raman lines. One is Placzek's concept[1] of describing the interaction between nuclear motion and electronic shell during a molecular vibration by the change of the molecular polarizability. It leads to the familiar result that the depolarization factor ρ is equal to 6/7 for all not totally symmetric vibrations, but less than 6/7 for the totally symmetric ones. This result is confirmed by experiment.

In order to find the particular values of ρ for the latter class of vibrations, we can use Silberstein's concept[2] of mutual (electrostatic) interaction of the dipoles induced by the field of the incoming radiation. This idea has been very fruitful in explaining the optical anisotropy responsible for Rayleigh scattering. However, the combination of the two concepts, in order to obtain the depolarization of Raman lines fails. Although it must be admitted that the failure may be due to the specific assumptions made in applying these concepts—and there are some indications that Silberstein's model of interactions must be refined—it seems worth while to retain the general concept, which easily lends itself to visualization and to introduce modifications rather than to reject it.

In previous work, I tried to reconcile the theory with the observations. I assumed[3] that not only does the molecular polarizability depend on the interatomic distance (by virtue of the interaction of the induced dipoles) but the atomic polarizabilities do also. It could be shown that this purely phenomeological assumption is indeed suitable for the purpose indicated. Later on we assumed[4] that the atomic polarizability is a function of the exciting field strength.[5] This is qualitatively equivalent to the first hypothesis, but a quantitative reduction to the first one would need a better understanding of the interaction of the radiation field with the field of the vibrating molecules than we have at the present time. This difficulty has been circumvented by a rather formal method of determining the variation of the field with the normal coordinate of the vibration. Because of this and the easier mathematical handling, the first method[3] is used in this paper again.

The treatment is now extended to polyatomic molecules in which more than one totally symmetric vibration is possible. These vibrations may have different depolarization factors; and it is assumed that this is due to the various vibration patterns, i.e., to the different possible combinations of distance changes. In the next section, the general method is outlined, which is then evaluated, for some linear molecules, in the last section.

GENERAL METHOD

We consider only molecules with two principal polarizabilities. These include all molecules with a distinguished symmetry axis of a multiplicity higher than two. Later on, we specialize to linear molecules.

The molecular polarizabilities A and B parallel and perpendicular, respectively, to the principal axis of the molecule are given by

$$A=F_a(\alpha_i, r_{ik}), \quad B=F_b(\alpha_i, r_{ik}), \tag{1}$$

in which F_a and F_b are certain functions of the atomic polarizabilities α_i and the interatomic distances r_{ik}. F_a and F_b are, in general, different from each other,[6] because of the different interaction of differently oriented dipoles. From A and B, the depolarization factor of Rayleigh scattering in gases can be determined from

$$\rho_{\text{Rayl}}=6/[7+45(a/b)^2] \text{ with } a=\tfrac{1}{3}(A+2B), \; b=A-B;$$

a is the average polarizability which can be determined from the molecular refraction. For diatomic molecules of the type XX, it is therefore possible to compute α and r from depolarization and refraction. The r-values are, in general, too high but of the correct order of mag-

[1] G. Placzek, in Marx, *Handbuch der Radiologie* (1934), Vol. VI, 2, p. 205.
[2] L. Silberstein, Phil. Mag. **33**, 92, 215, 521 (1917).
[3] F. Matossi, Physik. Z. **45**, 304 (1945).
[4] F. Matossi and R. Mayer, Phys. Rev. **74**, 449 (1948).
[5] The field dependence of polarizabilities has also been discussed independently and in another connection by O. Theimer, Proc. Indian Acad. Sci. **A28**, 506 (1948).
[6] For the specific expressions of F_a and F_b for certain types of molecules see, for instance, reference 3, or T. H. Havelock, Phil. Mag. **3**, 158, 433 (1927).

TABLE I.

	$r(10^{-8}$ cm)		ω(cm^{-1})	dr_1/dr_2	$\alpha(10^{-24}$ cm^3)	ρ_{obs}	$\rho_{th}(\alpha'=0)$	Remarks
NN	1.1		2330	...	0.9	0.19	0.54	spectr. radius
	1.6						0.63	scatt. radius
OO	1.22		1555	...	0.73	0.26	0.50	spectr. radius
	1.5						0.63	scatt. radius
NO	1.15		1877	...	0.9 (N) 0.73(O)	0.30	0.50	
CO	1.12		2155	...	0.85(C) 0.73(O)	0.29	0.50	
	r_1	r_2						
OCO	1.16	1.16	1335	1	0 (C) 1 (O)	0.21	0.81	
SCS	1.55	1.55	660	1	0 (C) 3.3 (S)	0.17	0.64	
NNN	1.2	1.2	1346	1	0.9	0.16	0.60	ion in solution
NNO	1.2	1.2	1285	0.5	0.9 (N)	0.22	0.50	
			2280	−1.25	0.73(O)	0.38	0.50	
NCS	1.15	1.54	750	0.2	0.9 (N)	0.08	0.25	ion in solution
			2066	−1.5	0.85(C) 3.0 (S)	0.37	0.33	
OCS	1.16	1.56	862	0.4	0.73(O)	0.1	0.6	
			2050	−1.4	0.85(C) 3.0 (S)	0.8	0.5	

nitude. This indicates that, in quantitative respect, the picture should be refined; but so far we do not have any better one. Some obvious improvements, such as multipole interactions and consideration of the finite size of the dipoles, can be shown to be of no avail.

According to the general concepts, the depolarization factor of Raman lines should be computable from the same equation as ρ_{Rayl} but with substitution of A' and B' for A and B, the primes indicating the change of the polarizabilities with the change of the molecular dimensions during the vibration,

$$\rho=6/[7+45(a'/b')^2]. \quad (2)$$

As a mathematical description of this change, we write

$$A'=\sum_{i,k}(\partial F_a/\partial r_{ik})dr_{ik}, \quad B'=\sum_{i,k}(\partial F_b/\partial r_{ik})dr_{ik}, \quad (3)$$

in which the sum is extended over all different distances $r_{ik}=r_{ki}$ and $\partial F/\partial r_{ik}$ is again some function of α_i and r_{ik}, and of $\alpha_i'=\partial\alpha_i/\partial r$. In general, α_i' may be different from zero. For simplification, it may be assumed that α_i is dependent only on those r_{ik}'s which refer to the distances from atom i to its nearest neighbors.

For the evaluation of Eq. (2), we consider the α_i's and the dr_{ik}'s to be known, the α_i's, from Rayleigh scattering data,[7] the dr_{ik}'s from the solution of the vibration equations which give the amplitudes of the atoms or rather their ratios, from which the ratios of the dr_{ik}'s can easily be determined.

We have as many Eqs. (2), with experimentally known values of ρ, as we have different vibrations of the totally symmetric species. Then we try to solve these equations for the unknowns α_i'. This method has some shortcomings which we now discuss.

First, we do not have, in general, enough equations, because the number of totally symmetric vibrations is considerably less than the number of atoms. The number of usable vibrations is still more reduced as the method is applicable to bond-stretching frequencies only. For bond-bending vibrations, all dr_{ik}'s become, in a first approximation, zero, and a'/b' becomes undetermined if we consider only the dr_{ik}'s along which chemical bonds are formed. Therefore, more or less reasonable and arbitrary assumptions must be made such as equality of the α_i''s for some atoms or vanishing of some α_i''s.

Second, Eqs. (2) do not give the sign of a'/b'. This leads to ambiguities. We have adopted, as valid solutions, only those for which all α_i''s are positive. Even with this restriction, we sometimes have some equally reasonable solutions. In order to be reasonable solutions, the α_i''s should not be too large. In our classical picture, α_i is a kind of measure of the atomic volume. Therefore, we should have $(\alpha'/\alpha)dr=(3/R)dR$ if R is the atomic radius. It is reasonable to restrict α' to such values that dR is not larger than the vibrational amplitude of the atom, which, however, is known only as to order of magnitude (about 0.07×10^{-8} cm).

Third, we have the choice of utilizing in the formulas either the r_{ik}-values determined from Rayleigh scattering or the spectroscopic values. The spectroscopic values are very accurate and may, therefore, be preferred as has been done in this paper (in contrast to the previous papers). But the utilization of the scattering values (as far as they are known) is also justifiable because it

[7] See J. Cabannes, *La diffusion moleculaire de la lumière* (Hermann et Cie., Paris, 1929), Chapter V. For a single molecule, only two data are available (depolarization and refraction), giving only two numbers A and B from which at most two α_i's (or one α_i and one r_{ik}) could be found. To overcome this restriction, it is assumed that the atomic polarizability is an additive property.

would mean that we use data obtained in a consistent manner from our system of equations.

Fourth, there are also some uncertainties with regard to the values of α_i (apart, of course, from inaccuracies of the experiments). For instance, different authors[7] have assumed different values for α_C in CO_2. The Rayleigh scattering data are not sufficient to give unambiguous values, and other considerations must furnish the missing data. For instance, the symmetry of the CO_2 molecule makes it plausible to assume (with Havelock) that $\alpha_C=0$. In other molecules, as in OCS, α_C might be different from zero. Indeed, the evaluation of the formulas for these two molecules shows that only a nonvanishing α_C leads to reasonable results for OCS, while $\alpha_C=0$ is possible in CO_2.

Fifth and last, the relative values of the amplitudes which determine the dr_{ik}'s depend on the force system used. But, as is well known, in most cases the force constants cannot be determined uniquely from the observations without some arbitrary though not unplausible assumptions. This refers not only to the force system as such (valence forces or central forces, with or without interactions) but also to the numerical values of the force constants. If it were possible to have some independent means of establishing reliable values for the α''s, we could reverse the procedure and check the force constants and even the molecular structure from the discussion of Raman line depolarization factors.

NUMERICAL RESULTS

The formulas used for A and B are given here for a linear XZY-molecule with r_1=distance XZ, $r_2=YZ$, $r=XY$; α_x, α_y, α_z=polarizabilities of X, Y, Z, respectively. They are obtained[3] by the previously mentioned dipole interaction calculation.

$$A=\frac{1}{N_a}\left\{\alpha_x+\alpha_y+\alpha_z+\frac{4}{r^3}\alpha_x\alpha_y+\frac{4}{r_2^3}\alpha_y\alpha_z+\frac{4}{r_1^3}\alpha_x\alpha_z+\left(\frac{8}{r_1^3r_2^3}+\frac{8}{r^3r_2^3}+\frac{8}{r^3r_1^3}-\frac{4}{r^6}-\frac{4}{r_1^6}-\frac{4}{r_2^6}\right)\alpha_x\alpha_y\alpha_z\right\};$$

$$N_a=1-\frac{4\alpha_x\alpha_y}{r^6}-\frac{4\alpha_y\alpha_z}{r_2^6}-\frac{4\alpha_x\alpha_z}{r_1^6}-\frac{16\alpha_x\alpha_y\alpha_z}{r^3r_1^3r_2^3};$$

$$B=\frac{1}{N_b}\left\{\alpha_x+\alpha_y+\alpha_z-\frac{2}{r^3}\alpha_x\alpha_y-\frac{2}{r_2^3}\alpha_y\alpha_z-\frac{2}{r_1^3}\alpha_x\alpha_z+\left(\frac{2}{r_1^3r_2^3}+\frac{2}{r^3r_2^3}+\frac{2}{r^3r_1^3}-\frac{1}{r^6}-\frac{1}{r_1^6}-\frac{1}{r_2^6}\right)\alpha_x\alpha_y\alpha_z\right\};$$

$$N_b=1-\frac{\alpha_x\alpha_y}{r^6}-\frac{\alpha_y\alpha_z}{r_2^6}-\frac{\alpha_x\alpha_z}{r_1^6}+\frac{2\alpha_x\alpha_y\alpha_z}{r^3r_1^3r_2^3}.$$

The data for the polarizabilities are taken from Cabannes[7] and Havelock.[6] The frequencies, the distances, and the observed depolarization factors are taken from Kohlrausch,[8] where the references to the original papers (mainly by Cabannes and Rousset) can be found. For the distances, the spectroscopic values have been chosen. Only for N_2 and O_2, the scattering data are also utilized for the evaluation in order to give an illustration of the influence of these data on the results. The force system from which the amplitude ratios are derived is a simplified central force system without interactions. N_3 is considered to be symmetric with respect to the forces. For the justification of this assumption, see reference 8. All data are listed in Table I, together with the theoretical ρ-values if the variability of α is disregarded. These values are obviously unsatisfactory. Therefore, the observed ρ-values have been used to calculate the variation of the polarizabilities in accordance with the method described in the previous section.

TABLE II. $\alpha'(10^{-16}$ cm$^3)$.

Molecule \ Atom	N	C	O	S	Remarks
NN	0.75—3.75	...	...	...	$r=1.6$
	3.5	...	...	...	$r=1.1$
OO	...	...	0.6	...	$r=1.5$
	...	...	0.9—1.2	...	$r=1.22$
NO	2.6	...	(2.6)	...	
CO	...	2.6	(2.6)	...	
OCO	...	0	0.45	...	
SCS	...	0	...	1.0	
NNN	2.1—2.6	...	...	...	
NNO	2.3	...	0.8	...	
NCS	0.63	(0.63)	...	5.4	
OCS	...	1.1	2.1	(5.0)	
	...	1.6	(1.6)	8.0	

Table II shows the values of α' computed from the observed depolarization factors and from the other data of Table I. As mentioned before, the method does not always give unique results, so that some assumptions must be made such as $\alpha_N'=\alpha_O'$ in NO and similar in other cases or such as $\alpha_S'=5$ in OCS. These are indicated by parentheses. A — separates equally possible solutions for different signs of a'/b'. All values satisfy the conditions mentioned in the previous section.

It was not possible to find acceptable solutions for NCS or OCS if α_C was assumed to be zero. This was expected. But neither was it possible to find any reasonable solution for molecules with a Cl-atom, as NCCl, probably because of the uncertain value of the polarizability of the Cl-atom in such molecules or because of the impossibility of unambiguously determining three α''s from two equations.

The fact that we obtain reasonable values for α' from the observed depolarization factors means that it is possible to account for the quantitative differences of the depolarization factors of different totally symmetric vibrations by assuming $d\alpha/dr$ to be different from zero.

[8] K. W. F. Kohlrausch, "Ramanspektren," *Hand- u. Jahrb. chem. Physik*, Vol. 9, Part VI, Secs. 23 and 24. For NNO, see W. S. Richardson and E. B. Wilson, Jr., J. Chem. Phys. **18**, 694 (1950).

Thus, the proposed method might open a practicable way of reconciling Silberstein's model and Raman effect data, although it cannot yet be utilized in obtaining unambiguous numerical values for the variation of the atomic polarizabilities. This would be possible only if we would have an independent theory of these variations, yielding, for instance, relations between the α''s of an atom in different molecules.

THE JOURNAL OF CHEMICAL PHYSICS VOLUME 19, NUMBER 8 AUGUST, 1951

Infrared and Mass Spectra of Some Deuterium-Containing Derivatives of Propane

FRANCIS E. CONDON, H. L. McMURRY, AND V. THORNTON
Phillips Petroleum Company, Research Department, Bartlesville, Oklahoma
(Received March 21, 1951)

Infrared and mass spectra of 2-deutero-2-propanol (from acetone and lithium aluminum deuteride), 2-chloro-2-deuteropropane (from 2-deutero-2-propanol and concentrated HCl and $ZnCl_2$), 2,2-dideuteropropane (from 2-chloro-2-deuteropropane via the Grignard reagent and D_2O), and 2-deutero-2-methylpropane (from *t*-butylmagnesium chloride and D_2O) are presented in comparison with the infrared and mass spectra of the corresponding compounds not substituted with deuterium.

IN a continuation of a study of spectra and molecular structure,[1] infrared and mass spectra have been obtained for 2,2-dideuteropropane and 2-deutero-2-methylpropane and for 2-deutero-2-propanol and 2-chloro-2-deuteropropane, intermediates obtained in the synthesis of 2,2-dideuteropropane from acetone by the reactions:

$$1.\ CH_3COCH_3 \xrightarrow[2.\ H_2O,\ HCl]{1.\ LiAlD_4,\ \text{ether}} CH_3CDOHCH_3\ (I)$$

$$2.\ (I) \xrightarrow[\text{mixture distilled}]{ZnCl_2,\ \text{conc. HCl}} CH_3CDClCH_3\ (II)$$

$$3.\ (II) \xrightarrow[2.\ D_2O]{1.\ Mg,\ \text{ether}} CH_3CD_2CH_3\ (III).$$

The heretofore undescribed 2,2-dideuteropropane distilled at −44° at 748 mm Hg and had a vapor pressure of 903 mm Hg at the temperature of melting mercury (where propane, bp −42° at 760 mm Hg, has 878 mm Hg). The over-all yield from 0.7-mole acetone was about 20 percent of theoretical.

The 2-deutero-2-methylpropane was prepared from *t*-butylmagnesium chloride and 99.8 percent deuterium oxide and had a vapor pressure of 1206 mm Hg at the temperature of melting ice (where 2-methylpropane has 1184 mm Hg).

The mass spectra (ion intensities relative to the intensity of the maximum peak as 100) of 2,2-dideuteropropane, 2-deutero-2-methylpropane, 2-deutero-2-propanol (I), and 2-chloro-2-deuteropropane (II) are presented in Table I together with similarly obtained spectra of propane, 1-deuteropropane,[1,2] 2-deuteropropane,[1,2] 2-methylpropane (isobutane), 2-propanol, and 2-chloropropane for comparison; and the infrared spectra of 2-deutero-2-methylpropane, 2-deutero-2-propanol, and 2-chloro-2-deuteropropane are presented in Fig. 1 and in Table II together with the infrared spectra of 2-methylpropane, 2-propanol, and 2-chloropropane for comparison. The infrared spectra of 1-deuteropropane, 2-deuteropropane, and 2,2-dideuteropropane have already been published.[1]

These spectra establish the identity and purity of the deuterium-substituted compounds. Thus the intensity of the mass 45 in the spectrum of 2-deutero-2-propanol indicates not more than 5.2 percent of 2-propanol; and the intensity of the mass 78 in the spectrum of 2-chloro-2-deuteropropane indicates not more than 2 percent of 2-chloropropane. These percentages must be considered as maxima because the pure deuterium-substituted compounds would be expected to yield ions with these masses. The infrared spectrum of 2-deutero-2-propanol indicates 1.5–2.0 percent of 2-propanol; the infrared spectrum of 2-chloro-2-deuteropropane indicates 1.8 percent of 2-chloropropane; the infrared spectrum of 2-deutero-2-methylpropane indicates 4.0 percent of 2-methylpropane. The infrared spectrum of the 2,2-dideuteropropane[1b] indicated less than 0.2 percent of 2-deuteropropane and less than 0.5 percent of propane, the limits of detectability of these compounds. A specimen of 2-deuteropropane obtained as a by-product during the preparation of the Grignard reagent from the 2-chloro-2-deuteropropane gave an infrared spectrum practically identical with the (corrected) spectrum of 2-deuteropropane previously published[1a] and thus provided evidence that the 2-deutero-2-propanol, the 2-chloro-2-deuteropropane, and the 2,2-dideuteropropane were practically free from isomers with deuterium in the "1" position.

The generally high isotopic purity maintained throughout the synthesis of 2,2-dideuteropropane indicates practically no hydrogen interchange under the

[1] a. McMurry, Thornton, and Condon, J. Chem. Phys. **17**, 918 (1949); b. H. L. McMurry and V. Thornton, *ibid.* **18**, 1515 (1950).
[2] Mass spectra of 1-deuteropropane and 2-deuteropropane have been previously published by Turkevich, Friedman, Solomon, and Wrightson, J. Am. Chem. Soc. **70**, 2638 (1948).

TABLE I. Mass spectra (relative ion intensities).[a]

$\frac{M}{e}$	Propane	Propane-1-*d*	Propane-2-*d*	Propane-2,2-d_2	2-Methyl-propane	2-Methyl-propane-2-*d*	2-Pro-panol	2-Pro-panol-2-*d*[b]	2-Chloro-propane	2-Chloro-propane-2-*d*
12	0.1	0.2	0.1	0.1	—	—	0.1	—	0.1	0.1
13	0.2	0.2	0.2	0.1	—	—	0.2	0.1	0.2	0.1
14	0.5	0.6	0.5	0.4	—	0.2	1.0	0.5	0.5	0.3
15	1.9	1.7	1.5	0.9	0.8	0.7	3.7	2.0	1.6	0.8
16	0.1	1.4	0.6	0.7	0.0	0.3	0.2	1.0	0.1	0.3
17	—	—	—	0.2	—	—	0.1	0.2	—	—
18	—	—	—	0 1	—	—	0.3	0.3	—	—
19	1.0	0.9	0.7	0.3	—	—	4.8	2.4	0.3	0.1
19.5	0.5	0.8	0.6	0.6	—	—	0.1	0.1	0.1	0.1
20	1.1	0.9	0.8	0.6	—	—	0.1	2.3	0.2	0.1
20.5	0.3	0.9	0.6	0.6	—	—	0.0	0.1	0.1	0.1
21	—	0.2	0.2	0.4	—	—	—	—	—	—
21.5	—	—	—	0.1	—	—	—	—	—	—
24	0.1	0.1	0.1	0.1	—	—	—	—	0.1	0.1
25	0.4	0.5	0.3	0.2	—	—	0.2	0.1	0.4	0.2
26	5.6	6.0	3.4	1.5	1.1	0.8	1.2	0.6	2.9	1.0
27	32.1	30.0	18.0	8.3	15.4	10.0	9.3	3.8	34.0	9.9
28	59.2	64.1	30.7	24.3	1.2	8.5	2.5	8.1	2.5	20.7
29	100	100	62.6	26.2	4.1	3.8	5.1	3.1	1.5	0.1
30	2.3	73.4	100	62.6	0.1	1.5	0.3	2.6	0.1	0.5
31	—	1.8	2.4	100	—	—	4.5	2.6	0.9	0.1
32	—	—	—	2.3	—	0.2	0.2	1.1	—	0.1
35	—	—	—	—	—	—	—	—	0.5	0.4
36	0.5	0.6	0.5	0.4	?	0.1	0.2	0.1	1.7	1.3
36.5	—	—	—	—	—	—	—	—	—	0.1
37	3.2	3.2	2.6	1.6	?	0.7	0.9	0.6	2.7	1.6
37.5	—	—	—	—	—	—	—	—	—	0.1
38	5.0	5.0	4.1	2.5	1.8	1.4	1.3	0.9	3.7	2.3
39	16.2	13.1	12.5	6.4	10.1	6.5	4.3	2.4	10.6	5.3
40	2.6	12.5	8.7	8.3	1.4	4.9	1.0	2.4	2.5	5.3
41	14.9	7.2	9.3	4.6	33.9	10.6	6.8	2.4	21.5	5.6
42	6.0	16.9	12.3	7.0	35.2	25.0	3.9	5.3	7.3	14.4
43	31.0	8.9	8.2	7.6	100	37.0	19.0	8.0	100	6.0
44	37.0	44.4	23.5	10.8	3.4	100	4.5	7.7	3.6	100
45	1.3	50.1	36.0	6.5	0.1	3.5	100	4.8	0.8	3.5
46		1.8	1.2	42.1	—	—	3.3	100	0.1	—
47				1.5	—	—	0.3	2.5	0.2	0.2
48					—	—	—	0.3	0.2	0.1
49					0.3	0.3	—	—	1.1	0.7
50					0.9	0.6	—	—	0.1	0.4
51					0.7	0.6	—	—	0.4	0.3
52					0.1	0.3	—	—	0.0	0.2
53					0.5	0.4	0.2	0.1	—	0.1
54					0.1	0.3	0.1	0.1	—	0.1
55					0.6	0.3	0.3	0.1	0.1	0.2
56					0.5	0.5	0.2	0.2	0.0	0.2
57					3.9	2.1	0.9	0.6	0.2	0.3
58					3.9	0.5	2.8	0.6	—	0.1
59					0.1	3.0	4.8	2.1	0.3	0.1
60					0.0	0.2	0.8	0.2	0.4	0.2
61							0.1	0.5	0.9	0.6
62									2.8	0.9
63									25.6	2.5
64									1.5	26.2
65									8.3	1.4
66									0.2	9.0
67–77[c]									1.5	1.5
78									23.6	0.5
79									1.0	24.7
80									7.6	1.0
81									0.3	8.0
82										0.4
R[d]	0.713	0.515	0.674[e]	0.632	1.13	1.24	1.09	1.17	0.620	0.747

[a] Obtained on a Westinghouse Type LV mass spectrometer with 75-volt electrons in the ionization chamber, an ion accelerating potential of about 550 volts, a catcher current of 6.5 microamps, and with the ionization chamber at about 210C.

[b] Contained 6.2 weight percent water by determination with Fischer reagent; but the method of sampling for mass spectrometry, vaporization from a frozen sample at low temperature and pressure, may have brought about some reduction in the water content of the sample reaching the ionization chamber.

[c] Sum of relative intensities of all ions with these masses.

[d] R = approximate intensity of maximum peak relative to the intensity of the mass 43 peak in the mass spectrum of *n*-butane obtained under the same conditions.

[e] 0.695 when corrected for 3 percent of propylene found by infrared spectrophotometry. (See reference 1a.)

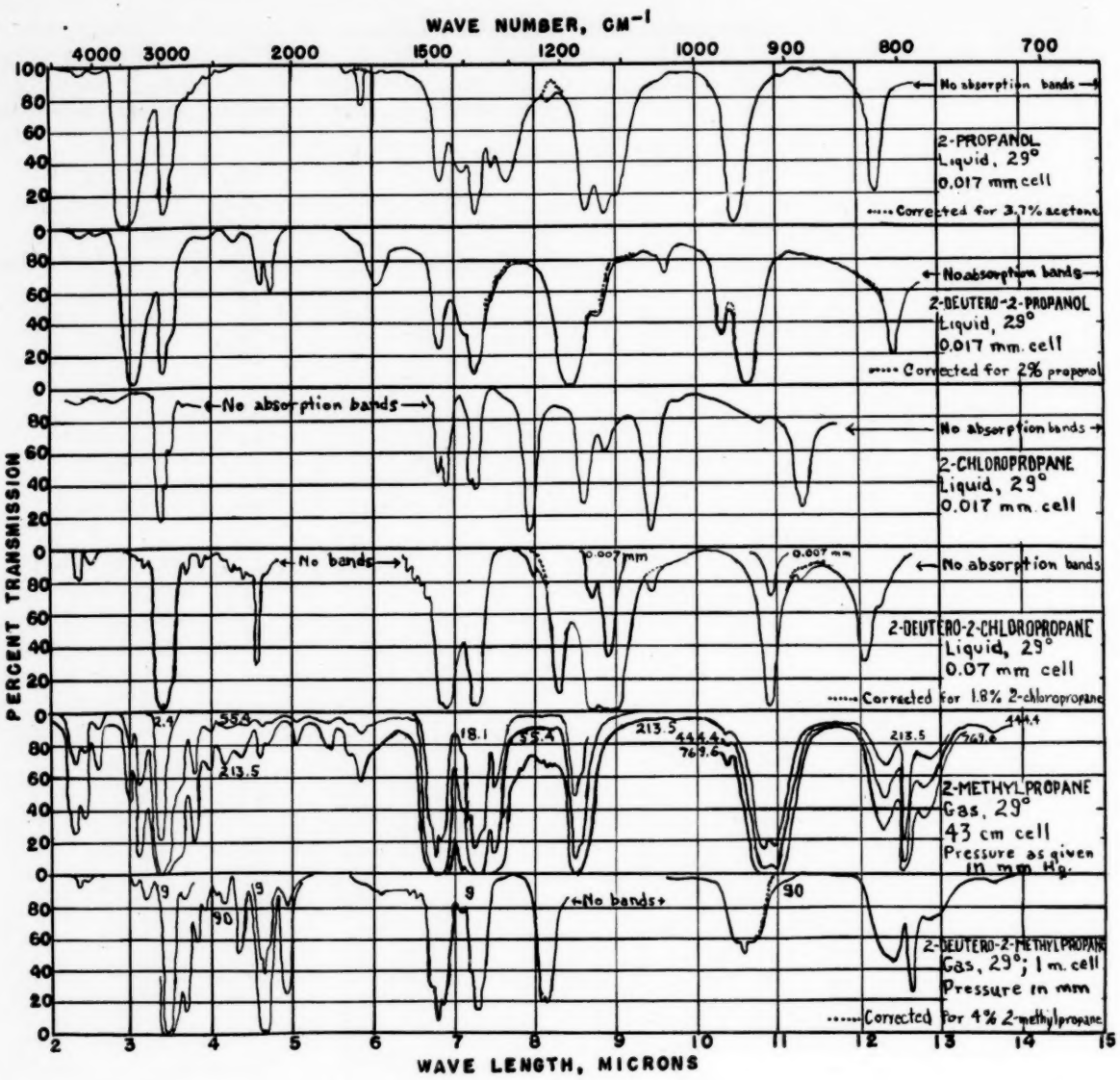

FIG. 1. Infrared absorption spectra.

conditions of the reactions. This is noteworthy expecially for reaction 2, which employed concentrated aqueous HCl and $ZnCl_2$ at temperatures approaching the boiling point of the mixture, acidic conditions resembling those for demonstrated catalytic hydrogen interchange with hydrocarbons.[3]

From the mass spectra of propane and 2,2-dideuteropropane, assuming that the presence of deuterium does not affect the ease of removal of hydrogens from adjacent carbons, and neglecting the small correction for C^{13}, it was calculated that electron impact removes a secondary hydrogen atom and an electron from propane

$$\frac{(31.0)(0.713)-(6.5)(0.632)}{(6.5)(0.632)}\times\frac{6}{2}=13$$

times as readily as a primary hydrogen atom and an electron. Using this factor and a factor of 1.2 for the relative ease of removal of hydrogen attached to carbon bearing a deuterium,[2,4] the relative intensities of the mass 44 peaks in the spectra of 1-deuteropropane and 2-deuteropropane were calculated as 21.7 and 14.9, respectively, in fair agreement with the observed values, $44.4\times0.515=22.9$ and $23.5\times0.674=15.8$, respectively.

Similarly, from the mass spectra of 2-methylpropane and 2-deutero-2-methylpropane, it was calculated that

[3] Ingold, Raisin, and Wilson, J. Chem. Soc. 1643 (1936); A. Farkas and L. Farkas, Ind. Eng. Chem. **34**, 716 (1942); T. M. Powell and E. B. Reid, J. Am. Chem. Soc. **67**, 1020 (1945); T. D. Stewart and D. Harman, *ibid.* **68**, 1135 (1946); Beeck, Otvos, Stevenson, and Wagner, J. Chem. Phys. **17**, 418 (1949).

[4] Evans, Bauer, and Beach, J. Chem. Phys. **14**, 701 (1946).

TABLE II. Infrared spectra.[a]

2-propanol			2-deutero-2-propanol			2-chloropropane			2-deutero-2-chloropropane			2-methylpropane			2-deutero-2-methylpropane		
ν (cm^{-1})	$\lambda(\mu)$	I[b]	ν (cm^{-1})	$\lambda(\mu)$	I[b]	ν (cm^{-1})	$\lambda(\mu)$	I[b]	ν (cm^{-1})	$\lambda(\mu)$	I[b]	ν (cm^{-1})	$\lambda(\mu)$	I[c]	ν (cm^{-1})	$\lambda(\mu)$	I[c]
816.3	12.25	m	803.2	12.45	m	886.5	11.28	m	815.0	12.27	w	781.3	12.80	w	777.6	12.86	w
953.3	10.49	s	939.0	10.65	s	930.2	10.75	w	829.9	12.05	m	796.8	12.55	w	792.4	12.62	w
1110	9.01	s	968.1	10.33	m	1028	9.73	w	917.4	10.90	s	812.2	12.31	w	807.1	12.39	w
1131	8.84	s	1041	9.61	m	1060	9.43	s	1124	8.90	s	913.1	10.95	w	940.7	10.63	w
1161	8.61	s	1136	8.80	m	1130	8.85	m	1152	8.68	s	925.8	10.80	w	947.0	10.56	w
1307	7.65	m	1183	8.45	s	1161	8.61	m	1208	8.28	m	964.3	10.37	w	956.0	10.46	w
1339	7.47	m	1304	7.67	w	1259	7.94	s	1389	7.20	m	1167	8.57	w	1229	8.14	w
1379	7.25	s	1332	7.51	w	1374	7.28	m	1376	7.27	m	1337	7.48	w	1239	8.07	w
1406	7.11	m	1376	7.27	s	1389	7.20	m	1453	6.88	s	1384	7.23	m	1374	7.28	m
1466	6.82	m	1397	7.16	m	1449	6.90	m	1471	6.80	m	1396	7.16	w	1383	7.23	w
1626	6.15	w	1464	6.83	m	1468	6.81	m	1508	6.63	w	1465	6.82	m	1393	7.18	w
1656	6.04	w	2110	4.74	m	1490	6.71	w	1522	6.57	w	1475	6.76	m	1410	7.09	w
1767	5.66	m	2174	4.60	m	2732	3.66	w	1541	6.49	w	1719	5.82	w	1460	6.85	m
2160	4.63	w	2342	4.27	w	2865	3.49	m	1563	6.40	w	1767	5.66	w	1475	6.78	m
2532	3.95	w	2545	3.93	w	2915	3.43	m	2155	4.64	m	1835	5.45	w	1490	6.71	m
2660	3.76	w	2857	3.50	m	2967	3.37	s	2198	4.55	w	1859	5.38	w	1504	6.65	w
2717	3.68	w	2959	3.38	s	3571	2.80	w	2252	4.44	w	1993	5.02	w	1536	6.51	w
2857	3.50	s	3322	3.01	s	3676	2.72	w	2294	4.36	w	2132	4.69	w	1555	6.43	w
2941	3.40	s	3953	2.53	w	3817	2.62	w	2342	4.27	w	2185	4.58	w	1653	6.05	w
3401[d]	2.94[d]	s	4255	2.35	w	4098	2.44	w	2364	4.23	w	2294	4.36	w	2033	4.92	w
3937	2.54	w				4292	2.33	w	2427	4.12	w	2410	4.15	w	2151	4.65	w
4237	2.36	w							2551	3.92	w	2519	3.97	w	2309	4.33	w
									2597	3.85	w	2646	3.78	w	2415	4.14	w
									2725	3.67	w	2740	3.61	w	2475	4.04	w
									2924	3.42	s	2962	3.37	s	2558	3.91	w
									2967	3.37	s	3209	3.11	w	2632	3.80	w
									3185	3.14	w	3338	2.99	w	2725	3.67	w
									3257	3.07	w	3837	2.60	w	2874	3.48	s
									3356	2.98	w	4105	2.43	w	2907	3.44	s
									4065	2.46	w	4318	2.31	w	3145	3.18	w
									4292	2.33	w				3289	3.04	w
									4367	2.29	w				4098	2.44	w
															4255	2.35	w

[a] Obtained with a Perkin-Elmer Model 12-B with G-M amplifier and Speedomax-G recorder.
[b] $I = 1/t \log(1/T)$, where T is the transmission and t is the cell thickness in mm. For strong (s) bands, $I > 60$; for medium (m) bands, $60 > I > 6$; and for weak (w) bands, $I < 6$.
[c] $I = 1/pl \log(1/T)$, where T is the transmission, p is the pressure in mm Hg, and l is the cell length in cm. For strong (s) bands, $I > 0.002$; for medium (m) bands, $0.002 > I > 0.001$; and for weak (w) bands, $I < 0.001$.
[d] Approximate.

electron impact removes a tertiary hydrogen atom and an electron

$$\frac{(3.9)(1.13)-(0.5)(1.24)}{(0.5)(1.24)} \times 9 = 55$$

times as readily as a primary hydrogen and an electron.

Comparison of the intensity of the mass 28 peak in the spectrum of propane with the intensity of the mass 30 peak in the spectrum of 2,2-dideuteropropane, and of the intensity of the mass 42 peak in the spectrum of 2-methylpropane with the intensity of the mass 43 peak in the spectrum of 2-deutero-2-methylpropane indicates that most of the ions resulting from loss of a methyl radical, a hydrogen atom, and an electron have an olefinic structure rather than an alkylidene structure.[5]

A detailed analysis of the infrared spectra is beyond the scope of this paper.

ACKNOWLEDGMENTS

Dr. E. E. Burgoyne assisted with the chemical syntheses. Miss Nora Potts plotted the infrared spectra. Messrs. T. D. Morgan and H. W. Rollmann obtained the mass spectra. Phillips Petroleum Company granted permission to publish the data.

[5] See D. P. Stevenson and J. A. Hipple, Jr., J. Am. Chem. Soc. **64**, 1588 (1942).

The Infrared Spectra of Propane and Its Symmetrical Deuterium Substituted Analogs

H. L. McMURRY AND V. THORNTON
Phillips Petroleum Company, Research and Development Department, Research Division, Bartlesville, Oklahoma

(Received January 29, 1951)

The infrared spectra of 2,2-dideuteropropane, 1,1,1,3,3,3-hexadeuteropropane, and octadeuteropropane are presented, together with that of propane for comparison. Complete assignments are proposed for the frequencies of the vibrations belonging to species A_1 and B_1, and partial assignments for the vibrations belonging to species B_2, in these molecules. They show that some low frequency vibrations (below 1350 cm^{-1}) in the deuterium substituted molecules cannot be described adequately in terms of simple group motions. The results suggest that this is true also for the corresponding vibrations in propane.

I. INTRODUCTION

THE vibrational frequencies below 1350 cm^{-1} in paraffin hydrocarbons are conveniently described in terms of group motions which are rocking motions of the CH_3 and CH_2 groups, vibrations of the carbon skeleton, etc. The impression is often left, however, that any given spectral frequency can be assigned uniquely to a single such group motion.[1] In a recent study of the spectra of propane and 2,2-dideuteropropane[2] it was concluded that this is not a realistic way to describe the low frequency vibrations of species B_1 in propane, but rather mixtures of CH_3 and CH_2 rocking motions and the unsymmetrical skeletal stretching motion must be considered.

This paper presents new spectral data for 1,1,1,3,3,3-hexadeuteropropane and octadeuteropropane, together with additional spectral data for 2,2-dideuteropropane and spectral data for propane (for comparison).

II. THE SPECTRA

The spectral data for propane is the same as that reported previously[3] and is from a sample of Phillips Research Grade certified by the N.B.S. to be 99.99 mole percent pure.

The 2,2-dideuteropropane was prepared in this laboratory by F. E. Condon.[4] Acetone was reacted with lithium aluminum deuteride to give 2-deuteropropanol, this product was reacted with zinc chloride to give 2-deutero-2-chloropropane, and then the Grignard reaction with D_2O was used to give the final product. The infrared spectrum of this material showed less than detectable amounts of 1-deuteropropane, 2-deuteropropane, and propane (less than one percent on any one). A specimen of 2-deuteropropane obtained as a by-product during the preparation of the Grignard reagent from 2-chloro-2-deuteropropane gave an infrared spectrum practically identical with the (corrected) spectrum of 2-deuteropropane in reference 3, and thus provided evidence that the dideuteropropane was practically free of isomers in the "1" position. It is felt that the purity is of the order of 98 percent. The simplicity of the spectrum (Fig. 1) is consistent with a high purity.

Details as to the preparations and purities of the 1,1,1,3,3,3-hexadeuteropropane and octadeuteropropane will be given elsewhere.[5] Mainly on the basis of mass spectral data[6] the hexadeuteropropane is believed to be 80 percent 1,1,1,3,3,3-hexadeuteropropane, and the octadeuteropropane 90 percent C_3D_8. The impurities are mainly isomers of $C_3H_3D_5$ and C_3HD_7 in the hexadeuteropropane and octadeuteropropane, respectively, but small amounts of the less deuterated compounds may be present in each sample.

Spectral Data

The infrared spectra between 2 and 15 microns for these materials in the gas phase are shown in Fig. 1. A Perkin Elmer Model 12B spectrometer equipped with a rocksalt prism, General Motors Amplifier, and Speedomax *G* recorder was used. Table I lists the band positions and intensities given as maximum extinction per unit concentration (in moles/cc) per unit path length (in centimeters) for the deuterated compounds. Similar data are given for propane in reference 3.

The spectrum of another sample of 1,1,1,3,3,3-hexadeuteropropane of lower purity (on the basis of its mass spectrum 73 percent 1,1,1,3,3,3-hexadeuteropropane) was available for comparison with that in Fig. 1. Only in the region of absorption around 710 cm^{-1} were there detectable differences in band structures, and the measured intensities of the other bands gave no conclusive evidence as to which of the bands in Fig. 1 may be due to impurities. A possible reason for this is that the most likely impurity, $CHD_2CH_2CD_3$ (on the basis of preparation method and the mass spectrum),[5] might have a spectrum closely resembling that of 1,1,1,3,3,3-hexadeuteropropane. The analysis in this report assumes that the 1,1,1,3,3,3-hexadeuteropropane

[1] See N. Sheppard, J. Chem. Phys. **16**, 690 (1948). Sheppard's terms "wagging," "rocking," and "twisting" are all termed "rocking" in the present work, the type of motion involved being clear from its symmetry species.
[2] H. L. McMurry and V. Thornton, J. Chem. Phys. **18**, 1515 (1950).
[3] McMurry, Thornton, and Condon, J. Chem. Phys. **17**, 918 (1949).
[4] F. E. Condon, unpublished work.
[5] F. E. Condon, to be published.
[6] H. W. Rollman and H. L. McMurry, (to be published).

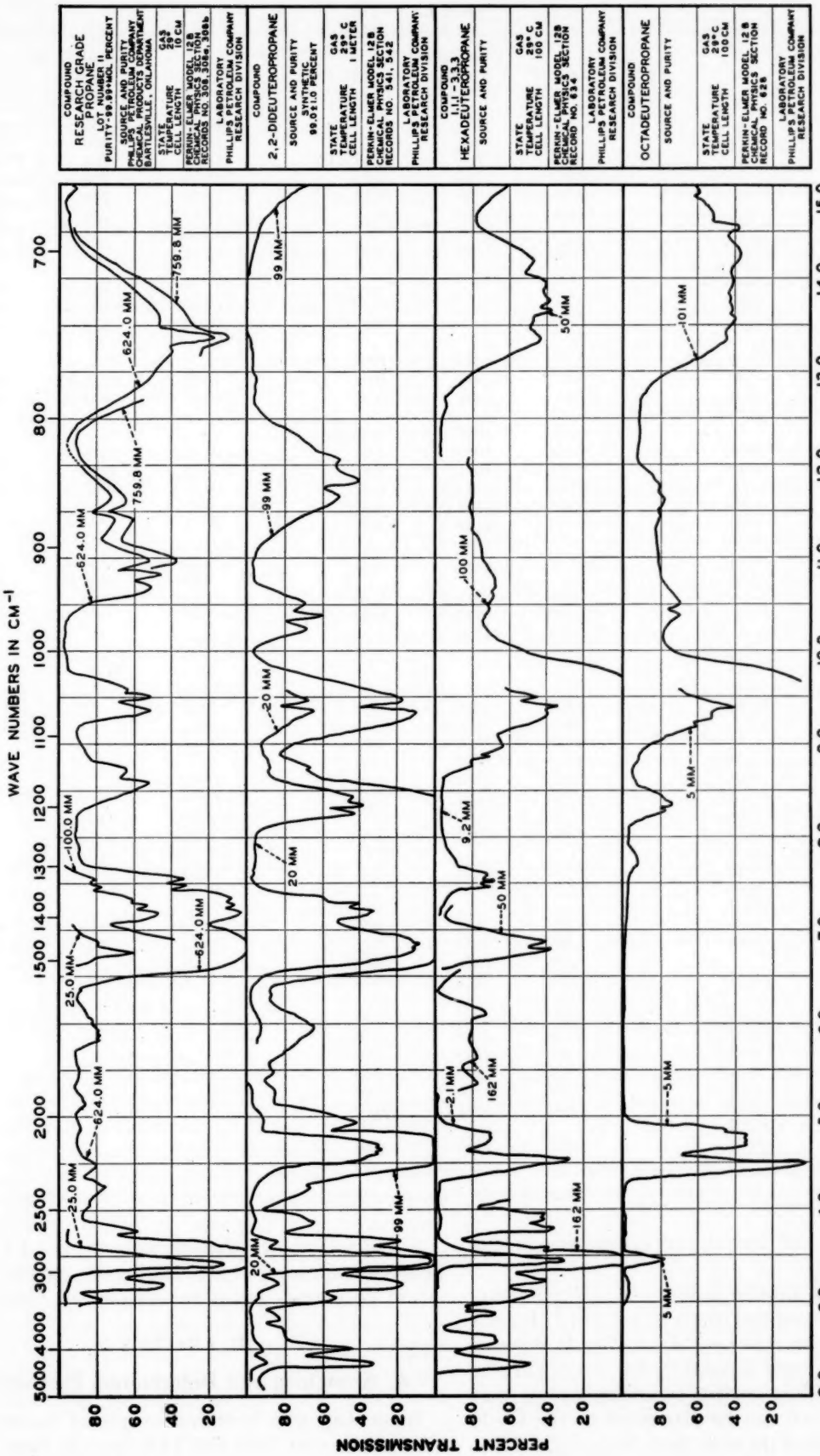

FIG. 1. Infrared spectra of propane, 2,2-dideuteropropane, 1,1,1,3,3,3-hexadeuteropropane, and octadeuteropropane.

TABLE I.

$CH_3CD_2CH_3$ (λ)	$CH_3CD_2CH_3$ (cm^{-1})	I[a]	$CD_3CH_2CD_3$ (λ)	$CD_3CH_2CD_3$ (cm^{-1})	I[a]	$CD_3CD_2CD_3$ (λ)	$CD_3CD_2CD_3$ (cm^{-1})	I[a]
						14.92	670	0.04×10^4
						14.64	683	0.05
						14.53	688	0.08
			14.19	705	0.13×10^4	14.23	703	0.08
			13.94	718	0.15	13.96	716	0.07
			13.78	726	0.15	13.78	726	0.07
			13.67	732	0.17	13.67	732	0.07
						13.56	738	0.08
			13.34	750	0.14	13.31	751	0.07
12.060	829.2	0.06×10^4						
11.840	844.6	0.08				11.75	851	0.02
11.663	857.5 *P*	0.06				11.62	860	0.02
						11.43	875	0.02
			10.70	935	0.03			
10.525	950.1 *R*	0.03	10.59	944	0.03	10.52	951 *R*	0.03
10.375	963.8 *Q*	0.04	10.44	958	0.03	10.37	965 *P*	0.03
10.226	978.0 *P*	0.03						
			9.506	1052	0.68			
9.473	1055.6 *R*	0.17	9.406	1063	1.0	9.381	1016	1.5
9.356	1068.8 *P*	0.19	9.340	1071	0.85	9.273	1018	1.1
			8.984	1113 *R*	0.41	9.172	1090	0.84
			8.858	1129 *Q*	0.31			
8.786	1138	0.06	8.771	1139 *P*	0.21			
8.434	1186 *R*	0.36						
8.342	1199 *Q*	0.41				8.333	1200 *Q*?	0.53
8.259	1211 *P*	0.36				8.278	1208 *P*?	0.42
			7.586	1318 *R*	0.29	7.686	1300	0.15
			7.538	1327 *Q*	0.33			
			7.474	1338 *P*	0.33			
7.314	1367	shoulder						
7.281	1373	0.38						
7.216	1386	0.47						
6.882	1453	0.89	6.870	1456 *R*	0.15			
6.847	1460	1.2	6.801	1470 *P*	0.16			
6.790	1473	0.95	6.212	1616	0.02			
5.965	1677	0.04	5.952	1680	0.01			
5.473	1827	0.01	5.613	1782	0.01			
5.266	1899	0.01	5.340	1873	0.01			
4.929	2029	0.08				4.836	2068	1.3
4.690	2132	0.52	4.788	2089	1.4	4.788	2089	1.8
4.643	2154	0.55				4.707	2124	1.8
4.594	2177	0.50	4.530	2208	5.0	4.674	2139	1.8
4.546	2200	0.41				4.480	2232	5.5
4.237	2360	0.03						
3.906	2560	0.03	3.942	2535	0.05	3.440	2930	0.45
3.848	2599	0.04	3.896	2573	0.05	3.14	3180	0.10
			3.778	2647	0.06			
3.652	2738	0.15	3.558	2811	0.05			
3.423	2921	vs	3.442	2905	4.8			
3.186	3138	0.15	3.186	3138	0.05			
3.041	3288	0.05	3.106	3219	0.04			
			2.936	3406	0.01			
2.811	3557	0.02	2.852	3506	0.02			
2.686	3723	0.02	2.603	3842	0.02			
2.499	4002	0.07						
2.336	4281	0.08	2.326	4318	0.04			

[a] The intensities (I) are expressed as maximum extinction per mole per cc per cm of absorbing path. Extinctions are not corrected for stray radiation which was less than two percent at all wavelengths.

contributes to all of the absorption regions in the spectrum of Fig. 1.

The spectrum of another sample of C_3D_8 containing (according to its mass spectrum) 87 percent C_3D_8 was nearly identical with that for C_3D_8 in Fig. 1. It seems evident that C_3D_8 must account for the major parts of the strong absorptions in this spectrum, except that at 2900 cm^{-1}, which can be attributed to the C—H stretching vibration of the most likely impurity, C_3HD_7.

For brevity the 2,2-dideuteropropane and 1,1,1,3,3,3-hexadeuteropropane will hereafter be referred to as symm. propane-d_2 and symm. propane-d_6, respectively.

III. ANALYSIS

A. Stretching and Deformation Frequencies

By analogy with hydrocarbon spectra the unresolved absorptions near 2900 and 1460 cm^{-1} in these spectra

may be attributed to stretching and unsymmetrical deformation vibrations, respectively, within the CH_3 and CH_2 groups, and the absorptions at 1380 cm^{-1} to symmetrical CH_3 deformation vibrations. Table II lists assignments for these and other frequencies in these molecules.

The assignments in Table II for the C−D stretching frequencies assume that the unsymmetrical CD_3 stretching vibrations have higher frequencies than the symmetrical. This is consistent with the assignments[7] for C_2D_6.

In C_2D_6 the CD_3 deformation vibrations have been assigned[7] frequencies between 1055 and 1158 cm^{-1}.

TABLE II. Vibrational assignments for propanes.

Symmetry	Description[a,b]	Frequency (cm^{-1})[d] C_3H_8	$C_3H_6D_2$	$C_3H_2D_6$	C_3D_8
A_1	$CH_3(CD_3)$ u. st.	2940	2920	(2210)	(2230)
	$CH_3(CD_3)$ sy. st.	2940	2920	2090	2120
	$CH_2(CD_2)$ sy. st.	2940	(2160)	2905	(2120)
	$CH_3(CD_3)$ u. def.	(1460)	(1460)	(1070)	(1070)
	$CH_2(CD_2)$ sy. def.	(1460)	1062	1463	(1070)
	$CH_3(CD_3)$ sy. def.	(1380)	(1380)	(1070)	(1070)
	$CH_3(CD_3)$ r., C_3 sy. st.	1155	1130	940	958
	$CH_3(CD_3)$ r., C_3 sy. st.	870	(850)	(720)	(720)
	C_3 sy. def.	372	370[p]	350[p]	340[p]
B_1	$CH_3(CD_3)$ u. st.	2940	2920	(2210)	(2230)
	$CH_3(CD_3)$ sy. st.	2940	2920	2090	2120
	$CH_3(CD_3)$ u. def.	(1460)	(1460)	1140[c]	(1070)
	$CH_3(CD_3)$ sy. def.	(1380)	(1380)	(1070)	(1070)
	$CH_2(CD_2)$ r., C_3 u. st.	1336	1199	1327	1200
	$CH_2(CD_2)$ r., C_3 u. st.	1053	964	940	860
	$CH_3(CD_3)$ r.	923	(850)	680[p]	650[p]
B_2	$CH_3(CD_3)$ u. st.	2940	2920	(2210)	(2230)
	$CH_2(CD_2)$ u. st.	2940	(2160)	2905	(2120)
	$CH_3(CD_3)$ u. def.	1478[c]	(1460)	(1070)	(1070)
	$CH_3(CD_3)$ r.	—	—	—	—
	$CH_2(CD_2)$ r.	748	(720)	<670	<670
	$CH_3(CD_3)$ r.	<670	<670	<670	<670

[a] The abbreviations u. st., sy. st., u. def., sy. def., denote vibrations which are unsymmetrical stretching, symmetrical stretching, unsymmetrical deformation, and symmetrical deformation, respectively, within the groups indicated. The letter r denotes a vibration involving a rocking motion of the indicated group. The descriptions are only qualitative.
[b] Table I of reference 3 suggests more detailed forms for some of these modes.
[c] This is the position of the Q branch in this region.
[d] Values in parentheses are near the centers of absorption regions.
[p] Predicted from the product rule.

On this basis the absorptions near 1070 cm^{-1} in the spectra of the symm. propane-d_6 and propane-d_8, and the band with a Q branch at 1130 cm^{-1} in the symm. propane-d_6 spectrum, have been assigned to vibrations involving CD_3 deformations. In particular, the 1130 cm^{-1} frequency in symm. propane-d_6 has been assigned to a vibration belonging to species B_1 and involving unsymmetrical CD_3 deformations. This choice was by analogy with hydrocarbons in which the unsymmetrical CH_3 deformations come at higher frequencies (near 1460 cm^{-1}) than the symmetrical (near 1380 cm^{-1}). However, some assignments for C_2D_6 are in violation of this rule[7] and the 1130 cm^{-1} frequency may involve symmetrical CD_3 deformations.

[7] G. Herzberg *Infrared and Raman Spectra* (D. Van Nostrand Company, Inc., New York, 1945), p. 344.

TABLE III. Ratios predicted from the Teller-Redlich equation.[a]

Modes involved	π_1	π_2	π_3
A_1	0.51	0.19	0.10
A_2	0.72	0.29	0.21
B_1	0.74	0.21	0.16
B_2	0.58	0.32	0.17

[a] Under π_1 are listed, for each species, the ratios predicted from the Teller-Redlich equation for the products of the propane frequencies to the products of the symm. propane-d_2 frequencies. Similarly, under π_2, π_3, are given the corresponding ratios for propane and symm. propane-d_6, and propane-d_8, respectively.

The band at 1062 cm^{-1} in the symm. propane-d_2 spectrum must involve the CD_2 deformation. This band in clearly resolved and has the proper shape.[3]

B. Skeletal and Rocking Frequencies

1. General

The stretching and deformation vibrations account for thirteen $(6A_1+4B_1+3B_2)$ of the infrared active vibrations (assuming C_{2v} symmetry) in each of these molecules. Nine infrared active vibrations $(3A_1+3B_1+3B_2)$ remain to be assigned. Assuming they do not interact with the stretching and deformation vibrations, they may be described in terms of motions of the carbon skeleton and rocking motions of the CH_3 (or CD_3) and CH_2 (or CD_2) groups. In what follows, the Teller-Redlich product rule[8] will be used in establishing assignments for these frequencies. Ratios calculated using this rule for the products of the frequencies for each species in propane to the corresponding frequency products in symm. propane-d_2, symm. propane-d_6, and propane-d_8 are shown in Table III, where they are listed under π_1, π_2, π_3, respectively. The moments of inertia used in calculating these ratios are shown in Table IV.

2. The Three Vibrations Belonging to Species A_1.

In propane these vibrations have the frequencies 1155(?), 870, and 375 cm^{-1}.

The weak bands at 1140, 940, and 958 cm^{-1} in the spectra of symm. propane-d_2, symm. propane-d_6, and propane-d_8, respectively, have been taken to be the analogs of the 1155 cm^{-1} propane frequency. Of these only the band at 958 cm^{-1} in the propane-d_8 spectrum

TABLE IV. Moments of inertia of the propanes.[a]

	x	y	z
$CH_3CH_2CH_3$	67.6	17.3	59.6
$CH_3CD_2CH_3$	70.4	21.9	61.3
$CD_3CH_2CD_3$	86.9	24.0	78.9
$CD_3CD_2CD_3$	90.1	28.7	80.5

[a] The z axis is the symmetry axis. The x and y axes are principal axes normal to the z axis, and normal to the plane of the carbons and in this plane, respectively. The units are atomic weight times angstroms squared. The C−C and C−H (or C−D) distances are 1.54 and 1.09A, respectively. All angles are tetrahedral except the C−C−C angle, which is 111°30′ (see Pitzer, J. Chem. Phys. 12, 310 (1944)).

[8] See reference 7, p. 232.

is clearly resolved. The others appear to have comparable intensities and their relative positions can be explained if the CH_3 (or CD_3) rocking motions contribute to these vibrations.

The analogs to the 870 cm^{-1} propane frequency are taken to be 850, 720, and 720 cm^{-1} in symm. propane-d_2, symm. propane-d_6, and propane-d_8, respectively. The choice is clear for symm. propane-d_2. The 720 cm^{-1} frequency for the other molecules could not be much higher if the associated bands have appreciable intensities.

When the above analogs of the 1155 and 870 cm^{-1} propane frequencies are used in the product rule, the frequencies 370, 350, and 340 cm^{-1} are predicted for the skeletal deformation frequencies of the symm. propane-d_2, symm. propane-d_6, and propane-d_8, respectively. These are very reasonable in comparison with the 375 cm^{-1} frequency for propane. No other equally plausible assignments for these vibrations could be found.

3. The Three Vibrations Belonging to Species B_1.

In propane these frequencies are 1336, 1053, and 923 cm^{-1}. Their analogs in symm. propane-d_2 have been assigned unambiguously (see reference 2 and Table II).

The analogs to the 1336 cm^{-1} frequency clearly come at 1327 and 1200 cm^{-1} in symm. propane-d_6 and propane-d_8, respectively.

The analogs to the others are less clear. If it is assumed that parts of the absorptions with comparable intensities at 940 and 860 cm^{-1} in the symm. propane-d_6 and propane-d_8 spectra, respectively, are the analogs to the 1053 cm^{-1} band in the propane spectrum, the product rule predicts the frequencies 680 and 650 cm^{-1}, respectively, for the remaining frequencies. There is evidence of a band just below 670 cm^{-1} in the symm. propane-d_6 spectrum.

4. The Three Vibrations Belonging to Species B_2.

One of these frequencies in propane, and two in each of the other molecules, are too low for detection with a rocksalt prism. Therefore, the product rule is of limited value. Only partial assignments for the frequencies of these modes are given in Table II.

IV. DISCUSSION

One object of the present work was to determine if the low frequency vibrations in propane could be classified simply as follows:

1. Vibrations involving only rocking motions of the CH_3 groups.
2. Vibrations involving only rocking motions of the CH_2 group.
3. Vibrations in which the groups move as mass points.

The validity of this classification can be tested for the vibrations of species A_1 and B_1. In both cases it fails. For the A_1 vibrations the substitution of CD_3 for CH_3 reduces the two higher frequencies by about the same ratio from their values in propane (1155, 870 cm^{-1}). This would hardly be expected if one pair of analogs involved only group rocking motions and the other pair skeletal stretching motions. Similarly, for the frequencies of the B_1 vibrations the substitution of CD_2 for CH_2 in $CH_3CD_2CH_3$ reduces all three frequencies from their propane values (1336, 1053, 923 cm^{-1}) by about the same ratio (0.90). This would not be expected if simple group motions adequately described these vibrations in both molecules.

It seems evident from this that the rocking motions of different groups must interact with each other and with the skeletal stretching motions to produce vibrations which are mixtures of these motions. Possibly the magnitude of these interactions increases with the ratio X/C (X is mass of the H or D atom and C the mass of the carbon atom) and is more important for the deuterated molecules than the undeuterated.

Some of the assignments in Table II are open to question, but it does not seem possible to choose any set which would alter the conclusion that simple group motions are inadequate to describe the low frequency vibrations in the deuterated compounds and possibly also in propane. A theoretical analysis aimed at describing the low frequency vibrations in these molecules as mixtures of group motions might, if used with the present data, answer the question as to the importance of these interactions in propane.

Contribution to the Theory of Critical Phenomena

BRUNO H. ZIMM*
Department of Chemistry, Harvard University, Cambridge, Massachusetts
(Received April 18, 1951)

If one considers the critical point between the liquid and gaseous phases, it may be shown that the "principle of superposition" leads to the result that the critical point is a singularity in the isotherm of fugacity or pressure against density. At this singularity the derivatives of every order of the fugacity or pressure with respect to the density are zero, not only the first two derivatives as in the van der Waals theory. It is postulated that these relations are true despite the uncertain nature of the superposition approximation.

If the critical point is such a singular point, it can be shown that Mayer's theory of critical phenomena leads quite reasonably to a single characteristic temperature instead of two separate temperatures for the vanishing of the slope of the isotherm and for the appearance of a surface tension. Experimental observations on the anomalous shape of the isotherms near the critical point are in accord with the theory.

THE exact nature of the critical point between liquid and gas does not yet seem to be established. Certainly the classical ideas based on the theory of van der Waals have never been demonstrated to represent the true state of affairs beyond question. The much more penetrating general theory of Mayer and co-workers,[1] strongly suggests the existence of a critical region between two characteristic temperatures instead of the single critical point of the classical theory. However, the only rigorous study of a special case, the two-dimensional Ising lattice as treated by Onsager and Kaufman,[2] shows a single critical temperature. There is also experimental evidence against the existence of two temperatures.[3] On the other hand, the experiments of Maass and co-workers[4] show some otherwise unexplained phenomena that have been interpreted in terms of Mayer's theory. In this connection see also a discussion by Rice[5] and a recent review by Hildebrand and Scott.[6]

By applying some simplifying assumptions to the general equations that Mayer developed,[1] we have encountered what seems to be a new property of the critical point. Our simplified equations give a critical point that is a peculiar kind of singularity in the function-theoretical sense. There is evidence that real critical points are the same kind of singularity. This result is especially interesting in that the interpretation of Mayer's theory seems to be altered so that a critical region with two characteristic temperatures is no longer necessary.

For simplicity we will consider only the liquid-vapor critical point of a one-component system, but the principal features of the results can be shown to apply also to some other types of critical points.

THE DERIVATIVES OF THE FUGACITY NEAR A CRITICAL POINT

The simplest relations seem to appear when we express the state of the system in terms of the fugacity, z, and the density, ρ, measured in numbers of molecules per unit volume. The fugacity is defined as

$$z=z_0 \exp(\mu/kT), \tag{1}$$

where μ is the chemical potential, k Boltzmann's constant, T the absolute temperature, and z_0 is such a constant that z approaches ρ as ρ is made to approach zero. We will also use the function $\varphi=p/kT$, where p is the pressure.

Mayer[7] has derived the following general formula for the nth derivative of φ with respect to z:

$$d^n\varphi/dz^n=n!\, b_n(z)(\rho/z)^n. \tag{2}$$

This formula is based on the grand partition function of Gibbs; its derivation should be valid except at a singularity of φ or z. To keep away from possible singularities, we will confine our initial investigations to a region of temperature slightly above the critical point where empirical information makes it seem improbable that there are singularities. The quantities $b_n(z)$ are so-called "cluster integrals" of distribution functions of n molecules as defined in Mayer's paper.[5] They are to be evaluated using the distribution functions appropriate to the system at fugacity z. In this respect they are to be distinguished from the cluster integrals employed in the original condensation theory.[1] For brevity we will omit the z hereafter, writing merely b_n.

We wish to find the derivatives of z with respect to ρ in terms of the cluster integrals. To do this we find it convenient to find first the derivatives of ρ with

* Visiting Lecturer at Harvard University during 1950–1951. Present address: Research Laboratory of the General Electric Company, Schenectady, New York.

[1] J. E. Mayer, J. Chem. Phys. **5**, 67 (1937); J. E. Mayer and S. F. Harrison, *ibid.* **6**, 87, 101 (1938); W. G. McMillan and J. E. Mayer, *ibid.* **13**, 276 (1945).

[2] L. Onsager, Phys. Rev. **65**, 117 (1944); B. Kaufman, *ibid.* **76**, 1232 (1949); B. Kaufman and L. Onsager, *ibid.* **76**, 1244 (1949).

[3] B. H. Zimm, J. Phys. and Colloid Chem. **54**, 1306 (1950).

[4] Tapp, Steacie, and Maass, Can. J. Research **9**, 217 (1933); S. N. Naldrett and O. Maass, *ibid.* **B18**, 118 (1940); S. G. Mason and O. Maass, *ibid.* **B26**, 592 (1948).

[5] O. K. Rice, J. Chem. Phys. **15**, 314 (1947); Chem. Revs. **44**, 69 (1949); J. Phys. and Colloid Chem. **54**, 1293 (1950).

[6] J. H. Hildebrand and R. L. Scott, *Solubility of Nonelectrolytes* (Reinhold Publishing Corporation, New York, 1950); *Annual Review of Physical Chemistry* (Annual Reviews, Inc., Stanford, California, 1950), Vol. I.

[7] J. E. Mayer, J. Chem. Phys. **10**, 629 (1942), Eq. (45).

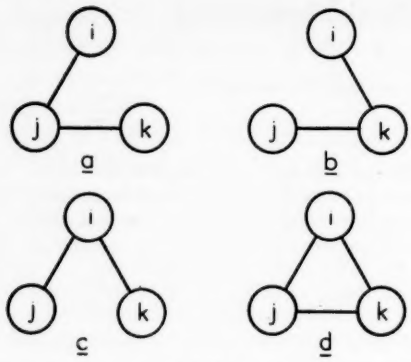

FIG. 1. "Bond figures" for the cluster integral b_3.

respect to z. The first cluster integral, $b_1(z)$, is identically unity. Hence, from Eq. (2), we get

$$d\varphi/dz=\rho/z, \tag{3a}$$

$$d^n\varphi/dz^n=d^{n-1}(\rho/z)/dz^{n-1}=n!\,b_n(\rho/z)^n. \tag{3b}$$

Solving this set of equations yields formulas for $d^n\rho/dz^n$:

$$d^n\rho/dz^n=(n+1)!\,b_{n+1}z(\rho/z)^{n+1}+n\cdot n!\,b_n(\rho/z)^n. \tag{4}$$

Before proceeding it is convenient to introduce a simplifying approximation. We shall show later that near the critical point $b_{n+1}\rho$ is much greater than b_n. Hence, we may ignore the last term of each of the equations in Eq. (4) and write simply

$$d^n\rho/dz^n=(n+1)!\,b_{n+1}z(\rho/z)^{n+1}. \tag{5}$$

To invert these derivatives we note that the operator $d/d\rho=(d\rho/dz)^{-1}d/dz$ and that $dz/d\rho=(d\rho/dz)^{-1}$. Hence, we get the general formula

$$dz^n/d\rho^n=[(d\rho/dz)^{-1}d/dz]^{n-1}(d\rho/dz)^{-1}. \tag{6}$$

The expansion of this equation and its explicit expression in terms of the cluster integrals lead to very complicated formulas for the higher derivatives. For the present purpose it is necessary to find only the orders of magnitude of the various derivatives, and this information may be obtained by simpler procedures.

THE CLUSTER INTEGRALS NEAR THE CRITICAL POINT

The first cluster integral that has a nontrivial value is

$$b_2=-\frac{1}{2}\int[F_2(r)-1]4\pi r^2dr, \tag{7}$$

where $F_2(r)$ is the radial distribution function.[6,7] From Eqs. (4) and (6) we find

$$d\ln z/d\ln\rho=1/(2b_2\rho+1). \tag{8}$$

At the critical point itself this derivative becomes practically zero, and near the critical point it becomes very small, while, of course, ρ remains finite. Therefore, b_2 must approach infinity as the critical point is approached.

It is now necessary to examine the integrand, $F_2(r)-1$. The radial distribution function, $F_2(r)$, is the ratio of the local density at a distance r from a fixed molecule to the average density. Since the density of the critical state of simple compounds is about twice the close-packed density, $F_2(r)$ can never be greater than two over a range of more than a molecular radius without forcing the molecules into a density greater than close packing. The experimentally measured $F_2(r)$ for argon in the critical region[8] is never greater than two, and it approaches two only for a very small region. Hence, the integrand, $F_2(r)-1$, is smaller than unity over most of its range. On the other hand, since $b_2(z)$ has been seen to be very large, the integrand must be appreciable, although small compared with unity, over a distance of many molecular diameters when the system is near the critical point.

The higher cluster integrals are more complicated. However, if we assume that the "superposition principle"[9] is applicable, at least approximately, the higher cluster integrals may all be expressed in terms of the functions

$$g(ij)=F_2(r_{ij})-1,$$

where r_{ij} is the distance between molecules i and j.[1,7] We shall discuss the cluster integrals in terms of the symbolic representation of them in terms of diagrams in a plane.[1] If a set of n numbered points representing the molecules are placed in a plane, a line drawn to connect the pair i and j will represent the function $g(ij)$. A number of diagrams may be constructed in which each point (molecule) is connected to every other point, either directly or indirectly through intermediate points, by lines (functions $g(ij)$). The product of the functions $g(ij)$ associated with such a diagram makes up one term in the integrand of the cluster integral b_n. The complete integrand is formed by adding together the terms corresponding to all possible diagrams in which each of the n points is connected directly or indirectly to each of the other points. The integrand is then multiplied by a numerical factor and integrated over the coordinates of all the molecules but one (the choice of this latter being unimportant). An illustration is given below.

For example, consider the cluster integral b_3. The four terms that make up the integrand are symbolized by the diagrams in Fig. 1. The first three of these terms may be integrated at once by integrating first over the coordinates of one of the end molecules and then over the middle molecule. The result in each case is b_2^2. The fourth term cannot be handled in this manner, but as we have seen that $g(ij)$ is less than unity over most of its range, this fourth term cannot be greater than $(2b_2)^2$. Therefore, b_3 is less than $4(2b_2)^2$.

[8] A. Eisenstein and N. S. Gingrich, Phys. Rev. **58**, 307 (1940); *ibid.* **62**, 261 (1942).

[9] Kirkwood, Maun, and Alder, J. Chem. Phys. **18**, 1040 (1950); and other references therein.

The same procedure may be applied to obtain the order of magnitude of the higher integrals. Each term of the integrand will yield a contribution of $(2b_2)^{n-1}$ or less to b_n. We have been unsuccessful in finding a tractable formula for the number of such terms in the general integral; however, an approximate formula, which sets an upper bound on the number of terms, has been found (see Appendix):

$$(\text{number of terms})<n\,!(2-1)(2^2-1)(2^3-1)\cdots(2^{n-1}-1)\cong n\,!2^{n(n-1)/2}.$$

(Actually, this formula makes a very considerable overestimate of the number of terms.) The cluster integral is defined as $(1/n\,!)$ times the integral of the sum of products. Our considerations then lead to the inequality

$$b_n<2^{n(n-1)/2}(2b_2)^{n-1}. \tag{9}$$

Now returning to Eq. (6), we may write explicit formulas for the first three derivatives:

$$\begin{aligned}
&dz/d\rho=1/(d\rho/dz),\\
&d^2z/d\rho^2=-(d^2\rho/dz^2)/(d\rho/dz)^3,\\
&d^3z/d\rho^3=-[(d^3\rho/dz^3)/(d\rho/dz)^4]\\
&\qquad\qquad+3(d^2\rho/dz^2)/(d\rho/dz)^5.
\end{aligned}\tag{10}$$

Substituting now from Eqs. (5) and (9), we may establish limits on these derivatives:

$$\begin{aligned}
&(\rho/z)(dz/d\rho)=1/2b_2\rho,\\
&|(\rho^2/z)(d^2z/d\rho^2)|<18/2b_2\rho,\\
&|(\rho^3/z)(d^3z/d\rho^2)|<942/2b_2\rho.
\end{aligned}\tag{11}$$

These equations show that if the first derivative becomes very small as the system approaches the critical point, the second and third derivatives must become small also.

Derivatives of higher order may be obtained by repeated operation with $(d\rho/dz)^{-1}d/dz$. It is shown below that the application of this operator changes the order of magnitude by at most a finite amount, so that if the first derivative may be made arbitrarily small as the critical point is approached, any higher derivative may also be made arbitrarily small.

Repeated application of the operator $(d\rho/dz)^{-1}d/dz$ to the third derivative, $d^3z/d\rho^3$, produces nothing but more terms of the type of those in the right-hand members of Eq. (10), terms whose factors are either $(d\rho/dz)^{-x}$ or $d^y\rho/dz^y$, where x is less than or equal to $2n-1$, and y is less than or equal to n, with n the order of the derivative. If $(d\rho/dz)^{-1}d/dz$ is allowed to operate again to produce the next higher derivative, it multiplies these factors by $-x(d\rho/dz)^{-2}d^2\rho/dz^2$ or $(d\rho/dz)^{-1}(d^{y-1}\rho/dz^{y-1})/(d^y\rho/dz^y)$, respectively. Using Eq. (9), we see that these multipliers have absolute values less than $18x/\rho$ or $(y+1)\,(2^y-1)/\rho$, respectively. In addition, the number of terms in any derivative of finite order is finite. Hence, the limit on $(\rho^{n-1}/z)d^{n-1}z/d\rho^{n-1}$ differs from the limit on $(\rho^n/z)d^nz/d\rho^n$ by a factor of finite magnitude. The true value of this factor is probably much less than its upper limit as given by the use of Eq. (9); actual calculation shows this to be the case for the first few derivatives.

The conclusion is that as the critical point is approached and $(\rho/z)dz/d\rho$ becomes small, the immediately higher derivatives must also become small. If $(\rho/z)dz/d\rho$ may be allowed to become small without limit, any given higher derivative may be made as small as desired.

The question of the existence of a lower bound for $(\rho/z)dz/d\rho$ requires discussion. All our formulas depend ultimately on the grand partition function. Gibbs[10] showed that in this case the derivative is related to the fluctuations in the number of molecules in a given system of the grand ensemble. In our notation, we have

$$(\rho/z)(dz/d\rho)=\langle\nu\rangle_{Av}/\langle(\nu-\langle\nu\rangle_{Av})^2\rangle_{Av}, \tag{12}$$

where ν is the number of molecules in a given system, and $\langle\nu\rangle_{Av}$ is the mean number of molecules per system of the ensemble. For a finite system it is clear that there is a lower bound on $(\rho/z)dz/d\rho$ of the order of the reciprocal of the number of molecules in the system. The derivative may be made small without limit only in an infinite system. It is not clear from our formulas, which are quite inexact, by how much a finite system containing 10^{23} molecules would differ from an infinite system. We will nevertheless adopt the usual procedure of assuming that there are only trivial differences between the observable quantities of ordinary systems and infinite systems.

All the preceding results concerning the derivatives of second order and higher depend upon the validity of the superposition approximation. At the present time it seems impossible to prove that this approximation is adequate, even for the arguments concerning order of magnitude advanced here. In fact, it is easy to show that the approximation may lead to serious errors; for example, $d^2z/d\rho^2$ as we have calculated it can never be positive in the neighborhood of the critical point, yet it must be positive on one side of the critical point if the point is to be one of inflection. The source of the difficulty seems to lie in the superposition approximation used in finding b_3. The exact expression[7] for the integrand of b_3 is

$$F_3(i,j,k)-F_2(i,j)-F_2(j,k)-F_2(k,i)+2,$$

where $F_3(i,j,k)$ is the distribution function of the three molecules i, j, and k. In using the superposition approximation we assume that

$$F_3(i,j,k)=F_2(i,j)F_2(j,k)F_2(k,i).$$

This assumption leads immediately to the diagrams of Fig. 1. However, we now see that the integrand of b_3 is the difference between $F_3(i,j,k)$ and another compar-

[10] J. Willard Gibbs, *Collected Works* (Yale University Press, New Haven, Connecticut), Vol. II, p. 201, Eq. (530).

able quantity, so that it is sensitive to a small error in $F_3(i, j, k)$.

We can only claim, therefore, that the preceding arguments may have heuristic value; and the results will eventually have to be justified in other ways.

THE CRITICAL POINT AS A SINGULARITY

We have shown in the preceding section that if the first derivative of the fugacity with respect to density goes to zero at the critical point, any other derivative of finite order probably will also go to zero, at least if the size of the system is not restricted. We have not proved that the first derivative *must* go to zero at the critical point, and to our knowledge no such proof exists. However, experimental results indicate that the first derivative does become very small as the critical point is approached. We will, therefore, assume that it and the higher derivatives approach zero and examine the consequences of this assumption.

The first consequence is that the critical point must be a singularity in the function-theoretical sense, apparently an essential singularity, in the isothermal of fugacity as a function of density. (Hence, also in view of Eqs. (3) and (5) the isothermal of pressure against density is singular.) This is true because a function can have an infinite number of its derivates zero at a point only if it is a constant or if it cannot be expanded in a power series about the point. Since the fugacity is manifestly not constant, it must be incapable of expansion about the critical point, and it is, therefore, singular at the critical point. The appearance of the experimental curves suggests that the singularity is isolated, as long as the temperature is constant, although this is not proven theoretically. Rice[5] has indeed suggested that there may be a finite flat portion in the isothermal.

Before proceeding, perhaps we should clarify one point. We have not assumed that Eq. (2) is valid at the critical point itself. It is not immediately clear that Mayer's derivation is valid when there is a singularity in z, although it seems probable that Eq. (2) may be derived in other ways not subject to the same restriction. For example, the right-hand member of Eq. (12) may be transformed into the right-hand member of Eq. (8) without using Eq. (2). Equation (12) assumes only the validity of the use of the grand canonical ensemble. However, it is not really necessary to consider this point. Our equations should be valid up to a singularity, so that they can tell us now the thermodynamic functions approach the limit, and thus indicate the nature of the singularity.

DISCUSSION

The possibility that the critical point is a singularity has an effect on the argument employed by Mayer[1] to show that there should be two characteristic temperatures, a critical temperature where the derivative of the isothermal becomes zero and a second (lower) temperature where the first-order transition between the liquid and gas phases first makes its appearance. The argument may perhaps be summarized very briefly as follows. The derivative $d\varphi/d\rho$, which is equal to our $(\rho/z)dz/d\rho$, can be shown to be represented by a power series in ρ with coefficients that are functions of the temperature and which are known in principle. The critical point is the first point at which the series attains a vanishing value as the temperature is lowered. The phase transition is a singularity of the function, which was shown to be a certain type of divergence of the power series representing the function. If the critical point is a regular point characterized only by the value of zero, there is no reason why divergence should appear at this point also; hence, there is no reason for the singularities representing the phase transition to appear immediately. Therefore, it is postulated that the phase transition actually appears at a lower temperature. For the phase transition to appear immediately below the critical point it would be necessary that there be some other condition on the critical point other than the condition that the first derivative of φ with respect to ρ have a minimum touching zero.

We can now claim to have indicated that another condition on the critical point probably does exist, since the point may itself be a singularity with an infinite number of derivatives vanishing. It is, therefore, not unreasonable that the singularities representing the phase transition should appear at an immediate lower temperature; these singularities could arise by cleavage and migration of the singularity at the critical point.

There exists a simple function that has many of the properties just suggested, the function $\exp[-1/(x^2+t)]$, where x is a variable corresponding to density, and t a parameter corresponding to temperature. When t is positive, the function has a minimum at $x=0$ but no singularities on the real axis. When $t=0$, there is an essential singularity at $x=0$, at which point also all the derivatives of the function with respect to x vanish. When t is negative, there are two singularities on the real axis at $x=\pm t^{\frac{1}{2}}$. The analogy cannot be pressed much further, because the limit of the ratio of two successive derivatives as the singularity is approached is infinite for this function but finite at the actual critical point.

The argument as given here does not prove or disprove the existence of separate temperatures for the first vanishing of the slope of the isotherm and the first appearance of a phase transition. However, it does make the equality of these temperatures seem at least as as reasonable as their inequality. In the latter respect it differs from Mayer's original argument.[1]

It is also to be remarked that the critical point as it appears here has properties not contemplated in the theory of van der Waals or other classical theories of a

similar nature. It has been generally assumed[11] that the isothermals are analytic through the critical point and that only the first and second derivatives of pressure (and, hence, fugacity) with respect to density are zero. Among other consequences, this leads to the prediction that the envelope of the two-phase region would have a parabolic (quadratic) form on the conventional density-temperature diagram. Actually, the envelope appears to be cubic in the density.[12]

Further, it seems probable that the nearness of a singularity will make it very difficult to fit the isotherms, in the neighborhood of the critical point, with polynomial interpolation formulas. This difficulty has already been remarked by Michels and Michels, who were forced to fit their accurate data on CO_2 with different polynomials for the densities corresponding to liquid and vapor even at temperatures above the critical.[13]

Finally, we present a comparison with experiment. The most satisfactory data for the purpose seem to be those presented earlier[3] on a two-component system, since the first derivative of the fugacity with respect to density of one of the components was directly measured, and thereby numerical differentiation of fugacity or pressure data with the accompanying uncertainties was avoided. Let the activity (relative fugacity) of one component be a_1, its density relative to the pure component be φ_1; then the quantities of interest are the derivatives $(\varphi_1/a_1)\partial a_1/\partial\varphi_1$ and $(\varphi_1^3/a_1)\partial^3 a_1/\partial\varphi_1^3$, since the second derivative is identically zero at the critical point, the latter being a point of inflection. The first derivative was measured directly,[3] and an approximate value of the third derivative was found from these data by the method of finite differences, starting with the experimental points themselves. The data were not accurate enough for significant values of higher derivatives to be found. The results for the critical composition are shown in Fig. 2. It is striking that the third derivative does tend toward zero as the critical point is approached, in a manner parallel to the first derivative, despite the inaccuracy of the finite-difference approximation. It must be emphasized that such a result is not contained in the classical theory, where the third derivative is explicitly assumed to remain finite at the critical point.

[11] For a discussion see R. H. Fowler and E. A. Guggenheim, *Statistical Thermodynamics* (Cambridge University Press, London), Chapter VII.

[12] E. A. Guggenheim, J. Chem. Phys. **13**, 253 (1945); see also references 3, 6, and 13.

[13] A. Michels and C. Michels, Proc. Roy. Soc. (London) **A160**, 348 (1937).

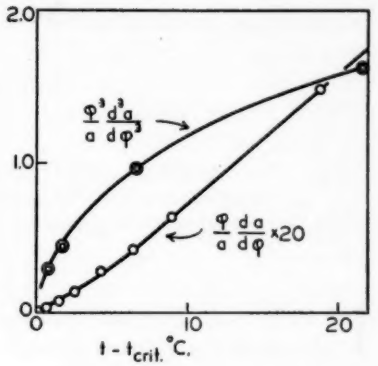

FIG. 2. First and third derivatives of activity, a, with respect to volume fraction, φ, for C_7F_{14} in solution in CCl_4, as functions of temperature less the critical temperature at which two liquid phases appear. Data from reference 3.

The true isothermals here are much flatter than the cubic curves of the classical theory, a condition that is plainly shown by the experimental data.[3,13]

ACKNOWLEDGMENT

The author would like to acknowledge his indebtedness to Professor J. E. Mayer, both for the original suggestion of this problem a number of years ago and for stimulating discussions on a number of subsequent occasions.

APPENDIX. A FUNCTION OF n WHICH IS GREATER THAN THE NUMBER OF TERMS IN THE nTH CLUSTER INTEGRAL

The diagram corresponding to any term of the cluster integral may be formed as follows: A point is chosen, and to it is coupled another point by a line. To the diagram thus formed is coupled another point, and so on until the desired diagram has been formed. The number of ways that a given point may be coupled to a diagram already containing n points is 2^n-1, since with any point already in the diagram a bond may be formed or not, giving two ways; there are n points, so there are 2^n ways in which bonds may or may not be formed to the given point; of these, all except one contain at least one bond to the given point. Of the new diagrams formed in this way, any one of the $n+1$ points could have been chosen as the given point, so that there may be $(n+1)(2^n-1)$ different ways of forming the diagram corresponding to $n+1$ points bonded together. This then is the upper limit on the ratio of the number of terms in b_{n+1} to the number of terms in b_n. Actually, this number is greater than the number of distinguishable terms, since many of the diagrams formed in this way will differ from each other only by symmetry operations, not in the relative positions of the bonds and points. For example, the complete triangle d in Fig. 1 could have been formed by coupling any one of the points 1, 2, or 3 to the other two, but the resulting diagrams differ from each other at the most by the arrangement of the three points on the corners of the triangle, and they correspond to the same term in b_3.

Starting in this way with the first cluster integral which is known to have one term, we find that

$$(\text{number of terms in } b_n) < n!(2-1)(2^2-1)(2^3-1)\cdots(2^{n-1}-1).$$

Note on the Theory of Critical Phenomena

JOSEPH E. MAYER
Institute for Nuclear Studies, University of Chicago, Chicago, Illinois
(Received April 25, 1951)

Zimm's theoretical considerations of the preceding paper are compared with the earlier conclusion of this author. Some of the consequences which must be drawn if one is not to accept Zimm's conclusions are pointed out. It appears that Zimm's conclusions are at least as plausible as this author's earlier hypotheses.

IN 1938, S. F. Harrison and the author[1] presented a plausibility argument for the existence of an anomalous region above the temperature of the usually observed critical point. In particular, they predicted that for a finite temperature range above the temperature, T_m, at which the meniscus disappears there would exist pressure isotherms which were independent of density over a finite density range, but for which $(\partial P/\partial\rho)_T$ would approach zero as the flat portion was reached, contrary to the behavior below T_m.

A considerable amount of experimental evidence exists to show that the behavior near the critical point is not that predictable from a simple van der Waals type of equation. Most of this evidence is consistent with the assumption of the anomalous behavior referred to above. However, the recent experiments of Zimm[2] definitely indicate different behavior.

The plausibility argument previously given can be stated in a more concise and convincing form than in the previous articles. By a rigorous application of the Gibbs statistics to a grand canonical ensemble one may derive for a one-component system an equation,

$$P/kT=\sum_{n\geq 1}b_n(V)z^n, \tag{1}$$

in which P is the pressure, z is the activity, normalized, so that it becomes equal to the number density, ρ, at infinite dilution, and the b_n's are coefficients, $b_1\equiv 1$, which are expressible as integrals over the coordinates of n molecules in the volume, V, of an integrand dependent on the potential energy of n or fewer molecules. In the derivation using the grand canonical ensemble[3] the b_n's do *not* depend upon the density and for finite values of n go to a definite value $b_n^{(0)}$ in the limit $V\to\infty$ provided the forces are sufficiently convergent. Now for any system of *finite* volume, V, the pressure must be a continuous function of z, without singularities. Singularities occur only in the limit $V\to\infty$, and there will be one at every activity z_0 for which there is a thermodynamic phase change. The pressure P_0 of condensation may, therefore, be associated with the first singularity of the equation

$$P/kT=\lim_{V\to\infty}\sum_{n\geq 1}b_n(V)z^n, \tag{1a}$$

which we assume[4] to be the same as that of the first singularity of

$$P/kT=\sum_{n\geq 1}b_n^{(0)}z^n \tag{1b}$$

on the positive real axis of z.

By an appropriate definition of coefficients β_m in terms of $b_n^{(0)}$'s for $n\leq m+1$ one may rewrite Eq. (1) in the form

$$\varphi=P/kT=x[1-\sum_{m\geq 1}[m/(m+1)]\beta_m x^m], \tag{2}$$

$$(\partial\varphi/\partial x)_T=[\partial(P/kT)/\partial x]_T=1-\sum_{m\geq 1}m\beta_m x^m, \tag{3}$$

in which x is defined in terms of a power series in z:

$$x=\sum_{n\geq 1}nb_n^{(0)}z^n=z[\partial(P/kT)/\partial z]_T. \tag{4}$$

From Eq. (4) it follows that $x=\rho$, the number density. Now it can be shown[5] that the first singularity in Eq. (1a) occurs at the lowest value on the positive real axis of x for which either

$$\sum_{m\geq 1}m\beta_m x^m=\text{singular} \tag{5a}$$

or

$$1-\sum m\beta_m x^m=0. \tag{5b}$$

If we define

$$\beta_0(T)=\lim_{m\to\infty}[\beta_m]^{1/m}, \tag{6}$$

condensation then occurs because of the condition (5a) at $\rho_0=1/\beta_0$ unless (5b) is satisfied for some value of x lower than $x=\rho_0$. In the latter case condensation occurs at that value of x for which (5b) is satisfied. In the former case $(\partial P/\partial\rho)_T>0$ as the point of condensation is reached. This corresponds to normal condensation below the observed critical point. If any finite temperature range exists for which Eq. (5b) determines the density at which condensation occurs, $(\partial P/\partial\rho_0)_T$ will approach zero in value as the condensation is approached. This will lead to anomalous properties in which no surface tension exists between the two thermodynamic phases, and a homogeneous density between those of the two phases can be maintained.

Now the plausibility argument for the existence of a finite temperature range for which (5b) determines the

[1] J. E. Mayer and S. F. Harrison, J. Chem. Phys. **6**, 87–104 (1938).
[2] B. H. Zimm, J. Phys. and Colloid Chem. **54**, 1306 (1950).
[3] Joseph E. Mayer, J. Chem. Phys. **10**, 629–643 (1942).
[4] S. Katsura and H. Fujita, J. Chem. Phys. **19**, 795 (1951), have pointed out that the transition from (1a) to (1b) is not necessarily correct and believe that the first singularities of (1a) and (1b) differ.
[5] M. Born and K. Fuchs, Proc. Roy. Soc. (London) **A166**, 391 (1938).

condensation may be stated as follows: both from theoretical considerations and from the experimental behavior of real substances, we know that $\beta_n \ll \beta_0^n$ for small values of n at very low temperatures. In this case, (5a) determines the condensation, and the sum in the expression on the left-hand side of (5b) is nearly zero at condensation, so that the saturated vapor behaves approximately as a perfect gas. Presumably, at sufficiently high temperatures the pressure is analytic through the density of the critical region and up to some density approximately that of the crystal. If the temperature is raised from low values, the first singularity determined by (5a) disappears from the positive real axis of z into the complex plane at a branch point of the position of the singularity in the z plane. Now if one is to have the classical behavior at the critical point predicted by an equation similar to that of van der Waals, this disappearance of the singularity must occur when (5b) also holds and, furthermore, when $(\partial^2 P/\partial \rho^2)_T = 0$.

This means that four requirements must be met simultaneously:

(A) $\sum m\beta_m x^m$ singular,

(B) The position of the singularity is at a branch point,

(C) $\sum m\beta_m x^m \to 1$ (as the singularity is approached),

(D) $\sum m^2\beta_m x^m \to 0$ (as the singularity is approached).

The simultaneous fulfillment of all four conditions seem to require a rather miraculous behavior of the coefficients β_m.

There remain two other possibilities; the singularity disappears when the expression on the left-hand side of (5b) is greater than zero or is less than zero. In the former case, $(\partial P/\partial \rho)_T > 0$ at the critical point, a condition which is thermodynamically possible but certainly not observed experimentally. In the latter case, there would necessarily be a temperature range for which (5b) determines the point of condensation and in which the experimental behavior would be anomalous. The true critical point, above T_m, would be the temperature at which only (C) and (D) were satisfied, but not at a singularity.

These conclusions have been variously criticized in the literature. Some of the criticisms were completely erroneous, since they were based on an assumption that the b_n's of Eq. (1) depended upon the density, an assumption which was understandable in view of the first derivations but which is completely excluded by the derivation in terms of the grand canonical ensemble.[5]

Another criticism given by Kahn and Uhlenbeck[6] was much more pertinent. The argument above has been given in such a form as to lend the greatest force to this criticism. The transition from Eq. (1) to Eq. (2) is based on a purely mathematical formulation. The same method could be used to deduce that *any* function $P(z, T)$ given in the form of (1b) had these properties, as a singularity disappeared owing to a change in some parameter, T, of the function. The argument of the author was, however, not quite so foolish as this criticism would imply. Although formally the β_m's are defined in terms of the b_n's, they do have a very simple significance if the potential energy is expressible as a sum of potentials between pairs of molecules. In this sense they seem to be as fundamental in meaning as the b_n's. It would, therefore, seem reasonable to assume that they were not so miraculously constructed that the four conditions, A, B, C, and D, could be simultaneously satisfied for all the various types of potential energies which must exist between real molecules.

The paper by Zimm immediately preceding this one raises a much more cogent argument against the assumptions made above. The argument is by no means decisive but certainly weakens the case for the existence of an anomalous critical region.

Equations (1), (1a), (1b), and (2) are also valid if P is interpreted to be the difference in pressure between two activities,

$$P = P(z_2) - P(z_1), \tag{7}$$

if z is proportional to the difference between the two activities,

$$z = (z_2 - z_1)\rho(z_1)/z_1, \tag{8}$$

and the coefficients

$$\left.\begin{aligned} b_n &= b_n(z_1) \\ \beta_m &= \beta_m(z_1) \end{aligned}\right\} \tag{9}$$

are calculated from the potentials of average force at the activity z_1. In this case one has

$$x = [1 - (z_1/z_2)]\rho(z_2). \tag{10}$$

In the limit $z_1 = 0$, since $\rho(z_1)/z_1$ is then unity, one has $z = z_2$, $x = \rho(z_2)$.

Now one finds, in general, that

$$(\partial \varphi/\partial x)_{x=0} = 1, \tag{11a}$$

$$(\partial^m \varphi/\partial x^m)_{x=0} = (m-1)!\,\beta_{m-1} \quad (m > 1), \tag{11b}$$

and

$$(\partial \varphi/\partial \rho)_T = 1/(1+\rho\beta_1) = (\partial x/\partial \rho)_{T(x=0)}, \tag{12}$$

where the β's are to be computed at the densities at which the derivatives are taken.

The features to which Zimm calls attention may be stated in a fashion alternative to his method as follows: If, as one assumes and as seems certainly to be the experimental case, $(\partial \varphi/\partial \rho)_T = (1/kT)(\partial P/\partial \rho)_T$ approaches zero in value as the critical density is approached, then $(\partial x/\partial \rho)_T$ also approaches zero, from Eq. (12). Now set $(\partial \varphi/\partial \rho)_T = \epsilon$, which may be arbitrarily small. Repeated differentiation with respect to ρ shows that $\rho^n(\partial^{n+1}\varphi/\partial \rho^{n+1})_T$ will be of order ϵ or smaller until, for some minimum n, the term $\rho^n\beta_n$ is of the order ϵ^{-n-1} or greater.

[6] B. Kahn and G. E. Uhlenbeck, Physica **5**, 399 (1938).

If "superposition" is assumed, the leading and largest term of β_n is

$$I_n=\frac{1}{n!}\int\int\cdots\int g(r_{01})g(r_{12})\cdots g(r_{n-1,n})g(r_{n,0})d\tau_1\cdots d\tau_n, \quad (13)$$

where

$$g(r)=F_2(r)-1, \quad (14)$$

and F_2 is the radial distribution function. As Zimm points out, $g(r)$ is presumably always less than unity. If the last factor, $g(r_{n,0})$, were omitted from the integrand of (13), the integral would be β_1^n, of the order $(\epsilon/\rho)^{-n}$. The inclusion of the last factor can only decrease the order. Therefore, the magnitude of $\rho^n\beta_n$ cannot exceed ϵ^{-n}, if "superposition" is assumed.

It is worth while emphasizing that the Eqs. (1b) and (2) with Eqs. (7), (8), (9), and (10) for any z_2 and z_1 form a self-consistent system. If one assumes any values of β_m at $z_1\equiv 0$ such that conditions C and D are satisfied for some $x=\rho_0$ with no singularity in the neighborhood, $(\partial^3\varphi/\partial\rho^3)_T\neq 0$, then one can, in principle at least, compute the $\beta_m(z)$ as the activity of ρ_0 is approached. One will, of course, find $\rho^2\beta_2=0(1+\rho\beta_1)^{-3}$. The only conclusion to be drawn from Zimm's argument is that this is inconsistent with "superposition" for the distribution functions.

One may point out that superposition is certainly not exactly correct. The large magnitude of β_1 near the critical point is due to the fact that $g(r)$ converges very slowly to zero at large r-values. This means that $F_2(i,j)\neq F_1(i)F_1(j)=1$ even when the distance r_{ij} is large. That is, the knowledge that one molecule is at a position x_i, y_i, z_i influences the probability that another be at x_j, y_j, z_j even when r_{ij} is large. This, in itself, is a curious state of affairs. The "superposition" principle assumes that

$$F_3(i,j,k)=F_2(j,k)F_2(k,i)F_2(i,j).$$

If Zimm's conclusion that $(\partial^n\varphi/\partial\rho^n)_T=0$ for all n's is not to be accepted, one must assume that $F_3(i,j,k)$ differs from unity at large r_{jk}, r_{ki}, r_{ij} values by significantly more than the product of the three F_2's. It hardly seems possible, with the present lack of knowledge, to know whether this is reasonable or not.

It certainly does not appear that Zimm's argument is final. However, it seems to this author, at the present time, that it is at least as plausible as the argument advanced previously that the four conditions, A, B, C, and D, were too much to satisfy simultaneously.

THE JOURNAL OF CHEMICAL PHYSICS VOLUME 19, NUMBER 8 AUGUST, 1951

A Study of Metallic Electrodes Prepared by Sublimation

BENJAMIN C. BRADSHAW
Signal Corps Engineering Laboratories, Fort Monmouth, New Jersey

(Received May 3, 1951)

The relative electromotive force of zinc crystals deposited from the vapor phase in high vacuum was measured and found to be of the order of 100 microvolts. It is concluded that zinc crystals formed by evaporation of zinc are practically strain free and, as such, are highly suitable where reversible zinc electrodes are needed.

INTRODUCTION

WHEN a metal solidifies, strains are introduced by uneven cooling among other things. Several authors, among whom are F. H. Getman,[1] and W. J. Clayton and W. C. Vosburgh,[2] succeeded in preparing strain-free zinc electrodes by annealing. Reversible silver chloride electrodes were prepared by the thermal decomposition of silver oxide.[3] The writer has prepared electrodes by the condensation of zinc on platinum wires and found that they agree in potential among themselves and with standard zinc amalgam electrodes to within 105 microvolts. A preliminary report of this work has been made.[4] The results of further investigation are given in the present paper.

TABLE I. The relative potential of zinc electrodes measured in microvolts.

Electrode No.[a]	A	1	2	3
A		8	27	3
1	8		23	6
2	27	23		10
3	3	6	10	

[a] Electrodes 1–2–3 were made by condensation of zinc on platinum wire. Electrode A was made by placing an aggregate of zinc crystals in a loop of platinum wire, immersing in a solution of mercurous nitrate for about 1 second, removing, and thoroughly washing.

METHODS OF PREPARATION

Electrodes were prepared in vacuum by sealing platinum wire into soft glass tubes. These were placed in a Pyrex tube containing a pellet of spectroscopically pure zinc, so that the wires were about 20 cm above the

[1] F. H. Getman, J. Phys. Chem. **35**, 2749 (1931).
[2] W. J. Clayton and W. C. Vosburgh, J. Am. Chem. Soc. **58**, 2093 (1936).
[3] G. Jones and S. A. Baeckstrom, J. Am. Chem. Soc. **56**, 1524 (1934).
[4] B. C. Bradshaw, J. Chem. Phys. **17**, 344(L) (1949).

TABLE II. The relative potential of zinc electrodes measured in microvolts.

Electrode No.[a]	A	B	1	2	3	4
A		16	70	45	18	33
B	16		93	61	37	50
1	70	93		30	58	44
2	45	61	30		25	11
3	18	37	58	25		14
4	33	50	44	11	14	

[a] Electrodes A and B were made by placing loose aggregates of zinc crystals in spirals of platinum wire; electrodes 1–2–3–4 by condensing zinc onto platinum wires.

TABLE III. The relative potential of zinc electrodes measured in microvolts.

Electrode No.[a]	1	2	3	4	5	6	7	8
1		52	67	33	48	38	13	143
2	52		13	22	98	93	72	87
3	67	13		39	105	99	100	78
4	33	22	39		81	74	64	108
5	48	98	105	81		7	22	183
6	38	93	99	74	7		51	178
7	13	72	100	63	22	51		110
8	143	87	78	108	183	178	110	

[a] Electrodes 1–2–3–4 (Group A) were made by evaporating zinc at 250°C and allowing it to condense on platinum wires; electrodes 5–6–7–8 (Group B) were made by evaporating zinc at 450°C.

zinc pellet. The pressure was then reduced to 10^{-7} mm of mercury, dry ice traps having been placed between the vacuum pump and the MacLeod gauge and the zinc plating system, to prevent contamination of the zinc with mercury. After evacuation, the Pyrex tube was heated by means of a cylindrical electric furnace so placed that the zinc pellet was near its midpoint and the electrode about 1 cm below its upper opening. The temperature was then raised until the zinc began to vaporize and condense on the platinum wires, the glass tubes into which the platinum wires were sealed, and the walls of the enveloping tube. The zinc collected at first in the form of a mirrorlike coating which was overlaid by an agglomeration of fine, loosely adhering crystals.

Other electrodes were made by bending platinum wires into spirals and placing in each of them a coherent mass of zinc crystals taken from the walls of the enveloping tube. Additional electrodes were prepared by amalgamating the surfaces of zinc crystals by immersing them in a solution of mercurous nitrate for a second or two and thoroughly washing them.

More recently experiments were conducted using groups of eight electrodes prepared in subgroups of four each. Subgroup A was prepared by heating the zinc pellet to 250°C and extending the evaporation period to approximately two weeks. Subgroup B was prepared by heating the zinc pellet to 450°C for a few hours.

All the electrodes thus prepared were placed in a dilute solution of pure zinc chloride (about 0.1 molar) and saturated with basic zinc carbonate; air was rigorously excluded. Several sets were made at various times, and their electromotive force was measured.

DISCUSSION

It was possible by comparing the relative potential of the electrodes of groups A and B to determine whether or not there was any relation between the degree of strain of the crystals and the time of crystal formation.

Table I shows that the maximum variation between an amalgamated zinc electrode and three evaporated zinc electrodes was 27 microvolts. Table II shows that the maximum deviation between electrodes made by placing aggregates of zinc crystals in platinum spirals, and those made by direct condensation of zinc on platinum wires was 93 microvolts. Table III shows that if electrode 8, which was bent in preparation, is excluded, then the group prepared by long evaporation at 250°C differ among themselves by less than 70 microvolts. The members of the group prepared by rapid evaporation at 450°C differ among themselves by less than 60 microvolts. The maximum deviation between any two electrodes is 105 microvolts. If electrode 8 is included, the greatest variation is 183 microvolts. The data presented here are but a small part of those taken; however, they are believed by the writer to be representative.

The useful lifetime of the electrodes is not known; it is certainly greater than eight weeks. The electrodes could be used repeatedly provided that they were washed and stored in distilled water while they were not in use. Sometimes they were slow in returning to equilibrium when they were reused; at other times they came to equilibrium as soon as they could be measured; new electrodes came to equilibrium immediately. In no case was it necessary to wait for more than a few hours.

CONCLUSIONS

The writer concludes that there is very little strain in any of the zinc electrodes described above, since all showed the reversible potential to within 105 microvolts except those that had been strained by bending.

Bromination of Hydrocarbons. V. Neopentane and Hydrogen Chain Lengths. Efficiency of Neopentane as a Third Body

FRANCIS E. SCHWEITZER* AND ERVIN R. VAN ARTSDALEN
Department of Chemistry, Cornell University, Ithaca, New York
(Received May 10, 1951)

A direct comparison of the rates of photochemical bromination of neopentane and hydrogen has been made, which shows the neopentane reaction to be 94 times faster at 470.6°K. It is shown that neopentane is of the order of 175 times more effective than hydrogen in promoting homogeneous bromine atom recombination. An estimate of the chain lengths for both photo and thermal bromination has been made, and it appears definite that the chain with neopentane has several hundred links. It is suggested that this is in part the result of a high radical concentration, favored by the fact that the heat of formation of neopentyl radical is only very slightly endothermic as contrasted with that for methyl radical or hydrogen atom.

THE kinetics of both photochemical and thermal bromination of neopentane has been investigated recently by Hormats and Van Artsdalen[1] in Paper IV of this series. It was shown that the reaction involves an atom and radical chain; and it appeared that the chain length is considerably greater than unity, at least for the thermal reaction. The present study was undertaken in the hope that it would be possible to make a more direct determination of the photochemical chain length and to compare it with that of the thermal reaction as well as chain lengths of other brominations.

EXPERIMENTAL METHOD AND RESULTS

Phillips reagent grade neopentane from the same lot used in our previous work was prebrominated to remove material which might brominate faster than neopentane, after which it was separated from the bromo products and repeatedly distilled under high vacuum to obtain a water white fraction which was stored entirely in the gas phase. Bromine was purified as described in Paper IV and supplied through the kindness of Professor H. A. Scheraga.

The apparatus was essentially the same one used by Hormats and Van Artsdalen, although the light intensity of the photochemically activating beam was lower in the studies reported in the present paper and the geometry was somewhat different, resulting also in lower incident light intensity. One additional change was made in the type of stopcock grease. In the present work we used Fluorolube FCX334[2] to lubricate those stopcocks exposed to bromine. This material, which permitted the attaining of a good vacuum, remained entirely unattacked by bromine, although bromine was very slightly soluble in the fluorolube. Our only objection to the fluorolube was that stopcocks greased with it alone and exposed to bromine tended to "freeze" rather easily at room temperature, though they could be freed by warming slightly.

Pressures of reactants were measured with a quartz spiral null-point manometer and the concentration of bromine as a function of time of illumination was followed photometrically as described in Paper IV. The data were extrapolated to obtain the rates at zero time, which were used in all calculations.

A series of measurements was made to determine the relative rates of photochemical bromination of neopentane and of hydrogen, both at the same constant light intensity. Rate constants were calculated using the rate expression found applicable in previous work:

$$-d[\mathrm{Br}_2]/dt = k_I[\mathrm{RH}][\mathrm{Br}_2]^{\frac{1}{2}}[1/P]^{\frac{1}{2}}, \qquad \text{(I)}$$

where RH represents either neopentane or hydrogen and P the total pressure of all gases present. It quickly became evident that the reaction with neopentane takes place so much faster than that with hydrogen that the two reactions could not be measured with satisfactory precision at the same temperature. We made a few measurements of the initial rate of photobromination of neopentane, in the absence of hydrogen bromide, over the temperature range 124 to 181°C using the above rate expression. One can estimate from measured rates of thermal bromination at 197.4°C[1] that the dark reaction should be negligible in this temperature range, and this was verified experimentally. The activation energy was calculated from the temperature dependence of these measurements to be 18.0 kcal/mole in excellent agreement with 18.1 kcal/mole obtained by Hormats and Van Artsdalen[1] in their more exhaustive study of temperature effects. Temperatures of about 225 to 250°C were required in order to obtain comparable rates with hydrogen. Hence, it is necessary to extrapolate rates to some uniform temperature for purposes of comparison. We therefore decided to compare all rates and steric effects at 197.4°C (470.6°K), the temperature of thermal bromination studies reported in Paper IV.

The rate constant for photobromination of neopentane, defined in Eq. (I), was found to be

$$k_{I(\mathrm{NpH})} = 3.18(\pm 0.15)\times 10^{-4}\ \mathrm{sec}^{-1} \text{ at } 171.5°\mathrm{C}(\pm 0.3°),$$

* Present address: Fabrics and Finishes Department, E. I. duPont de Nemours and Company, Philadelphia, Pennsylvania.

[1] E. I. Hormats and E. R. Van Artsdalen, J. Chem. Phys. **19**, 778 (1951).

[2] This material was supplied to us through the courtesy of Dr. S. W. McCune, III, Organic Chemicals Department, E. I. duPont de Nemours and Company, Wilmington, Delaware.

which when extrapolated using the experimental energy of activation 18.1 kcal/mole gives $k_{I(\mathrm{NpH})}=9.8\times10^{-4}$ sec^{-1} at 197.4°C. The corresponding experimental rate constant for photobromination of hydrogen under the same conditions was

$$k_{I(\mathrm{H_2})}=3.16(\pm0.03)\times10^{-5}\ \mathrm{sec}^{-1}\ \text{at}\ 226.0°\mathrm{C}\ (\pm0.2°).$$

This was extrapolated to 197.4° by means of the well-established activation energy[3] 17.64 kcal/mole giving $k_{I(\mathrm{H_2})}=1.04\times10^{-5}$ sec^{-1} at 197.4°C. Since the ratio of these two rate constants at 197.4° is 94, the rate of photobromination of neopentane is 94 times faster than of hydrogen, even though there is a balance of 0.5 kcal/mole activation energy favoring the hydrogen reaction. These data are collected in Table I.

DISCUSSION

It has been shown in Paper IV that in the case of neopentane

$$k_I=k_2(k_{\mathrm{app}}\alpha I_0/k_5)^{\frac{1}{2}}, \qquad \text{(II)}$$

where k_2 is the specific rate constant for the rate determining step

$$\mathrm{NpH+Br=Np+HBr}, \qquad (2)$$

k_{app} is an apparatus constant, α the absorption coefficient of Br_2, I_0 the incident light intensity, and k_5 the specific rate constant for recombination of Br atoms

$$\mathrm{2Br+M=Br_2+M}. \qquad (5)$$

It has also been demonstrated that the value of k_5 depends on the nature of M. An exactly analogous situation obtains for photobromination of hydrogen. Thus, the ratio of the over-all experimental rate constants for these two reactions becomes

$$\frac{k_{I(\mathrm{NpH})}}{k_{I(\mathrm{H_2})}}=\frac{k_{2(\mathrm{NpH})}}{k_{2(\mathrm{H_2})}}\left\{\frac{k_{5(\mathrm{H_2})}}{k_{5(\mathrm{NpH})}}\right\}^{\frac{1}{2}}, \qquad \text{(III)}$$

since all the other constants cancel out. We see that this ratio of rate constants for the photochemical case depends not only on the chain propagating step (2), but also inversely on the square root of the recombination rates of bromine atoms in presence of hydrogen or neopentane. Unfortunately, the values for the respective k_5's have to be averages for the particular gases and pressures used.

We also showed in Paper IV that in the case of thermal bromination the over-all rate constant, k, had the relationship

$$k=k_2K_{\mathrm{eq}}^{\frac{1}{2}}, \qquad \text{(IV)}$$

where $K_{\mathrm{eq}}=[\mathrm{Br}]^2/[\mathrm{Br_2}]$ is the equilibrium constant for thermal dissociation of bromine. Thus, for thermal bromination we may write

$$k_{(\mathrm{NpH})}/k_{(\mathrm{H_2})}=k_{2(\mathrm{NpH})}/k_{2(\mathrm{H_2})} \qquad \text{(V)}$$

and we note that the ratio of rates in this case does not depend on the efficiency of the third bodies in homogeneous recombination of bromine atoms. The experimental rate constant for thermal bromination of neopentane reported by Hormats and Van Artsdalen[1] is $k_{(\mathrm{NpH})}=2.00(\pm0.19)\times10^{-2}$ (cc mole^{-1})$^{\frac{1}{2}}$ sec^{-1} at 197.4°C. Bodenstein and Lind[4] have studied the thermal reaction between hydrogen and bromine in the temperature range 301 to 226°C. A least squares extrapolation of their data through about 29° gives for this rate constant

$$k_{(\mathrm{H_2})}=1.61\times10^{-5}\ (\mathrm{cc\ mole}^{-1})^{\frac{1}{2}}\ \mathrm{sec}^{-1}\ \text{at}\ 197.4°\mathrm{C}.$$

Thus, the ratio of the rate of thermal bromination of neopentane to that of hydrogen is 1240, and we consider that this is also the ratio of the rate constants of the chain propagating reaction step (2).

We have made use of Eqs. (III) and (V) to obtain a comparison between the efficiencies of neopentane and hydrogen in promoting recombination of bromine atoms. From Eq. (V) and data cited above we obtain $k_{2(\mathrm{NpH})}/k_{2(\mathrm{H_2})}=1240$ and on substituting this into Eq. (III) obtain

$$k_{5(\mathrm{NpH})}/k_{5(\mathrm{H_2})}=\{1240/94\}^2=174,$$

indicating that neopentane is of the order of 174 times more efficient as a homogeneous third body in reaction (5) than is hydrogen. This result is qualitatively what we would expect, though the magnitude of difference between the two molecules looks quite large. It is difficult to estimate the probable error, since four different rates are involved, three of which had to be extrapolated. However, it is our considered opinion that the above value should be correct to within a factor of about two or three.

Making use of Eq. (III) and the relationship $k_2=sZe^{-E/RT}$, where s is the steric factor, Z the collision number, and E the experimentally determined activation energy, we obtain for the ratio of steric factors of the neopentane and hydrogen brominations

$$\frac{s_{(\mathrm{NpH})}}{s_{(\mathrm{H_2})}}=\frac{k_{I(\mathrm{NpH})}}{k_{I(\mathrm{H_2})}}\left\{\frac{k_{5(\mathrm{NpH})}}{k_{5(\mathrm{H_2})}}\right\}^{\frac{1}{2}}\frac{Z_{(\mathrm{H_2})}}{Z_{(\mathrm{NpH})}}\times\exp\left[\frac{E_{\mathrm{NpH}}-E_{\mathrm{H_2}}}{RT}\right]. \qquad \text{(VI)}$$

TABLE I. Rates of bromination at 197.4°C.

Photoreaction, k_I in sec^{-1}			Thermal reaction, k in (cc mole^{-1})$^{\frac{1}{2}}$ sec^{-1}		
NpH[a]	H_2[a]	NpH/H_2	NpH[b]	H_2[c]	NpH/H_2
9.8×10^{-4}	1.04×10^{-5}	94	2.00×10^{-2}	1.61×10^{-5}	1240

[a] This research. [b] Reference 1. [c] Calculated from reference 4.

[3] M. Bodenstein and H. Lütkemeyer, Z. physik. Chem. **114**, 208 (1924). W. Jost, *ibid.* **134**, 92 (1928). W. Jost and G. Jung, *ibid.* **3B**, 83 (1929). G. Jung, *ibid.* **3B**, 95 (1929). G. B. Kistiakowsky and E. R. Van Artsdalen, J. Chem. Phys. **12**, 469 (1944).

[4] M. Bodenstein and S. C. Lind, Z. physik. Chem. **57**, 168 (1907).

The ratio of the collision numbers $Z_{(H_2)}/Z_{(NpH)}$ was computed to be 1.80, using 3.0A for the diameter of the Br atom, 6.0A for neopentane, and 2.88A for hydrogen. Certainly 1.8 must be fairly close to the true value. Other values required in Eq. (VI) to compute the frequency factor ratio have been obtained above from experimental data. We find

$$s_{(NpH)}/s_{(H_2)}=94\times(174)^{\frac{1}{2}}\times 1.8\times e^{500/RT}=3800$$

at 470.6°K. This ratio corresponds to the ratio of chain lengths in the thermal reaction. However, the ratio of apparent chain lengths for the photochemical reaction will be decreased below this value by the term $(174)^{\frac{1}{2}}$, accounting for the lower steady-state concentration of bromine atoms during illumination in neopentane than in hydrogen, which is caused by the different efficiencies of neopentane and hydrogen as third bodies for homogeneous recombination of bromine atoms. Thus, the apparent chain length for photobromination of neopentane is only 290 times that for hydrogen instead of 3800. The steric factor for the hydrogen reaction has been accepted to be about 0.1,[5] whence the steric factor for the reaction of neopentane with a bromine atom is estimated to be 380 from these data. This is in good agreement with the value $s=473$ calculated in Paper IV from the thermal rate and bromine-bromine atom equilibrium constant. We conclude that both photochemical and thermal bromination of neopentane involve fairly long chains.

It is interesting to speculate concerning the reason for a long chain in bromination of neopentane in contradistinction to the cases with hydrogen, methane, and ethane. We suggest that this is closely connected with our finding that the heat of formation of the neopentyl radical is nearly zero[1] under the conditions of our experiments, while heats of formation of radicals for the other reactions are strongly endothermic. Therefore, on energetical grounds, the conditions are more favorable in the case of neopentane to the accumulation of the chain-propagating neopentyl radical than of methyl radical in the methane reaction. Since the chain length is dependent, among other things, on the concentration of the hydrocarbon radical, we may expect a higher radical concentration to lead to longer chains.

[5] G. B. Kistiakowsky and E. R. Van Artsdalen, J. Chem. Phys. **12**, 469 (1944).

THE JOURNAL OF CHEMICAL PHYSICS VOLUME 19, NUMBER 8 AUGUST, 1951

Binding Energy and Dipole Moment of Alkali Halide Molecules*

EDMUND S. RITTNER
Philips Laboratories, Inc., Irvington-on-Hudson, New York

(Received March 23, 1951)

A simple theory of alkali halide gas molecules in the spirit of Born-Mayer lattice theory is presented. The molecule is considered to be constituted of ions, each of which is polarized by the electrostatic field of the other. This deformation polarization has two important consequences: (1) the net dipole moment of the molecule becomes appreciably lower than that given by the product of the electric charge e, and the internuclear separation a; (2) the repulsion constants (determined from empirical data) become different from the corresponding constants for the crystal. The theory yields satisfactory results for the binding energy, vibration frequency, and dipole moment, μ, in all instances where necessary data are available. In cases where the internuclear distances are not known experimentally, they are calculated from the theory using experimental binding energies. It is possible to assign to the ions Goldschmidt-like radii, the sums of which reproduce reasonably well both the calculated and the observed internuclear distances. Finally, item (1) above explains why Pauling's criterion for the fraction of ionic character, $f=\mu/ea$, is not a very good measure of ionicity for these completely ionic substances.

I. INTRODUCTION

NUMEROUS attempts[1–6] have been made to calculate the binding energy of alkali halide gas molecules from Born lattice theory. All of these calculations are based upon the assumption that the repulsion constants are the same for the gas molecules as for the crystals, an assumption which will be shown below to be invalid. Because of this circumstance the earlier attempts,[1–3] which derived internuclear distances for the gas molecules from the corresponding distances in the crystals via the theory, were rather unsuccessful. The more recent treatment of this problem by Verwey and de Boer,[6] which employs directly the internuclear distances determined by electron diffraction,[7] has achieved a high measure of success. It is one of the primary purposes of the present paper to improve upon and to extend this work.

* Presented at the 304th meeting of the American Physical Society held in Pittsburgh on March 8–10, 1951.

[1] A. Reis, Z. Physik **1**, 294 (1920).

[2] M. Born and W. Heisenberg, Z. Physik **23**, 388 (1924).

[3] E. J. W. Verwey and J. H. de Boer, Rec. trav. chim. **55**, 431 (1936).

[4] A. May, Phys. Rev. **54**, 629 (1938).

[5] O. K. Rice, *Electronic Structure and Chemical Binding* (McGraw-Hill Book Company, Inc., New York, 1940), p. 249.

[6] E. J. W. Verwey and J. H. de Boer, Rec. trav. chim. **59**, 633 (1940).

[7] Maxwell, Hendricks, and Mosely, Phys. Rev. **52**, 968 (1937).

A few attempts[2,8] have also been made to calculate classically the dipole moment of alkali halide molecules. These calculations have not yielded good results, as they were carried out before the internuclear distances had been experimentally determined. The dipole moment is of some interest in connection with a commonly employed criterion[9] for the fraction of ionic character of a bond: $f=\mu/ea$ (μ=dipole moment, e=the electronic charge, and a=equilibrium interatomic separation). This criterion leads to the curious dilemma[10] for the alkali halides that, although the bonding is generally supposed to be completely ionic, the quantity f is experimentally found to be in the neighborhood of 0.7. Another object of the present paper is to recalculate values of the dipole moment based upon electron diffraction data[7] and to show that the dilemma mentioned above arises from the fact that the criterion neglects the mutual deformation polarization of the ions.†

The theory on which the present work is based is presented in Sec. II (1) for the dipole moment and in Sec. II (2) for the binding energy. The data employed in the calculation are listed in Sec. III; the numerical results obtained for the repulsion constants, binding energy, vibration frequency, and dipole moment are given in Sec. IV. The latter section also includes a set of Goldschmidt-like radii which reproduce reasonably well the internuclear distances. Finally, the implications of this work are briefly discussed in Sec. V.

II. THEORY

1. Dipole Moment

The alkali halide molecule is considered to be constituted of ions, each of which is polarized by the electrostatic field of the other. If the charges on the ions are designated $+e$, $-e$; the polarizabilities α_1, α_2; the induced moments μ_1, μ_2; and the equilibrium separation of the ion centers a; then the net dipole moment μ of the molecule is given by

$$\mu=ea-(\mu_1+\mu_2) \tag{1}$$

as may be seen from Fig. 1. Further designating the electrostatic field at the center of each ion as E_1, E_2, then the induced moments are given by

$$\mu_1=\alpha_1E_1=\alpha_1\left(\frac{e}{a^2}+\frac{2\mu_2}{a^3}\right), \tag{2}$$

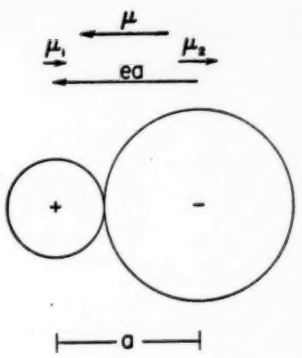

FIG. 1. Model of an alkali halide molecule showing the contributions to the net dipole moment.

$$\mu_2=\alpha_2E_2=\alpha_2\left(\frac{e}{a^2}+\frac{2\mu_1}{a^3}\right). \tag{3}$$

The simultaneous solution of Eqs. (2) and (3) yields[11]

$$\mu_1=\frac{a^4e\alpha_1+2ae\alpha_1\alpha_2}{a^6-4\alpha_1\alpha_2}, \tag{4}$$

$$\mu_2=\frac{a^4e\alpha_2+2ae\alpha_1\alpha_2}{a^6-4\alpha_1\alpha_2}. \tag{5}$$

It is convenient to develop Eqs. (4) or (5) in power series for later use in the expression for the binding energy. For the condition $a^6\gg4\alpha_1\alpha_2$, which is valid for all the alkali halides, the induced moments become

$$\mu_1=\frac{e\alpha_1}{a^2}+\frac{2e\alpha_1\alpha_2}{a^5}+\frac{4e\alpha_1^2\alpha_2}{a^8}+\cdots, \tag{6}$$

$$\mu_2=\frac{e\alpha_2}{a^2}+\frac{2e\alpha_1\alpha_2}{a^5}+\frac{4e\alpha_1\alpha_2^2}{a^8}+\cdots. \tag{7}$$

Returning again to Eqs. (4) and (5) and combining them with Eq. (1), we obtain

$$\mu=ea-\left(\frac{a^4e(\alpha_1+\alpha_2)+4ae\alpha_1\alpha_2}{a^6-4\alpha_1\alpha_2}\right). \tag{8}$$

While it is clear that Eqs. (2) and (3), and hence also (8), are valid for internuclear separations large compared with the ion dimensions, it is not immediately obvious that they apply at the small distances which actually obtain in alkali halide molecules, as the in-

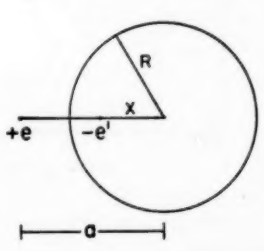

FIG. 2. Simplified model of an alkali halide molecule comprising a point charge $+e$ and a negatively charged metal sphere.

[8] P. Trautteur, Nuovo cimento **15**, 5 (1938).

[9] L. Pauling, *The Nature of the Chemical Bond* (Cornell University Press, Ithaca, New York, 1944), second edition, p. 46.

[10] G. H. Herzberg, *Molecular Spectra and Molecular Structure. I. Spectra of Diatomic Molecules* (D. van Nostrand Company, Inc., New York, 1950), second edition, p. 377.

† The importance of the deformation polarization in problems of this type has been repeatedly emphasized for many years by K. Fajans and his co-workers (see, for example, K. Fajans, Ceramic Age **54**, 288 (1949)). Recently, Pauling's criterion has also been subjected to criticism by D. Z. Robinson (J. Chem. Phys. **17**, 1022 (1949)) based on a quantum-mechanical calculation of the dipole moment in HCl.

[11] P. Debye, *Polar Molecules* (Dover Publications, New York, 1945), p. 60.

TABLE I.

Substance	a, Å (1200°C)	α_1, cm³ ×10⁻²⁴	α_2, cm³ ×10⁻²⁴	ω_e, cm⁻¹	μA, atomic wt. units	I_2, ev	E, ev
LiF		0.029	1.05		5.0846	75.28	4.13
LiCl			3.69		5.8056		3.72
LiBr			4.81		6.3872		3.49
LiI			7.16		6.582		3.14
NaF		0.181			10.4054	47.0	
NaCl	2.51			380	13.9508		
NaBr	2.64			315	17.8588		
NaI	2.90			286	19.4692		
KF		0.84			12.7894	31.7	
KCl	2.79			280	18.599		
KBr	2.94			231	26.260		
KI	3.23			212	29.896		
RbF		1.42			15.5486	27.3	
RbCl	2.89			(253)	25.068		
RbBr	3.06				41.313		
RbI	3.26				51.089		
CsF		2.44			16.6277	23.4	
CsCl	3.06				27.998		
CsBr	3.14			(194)	49.921		
CsI	3.41			142	64.935		

homogeneous electric field varies greatly from one part of the ion to another.

To examine this question further, let us consider a simplified model of the molecule comprising a point charge $+e$ situated a distance a away from the center of a metal sphere of radius R charged homogeneously with a total charge $-e$ (see Fig. 2). For such a simplified model, which would appear to be a reasonable representation of an alkali halide molecule with $\alpha_1 \ll \alpha_2$, a determination of the dipole moment μ_2 induced in the metal sphere represents a simple problem in electrostatics. If the sphere is grounded, then it may be shown[12] by the method of images that a charge $-e'$ is induced in the sphere at a distance x from the center, such that

$$|e'| = eR/a, \tag{9}$$

$$x = R^2/a. \tag{10}$$

At this stage, since the center of the sphere may be considered to contain a charge $+e'$ and another charge $-e'$, the field at any external point due to the presence of the sphere will be that of a point charge $-e'$ at the center of the sphere and that of a dipole moment $e'x$ slightly removed from the center of the sphere. The sphere may then be disconnected from ground and charged homogeneously first with a charge $+e'$, making it neutral, and then with the desired net charge $-e$. Neither of these charging processes will alter Eqs. (9) and (10). Hence, the final result is an induced moment in the negatively charged sphere of magnitude

$$\mu_2 = e'x = \frac{eR}{a}\frac{R^2}{a} = \frac{eR^3}{a^2}. \tag{11}$$

This may be written as

$$\mu_2 = \alpha_2 E_2, \tag{12}$$

where $\alpha_2 = R^3$ and E_2 is the electrostatic field at the center of the sphere due to the point charge $+e$. Equation (12) represents a justification for employing Eqs. (2), (3), and (8) at small internuclear distances.

Note that the preceding argument requires that $x < R$ or alternatively that $a > R$, a condition which is fulfilled for all of the alkali halides, as will be shown in Sec. IV.

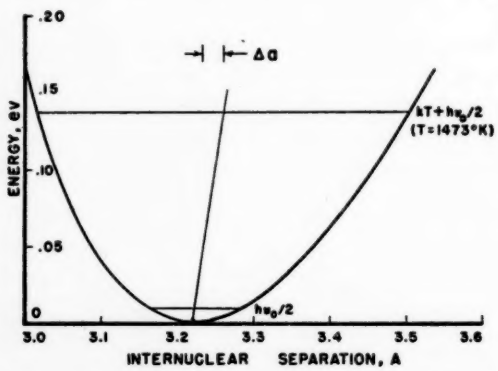

FIG. 3. Potential energy *versus* internuclear separation plot for RbI gas molecules showing the thermal expansion.

[12] J. H. Jeans, *Electricity and Magnetism* (Cambridge University Press, London, 1915), p. 189.

2. Binding Energy

Most of the energy binding the ions together in the molecule arises from purely electrostatic interactions between the ions: charge-charge interaction, charge-dipole interaction, dipole-dipole interaction, and quasi-elastic energy stored in the induced dipoles. Following Born and Heisenberg,[2] this portion ϕ of the total binding energy W may be expressed as a function of the internuclear separation r as follows:

$$\phi = -\frac{e^2}{r} - \frac{\mu_1 e}{r^2} - \frac{\mu_2 e}{r^2} - \frac{2\mu_1\mu_2}{r^3} + \frac{\mu_1^2}{2\alpha_1} + \frac{\mu_2^2}{2\alpha_2}. \tag{13}$$

Substituting the first two terms‡ of the series in Eqs. (6) and (7) (using the generalized r notation) into Eq. (13), we obtain

$$\phi = -\frac{e^2}{r} - \frac{e^2(\alpha_1+\alpha_2)}{2r^4} - \frac{2e^2\alpha_1\alpha_2}{r^7}. \tag{14}$$

The remainder of the binding energy we treat completely in the spirit of Born and Mayer lattice theory;[13] thus, are included a repulsion term of the exponential form, a van der Waals attraction term, and kinetic energy terms representing the difference in translational, rotational, and vibrational energy between the molecule and the free ions from which it is composed. The total

‡ For the observed internuclear distances in the alkali halides, convergence of the series is so rapid that use of only the first two terms of the series is adequate to determine the binding energy to within about a percent.

[13] M. Born and J. E. Mayer, Z. Physik **75**, 1 (1932).

TABLE II.

1 Substance	2 ρ	3 A, ev	4 $-W$ (calc) ev	5 $-W$ (exp) ev	6 a, (300°K) A	7 Σ ionic radii, A	8 ω_e (calc) cm^{-1}	9 ω_e (exp) cm^{-1}	10 μ (calc) D	11 μ (exp) D	12 ea, D
LiF		436		7.73	1.53[a]	1.42	773		5.04		7.35
LiCl		1330		6.80	1.97[a]	1.97	705		4.76		9.46
LiBr		1950		6.42	2.14[a]	2.12	650		5.11		10.28
LiI		3490		6.02	2.37[a]	2.40	616	450	5.15		11.38
NaF		964		6.26	2.00[a]	1.93	477		7.99		9.60
NaCl	0.303	3380	5.44	5.56	2.48	2.48	373	380	8.71		11.91
NaBr	0.318	4800	5.26	5.34	2.61	2.63	321	315	8.84		12.53
NaI	0.317	9470	4.91	5.03	2.87	2.91	291	286	9.33		13.78
KF		1590	5.94	6.08	2.17[b]	2.21	410	(390)	8.06	8.62	10.42
KCl	0.332	6760	4.95	4.98	2.76	2.76	296	280	10.09[c]	9.53	13.35[c]
KBr	0.328	10000	4.76	4.76	2.91	2.91	241	231	10.46[c]	10.85	14.07[c]
KI	0.311	20700	4.43	4.45	3.19	3.19	213	212	11.26[c]	11.05	15.42[c]
RbF		2290		5.69	2.31[a]	2.31	361	(340)	8.33		11.09
RbCl	0.306	9020	4.82	4.84	2.86	2.86	250	(253)	10.07		13.73
RbBr		13600	4.62	4.61	3.02	3.01	188		10.56		14.50
RbI		23600	4.42	4.30	3.22	3.29	163		10.75		15.46
CsF		3310	5.54	5.44	2.43[b]	2.47	345	(270)	8.06	7.61	11.67
CsCl		14000	4.63	4.62	3.02	3.02	229		10.39	9.97	14.50
CsBr	0.261	17900	4.56	4.43	3.10	3.17	171	(194)	10.49		14.89
CsI	0.308	35200	4.28	4.28	3.36	3.45	141	142	11.29[c]	12.1	16.28[c]
	Av= 0.31±0.01										

[a] Calculated from experimental binding energy.
[b] Value chosen to give best agreement for both binding energy and dipole moment.
[c] Calculated from a value at 900°K to permit direct comparison of μ with experimental value.

energy is then of the form:

$$W=\phi+Ae^{-r/\rho}-\frac{c}{r^6}+\frac{h\nu_0}{2}+\frac{h\nu_0}{e^{h\nu_0/kT}-1}-\frac{kT}{2}. \quad (15)$$

On the assumption that the repulsion constants are the same for crystals as for the corresponding gas molecules, Verwey and de Boer[6] have concluded that the exponential form of the repulsion term is not applicable to the gas molecules. Here, we determine the repulsion constants in a straightforward manner from experimental data by the use of the relations:

$$(dW/dr)_{r=a}=0 \quad (16)$$

and

$$(d^2W/dr^2)_{r=a}=p \text{ (the force constant)}. \quad (17)$$

Equilibrium internuclear distances, a, are taken from electron diffraction determinations;[7] and force constants, p, are taken from band spectra studies.[14] As will be seen in Sec. IV, the repulsion constants determined in this way for the gas molecules are not identical with those determined experimentally for crystals via the theory of Born and Mayer.[13]

As for the other quantities in Eq. (15), the van der Waals attractive constant, c, may be estimated by the method of London[15] and the vibration frequency, ν_0, is simply related to the force constant:

$$p=5.8883\times10^{-2}\mu_A\omega_e^2 \text{ dynes/cm},$$

where $\omega_e=\nu_0/c$ and μ_A is the reduced mass of the molecule in atomic-weight units. Finally, the binding energy may be calculated from Eqs. (14) and (15) taking $r=a$.

[14] See reference 10, p. 500.
[15] F. London, Z. Physik **63**, 245 (1930).

Application of conditions (16) and (17) to Eq. (15) leads to the result:

$$\rho=\frac{\dfrac{e^2}{a^2}+\dfrac{2e^2(\alpha_1+\alpha_2)}{a^5}+\dfrac{14e^2\alpha_1\alpha_2}{a^8}+\dfrac{6c}{a^7}}{p+\dfrac{2e^2}{a^3}+\dfrac{10e^2(\alpha_1+\alpha_2)}{a^6}+\dfrac{112e^2\alpha_1\alpha_2}{a^9}+\dfrac{42c}{a^8}}. \quad (18)$$

As will be shown in Sec. IV, ρ proves to be substantially constant in nine cases where data are available to permit evaluation. If the average value of ρ is considered to apply to all the alkali halides, then it becomes possible to calculate from Eq. (18) the force constant, and thus the vibration frequency.

III. DATA EMPLOYED

The data employed in the calculations are listed in Table I. The internuclear distances, a, measured at about 1200°C are taken from the electron diffraction studies of Maxwell, Hendricks, and Mosely.[7] The polarizability values chosen, α_1 and α_2, are those given by Pauling[16] as his α_1-values agree well with the more recent calculations of Mayer and Mayer[17] for the alkali ions. The final results for W and μ, however, are not sensitive to the particular choice of polarizabilities. The vibration frequencies, ω_e, and reduced masses, μ_A, are taken from the compilation of Herzberg.[14] The second ionization potentials, I_2, of the alkali atoms are taken from Bacher and Goudsmit;[18] and the electron affinities,

[16] L. Pauling, Proc. Roy. Soc. (London) (A) **114**, 191 (1927).
[17] J. E. Mayer and M. G. Mayer, Phys. Rev. **43**, 605 (1933).
[18] R. F. Bacher and S. Goudsmit, *Atomic Energy States* (McGraw-Hill Book Company, Inc., New York, 1932).

TABLE III.

Ion	Radius, A	$a^{\frac{1}{3}}$, A
F^-	1.04	1.02
Cl^-	1.59	1.57
Br^-	1.74	1.69
I^-	2.02	1.93
Li^+	0.38	0.31
Na^+	0.89	0.57
K^+	1.17	0.94
Rb^+	1.27	1.12
Cs^+	1.43	1.35

E, of the halogen atoms are taken from the work of Mayer and co-workers;[19–22] both quantities are needed to estimate the van der Waals attractive constant, c.

In order to compare calculated binding energies with experimental ones, it is convenient to calculate the energies corresponding to room temperature. Hence, it becomes necessary to correct the observed internuclear distances for thermal expansion. This has been done by the graphical method of Verwey and de Boer;[6] i.e., plots of W as $f(r)$ were made in accordance with Eqs. (14) and (15)' and Δa found by determining graphically the centers of the zero point level and of a horizontal line $h\nu_0/(e^{h\nu_0/kT}-1)(=kT$ at high temperatures) above this level (see Fig. 3 for an example). Because of the more complete energy expression employed by us in this correction, the anharmonicity of the potential curve and thus the thermal expansion were found to be less than that given by Verwey and de Boer[6] (calculated on the basis of only a couloumb and a repulsion term). An approximate expression for the expansion correction between 1200°C and room temperature, including the small effect of rotation on the internuclear separation, is $\Delta a/a=4\times10^{-3}a$. Application of this correction yields the a values shown without superscripts "a" or "b" in column 6 of Table II.

IV. RESULTS

Results of the calculation are presented in Tables II and III for the repulsion constants, binding energy, internuclear distance, ionic radii, vibration frequency, and dipole moment. These quantities are discussed below in sequence.

1. Repulsion Constants

The repulsion constant ρ was determined in those cases where values could be found for both the internuclear separation and the force constant. The constant ρ is found to be substantially the same in all of the nine cases considered, having the average value $0.31(\pm0.01)$ (see column 2 of Table II). The situation is thus similar to that prevailing[13] in the alkali halide crystals where, however, the average value of ρ is $0.345(\pm0.02)$, or about ten percent higher. The separation between closest neighbors in the crystals is also about ten percent higher than in the corresponding gas molecules, so that the ratio r/ρ is roughly the same in both cases.

The repulsion constant A was determined for all the alkali halides (using, where necessary, values of a calculated in a manner to be described below) with the results displayed in column 3 of Table II. These values, and hence the energy of repulsion per ion pair, are on the average about five times as large as those which obtain[19] in the crystals. This circumstance may possibly arise from increased overlap of the charge distributions of the ions produced by the polarization deformation in the gas molecule.

2. Binding Energy

The binding energy (at 300°K) was calculated for all cases in which internuclear separations were known. The results, shown in column 4 of Table II, are to be compared with the experimental values of the binding energy listed in column 5. Agreement is quite satisfactory, i.e., within ±3 percent. The experimental values are the negative of the sum $(D+I-E)$, where D is the dissociation energy of the molecule into neutral atoms, I the first ionization potential of the alkali atom, and E the electron affinity of the halogen atom. Values of D were taken from the compilation of Bichowsky and Rossini,[23] values of I from reference 18, and values of E from references 19–22 (see last column of Table I).

It is worth pointing out that the only terms in Eqs. (14) and (15) that contribute appreciably to the energy are the couloumb, repulsion, and $e^2(\alpha_1+\alpha_2)/2a^4$ terms.

The treatment of the substances KF and CsF requires special mention. The internuclear distance in these molecules has been determined recently by Grabner and Hughes[24] and by Trischka[25] using the electric resonance method of molecular beam spectroscopy.[26] The values obtained by these workers are 2.55A for KF and 2.34A for CsF. Using these particular numbers, the theory yields values of binding energy which do not agree well with the experimental values. It is important to realize, however, that the electric resonance method yields results of high accuracy for the product μ^2A (μ, the dipole moment, and A, the moment of inertia) but that the individual values of μ and A have been determined heretofore[26] only to a much lower accuracy.§ In the light of these facts, it is perhaps significant that it is possible to choose values for the internuclear separations in these molecules so as to yield good agreement between theory and experiment for both the binding energy and the dipole moment. Using the values shown in column 6

[19] J. E. Mayer and L. Helmholz, Z. Physik **75**, 19 (1932).
[20] P. P. Sutton and J. E. Mayer, J. Chem. Phys. **3**, 20 (1935).
[21] P. M. Doty and J. E. Mayer, Phys. Rev. **66**, 36 (1944).
[22] J. E. Mayer, Phys. Rev. **75**, 1282 (1949).
[23] F. R. Bichowsky and F. D. Rossini, *The Thermochemistry of the Chemical Substances* (Reinhold Publishing Corporation, New York, 1936).
[24] L. Grabner and V. Hughes, Phys. Rev. **79**, 819 (1950).
[25] J. W. Trischka, Phys. Rev. **76**, 1365 (1949).
[26] H. K. Hughes, Phys. Rev. **70**, 570 (1946).
§ It is a pleasure to acknowledge a helpful discussion with Professor I. I. Rabi in this connection.

of Table II: $a=2.17$A for KF and 2.43A for CsF, it may be seen from columns 4 and 5 that the corresponding calculated binding energies are in satisfactory agreement with the experimental ones. The dipole moments of these molecules will be considered below.

3. Internuclear Distances and Ionic Radii

In all cases where internuclear distances have not been determined by electron diffraction, they were calculated from the experimental binding energies by means of the theory. The values so obtained are designated by asterisks in column 6 of Table II. The application of this procedure to KF and CsF yielded values of a differing only by a few percent from those cited above.

Examination of the complete list of internuclear distances thus made available revealed regularities in the differences between a values for the various alkali halides entirely analogous to those observed in crystals. This suggests the possibility of assigning Goldschmidt-like radii to the gaseous ions, a possibility which is indeed realizable. One possible set of such radii is shown in Table III. This particular set is based upon the observed interatomic distance and upon Pauling's[27] values of the screening constants in the KCl molecule. For comparison with these radii, Table III includes values of $\alpha^{\frac{1}{3}}$, which is the radius of an equivalent metal sphere. Agreement between these two sets of radii is generally not unreasonable. That the sum of the ionic radii reproduce reasonably well both the calculated and observed internuclear distances may be seen from a comparison of columns 6 and 7 of Table II. Note that the condition $a>R$ is fulfilled for all of the alkali halides.

4. Vibration Frequency

Using the internuclear distances of column 6 of Table II and the average value of $\rho=0.31$, the vibration frequency, ω_e, was calculated for all of the alkali halides with the results shown in column 8. These may be compared with the experimental values listed in column 9 taken from reference 14 and from the recent work of Hughes and Grabner.[28] In view of the uncertainties in the experimental values and of the fact that we are dealing here with the second derivative of the energy, agreement between theory and experiment may be judged satisfactory.

A notable exception, however, is represented by LiI, where the agreement is rather poor. It is perhaps worth mentioning that a similar situation occurs with respect to the LiI crystal, where the value of the repulsion constant ρ calculated by Born and Mayer[13] is completely out of line with the ρ-values for all the other alkali halides. It is possible that a purely ionic model is not too satisfactory a representation of the situation for this particular material.

[27] See reference 9, p. 344.
[28] V. Hughes and L. Grabner, Phys. Rev. **79**, 314 (1950).

5. Dipole Moment

Values of the dipole moment shown in column 10 of Table II were calculated from 300°K a values for all the alkali halides save KCl, KBr, KI, and CsI. In these cases the calculations were based upon 900°K a values to permit direct comparison with the experimental results of Rodebush, Murray, and Bixler[29] (shown in column 11) obtained by deflection of a beam of molecules in a nonhomogeneous field. The other "experimental" values of μ listed in column 11 of Table II are computed from the μ^2A results obtained by the electric resonance method by Grabner and Hughes,[24] Trischka,[25] and Luce and Trischka,[30] the computation being based upon the 300°K a values in column 6, Table II, and upon the reduced mass (μ_A) values in Table I. The theoretical and experimental values of the dipole moment agree to within ± 6.5 percent in the seven cases where data are available. Note from a comparison of columns 10 and 12 of Table II that the net dipole moment of an alkali halide molecule is appreciably lower than the product ea, owing to the mutual polarization of the ions.

V. CONCLUDING REMARKS

In so far as it is allowable to draw conclusions from a semi-empirical, classical theory of the type presented above, it appears that the picture of an alkali halide gas molecule being constituted of ions, each of which is distorted by the electrostatic field of the other, accounts quite well for the important properties of the molecule. The predicted values of internuclear separation, vibration frequency, and dipole moment listed in Table II may prove useful until such time as new work establishes the values definitely on an experimental basis.

The failure of Pauling's[9] criterion for the fraction of ionic character of a bond (μ/ea) in the case of the alkali halides stems from the fact that the criterion fails to include the far from negligible polarization deformation of the ions.

ACKNOWLEDGMENTS

The writer wishes to express his indebtedness to Professor G. E. Uhlenbeck and Dr. F. K. du Pré for their encouragement and advice.

Note added in proof: It has been pointed out to the writer by Professor K. Fajans that the quantity "ionicity" has been defined by various workers in different ways. To avoid confusion, the meaning of the phrase "completely ionic" as employed in the text is illustrated by the following example. In Na^+Cl^-, the Na^+ has a neonlike quantum configuration and the Cl^- an argonlike configuration, although both charge distributions are not spherically symmetric with respect to the nuclei, owing to the polarization deformation. The fraction μ/ea has been defined by Fajans (see Z. Elektrochem. **34**, 502 (1928)) as the "degree of polarity" of a molecule and for completely ionic molecules is a measure of this deformation.

[29] Rodebush, Murray, and Bixler, J. Chem. Phys. **4**, 372 (1936).
[30] R. G. Luce and J. W. Trischka, Phys. Rev. **82**, 323 (1951).

Brownian Motion in a Gas of Noninteracting Molecules

MELVILLE S. GREEN
Natural Science Staff, College of University of Chicago, Chicago, Illinois
(Received April 12, 1950)

The Brownian motion of a hard spherical particle in a gas whose molecules interact only with the particle but not with each other is considered from three points of view. (a) The generalized Fokker-Planck equation for the process is derived by the classical method of Lord Rayleigh. (b) The hypothesis of the phenomenonological theory of Brownian motion that the distribution of changes of momentum of the particle is normal is investigated with some mathematical rigor. (c) The formula for the friction constant recently given by Kirkwood is applied to this case. It is found that the plateau value in this formula exists in this case and that the value obtained agrees with Rayleigh's method. The hypothesis of the phenomenonological theory is found to be justified for times long enough for many collisions to have taken place. The theoretical formula for the friction constant is compared with Millikan's data for the friction constant for oil droplets in air at low pressures. It is found to agree with Millikan's data with respect to the form of the dependence on density and temperature. The theoretical values for hard spheres are somewhat lower than the data for oil droplets.

THE purpose of this paper is to examine from three points of view the motion of a spherical Brownian particle in a gas of noninteracting molecules. The results obtained are, of course, quite different from those of the well-known case of Brownian motion in a liquid, or in a dense gas, where the surrounding molecules are anything but noninteracting. In particular, Einstein's formula relating the friction constant of the Brownian particle to the viscosity of the surrounding medium does not apply because a gas of noninteracting molecules has no property which can be described as a viscosity. The principal interest of this case is that it can be rather completely analyzed from the microscopic point of view. Nevertheless, it is not unreasonable to expect that the idealization of noninteracting surrounding molecules represents very well the actual behavior of a Brownian particle in a very tenuous gas in which the mean free path is large compared to the size of the particle.

The first method is due to Lord Rayleigh[1] and was applied by him to the motion of a Brownian particle in a one-dimensional gas. It consists in the calculation of the effect of the collisions of the surrounding gas molecules with the Brownian particle on the distribution of its phases. The second method consists in the calculation of the distribution of changes of momentum of the Brownian particle over a time interval long compared to the time of a collision, but short compared to the time to reach equilibrium. The third method is an application of a formula recently derived by Kirkwood which relates the correlation between the force on a Brownian particle at different times to the friction constant.[2]

In all these cases it is assumed that the time of collision is short compared to the average time between collisions so that the Brownian particle is interacting with, at the most, one of the surrounding molecules. As the sphere approaches the ideal of perfect hardness this assumption is more and more justified. To simplify calculations it is also assumed that the mass of the gas molecules is small compared to the mass of the Brownian particle and that they are maintained in maxwellian equilibrium by being immersed in a heat reservoir at temperature T.

I. METHOD OF LORD RAYLEIGH

Let us call the distribution function of the Brownian particle in its complete phase space $\rho(\mathbf{P}, \mathbf{X}, t)$ where $\mathbf{P}$ is its momentum vector, $\mathbf{X}$ its position vector, and t the time. We will derive a partial differential equation which this function must satisfy by equating its rate of change to the difference between the probability per unit time for entering and the probability per unit time for leaving the elementary phase volume $d\mathbf{P}d\mathbf{X}$. There are two ways in which this probability can change; the Brownian particle may enter or leave the volume $d\mathbf{X}$ due to its translatory motion, or its momentum may enter or leave the volume $d\mathbf{P}$ due to a collision with a surrounding molecule. These two processes are mutually independent. On the one hand, if the Brownian particle is near enough to the boundary of $d\mathbf{X}$ so that it will enter or leave it in a short time were there no possibility of a collision it will almost certainly enter or leave taking collisions into account, since the probability that it suffers no collisions in the interval dt approaches 1 as dt approaches 0. On the other hand, the collision with which we are dealing approaches the ideal of an instantaneous change of the momentum with no change of position, and the number of molecules which leave the volume $d\mathbf{X}$, as well as the momentum region $d\mathbf{P}$ during a collision will be small compared to those that leave $d\mathbf{P}$ but remain in $d\mathbf{X}$. The total rate of change of the probability for being in $d\mathbf{P}d\mathbf{X}$ is the sum of the rates of change due to these two independent effects.

The part of this total rate of change due to translation is the same as for a free particle and is well known from the calculations which lead to Liouville's equation.[3]

[1] Lord Rayleigh, Phil. Mag. 32, p. 424 (1891).
[2] This problem was also investigated by a simplified, but inexact method by M. v. Smoluchowski, Ann. Physik **21**, 756 (1906).
[3] See for instance J. W. Gibbs, *Elementary Principles of Statistical Mechanics* (Charles Scribner's and Sons, New York, 1902), chapter I.

It is simply,

$$-\nabla_x \cdot \mathbf{P}/M\rho d\mathbf{P}d\mathbf{X}, \tag{1}$$

where M is the mass of the Brownian particle.

The part due to collisions is equal to the difference of the probability per unit time that a Brownian particle located in $d\mathbf{X}$, but with momentum outside of $d\mathbf{P}$, suffers a collision which brings its momentum into $d\mathbf{P}$, and the probability per unit time that a Brownian particle in the volume $d\mathbf{X}$, and with momentum in the region $d\mathbf{P}$, suffers a collision which takes its momentum outside of $d\mathbf{P}$. Since $d\mathbf{P}$ is infinitesimal while the change of momentum in a collision is finite, any collision at all will do this.

Let us consider now the mechanics of a collision. We need not specify the force between a molecule and the Brownian particle except to state that it is radially symmetric and acts only within a very short distance of the surface of the particle. If this distance is small compared to the radius of the particle, every elementary momentum change which takes place will be very nearly parallel to the radius of the Brownian sphere to the point of closest approach of the molecule. The more closely the sphere approaches the ideal of perfect hardness the more nearly parallel the elementary momentum changes will be. We can assume then that the change of momentum of both the Brownian particle and the molecule will be in the direction of the normal at the point of contact. If we call $\mathbf{P}'$, $\mathbf{P}$ the momentum of the Brownian particle before and after the collision respectively, $\mathbf{p}'$ and $\mathbf{p}$ that of the molecule, $\mathbf{n}$ the unit normal at the point of collision and M the mass of the molecule we have

$$\mathbf{P}=\mathbf{P}'+\mathbf{n}a$$
$$\mathbf{p}=\mathbf{p}'+\mathbf{n}b,$$

where a and b are scalars. These two equations together with the equations of conservation of energy and momentum give

$$\mathbf{P}=\mathbf{P}'+2Mm/M+m(\mathbf{p}'/m-\mathbf{P}'/M)\cdot\mathbf{nn}, \tag{2a}$$

$$\mathbf{p}=\mathbf{p}'-2Mm/M+m(\mathbf{p}'/m-\mathbf{P}'/M)\cdot\mathbf{nn}. \tag{2b}$$

We note in passing for use later on that in a collision between a molecule of momentum $\mathbf{p}'$ and a Brownian particle of momentum $\mathbf{P}'$ the change of momentum is

$$2Mm/M+m(\mathbf{p}'/m-\mathbf{P}'/M)\cdot\mathbf{nn}.$$

In order to calculate the number of molecules entering $d\mathbf{P}$ we need to know what initial momentum $\mathbf{P}'$ of the Brownian particle is required in a collision with a molecule of initial momentum $\mathbf{p}'$ so that the final momentum is $\mathbf{P}$. In other words we need $\mathbf{P}'$ in terms of $\mathbf{p}'$ and $\mathbf{P}$. From (2a) we obtain

$$\mathbf{P}'=\mathbf{P}-2Mm/M-m(\mathbf{p}'/m-\mathbf{P}/M)\cdot\mathbf{nn}. \tag{3}$$

Now the probability that the Brownian particle enters the region $d\mathbf{P}d\mathbf{X}$ in a time dt because of a collision with a molecule in the momentum range $d\mathbf{p}'$ which occurs in a neighborhood dA of its surface is the product of the probability that the Brownian particle has a suitable momentum, and that there is a molecule near enough to dA for a collision to take place in a time dt. If its momentum is $\mathbf{p}'$ such a molecule must be contained in a region of base dA and altitude equal to the normal component of the relative displacement in time dt. The probability of one molecule in this region is practically equal to the average number of molecules in this region if this average is small compared to one. We have for the probability of a collision of the above type

$$-\rho(\mathbf{P}', \mathbf{X}, t)\mathbf{n}\cdot\left(\frac{\mathbf{p}'}{m}-\frac{\mathbf{P}'}{M}\right)d(2\pi mkT)^{-\frac{3}{2}} \times\exp-\frac{p'^2}{2mkT}d\mathbf{P}'d\mathbf{X}d\mathbf{p}'dAdt, \tag{4a}$$

where d is the density of the surrounding molecules.

(The minus sign takes account of fact that velocity of molecule with respect to the Brownian particle must be opposite to the normal for a collision to take place.)

Similarly, the probability that the Brownian particle will leave $d\mathbf{P}d\mathbf{X}$ in a time dt by a collision with a molecule of momentum in the range $d\mathbf{p}'$ which occurs in a neighborhood dA of its surface is the product of the probability that it is in $d\mathbf{P}d\mathbf{X}$ and that there is a molecule in the range $d\mathbf{p}'$ which is near enough to dA to collide in the time dt. We have for this probability

$$-\rho(\mathbf{P}, \mathbf{X}, t)\mathbf{n}\cdot\left(\frac{\mathbf{p}'}{m}-\frac{\mathbf{P}}{m}\right)d(2\pi mkT)^{-\frac{3}{2}} \times\exp-\frac{p'^2}{2mkT}d\mathbf{P}d\mathbf{X}d\mathbf{p}'dAdt. \tag{4b}$$

Let us express (4a) in terms of $\mathbf{P}$ and $\mathbf{p}'$ and take the difference of (4a) and (4b). We have from (3)

$$d\mathbf{P}'=M+m/M-md\mathbf{P},$$

while from (2a) together with (3) we have

$$\mathbf{n}\cdot\left(\frac{\mathbf{p}'}{m}-\frac{\mathbf{P}'}{M}\right)=\frac{M+m}{M-m}\mathbf{n}\cdot\left(\frac{\mathbf{p}'}{m}-\frac{\mathbf{P}}{M}\right).$$

Then the excess of the probability of entering $d\mathbf{P}d\mathbf{X}$ over that of leaving due to a collision with a molecule in the range $d\mathbf{p}'$ which occurs in the neighborhood of its surface dA is

$$-[(M+m/M-m)^2\rho(\mathbf{P}', \mathbf{X}, t)-\rho(\mathbf{P}, \mathbf{X}, t)] \times\mathbf{n}\cdot(\mathbf{p}'/m-\mathbf{P}/M)d(2\pi mkT)^{-\frac{3}{2}} \times\exp-p'^2/2mkTd\mathbf{P}d\mathbf{X}d\mathbf{p}'dAdt. \tag{5}$$

We note that the condition on $\mathbf{p}'$ for a collision in which the Brownian particle enters $d\mathbf{P}d\mathbf{X}$ is $\mathbf{n}\cdot(\mathbf{p}'/m-\mathbf{P}'/M)<0$ while that for a collision in which it leaves $d\mathbf{P}d\mathbf{X}$ is $\mathbf{n}\cdot(\mathbf{p}'/m-\mathbf{P}/M)<0$. Because of the relation between these two quantities they are positive

or negative together. To find the total change in probability we must integrate (5) over all $\mathbf{p}'$ for which $\mathbf{n}\cdot(\mathbf{p}'/m-\mathbf{P}/M)<0$ and over all surface elements dA.

We obtain in this way the linear differentio-integral equation for ρ

$$\frac{\partial\rho}{\partial t}+\nabla_x\cdot\frac{\mathbf{P}}{M}\rho=-d(2\pi mkT)^{-\frac{1}{2}}\times\int dA\int\left[\left(\frac{M+m}{M-m}\right)^2\rho(\mathbf{P}',\mathbf{X},t)-\rho(\mathbf{P},\mathbf{X},t)\right]\times\mathbf{n}\cdot\left(\frac{\mathbf{p}'}{m}-\frac{\mathbf{P}}{M}\right)\exp-p'^2/2mkTd\mathbf{p}'d\mathbf{A}. \quad (6)$$

This equation may be used to predict the future course of the distribution when it is known at one initial time.

If ρ is smooth enough so that it may be approximated by the first few terms of a power series in the neighborhood of any momentum $\mathbf{P}$ we can reduce (6) to the form of Chandrasekhar's generalized Fokker-Planck equation.[4] The power series approximation must hold for $|\Delta\mathbf{P}|$ less than some representative value of the change of momentum in a single collision. Such a representative value is the root-mean-square momentum of one of the colliding molecules or $(mkT)^{\frac{1}{2}}$. We expand the first term of the integrand in (6) in a power series around $\mathbf{P}$ and obtain

$$\frac{\partial\rho}{\partial t}+\nabla_x\cdot\frac{\mathbf{P}}{M}\rho=\left[\left(\frac{M+m}{M-m}\right)^2-1\right]A\rho+\left(\frac{M+m}{M-m}\right)\mathbf{B}\cdot\nabla_P\rho+\left(\frac{M+m}{M-m}\right)^2\boldsymbol{C}:\nabla_P\nabla_P\rho, \quad (7)$$

$+$higher order terms,

where the scalar A is

$$-d(2\pi mkT)^{-\frac{1}{2}}\times\int_{\text{surface of sphere}}dA\int_{\mathbf{n}\cdot(\mathbf{p}'/m-\mathbf{P}/M)<0}\mathbf{n}\cdot\left(\frac{\mathbf{p}'}{m}-\frac{\mathbf{P}}{M}\right)\times\exp-p'^2/2mkTd\mathbf{p}', \quad (8a)$$

the vector $\mathbf{B}$ is

$$\frac{2Mm}{M-m}d(2\pi mkT)^{-\frac{1}{2}}\times\int_{\text{surface of sphere}}dA\int_{\mathbf{n}\cdot(\mathbf{p}'/m-\mathbf{P}/M)<0}\mathbf{n}\left(\mathbf{n}\cdot\left(\frac{\mathbf{p}'}{m}-\frac{\mathbf{P}}{M}\right)^2\right)\times\exp-\mathbf{p}'^2/2mkTd\mathbf{p}', \quad (8b)$$

and the dyadic $\boldsymbol{C}$ is

$$-\frac{2M^2m^2}{(M-m)^2}d(2\pi mkT)^{-\frac{1}{2}}\times\int_{\text{surface of sphere}}dA\int_{\mathbf{n}\cdot(\mathbf{p}'/m-\mathbf{P}/M)<0}\mathbf{nn}\left(n\cdot\left(\frac{\mathbf{p}'}{m}-\frac{\mathbf{P}}{M}\right)\right)^3\times\exp-\mathbf{p}'^2/2mkTd\mathbf{p}'. \quad (8c)$$

The double dot : in (7) means the double contraction of the dyadic $\boldsymbol{C}$ with the dyadic whose components are the second order derivatives of ρ with respect to the components of $\mathbf{P}$.

We can carry out these integrals most simply by using a coordinate system for $\mathbf{p}'$ in which one of the axes is the unit normal $\mathbf{n}$ and by making the substitution

$$-z/m=\mathbf{n}\cdot(\mathbf{p}'/m-\mathbf{P}/M). \quad (9)$$

Since in our problem the mass of the colliding molecules is small compared to that of the Brownian particle while their velocity is much larger than that of the Brownian particle we obtain retaining only lowest powers in m/M and $\mathbf{P}$

$$A=2/mdR^2(2\pi mkT)^{\frac{1}{2}}, \quad (10a)$$

$$\mathbf{B}=8/3MdR^2(2\pi mkT)^{\frac{1}{2}}\mathbf{P}, \quad (10b)$$

$$\boldsymbol{C}=8/3dR^2(2\pi mkT)^{\frac{1}{2}}kT\boldsymbol{I}, \quad (10c)$$

where $\boldsymbol{I}$ is the unit dyadic.

Substituting these values in (7) we obtain

$$\frac{\partial\rho}{\partial t}+\nabla_x\cdot\frac{\mathbf{P}}{M}\rho=\frac{8}{3}dR^2(2\pi mkT)^{\frac{1}{2}}kT\times\left(\frac{3\rho}{MkT}+\frac{\mathbf{P}}{MkT}\cdot\nabla_P\rho+\nabla_P{}^2\rho\right)=\frac{8}{3}dR^2(2\pi mkT)^{\frac{1}{2}}kT\left(\nabla_P\cdot\frac{\mathbf{P}}{MkT}\rho+\nabla_P{}^2\rho\right). \quad (11)$$

Equation (11) is in the form of Chandrasekhar's equation, with a friction constant $\beta=8/3MdR^2(2\pi mkT)^{\frac{1}{2}}$.

II. THE CALCULATION OF THE DISTRIBUTION OF CHANGES OF MOMENTUM OF THE BROWNIAN PARTICLE

Equation (11) has been derived by Chandrasekhar[4] from the assumption that for times Δt short compared to the time to reach equilibrium the distribution of changes of momentum $\Delta\mathbf{P}$ of a Brownian particle with an initial momentum $\mathbf{P}$ is normal, with a mean value $\beta\mathbf{P}\Delta t=8/3MdR^2(2\pi mkT)^{\frac{1}{2}}\mathbf{P}\Delta t$ and a mean square deviation $\beta MkT\Delta t=16dR^2(2\pi mkT)^{\frac{1}{2}}kT\Delta t$. (The distribution of $\Delta\mathbf{P}$ is supposed to be spherically symmetric about its mean value.)

$$\varphi(\Delta\mathbf{P})d\Delta\mathbf{P}=(2\pi\beta MkT\Delta t)^{-\frac{3}{2}}\times\exp-|\Delta\mathbf{P}-\beta\mathbf{P}\Delta t|^2/2\beta MkT\Delta td\Delta\mathbf{P}. \quad (12)$$

[4] S. Chandrasekhar, Revs. Modern Phys. **15**, 2 (1943).

For the particular case with which we are concerned it has been possible to test this assumption by obtaining rigorous estimates of φ. We shall see that the actual distribution $\Delta\mathbf{P}$ differs quite considerably from (12) for times of the order of the average time between collisions. For times long enough for many collisions to have taken place, however, the actual distribution is asymptotic to (12).

Let us consider the phase space of one of the surrounding molecules of the gas. We are interested particularly in that part of it in which the molecule is close to the surface of the Brownian particle, close enough so that it will hit it in short time Δt. We can conveniently use as coordinates in configuration space the length, l, of the perpendicular dropped to the surface of the sphere together with the outward unit normal, $\mathbf{n}$, at the foot of this perpendicular. A molecule near the surface of the Brownian particle will collide with it within a time Δt if the normal component of the relative velocity of the molecule and the Brownian particle is negative and greater in absolute value than $l/\Delta t$,

$$-\mathbf{n}\cdot(\mathbf{p}/m-\mathbf{P}/M)\Delta t>l. \tag{13}$$

The probability that this particular molecule will collide with the Brownian particle is the probability that it be in the part of its phase space which satisfies (13). This probability is

$$-\Delta t\int_{\substack{\text{surface of}\\ \text{sphere}}} dA \int_{\mathbf{n}\cdot(\mathbf{p}/m-\mathbf{P}/M)<0} V^{-1}(2\pi mkT)^{-\frac{3}{2}} \times\exp-\mathbf{p}^2/2mkT\,\mathbf{n}\cdot\left(\frac{\mathbf{p}}{m}-\frac{\mathbf{P}}{M}\right)d\mathbf{p}, \tag{14}$$

where dA is an element of the surface of the sphere, and V is the volume of the space where the molecule is free to move. The average number of collisions, $\bar\nu$, in the time Δt is the average number of molecules whose phases satisfy (13) or N times (14). We have already essentially found the value of (14) in Eqs. (8a) and (10a). We find thus

$$\bar\nu=2/mdR^2(2\pi mkT)^{\frac{1}{2}}\Delta t. \tag{15}$$

The actual number of collisions, ν, or what is the same thing, the actual number of molecules whose phases satisfy (12) may fluctuate from this average value and indeed by relatively large amounts for small $\bar\nu$. Since the phases of the surrounding molecules are independent random variables, and since $\bar\nu$ is small compared to N the distribution of ν will be a poisson distribution.

$$P_\nu=\bar\nu^\nu/\nu!\exp-\bar\nu. \tag{16}$$

In the same way the actual change of momentum of the Brownian particle will be the sum of the changes due to all the molecules in the region which satisfies (13). If we neglect the variation in momentum of the Brownian particles each colliding molecule contributes an amount

$$2m(\mathbf{p}/m-\mathbf{P}/M)\cdot\mathbf{nn}$$

up to the first order in m/M where $\mathbf{P}$ is the momentum of the Brownian particle at the beginning of the interval Δt. This assumption is justified as long as Δt is short compared to the time to reach equilibrium. If at the beginning of the interval Δt there are ν molecules with phases $(\mathbf{n}_i, l_i, \mathbf{p}_i)$ which satisfy (13) the change in momentum of the Brownian particle during the whole interval will be

$$\Delta\mathbf{P}_\nu=\sum_{i=1}^{\nu} 2m\left(\frac{\mathbf{p}_i}{m}-\frac{\mathbf{P}}{M}\right)\cdot\mathbf{n}_i\mathbf{n}_i. \tag{17}$$

We can easily determine the distribution of $\Delta\mathbf{P}_\nu$ since it is the sum of independent random variables. If $\rho_1(\Delta\mathbf{P}_1)$ is the distribution of the change in momentum due to a single collision, and $\rho_\nu(\Delta\mathbf{P}_\nu)$ the distribution of the sum of the change due to ν collisions we have

$$\rho_\nu(\Delta\mathbf{P}_\nu)=\int\rho_1(\mathbf{x}_1)\rho_1(\mathbf{x}_2)\cdots \rho_1(\mathbf{x}_{\nu-1})\rho_1(\Delta\mathbf{P}_\nu-\sum_{r=1}^{\nu-1}\mathbf{x}_r)d\mathbf{x}_1\cdots d\mathbf{x}_{\nu-1}. \tag{18}$$

The total probability of a change in momentum $\rho(\Delta\mathbf{P})$ is

$$\rho(\Delta\mathbf{P})=\sum_{\nu=0}^{\infty}P_\nu\rho_\nu(\Delta\mathbf{P})=\left(\sum_{\nu=0}^{\infty}\frac{\bar\nu_\nu}{\nu!}\rho_\nu(\Delta\mathbf{P})\right)\exp-\bar\nu. \tag{19}$$

This expression has a simple meaning when $\bar\nu$ is small compared to 1, that is to say, when Δt is so short that there is only a small probability that there will be a collision. If there are no molecules whose phase satisfies (13) $\Delta\mathbf{P}$ will certainly be 0 and the first term of (19) will be $\delta(\Delta\mathbf{P})\exp-\bar\nu$ where δ is the Dirac delta-"function." Up to the first order in $\bar\nu$ (19) is

$$\delta(\Delta\mathbf{P})(1-\bar\nu)+\bar\nu\rho_1(\Delta\mathbf{P}). \tag{20}$$

Let us determine $\rho_1(\Delta\mathbf{P})$ explicitly. To do this we note that

$$V^{-1}(2\pi mkT)^{-\frac{3}{2}} \times\exp-(\mathbf{n}\cdot\mathbf{p})^2/2mkT\,1/m(\mathbf{n}\cdot\mathbf{p})R^2d\omega d(\mathbf{n}\cdot\mathbf{p})dt \tag{21}$$

is the probability of a collision which occurs in a part of the surface of the Brownian particle which subtends a solid angle $d\omega$, and in which the normal component of the momentum of the colliding molecule is $\mathbf{n}\cdot\mathbf{p}$. The change of momentum $\Delta\mathbf{P}$, in a single collision, is a function of this normal component and of the normal at the point of collision. The magnitude of $\Delta\mathbf{P}$ is $-2(\mathbf{n}\cdot\mathbf{p}-m/M\mathbf{n}\cdot\mathbf{p})$ while its direction is that of $-\mathbf{n}$. We simply express (21) in terms of $\Delta\mathbf{P}$

$$\begin{aligned}\mathbf{n}\cdot\mathbf{p}&=-(\Delta P/2-m/M\mathbf{n}\cdot\mathbf{P}),\quad d(\mathbf{n}\cdot\mathbf{p})=\tfrac{1}{2}d(\Delta P),\\ &=-(\Delta P/2+m/M\Delta\mathbf{P}\cdot\mathbf{P}/\Delta P),\end{aligned} \tag{22}$$

where ΔP is the magnitude of $\Delta\mathbf{P}$.

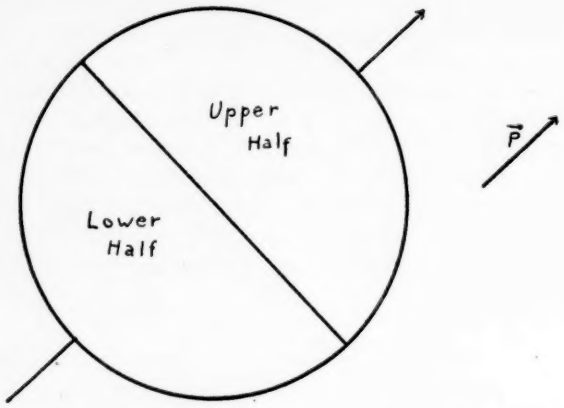

FIG. 1. The two half-spheres of the Brownian particle. The axis of the sphere is in the direction of the momentum vector **P**.

Dividing by a normalizing factor which is the probability of a collision in the interval Δt and by the volume element $\Delta P^2 d\Delta P d\omega$ we obtain for the distribution of the change in momentum due to a single collision

$$(16\pi mkT\Delta P)^{-1} \times \exp-(\tfrac{1}{2}\Delta P + m/M\Delta\mathbf{P}\cdot\mathbf{P}/\Delta P)^2/2mkT. \quad (23)$$

This distribution has a singularity at $\Delta\mathbf{P}=0$. In the neighborhood of $\Delta\mathbf{P}=0$, $\rho_1(\Delta\mathbf{P})$ behaves like

$$\Delta P^{-1} \exp-(m^2/M^2 \cos^2\theta P^2)/2mkT,$$

where θ is the angle between **P** and $\Delta\mathbf{P}$.

For a given value of ΔP the most probable direction of $\Delta\mathbf{P}$ is opposite to **P**. Those collisions which oppose the already existing motion of the Brownian particle are the most probable. If we had not assumed that the momenta of the surrounding molecules are distributed maxwellianly, this would not necessarily be true. It is always true, however, that the mean of $\Delta\mathbf{P}$ is always in the direction of $-\mathbf{P}$. We can see this in the following way. Let us consider the two hemispheres of the Brownian particle whose axis is the direction of **P** (Fig. 1), and let us compare the part of the mean of $\Delta\mathbf{P}$ contributed by collisions with the *same* normal component of momentum of the colliding molecule. Since the distribution of the phases of the molecule must in any case be spacially homogeneous, and isotropic, it is uniformly probable to find the molecule with the given normal component near any part of the surface of the sphere. There will, however, be more probability of a collision, in Δt, on the upper hemisphere than on the lower since the particle moves to meet a molecule in the neighborhood of the upper hemisphere, but moves away from a molecule in the neighborhood of the lower. Moreover, the magnitude of the momentum change of collisions on the upper hemisphere is greater than for the lower, since the absolute value of the normal component of the relatively velocity is greater on the upper hemisphere. Due to these two effects the magnitude of the contributions to the mean change of momentum is greater from the upper hemisphere than from the lower, and since the direction of that from the upper is opposite to **P** the total mean momentum change will be opposite to **P**.

Let us now turn to the investigation of the distribution $\rho(\Delta\mathbf{P})$ of changes of momentum for an average number of collisions which is not small compared to 1. It will be more convenient to work with the fourier transform, or what is called in the mathematical theory of probability the characteristic function,[5] $L(\mathbf{y})$, of this distribution, because this can be expressed very simply in terms of $L_1(\mathbf{y})$ the characteristic function of $\rho_1(\Delta\mathbf{P})$.

From (19) we have

$$L(\mathbf{y}) = \int \exp i\mathbf{y}\cdot\Delta\mathbf{P}\rho(\Delta\mathbf{P})d\Delta\mathbf{P}$$

$$= \exp-\bar{\nu}\sum_{\nu=0}^{\infty}\frac{\bar{\nu}^\nu}{\nu!}\int \exp i\mathbf{y}\cdot\Delta\mathbf{P}\rho_\nu(\Delta\mathbf{P})d\Delta\mathbf{P}.$$

$\rho_\nu(\Delta\mathbf{P})$ however, is the ν-fold Faltung of $\rho_1(\Delta\mathbf{P})$ and using the formula that the characteristic function of the Faltung of a set of functions is the product of their characteristic functions,[5] we have

$$L(y) = \exp-\bar{\nu}\sum_{\nu=0}^{\infty}\frac{\bar{\nu}^\nu}{\nu!}L_1(\mathbf{y})^\nu = \exp\bar{\nu}(L_1(\mathbf{y})-1). \quad (24)$$

If $\bar{\nu}$ is an integer we note that we would have obtained the same formula for $L(\mathbf{y})$ if it were the characteristic function of the sum of $\bar{\nu}$ independent random variables, each having the distribution $\bar{\rho}_1(\Delta\mathbf{P})$ with the characteristic function $\exp(L_1(\mathbf{y})-1)$. Now there is a group of theorems of the mathematical theory of probability called central limit theorems which state that under quite general conditions on $\bar{\rho}_1(\Delta\mathbf{P})$ the distribution of such a sum is asymptotic to a normal distribution as $\bar{\nu}$ goes to infinity. The first and second moments of the normal distribution are the sum of the first and second moments of the component variables. One such theorem states that if $\bar{\rho}_1(\Delta\mathbf{P})$ has finite moments of the first and second orders, the probability that the total momentum changes lies in a certain region of finite volume of $\Delta\mathbf{P}$ space is asymptotic to the probability assigned to such a region by a normal distribution with the above first and second moments. An equivalent condition is that $\exp(L_1(y)-1)$ has finite second derivatives at $\mathbf{y}=0$. As we shall see this last condition is in fact satisfied and the distribution of changes of momentum approaches the normal distribution (12).

The above central limit theorem states that the probability that the momentum change lies in any particular region approaches the probability which would be assigned to the same region by a certain normal distribution. It does not assure us, however, that for a fixed $\bar{\nu}$ the approximation is equally good for all regions, and, indeed, since the singularity of $\rho_1(\Delta\mathbf{P})$ for $\Delta\mathbf{P}=0$

[5] See H. Cramer, *Mathematical Methods of Statistics* (Princeton University Press, Princeton, 1946.)

and since there is always a finite probability for $\Delta\mathbf{P}=0$, there is always a region in the neighborhood of $\Delta\mathbf{P}=0$ in which the normal approximation is very bad. In order to delimit this region more precisely we will need more information about $\rho_1(\Delta\mathbf{P})$ and $L_1(\mathbf{y})$.

Let us calculate $L_1(\mathbf{y})$.

$$L_1(y)=\int \Delta P \exp(i\Delta\mathbf{P}\cdot\mathbf{y})$$
$$\times\exp-(\tfrac{1}{2}\Delta P+m/M\Delta\mathbf{P}\cdot\mathbf{P}/\Delta P)^2/2mkTd\Delta Pd\omega. \quad (25)$$

Since in our problem m/M is a small number it will be convenient to expand $L_1(\mathbf{y})$ in a power series in $\mathbf{P}$ and keep only terms of the zeroth and first order. We have then

$$L_1(\mathbf{y})=\int d\Delta Pd\omega\Delta P\exp(i\Delta\mathbf{P}\cdot y-\Delta P^2/8mkT)$$
$$\times(1-\mathbf{P}\cdot\Delta\mathbf{P}/2mkT+0(\Delta P^2)).$$

We can carry out the integration over $d\omega$ if we call θ the angle between $\mathbf{y}$ and $\Delta\mathbf{P}$, α that between $\mathbf{y}$ and $\mathbf{P}$, and φ the angle that the plane $(\mathbf{y},\Delta\mathbf{P})$ makes with the plane $(\mathbf{y}\cdot\mathbf{P})$ (Fig. 2).

If β is the angle between $\mathbf{P}$ and $\Delta\mathbf{P}$, then by the law of cosines of spherical trigonometry

$$\cos\beta=\cos\theta\cos\alpha+\sin\theta\sin\alpha\cos\varphi.$$

Moreover $d\omega=\sin\theta d\theta d\varphi$. Thus, we obtain

$$L_1(\mathbf{y})=(4mkT)^{-1}\Big\{(1/y-iP\cos\alpha/2mkTy^2)$$
$$\times\int_0^\infty \exp-\Delta P^2/8mkT\sin y\Delta Pd\Delta P$$
$$+iP\cos\alpha/2mkTy\int_0^\infty \Delta P$$
$$\times\exp-\Delta P^2/8mkT\cos y\Delta Pd\Delta P+0(p^2)\Big\}. \quad (26)$$

The second integral on the right is the derivative of the first with respect to y. If we call the first integral $g(y)$, a partial integration shows that the second is $4mkT(1-yg(y))$. In what follows we will need to know $g(y)$ only for very large, and very small values of y. We can derive a power series, everywhere convergent, for $g(y)$ by expanding the sine function in a power series in $y\Delta P$. We can derive a power series, asymptotically convergent in $1/y$, by successive partial integration. In both of these series the error is of the order of the last term dropped.

For small y

$$g(y)=4mkTy-16/3(mkT)^2y^3$$
$$+64/15(mkT)^3y^5+0(y^7). \quad (27a)$$

For large y

$$g(y)=1/y+1/4mkTy^3+0(1/y^5). \quad (27b)$$

We obtain thus

$$L_1(y)=1-i4/3m/MP\cos\alpha y-4/3mkTy^2$$
$$+i32/15m/MP\cos\alpha mkTy^3+0(y^4), \quad (28a)$$
$$L_1(y)=1/4mkT(1/y^2+iP\cos\alpha/MkTy^3+0(1/y^4)). \quad (28b)$$

We can immediately confirm the formulas for the first and second moments of the distribution of $\Delta\mathbf{P}$ which were derived from Rayleigh's partial differential equation. From the definition of $L(\mathbf{y})$ we have

$$\langle\Delta\mathbf{P}\rangle=-i[\nabla_y L(\mathbf{y})]_{y=0}$$
$$\langle\Delta\mathbf{P}\Delta\mathbf{P}\rangle=-[\nabla_y\nabla_y L(\mathbf{y})]_{y=0}$$
$$\nabla_y L(\mathbf{y})=\nabla_y\exp\bar{\nu}(L_1(\mathbf{y})-1)=\bar{\nu}\nabla_y L_1(\mathbf{y})$$
$$\times\exp\bar{\nu}(L_1(y)-1)$$
$$\nabla_y\nabla_y L(\mathbf{y})=[\bar{\nu}\nabla_y\nabla_y L_1(\mathbf{y})+\bar{\nu}^2(\nabla_y L_1(y)^2]$$
$$\times\exp\bar{\nu}(L_1(y)-1). \quad (29)$$

At $\mathbf{y}=0$, $L_1(\mathbf{y})=1$ so

$$\langle\Delta\mathbf{P}\rangle=-i\bar{\nu}[\nabla_y L_1(\mathbf{y})]_{y=0}$$
$$\langle\Delta\mathbf{P}\Delta\mathbf{P}\rangle=-\bar{\nu}[\nabla_y\nabla_y L_1(\mathbf{y})]_{y=0}-\bar{\nu}^2[\nabla_y L_1(\mathbf{y})]^2.$$

For

$$\langle(\Delta\mathbf{P}-\langle\Delta\mathbf{P}\rangle)(\Delta\mathbf{P}-\langle\Delta\mathbf{P}\rangle)\rangle=\langle\Delta\mathbf{P}\Delta\mathbf{P}\rangle-\langle\Delta\mathbf{P}\rangle\langle\Delta\mathbf{P}\rangle,$$

we obtain

$$-\bar{\nu}[\nabla_y\nabla_y L_1(\mathbf{y})]_{y=0}.$$

Remembering that $Py\cos\alpha=\mathbf{P}\cdot\mathbf{y}$

$$[\nabla_y L_1(\mathbf{y})]_{y=0}=-i4/3m/M\mathbf{P}$$
$$[\nabla_y\nabla_y L_1(\mathbf{y})]_{y=0}=-8/3mkT\boldsymbol{I},$$

where $\boldsymbol{I}$ is the unit dyadic. We have, finally,

$$\langle\Delta\mathbf{P}\rangle=-4/3\bar{\nu}m/M\mathbf{P}=-8/3MdR^2(2\pi mkT)^{\frac{1}{2}}\mathbf{P}\Delta t, \quad (30a)$$
$$\langle(\Delta\mathbf{P}-\langle\Delta\mathbf{P}\rangle)(\Delta\mathbf{P}-\langle\Delta\mathbf{P}\rangle)\rangle=8/3\bar{\nu}mkT\boldsymbol{I}$$
$$=16/3dR^2(2\pi mkT)^{\frac{1}{2}}KT\Delta t\boldsymbol{I}. \quad (30b)$$

The method which we will use to determine an asymptotic formula for $\rho(\Delta\mathbf{P})$ parallels that of a proof by Khintchin of the central limit theorem.[6] Our problem

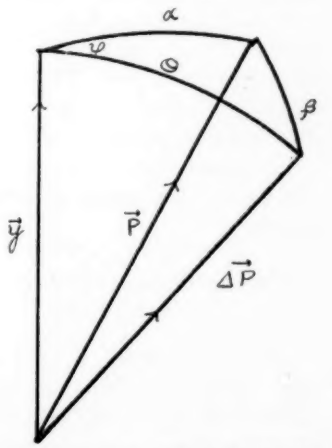

FIG. 2. The spherical triangle formed by the three vectors $\mathbf{y}$, $\mathbf{P}$, $\Delta\mathbf{P}$.

[6] Khintchin, *Mathematical Foundations of Statistical Mechanics* (Dover Publications, New York, 1949).

is to find the distribution whose characteristic function is $L(\mathbf{y})$. By the inversion formula for fourier transforms we have

$$\rho(\Delta\mathbf{P})=(2\pi)^{-3}\int \exp -i\mathbf{y}\cdot\Delta\mathbf{P}L(\mathbf{y})d\mathbf{y}$$

$$=(2\pi)^{-3}\int \exp(-i\mathbf{y}\cdot\Delta\mathbf{P}+\bar{\nu}(L_1(\mathbf{y})-1))d\mathbf{y}. \quad (31)$$

The general idea of the method is to use the approximation (28a) to estimate the characteristic function for small y, and the distribution function for large $\Delta\mathbf{P}$, while using (28b) to estimate the characteristic function for large "y," and the distribution for $\Delta\mathbf{P}$ in the neighborhood of zero. Let us try to determine the region in the integral (31) in which (28a) is a suitable approximation. We have

$$L(y)=\exp[-i\bar{\nu}4/3m/MP\cos\alpha y-4/3\bar{\nu}mkTy^2$$
$$+i\bar{\nu}32/15P\cos\alpha mkTy^3+0(y^4)]$$
$$=\exp[-i\bar{\nu}4/3m/MP\cos\alpha y-4/3\bar{\nu}mkTy^2]$$
$$\times\exp[i\bar{\nu}32/15P\cos\alpha mkTy^3+0(y^4)].$$

Now the first factor is the characteristic function of a normal distribution with mean $-4/3\bar{\nu}m/M\mathbf{P}$ and mean square deviation $4/3\bar{\nu}mkT$. Its absolute value approaches zero very rapidly for $y\gg(\bar{\nu}mkT)^{-\frac{1}{2}}$. The second factor approaches 1 for values of y for which $\bar{\nu}y^3$ approaches zero. This condition will be satisfied and the first factor will be a satisfactory approximation for the range of integration $y<(\bar{\nu}mkT)^{-\frac{1}{3}}\log\bar{\nu}$. We can increase the accuracy of our approximation by expanding the second factor in powers of y.

$$L(\mathbf{y})=\exp(-i\bar{\nu}4/3m/MP\cos\alpha y-4/3\bar{\nu}mkTy^2)$$
$$\times(1+i32/15m/M\bar{\nu}P\cos\alpha mkTy^3$$
$$+16/15\bar{\nu}m^2k^2T^2y^4+0(\bar{\nu}|y|^5+\bar{\nu}^2|y|^2)) \quad (32)$$

for $y<(mkT\bar{\nu})^{-\frac{1}{4}}\log\bar{\nu}$ (Region I).

We note that the diameter of the region where (32) is a satisfactory approximation approaches zero as $\bar{\nu}$ approaches ∞. This region will, however, always contain those values of $\mathbf{y}$ for which $L(\mathbf{y})$ differs significantly from zero. Indeed, at the boundary of the region $y=(\bar{\nu}mkT)^{-\frac{1}{3}}\log\bar{\nu}$, $|L(\mathbf{y})|$ is of the order of $\bar{\nu}^{-4/3}$ which approaches zero as $\bar{\nu}\to\infty$.

Let us turn now to the region where the inverse power series (28b) leads to a suitable approximation to $L(\mathbf{y})$. We have

$$L(\mathbf{y})=\exp-\bar{\nu}\exp\left[\bar{\nu}/4mkTy^2+\frac{i\bar{\nu}\mathbf{P}\cdot\mathbf{y}}{MkTy^4}+0(\bar{\nu}/y^4)\right]. \quad (33)$$

The first factor is the characteristic function of $\exp-\bar{\nu}\delta(\Delta\mathbf{P})$ while the second factor will be very nearly one so long as $\bar{\nu}/4mkTy^2\ll1$. This will certainly be the case for large $\bar{\nu}$ if $y>\bar{\nu}^{\frac{1}{4}}\log\bar{\nu}(mkT)^{\frac{1}{4}}$. As before the approximation may be improved by expanding the second factor. We obtain thus

$$L(\mathbf{y})=\exp-\bar{\nu}+\bar{\nu}\exp-\bar{\nu}\left(1/4mkTy^2\right.$$
$$\left.+\frac{i\mathbf{P}\cdot\mathbf{y}}{4mMk^2T^2y^4}+0(\bar{\nu}/y^4)\right). \quad (34)$$

In the region where (34) is a good approximation $|L(\mathbf{y})|$ is of the order $\exp-\bar{\nu}$ as $\bar{\nu}\to\infty$. Since this region extends to infinity, however, it may give a significant contribution to the distribution $\rho(\Delta\mathbf{P})$ especially when $\Delta\mathbf{P}$ is small.

In the region $\bar{\nu}^{\frac{1}{4}}\log\bar{\nu}(mkT)^{-\frac{1}{4}}>y\gtrsim(\bar{\nu}mkT)^{-\frac{1}{4}}\log\bar{\nu}$, $|L(\mathbf{y})|$ approaches zero exponentially for every value of y since $L_1(y)-1$ has a negative real part. While the volume of this region goes to infinity as $\bar{\nu}\to\infty$, the magnitude of the integrand is so small that it does not make a significant contribution to $\rho(\Delta\mathbf{P})$. It will be convenient to divide this region into two parts.

$$\bar{\nu}^{\frac{1}{4}}\log\bar{\nu}(mkT)^{-\frac{1}{4}}>y\gtrsim\delta \quad \text{(Region III)}$$

$$\delta>y\gtrsim(\bar{\nu}mkT)^{-\frac{1}{4}}\log\bar{\nu} \quad \text{(Region IV)}$$

where δ is a suitable chosen number independent of $\bar{\nu}$. In region III there is always a positive constant b, independent of $\bar{\nu}$ such that

$$|L(\mathbf{y})|<\exp-b\bar{\nu}.$$

This is a consequence of the fact that $|L_1(\mathbf{y})|<1$ for $y\neq0$, $|L_1(\mathbf{y})|\to0$ as $y\to\infty$ and the $L_1(\mathbf{y})$ is continuous for all $\mathbf{y}$. We cannot make such an estimate of $|L(\mathbf{y})|$ in region IV because the lower boundary of this region approaches zero as $\bar{\nu}\to\infty$, and we would have to make b smaller and smaller as $\bar{\nu}\to\infty$. We now choose δ so that for $y<\delta$

$$|L(\mathbf{y})|=|\exp\bar{\nu}(L_1(\mathbf{y})-1)|<\exp-\tfrac{2}{3}\bar{\nu}mkTy^2.$$

Since the dominant term in $L_1(\mathbf{y})-1$ for small y is $-4/3mkTy^2$, this will be the case when the absolute value of the higher order terms in $L_1(\mathbf{y})-1$ is less than $\frac{1}{2}$ of the dominant term which can certainly be achieved for small enough δ.

$\rho(\Delta\mathbf{P})$ will be the sum of four terms.

$$\rho(\Delta\mathbf{P})=K_I+K_{II}+K_{III}+K_{IV}, \quad (35)$$

$$K_I=\frac{1}{8\pi^3}\int_{\text{Region I}}\exp(-i\Delta\mathbf{P}\cdot\mathbf{y}+\bar{\nu}(L_1(\mathbf{y}^1-1))d\mathbf{y}$$

$$K_{II}=\frac{1}{8\pi^3}\int_{\text{Region II}}$$

$$K_{III}=\frac{1}{8\pi^3}\int_{\text{Region III}}$$

$$K_{IV}=\frac{1}{8\pi^3}\int_{\text{Region IV}}.$$

For K_I we will use the approximation (32) for $L(\mathbf{y})$. Since the domain of integration extends well beyond the region where the absolute value of the integrand differs appreciably from zero, we may conveniently extend the domain of integration to infinity and estimate the additional terms introduced thereby. We have to evaluate

$$\int_{y<\infty} \exp -i(\mathbf{\Delta P}+4/3\bar{\nu}m/M\mathbf{P})\cdot\mathbf{y} \times\{1+i32/15m/M\bar{\nu}\mathbf{P}\cdot\mathbf{y}y^2+16/15\bar{\nu}mkTy^4 +0(\bar{\nu}|y|^5+\bar{\nu}^2|y|^3)\}d\mathbf{y}. \quad (36)$$

The contribution of the last two terms in the brackets is less than

$$\int_{y<\infty} \exp -4/3\bar{\nu}mkTy^2(\bar{\nu}|y|^5+\bar{\nu}^2|y|^3)d\mathbf{y}=0(1/\bar{\nu}^3).$$

The contribution of the first term is simply

$$(2\pi\bar{\nu}mkT)^{-\frac{3}{2}} \exp -(\mathbf{\Delta P}+4/3\bar{\nu}m/M\mathbf{P})^2/16/3\bar{\nu}mkT =\rho_0(\mathbf{\Delta P}).$$

The contributions of the second and third terms may be evaluated from successive differentiations with respect to the components of $\mathbf{\Delta P}$. We have then for the integral (35)

$$(1+3/15m/M\bar{\nu}mkT\mathbf{P}\cdot\nabla_{\mathbf{\Delta P}}\nabla_{\mathbf{\Delta P}}{}^2+16/15\bar{\nu}m^2k^2T^2 +\nabla_{\mathbf{\Delta P}}{}^2\nabla_{\mathbf{\Delta P}}{}^2)\rho_0(\mathbf{\Delta P})+0(1/\bar{\nu}^3)$$
$$=\rho_0(\mathbf{\Delta P})[1+3/16\mathbf{P}\cdot\mathbf{\Delta P}/\bar{\nu}mkT(5-\Delta P^2/8/3\bar{\nu}mkT) +3/20\bar{\nu}(15-10\Delta P^2/8/3\bar{\nu}mkT+\Delta P^4/(8/3\bar{\nu}mkT)^2)] +0(1/\bar{\nu}^3).$$

The error introduced by extending the region of integration to infinity is of an order less than $\exp -\frac{1}{4}\log^2\bar{\nu}$ for large $\bar{\nu}$.

For K_{II} we will use the approximation (34). We have for the contribution from this region

$$1/8\pi^3 \int_{y>\bar{\nu}^{\frac{1}{3}}\log\bar{\nu}(mkT)^{-\frac{1}{2}}} d\mathbf{y}\left(\exp-\bar{\nu}+\bar{\nu}\exp-\bar{\nu}/4mkTy^2 +\bar{\nu}\exp-\bar{\nu}\cdot\frac{i\mathbf{P}\cdot\mathbf{y}}{4Mmk^2T^2y^4}+0\left(\frac{\bar{\nu}\exp-\bar{\nu}}{y^4}\right)\right).$$

In the first term we will extend the region of integration to include the whole space. The error introduced thereby is less than

$$\exp-\bar{\nu}\int_{y<\bar{\nu}^{\frac{1}{3}}\log\bar{\nu}(mkT)^{\frac{1}{2}}} d\mathbf{y}=4/3\pi\bar{\nu}^{\frac{1}{2}}(mkT)^{-\frac{3}{2}}\log\bar{\nu}^3\exp-\bar{\nu},$$

which approaches zero faster than any negative power of $\bar{\nu}$. The first term yields

$$\exp-\bar{\nu}\delta(\mathbf{\Delta P})+0(\bar{\nu}^{\frac{3}{2}}(\log\bar{\nu})^3\exp-\bar{\nu}).$$

The second term is

$$\frac{1}{8\pi^3}\frac{\bar{\nu}\exp-\bar{\nu}}{4mkT}\int_{y>\bar{\nu}^{\frac{1}{3}}\log\bar{\nu}(mkT)^{-\frac{1}{2}}} dy\int_0^{\pi}d\theta\int_0^{2\pi}d\varphi \times\exp(-iy\Delta P\cos\theta)\sin\theta$$
$$=\frac{1}{8\pi^3}\frac{\bar{\nu}\exp-\bar{\nu}}{4mkT}\cdot 4\pi\cdot\int_{y>\bar{\nu}^{\frac{1}{3}}(mkT)^{-\frac{1}{2}}\log\bar{\nu}}\frac{\sin y\Delta P}{y\Delta P}dy$$
$$=\frac{1}{8\pi^2}\frac{\bar{\nu}\exp-\bar{\nu}}{mkT}\cdot\frac{1}{\Delta P}\int_{z>\Delta P\bar{\nu}^{\frac{1}{3}}(mkT)^{-\frac{1}{2}}\log\bar{\nu}}\frac{\sin z}{z}dz.$$

If we use the same notation as was used in the derivation of Eq. (26) the third term is

$$-\frac{1}{8\pi^3}\frac{\bar{\nu}\exp-\bar{\nu}}{4mkT}\frac{P\cos\beta}{MkT}\cdot 4\pi\int_{\bar{\nu}^{\frac{1}{3}}\log\bar{\nu}\Delta P(mkT)^{-\frac{1}{2}}}^{\infty}\frac{\sin z-z\cos z}{z}dz.$$

The integral approaches the limit $\pi/2$ when $\Delta P\to 0$ and is bounded for all ΔP. For $\Delta P=0$ this term is $-\bar{\nu}\exp-\bar{\nu}/16\pi mkT\mathbf{P}\cdot\mathbf{\Delta P}/\Delta P$ and is of order $\bar{\nu}\exp-\bar{\nu}$ for all ΔP.

The fourth term is of the order

$$\bar{\nu}^2\exp-\bar{\nu}\int_{\bar{\nu}^{\frac{1}{3}}\log\bar{\nu}(mkT)^{-\frac{1}{2}}}^{\infty}dy/y^2=0(\bar{\nu}^{-\frac{1}{3}}\exp-\bar{\nu}/\log\bar{\nu}).$$

For K_{III} and K_{IV} we will not need to determine the dependence on ΔP, but simply show that they both approach zero faster than any negative power of $\bar{\nu}$.

$$K_{III}\leqq 1/8\pi^3\int_{\bar{\nu}^{\frac{1}{3}}\log\bar{\nu}(mkT)^{-\frac{1}{2}}>y\geqq\delta}\exp-|b|\bar{\nu}dy =0(\exp-|b|\bar{\nu}\bar{\nu}^{\frac{1}{3}}\log\bar{\nu}),$$

$$K_{IV}\leqq\int_{\delta>y\geqq\log\bar{\nu}(\bar{\nu}mkT)^{-\frac{1}{2}}}\exp-\tfrac{2}{3}\bar{\nu}mkTy^2dy,$$
$$\leqq\int_{\infty>y>\log\bar{\nu}(\bar{\nu}mkT)^{-\frac{1}{2}}}\exp-\tfrac{2}{3}|b|\bar{\nu}mkTy^2d\mathbf{y} =0(\exp-\tfrac{1}{3}\log^2\bar{\nu}),$$

which approaches zero faster than any negative power of $\bar{\nu}$.

Collecting all our estimates together we have

$$\rho(\Delta\mathbf{P})=\rho_0(\Delta\mathbf{P})\Big(1+\frac{3}{10}\frac{1}{\bar\nu}\frac{\mathbf{P}\cdot\Delta\mathbf{P}}{MkT}\Big(5-\frac{\Delta P^2}{8/3mkT}\Big)$$
$$+\frac{3}{20}\frac{1}{\bar\nu}\Big(15-10\frac{\Delta P^2}{8/3mkT}+\frac{\Delta P^4}{(8/3mkT)^2}\Big)\Big)$$
$$+\exp-\bar\nu\delta(\Delta\mathbf{P})+\frac{\bar\nu\exp-\bar\nu}{8\pi^2mkT}\frac{1}{\Delta P}$$
$$\times\int_{z=\bar\nu^{\frac12}\log\bar\nu(mkT)^{-\frac12}\Delta P}\frac{\sin z}{z}dz+0(1/\bar\nu^{\frac12}). \quad (37)$$

We note that while the term $0(1/\bar\nu^{\frac12})$ in our estimate of $\rho(\Delta\mathbf{P})$ approaches zero for large $\bar\nu$ it is a constant for any given value of $\bar\nu$. This means that our estimate may be relatively quite bad for large ΔP since we know that $\rho(\Delta\mathbf{P})$ must approach zero for large ΔP. By considering the ratio between the magnitude of our estimate for large ΔP and the $0(1/\bar\nu^{\frac12})$ term we see that we have a good estimate if $\Delta\mathbf{P}$ is confined to a sphere of radius $R(\bar\nu)$ which approaches infinity slower than $(\log\bar\nu)^{\frac12}$.

On the other hand for ΔP in the neighborhood of zero $\rho(\Delta\mathbf{P})$ becomes infinite. The first singular term is a delta-function and represents the finite probability for no collision to have taken place. In order that the second singular term should be of the order of the rest of the estimate

$$\Delta P\sim\bar\nu^2\exp-\bar\nu(1-1/3m/MP^2/mkT)(8/3mkT)^{\frac12}$$

or less.

We can summarize our analysis of the distribution of changes of momentum of a Brownian particle in a gas of noninteracting particles by the statement that this distribution approaches

$$\rho_0(\Delta\mathbf{P})=(16/3\pi\bar\nu mkT)^{-\frac12}$$
$$\times\exp-(\Delta\mathbf{P}+4/3m/M\bar\nu\mathbf{P})^2/16/3\bar\nu mkT$$

asymptotically, but the ratio of the true distribution to the asymptotic limit approaches 1 nonuniformly. The convergence is slow in the neighborhood of $\Delta\mathbf{P}=0$ and in the neighborhood of $\Delta\mathbf{P}=\infty$.

III. KIRKWOOD'S FORMULA FOR THE FRICTION CONSTANT

The method of Lord Rayleigh, and the method we used to derive the distribution of changes of momentum are both applicable only to the particular case where the Brownian motion can be analyzed in terms of independent collisions. Kirkwood's analysis of Brownian motion is designed to apply generally. The purpose of this section is to show that Kirkwood's formula[7] for the friction constant leads to the same result as both previous methods.

This formula is

$$\beta=1/3MkT\int_{-\tau}^{0}\overline{\mathbf{F}(0)\cdot\mathbf{F}(S)}dS, \quad (38)$$

where $\mathbf{F}(0)$ is the force on the Brownian particle at some particular phase of the system Brownian particle plus surrounding molecules, $\mathbf{F}(S)$ is the force on the particle S seconds later, τ is a suitably chosen time, and the bar means averaging over all the particular initial phases of the surrounding molecules, which are supposed to be distributed as they would be in an equilibrium ensemble.

The force on the Brownian particle is in our case the sum of forces due to individual molecules.

$$\mathbf{F}(0)=\sum_i\mathbf{F}_i(0)$$
$$\mathbf{F}(S)=\sum_i\mathbf{F}_i(S) \qquad i=1\cdots N, \quad (39)$$

where $\mathbf{F}_i(S)$ is the force on the Brownian particle due to the ith molecule at time S, and N is the total number of molecules. We have

$$\beta=\frac{1}{3MkT}\Big(\sum_i\int_{-\tau}^{0}\overline{\mathbf{F}_i(0)\cdot\mathbf{F}_i(S)}dS$$
$$+\sum_{i\neq j}\int_{-\tau}^{0}\overline{\mathbf{F}_i(0)\cdot\mathbf{F}_j(S)}dS\Big). \quad (40)$$

Now for every configuration in which a molecule is colliding with the Brownian particle we will get a contribution to the first group of terms of $F^2\theta$ where F is some representative value of the force, and θ the time of collision. Since we have assumed that the time of collision is short compared to the time between collisions, the average number of molecules colliding the Brownian particle will be some number, n, much less than one. The total contribution of the first group of terms will be of the order $nF^2\theta$. Similarly for each configuration in which a molecule is colliding with the Brownian particle there will be a contribution to the second group of terms of $F^2\theta$, only if another molecule has collided less than τ seconds earlier. For each such configuration there will be a total contribution of $F^2\theta\bar\nu$ where $\bar\nu$ is the average number of collisions in the time τ, or $nF^2\theta\bar\nu$ for all the n molecules which are on the average colliding at one time. If we choose τ to be longer than the time of collision but short enough so that $\bar\nu$ is small compared to one, the integral in the definition of β will have a plateau value, i.e., it will have practically the same value for all possible τ's such that τ more than the time of collision but very small compared to the time between collisions. In order to evaluate this plateau value we need consider only the first group of terms.

[7] J. G. Kirkwood, J. Chem. Phys. 14, 180 (1946).

Taking these remarks into consideration we see that we have simplified our problem very considerably. We have reduced the integrand defining β to a group of terms each of which depends only on the phase of a single molecule. We can immediately carry out the integration over S and write

$$\beta=\frac{N}{3MkT}\overline{\mathbf{F}(0)\cdot\Delta\mathbf{P}}, \tag{41}$$

where $\Delta\mathbf{P}$ is the change in momentum of the Brownian particle from $-\tau$ (which is long before the collision starts) to the time zero. The bar now means averaging over the phases of a single molecule.

Let us consider the mechanism of a collision. In order to simplify the further calculations we will suppose that the Brownian particle is originally at rest and that its mean is so large that we can neglect its motion during any one collision. We must now make some explicit assumptions about the potential of the interaction between the molecule and the Brownian particle. We suppose that it is normal to the surface of the Brownian particle, that it is infinite at this surface, and that it drops off rapidly to zero within a distance small compared to the radius. It will be convenient to express this potential in terms of the normal distance X to the surface, $V(X)$. By the principle of the conservation of momentum the change of momentum of the Brownian particle is equal and opposite to that of the molecule, and in what follows we need concern ourselves only with the motion of the molecule.

As a molecule enters the region where $V(X)$ is different from zero its direction of its motion starts to change As it approaches the surface of the Brownian particle the direction changes more and more quickly until it is such as to increase rather than decrease the mutual distance of the two bodies. This mutual distance increases until it has left the region where $V(X)$ differs from zero and thereafter travels with a constant velocity, different from its original velocity. Since the region where $V(X)$ is different from zero is very thin compared to the radius of the molecule, the normal from the point where the molecule entered this region will be practically parallel to that from the point where it left the region. If we call the perpendicular from the point of closest approach the normal at the point of contact we can consider the force acting on the molecule to be parallel to the normal at the point of constant. Any change of momentum of the molecule will be parallel to the normal to the point of contact. If we call $\mathbf{n}$ the unit outward normal at the point of contact and $p_n(t)$ the normal component of the momentum of the molecule we have, by the principle of the conservation of energy;

$$p_n^2(0)/2m+V(X(0))=p_n^2(-\tau)/2m. \tag{42}$$

In (42) we have taken account of the fact that τ is larger than the representative time of a collision and $V(X(-\tau))$ is zero. The normal component of the change of momentum of the molecule is

$$p_n(0)-p_n(-\tau)=p_n(0)+\left(2m\left(\frac{p_n^2(0)}{2m}+V(X(0))\right)\right)^{\frac{1}{2}},$$

where we have taken the negative sign in the square root because $p_n(-\tau)$ must be negative if a collision is to take place at a later time. We have then for the change of momentum of the Brownian particle,

$$\Delta\mathbf{P}=-\mathbf{n}\left[p_n(0)+\left(2m\left(\frac{p_n^2(0)}{2m}+V(X(0))\right)\right)^{\frac{1}{2}}\right]. \tag{43}$$

Then

$$\beta=\frac{N}{3MkT}\frac{\int\frac{dV}{dX}\left[p_n+\left(2m\left(\frac{p_n^2}{2m}+V(X)\right)\right)^{\frac{1}{2}}\right]\exp-\left(\frac{\mathbf{p}^2}{2m}+V(X)\right)\Big/kTd\mathbf{p}dv}{\int\exp-\left(\frac{\mathbf{p}^2}{2m}+V(X)\right)\Big/kTd\mathbf{p}dv}, \tag{44}$$

where we have substituted $-\mathbf{n}dV/dX$ for $\mathbf{F}(0)$ and have written p_n for $p_n(0)$, X for $X(0)$. dv is the volume element in configuration space and $\mathbf{p}$ is the momentum vector of the molecule at time zero. In (44) we observe immediately that the term p_n in the parentheses contributes nothing to the integral because positive and negative normal components at time zero are equally probable.

Because the factor dV/dX is zero a short distance from the surface of the Brownian particle we may conveniently use $dAdX$ for the volume element in the integral in the numerator of (44) where dA is an element of the surface of the particle. Carrying out the integration over the tangential components of the momentum in the numerator and over the whole phase space in the denominator we have

$$\beta=\frac{N}{3MkTv}(2\pi mkT)^{-\frac{1}{2}}\times\int\frac{dV}{dX}\left(2m\left(\frac{p_n^2}{2m}+V(X)\right)\right)^{\frac{1}{2}}\times\exp-\left(\frac{p_n^2}{2m}+V(X)\right)\Big/kTdp_ndXdA, \tag{45}$$

where v is

$$\int \exp -V(X)/kTdv$$

and is practically equal to the volume outside of the Brownian particle. We change the variables in (45) to

$$E=p_n^2/2m+V(X) \qquad dV/dXdXdp_n=dEdp_n$$
$$p_n=p_n$$

$$\beta=N/3MkTv(2m)^{\frac{1}{2}}/(2\pi mkT)^{\frac{1}{2}} \times \int dA \int_{-\infty}^{+\infty} dp_n \int_{p_n^2/2m}^{\infty} (E)^{\frac{1}{2}} \exp -E/kTdE \quad (46)$$

since $E=\infty$ when $X=0$ and $E=p^2/2$ $m$when $X=\infty$. If we integrate over dA and reverse the order of the remaining integrations we obtain

$$\beta=N/3MkTv(2\pi mkT)^{-\frac{1}{2}}\cdot 4\pi R^2 \cdot 2m\cdot 2\int_0^{\infty} E\exp -E/kTdE$$
$$=16d/3MkT\pi R^2(2\pi mkT)^{-\frac{1}{2}}mk^2T^2$$
$$=8/3MdR^2(2\pi mkT)^{\frac{1}{2}}kT, \quad (47)$$

which coincides with the value obtained in parts I and II.

BIBLIOGRAPHIC NOTE

The problem of the motion of a particle in a gas of noninteracting molecules was apparently first discussed by Lord Rayleigh in the reference cited. The method he used was essentially the same as ours, but the particle and the molecules of the gas were constrained to move in one dimension. The three-dimensional case was discussed by Smoluchowski[6] in one of the earliest papers in which the true nature of Brownian motion was understood. His method was admittedly approximate and the formula which he obtained for the friction constant was the same as ours in its dependence on the temperature of the gas, the mass of the particle and the mass, and concentration of the molecules, but with a different, and incorrect numerical constant. The correct formula was obtained by H. A. Lorentz[8] by a method which was equivalent to our modification of Rayleigh's method.

As stated above, the idealized case considered in this paper has an experimental realization in Brownian motion in a real gas in which the mean free path of the molecules is large compared to the size of the particle. Millikan[9] observed the friction constant for charged oil droplets for a wide range of pressure in air, and obtained the following empirical formula:

$$M\beta=6\pi\eta R(1+l/R(.824+.32\exp -1.54R/l))^{-1},$$

where η is the viscosity of the gas, R the radius, and M the mass of the particle, and l the mean free path. For $l \ll R$ the formula approaches the Einstein formula. For $l \gg R$ it approaches

$$16.47\eta R^2/l.$$

Using the formula of the kinetic theory of gases

$$\eta=.558d(mkT)^{\frac{1}{2}}lM^{-1}$$
$$\beta_{l/R\to\infty}=9.04dR^2(mkT)^{\frac{1}{2}}M^{-1}.$$

The formula given above gives

$$8/3(2\pi)^{\frac{1}{2}}dR^2(mkT)^{\frac{1}{2}}M^{-1}=6.66dR^2(mkT)^{\frac{1}{2}}M^{-1}.$$

The limiting formula obtained by Millikan thus gives a rather larger value for the friction constant than our formula. We can interpret this result as meaning that the surface of an oil droplet is somewhat rougher with respect to a diatomic gas than the surface of an ideal hard sphere with respect to monatomic molecules.

ACKNOWLEDGMENT

I wish to thank Professor E. P. Wigner, who pointed out the interest of the present problem, and Professor J. G. Kirkwood who read and commented on the manuscript.

[8] H. A. Lorentz, *Les Theories Statistiques en Thermodynamique* (B. G. Teubner, Leipzig, 1912).
[9] R. A. Millikan, Phys. Rev. **1**, 218 (1913).

THE JOURNAL OF CHEMICAL PHYSICS VOLUME 19, NUMBER 8 AUGUST, 1951

The Rate Equation of Ammonia-Synthesis on Iron-Type Catalysts of Different Composition*

R. BRILL
Polytechnic Institute of Brooklyn, Brooklyn, New York,
AND
Research Department, Phillips Petroleum Company, Bartlesville, Oklahoma
(Received April 2, 1951)

Investigations on the rate equation of ammonia synthesis on iron catalysts have been carried out. The results agree in a general way with the rate equation of Temkin and Pyzhev. An improvement of this equation is given, which leads to a better agreement between observed and calculated synthesis rates. Experiments carried out at low temperatures show that the rate equation is the same for the three catalysts which have been investigated: (1) pure iron, (2) iron containing 3 percent alumina, and (3) iron containing 3 percent alumina and 2 percent potassium oxide. By means of the improved Temkin and Pyzhev equation a formal explanation can be given for the results obtained by Love and Emmett on ammonia decomposition on a singly promoted iron catalyst between 400 and 450C.

FOR the decomposition of ammonia on iron catalysts, different rate equations have been given,[1,2] and by Love and Emmett[3] it was shown that the rate of ammonia decomposition on an iron synthetic ammonia catalyst (No. 931) containing 1.3 percent alumina and 1.6 percent potassium oxide especially is given by

$$-\frac{dp_{NH_3}}{dt}=k\frac{p_{NH_3}{}^{0.60}}{p_{H_2}{}^{0.85}}. \tag{1}$$

It is stated in a paper of Emmett and Kummer[4] that the decomposition kinetics on an iron catalyst which contains only alumina are quite different from those on a catalyst containing potassium also.

For the rate of formation of ammonia on iron catalysts the following equation was given by Temkin and Pyzhev:[5]

$$\frac{dp_{NH_3}}{dt}=k_1\frac{p_{N_2}p_{H_2}{}^{1.5}}{p_{NH_3}}-k_2\frac{p_{NH_3}}{p_{H_2}{}^{1.5}}. \tag{2}$$

This formula has been explained by these authors using the equation of Zeldowitsch[6] for the rates of adsorption and desorption of gases on surfaces.† But, in agreement with the experiments on ammonia decomposition, the validity of Eq. (2) seems to be restricted to doubly promoted catalysts according to Emmett and Kummer.[4]

The following experiments have been carried out with the intention of studying further the influence of the composition of the catalyst on the mechanism of reaction.

EXPERIMENTAL

The experiments were made at atmospheric pressure in the following way:

Pure ammonia was liquified and redistilled several times. Then it was evaporated, and the gas was led at 1000°C over an ammonia catalyst. In this way a gas mixture was obtained containing N_2 and H_2 in the ratio 1:3. This mixture was carefully purified by passing it through a solution of phosphoric acid to get rid of the small amount of ammonia which was still in the gas after the decomposition. Then the gas was dried by silica gel at room temperature and, in addition, by silica gel in three liquid air traps which were put in series.

The purified gas was used for ammonia synthesis. The catalyst was located in a Pyrex glass tube placed in a bath of molten metal alloy, the temperature of which was kept constant within a range of ±0.1°C. The temperature was measured by thermocouples in the metal bath as well as in the catalyst.

The flow rate was measured by manometers and checked by measuring the total amount of gas which passed the catalyst during one experiment by means of an accurate gasmeter (1 cycle per liter). The amount of ammonia which is formed was measured by leading the gas through a gas scrubber which was filled with a given amount of HCl solution of a known concentration and determining the time which was necessary to use up the acid.

The measurements were carried out on three different catalysts: (1) pure iron, (2) iron containing 3 percent alumina, and (3) iron containing 3 percent alumina and 2 percent potassium oxide. All those catalysts were prepared by fusing iron, or a mixture of iron and alumina, or alumina and potassium nitrate, in a stream of oxygen and reducing them at 450°C by the nitrogen-hydrogen

* Experiments carried out by W. Hennige.
[1] E. Winter, J. Phys. Chem. B **13**, 401 (1931).
[2] C. H. Hinshelwood and H. Burk, J. Chem. Soc. **127**, 1105 (1925).
[3] K. S. Love and P. H. Emmett, J. Am. Chem. Soc. **63**, 3297.
[4] P. H. Emmett and J. T. Kummer, Ind. Eng. Chem. **35**, 677 (1943).
[5] M. I. Temkin and V. Pyzhev, Acta Physicochim. U. R. S. S. **12**, 327 (1940).
[6] J. Zeldowitsch, Acta Physicochim. U. R. S. S. **1**, 449 (1934).
† This procedure is critically treated in some papers by Emmett, Brunauer, and co-workers (see, for example, references 4 and 5); and also by A. Eucken in *Lehrbuch der Chemischen Physik* (Leipzig, 1944), Vol. II, 2, p. 1459 ff, so that it seems to be superfluous to go into this matter here.

TABLE I. Rate constants $2k_1$ for ammonia synthesis.

Catalyst	Fe-Al-K				Fe-Al				Fe			
temperature	317°		324°		321°		318°		317°		314°		321°	
Flow rate in 1/hr \ Column no.	1		2		3		4		5		6		7	
	% NH_3	$2k_1 \cdot 10^4$	% NH_3	$2k_1 \cdot 10^4$	% NH_3	$2k_1 \cdot 10^4$	% NH_3	$2k_1 \cdot 10^4$	% NH_3	$2k_1 \cdot 10^4$	% NH_3	$2k_1 \cdot 10^4$	% NH_3	$2k_1 \cdot 10^4$
14	0.212	1.38	0.212	1.13	0.238	1.38	0.221	1.19	0.203	0.94	0.159	0.61	0.132	0.42
12	...	...	...	...	0.253	1.34	...	...	0.221	0.96	...	...	0.138	0.39
10	...	...	...	...	0.283	1.40	...	...	0.241	0.94	...	...	0.148	0.38
8	0.272	1.05	0.275	1.08	0.297	1.23	0.263	0.96	0.250	0.82	0.180	0.45	0.164	0.37
6	0.302	0.90	0.308	1.01	0.340	1.23	0.285	0.85	0.284	0.79	0.195	0.39	0.190	0.37
4	0.367	0.89	0.378	1.02	0.407	1.19	0.362	0.93	0.344	0.78	0.243	0.41	0.227	0.36
Mean value		1.06 ±0.10		1.06 ±0.02		1.30 ±0.03		0.98 ±0.07		0.87 ±0.03		0.47 ±0.04		0.38 ±0.008
Mean error (percent)		9.4		2.3		2.5		6.7		3.6		8.8		2.1

mixture which was used for synthesis. Here 1 cm^3 of catalyst was used, and the flow rate of the nitrogen-hydrogen mixture during the reduction was 4 1/hr. The reduction period, i.e., the time within which the maximum yield at 450° was reached, depended very much upon the composition of the catalyst and amounted to from 20–80 hr.

The experiments were carried out at relatively low temperatures of about 320°C, because some preliminary measurements on the dependency of the rate constant upon the temperatures have shown that at elevated temperatures (450–500°) the rate of reaction becomes abnormal. This seems to indicate that at higher temperatures diffusion processes become rate determining.

The pure iron catalyst was investigated, because it was found, in 1938, by Dr. Hammacher and myself‡ that, in contradiction to the then-known facts, under the experimental conditions described above pure iron retains its catalytic activity for a very long time even at 450°C. The reason for this fact seems to be that the synthesis gases were very pure. Indeed, it could be shown that by the presence of traces of catalyst poisons (e.g., H_2S) this catalyst is poisoned very fast, whereas the aluminum containing catalyst is still active.

RESULTS

Some orienting measurements yielded the results given in Table I. Different rate equations were tried, but the best agreement was obtained by using the integration of Eq. (2). The values of k_1 calculated from the data with Eq. (2) are shown in Table I. From this table it is to be seen that the constancy of the values obtained for the rate constant at various flow rates of the synthesis gas is of the same order of accuracy for all the investigated catalysts of different composition. Therefore, to the extent indicated by the constancy of those values, it may be stated that all catalysts obey the Temkin Pyzhev equation at these low temperatures between 314 and 321°C. That would mean that the mechanism of reaction is the same for all these catalysts at 314 to 321° and also the same as for the doubly promoted catalysts at higher temperatures (400–450°C) where other authors have observed the validity of the Temkin and Pyzhev equation for this catalyst.[5,7,8] This result restricts the statement made by Emmett and Kummer,[4] that the theory of Temkin and Pyzhev does not seem to apply to catalysts singly promoted with alumina, to higher temperatures.

It is evident from Table I that the rate constants show a trend with the flow rate. All values obtained at lower flow rates are smaller than the values obtained at larger flow rates. This does not seem to be accidental, because experiments carried out with a high accuracy showed the same behavior (see Table II; X = measured ammonia pressure/ammonia pressure at equilibrium). Since the measurements with high flow rate were always carried out first, the higher activities at higher flow rates might appear due to a lowering of activity of the catalysts during an experiment. But this cannot be the case for the following reasons: (a) the activity of a catalyst is constant for a very long time and does not decrease appreciably during several hours; (b) the values given in column 2, Table I, are mean values of measurements on the same catalyst taken on two successive days (August 18 and 19, 1943). The single values, which were measured, are given here:

	Experiment on August 18, 1943			Experiment on August 19, 1943		
Flow rate (1/hr)	% NH_3	X	$2k_1 \cdot 10^4$	% NH_3	X	$2k_1 \cdot 10^4$
14	0.216	0.168	1.13	0.214	0.167	1.12
8	0.276	0.215	1.06	0.275	0.215	1.05
6	0.309	0.241	1.01	0.308	0.240	1.00
4	0.378	0.295	1.02	0.378	0.295	1.02.

‡ This result was not published until now.

[7] P. H. Emmett and Brunauer, J. Am. Chem. Soc. **56**, 35 (1934).
[8] Brunauer, Love, and Keenan, J. Am. Chem. Soc. **64**, 751 (1942).

The differences at the same flow rate are within the limit of error, and it is quite certain that no activity change takes place in the case of the doubly promoted catalyst.

In the case of the other two catalysts of Table I, one certainly gets the impression that the low k-value at the end of the one experiment is identical with the value at the start of the next one (see Table I, columns 4, 5 and 6, 7). But this should be purely accidental, because the experiments in columns 4 and 5 were carried out with different catalysts of the same composition; the same holds for the experiments in columns 6 and 7.

So the trend is present and indicates that while Eq. (2) may be a good approximation, it is not correct in this form. If one tries other rate equations (e.g., $dp_{NH_3}/dt = k_1 \cdot p_{N_2}{}^{0.5} \cdot p_{H_2}{}^{1.5} - k_2 p_{NH_3}$ or $dp_{NH_3}/dt = k_1 p_{N_2} \cdot p_{H_2}{}^3 - k_2 \cdot p_{NH_3}{}^2$) leading to k_1 proportional to

$$\ln[1/(1-X)] \quad \text{or} \quad \ln[(1+X)/(1-X)],$$

the trend gets larger. The integration of Eq. (2) leads to an expression

$$k_1 \sim (1/t) \ln[1/(1-X^2)].$$

Now if one writes this equation in a more general form,

$$k_1 \sim (1/t) \ln[1/(1-X^n)],$$

then n-values can be found between 2 and 2.5 by trial which give constants without a trend. This means that the equation of Temkin and Pyzhev can be put in a more general form:

$$\frac{dp_{NH_3}}{dt} = k_1 \left(\frac{p_{N_2}{}^{0.5} \cdot p_{H_2}{}^{0.75}}{p_{NH_3}{}^{0.5}} \right)^n - k_2 \left(\frac{p_{NH_3}{}^{0.5}}{p_{H_2}{}^{0.75}} \right)^n . \quad (3)$$

But the derivation of the Temkin and Pyzhev equation gives primarily

$$\frac{dp_{NH_3}}{dt} = k_1 \cdot p_{N_2} \left(\frac{p_{H_2}{}^3}{p_{NH_3}{}^2} \right)^{a/(a+b)} - k_2 \left(\frac{p_{NH_3}{}^2}{p_{H_2}{}^3} \right)^{b/(a+b)} . \quad (4)$$

If $a=b$, Eq. (4) goes over to Eq. (2). Here a and b are constants of the rate equation of Zeldowitsch for the activated adsorption and desorption of nitrogen on the catalyst:

$$dF/dt = k_A p_{N_2} e^{-(A+aF)/RT}, \quad (5)$$

$$-dF/dt = k_D e^{-(D-bF)/RT}, \quad (6)$$

where F represents the part of the surface which is occupied by the adsorbed substance, k_A and k_D are constants, A is the minimum activation energy of adsorption, and D the maximum activation energy of desorption. Equations (5) and (6) compensate for a certain variation of activation energy, which may be present at the different active centers of the surface of a catalyst.

This problem is treated more extensively by Brunauer, Love, and Keenan,[8] and it is shown by these authors that Eqs. (5) and (6) lead to an equation for the adsorption isotherm which is valuable only in a region where the fractional amount of the surface which is covered is neither very small nor very large. These authors also give equations which are more generally applicable. They find, furthermore, from measurements of the rate of adsorption and of the adsorption isotherm of N_2 on catalyst 931, that $b/(a+b)=0.276$. This gives for the decomposition of ammonia on this catalyst

$$-\frac{dp_{NH_3}}{db} = k \left(\frac{p_{NH_3}{}^2}{p_{H_2}{}^3} \right)^{0.276} = k \frac{p_{NH_3}{}^{0.55}}{p_{H_2}{}^{0.82}},$$

which is in a very good agreement with the experimental result of Love and Emmett[3] given here by Eq. (1).

Table II.

Total amount of gas in l	Time (min)	% NH_3 in the gas	X	$2k_1 \cdot 10^4$	Mean value	Mean error (percent)
		Catalyst: Fe-Al-K Temperature: 317°				
5.59	23.55	0.216	0.150	1.147	1.058±0.030	2.8
4.43	32.0	0.273	0.190	1.078		
4.00	38.33	0.303	0.210	1.004		
3.27	47.40	0.370	0.257	1.002		
		Catalyst: Fe Temperature: 317°				
9.07	40.92	0.133	0.0924	0.406	0.361±0.014	3.9
7.30	57.18	0.166	0.1153	0.364		
6.30	69.17	0.192	0.1333	0.346		
5.31	87.17	0.228	0.1583	0.329		

Now if $a \neq b$, we may write Eq. (4) in the form

$$\frac{dp_{NH_3}}{dt} = k_1 p_{N_2} \left(\frac{p_{H_2}{}^3}{p_{NH_3}{}^2} \right)^n - k_2 \left(\frac{p_{NH_3}{}^2}{p_{H_2}{}^3} \right)^{1-n} . \quad (7)$$

Integration of this equation gives

$$k_1 = \frac{1}{t} \frac{p_{NH_3,\,eq.}{}^{2n+1}}{p_{N_2} \cdot p_{H_2}{}^{3n}} X^{2n} \sum_{\nu=0}^{\infty} \frac{X^{(2\nu+1)}}{2(n+\nu)+1} . \quad (8)$$

In Table III the results of the experiments of Table I are evaluated by means of Eq. (8). On the bottom of each column the mean value and the limit of error are given, calculated in the usual way. In addition, the mean error of the mean value in percent is given. Table III has to be compared with Table I, which contains the rate constants for $n=0.5$. If $n=0.5$,

$$X^{2n} \sum_{\nu=0}^{\infty} \frac{X^{2\nu+}}{2(n+\nu)+1} = X \sum \frac{X^{2\nu+1}}{2(\nu+1)} = \tfrac{1}{2} \ln \frac{1}{1-X^2} .$$

One sees that it is almost possible to get rid of the trend which was observed for $n=0.5$ if n is chosen larger than 0.5. If one takes as a measure for the constancy of the rate constants the percentage of the limit of error, one sees that for the Fe-Al-K catalyst the best value for n may be closer to 0.6 than to 0.7. For the Fe-Al catalyst the best n value is 0.7 or even a little larger, and for the Fe catalyst n seems to be close to 0.6. In this

TABLE III. Rate constants $k_1 \cdot 10^4$ calculated by Eq. (8).

Catalyst	Fe-Al-K				Fe-Al				Fe					
Temperature	317°		324°		321°		318°		317°		314°		321°	
Flow rate (1/hr) \ n	0.6	0.7	0.6	0.7	0.6	0.7	0.6	0.7	0.6	0.7	0.6	0.7	0.6	0.7
14	0.29	0.085	0.32	0.094	0.40	0.108	0.35	0.080	0.27	0.077	0.165	0.046	0.109	0.029
12	...	...	...	...	0.40	0.121	...	...	0.28	0.081	...	...	0.104	0.028
10	...	...	...	...	0.43	0.133	...	...	0.28	0.083	...	...	0.102	0.028
8	0.32	0.098	0.33	0.101	0.38	0.120	0.29	0.070	0.24	0.073	0.123	0.035	0.102	0.028
6	0.28	0.087	0.31	0.099	0.39	0.125	0.26	0.064	0.24	0.075	0.110	0.032	0.106	0.030
4	0.29	0.093	0.32	0.109	0.39	0.131	0.29	0.076	0.25	0.080	0.121	0.036	0.105	0.031
Mean value	0.30 ±0.01	0.091 ±0.003	0.32 ±0.004	0.101 ±0.003	0.40 ±0.006	0.123 ±0.003	0.30 ±0.02	0.073 ±0.003	0.26 ±0.006	0.078 ±0.001	0.130 ±0.010	0.037 ±0.003	0.105 ±0.001	0.029 ±0.0005
Mean error (percent)	2.5	2.9	1.2	2.5	1.6	1.8	5.7	4.2	2.4	1.8	8.1	7	0.9	1.6

latter case the first measurement at 314°C at the flow rate of 14 1/hr does not seem to be very accurate, and, therefore, more weight is to be placed on the measurement at 321°C.

The evaluation of the precision measurements of Table II by means of Eq. (8) yields the figures given in Table IV. These evaluations show the best values at the Fe-Al-K catalyst for $n=0.65$ and at the Fe catalyst for $n=0.7$. If one considers that only 4 measurements are made in these cases, the limit of error is quite small. In spite of that, the exact determination of n would need still more measurements and, perhaps, more accurate measurements, especially if the catalysts activated in a different manner show differences in the exponent n. The measurements presented here show only that $n \neq 0.5$ and is probably close to 0.7 for all three catalysts. This gives for the ammonia decomposition

$$-dp_{NH_3}/dt = p_{NH_3}{}^{0.6}/p_{H_2}{}^{0.9}, \qquad (9)$$

in a very good agreement with the expression given by Love and Emmett,[3] quoted here in Eq. (1).

With $n=0.7$, we obtain $a/b=2.3$. The value $b/(a+b)=0.276$, given by Brunauer, Love, and Keenan, gives $a/b=2.6$. This means in connection with Eqs. (5) and (6), and if we accept the explanation of the formula given by Temkin and Pyzhev that the depth of the potential of the chemisorption of nitrogen varies less than the height of the potential wall which has to be overcome if activated adsorption occurs. This seems to be reasonable.

TABLE IV.

	Catalyst: Fe-Al-K Temperature: 317° $k_1 10^4$				Catalyst: Fe Temperature: 317° $k_1 \cdot 10^4$		
	X	$n=0.6$	$n=0.65$	$n=0.7$	X	$n=0.6$	$n=0.7$
	0.150	0.333	0.181	0.098	0.0924	0.107	0.0283
	0.190	0.329	0.182	0.101	0.1153	0.100	0.0278
	0.210	0.312	0.175	0.098	0.1333	0.099	0.0282
	0.257	0.324	0.184	0.106	0.1583	0.097	0.0286
Mean value	...	0.3257 ±0.004	0.1805 ±0.0017	0.1008 ±0.0017	...	0.1011 ±0.002	0.02823 ±0.00014
Mean error (percent)	...	1.2	0.9	1.6	...	1.9	0.5

The investigations of Love and Emmett[3] show that the behavior of the singly promoted catalyst is different from that of the doubly promoted one as far as the ammonia decomposition is concerned. These investigations were carried out at higher temperatures (375–450°C), and it was found that between 400 and 450°C the singly promoted catalyst (containing 10.5 percent Al_2O_3) decomposes ammonia after the following equation:

$$-dp_{NH_3}/dt = k(p_{H_2}{}^{1.2}/p_{NH_3}{}^{0.8}). \qquad (10)$$

The decomposition of ammonia is given by the second member of the right side of Eq. (7). One sees immediately that Eq. (10) results from this member of Eq. (7) if one puts $n=1.4$.

If one follows the deduction of Temkin and Pyzhev, a value of $n>1$ does not seem to have any sense, because $n>1$ means that either a or b has to be negative. But, anyhow, let's assume for trial that b is negative. A negative b in Eq. (6) would mean that when the surface is fully occupied, at first nitrogen molecules are desorbed which have to overcome the largest activation energy of desorption. This seems to be senseless. But one has to consider that on spots, where the activation energy of desorption is large, the heat of adsorption will be large too, and if the heat of adsorption is large, the interaction between the adsorbed particles and the surface is strong. Now, a strong interaction will cause a deformation of the adsorbed molecules or radicals; and, therefore, the probability for a chemical reaction may be much greater on these centers. Thus, if on these centers the rate of reaction is faster than on others with a lower heat of adsorption, the desorption of nitrogen will take place at first here, and only if most of these centers are empty will the slower reaction on the centers with the lower heat of adsorption play a role. A procedure like this will be described by Eq. (6) if b is a negative number. This is, of course, a formal attempt only for an explanation of the results of Love and Emmett.[3]

The experiments which are described here were carried out between 1942 and 1944 in the Eduard Zintl Institut fur Anorganische and Physikalische Chemie der Technischen Hochschule in Darmstadt, and it was planned to perform more experiments concerning the whole temperature range from 315 to 500°C. Furthermore, measurements of heats of activation were planned and the study of the influence of partial poisoning on the activation energy, etc. It was, however, not possible to continue the experiments after the end of the war, and I see no possibility at present of doing so. Therefore, I decided to publish this unfinished work, because I think that even the results obtained up till now give some contribution to the study of the problem of ammonia synthesis.

Magnetic Study of Some Organo-Metallic Compounds of Arsenic

MATA PRASAD AND L. N. MULAY
Chemical Laboratories, Institute of Science, Bombay, India

(Received April 23, 1951)

The susceptibility of As has been evaluated from the molecular susceptibilities of organo-metallic compounds of the type (i) $R.AsH_2$, R_2As, (ii) $R-As:As-R$, (iii) $RAs:O(OH)_2$, $R_2As:O(OH)$, and $R_3As(OH)_2$, using Pascal's constants for atoms and linkages in the organic radicals R and those derived for :O and $-OH$ groups in arsinic acids. The values obtained from (i) and (ii) are in agreement with Honda's value for arsenic element. These values, and that deduced from (iii), are much different from Slater's theoretical value for the As atom.

In the (i) arsines, (ii) arseno-compounds, and (iii) arsinic acids, a distinct linear relationship has been observed between the molecular susceptibility and the total number of electrons in the molecule. The linear relation has been used to evaluate the susceptibility of the As atom in these compounds, which is in agreement with Slater's theoretical value.

PASCAL[1] has shown that the magnetic susceptibilities of Sn and Hg deduced from the molecular susceptibilities of a homologous series of their organo-metallic compounds are in excellent agreement with those obtained from the pure metals. This method should therefore be very useful for deducing the atomic susceptibility of metals which cannot be obtained in a pure state. However, the susceptibilities of Sn and Hg atoms calculated according to Slater's method are considerably higher than those deduced by Pascal.

The present paper deals with a systematic study of the magnetic susceptibilities of a number of organo-metallic compounds of arsenic. The data obtained have been utilized to (i) deduce the susceptibilities of As in the tri- and pentavalent states and (ii) to see whether the molecular susceptibility of these compounds is a linear function of the number of electrons in the molecule. Pascal[1a] has also measured the magnetic susceptibilities of a few organo-metallic compounds of As, not belonging to a definite series, and has deduced from them that the atomic susceptibilities of As in the trivalent and pentavalent states are 20.9 and 43.2, respectively. These values are very different from those calculated for the As atom according to Slater's method.

EXPERIMENTAL

The organo-metallic compounds used were prepared in a chemically pure state by the known methods. Their purity was established before any measurements were made by estimating the As content according to Ewin's[2] method. Care was taken to see that ferromagnetic impurities were totally absent. Compounds of which the analysis is not given in the tables of results were obtained from the Bengal Immunity Research Laboratories, Calcutta, and the Cipla Laboratories, Bombay, and were guaranteed as pure. Throughout this discussion the nomenclature adopted by Newton Friend[3] for the organo-arsenic acids has been used.

The susceptibilities were measured on a modified form of Gouy's balance, specially constructed by Prasad, Dharmatti, and Gokhale.[4]

RESULTS

The results obtained are given in Tables I, II, and III. The formulas of the organo-arsenic compounds, their analysis, and the references to the method of preparation are given one below the other in column 1 of the tables; their specific (χ_a) and molecular (χ_m) susceptibilities in -1×10^{-6} cgs units are recorded in columns 2 and 3, respectively; columns 4 and 5 give the total number of electrons (Z) in the molecule of the compound and number of electrons (Z_R) in the organic part of the molecule. The susceptibility of the anhydrous compound has been obtained by subtracting the value of the susceptibility for two molecules of water ($\chi_{H_2O}=12.96$) from the molecular susceptibility of 3:3′ diamino-4:4′ dihydroxy arseno-benzene dihydrochloride dihydrate.

DISCUSSION OF RESULTS

The authors' value of the susceptibilities of triphenyl arsine, triphenyl arsine dihydroxide, arseno benzene, 3:3′ diamino-4:4′ dihydroxy arseno-benzene, and dimethyl arsinic acid are in good agreement with the corrected values of Pascal.[1a]

1. Susceptibility of As Atom

(i) As *from Arsines*

The values of χ_{As} have been calculated by deducting from χ_m the susceptibility contributions (χ_R) due to the organic radicals present in the compounds, calculated from Pascal's corrected values of atomic susceptibilities and the constitutive correction constants for the linkages involved in these radicals. The values of χ_R and χ_{As} are given in columns 6 and 7 of the Table I. Since the several values of χ_{As} are very nearly equal to each other, their mean values, 20.72, may be con-

[1] Pascal, Compt. rend. **156**, 323 (1913).
[1a] Pascal, Compt. rend. **174**, 1698 (1922).
[2] Ewin, J. Chem. Soc. **109**, 1356 (1916).
[3] Newton Friend, *A Textbook of Inorganic Chemistry* (1930), Vol. II, pp. 35, 153.
[4] Prasad, Dharmatti, and Gokhale, Proc. Indian Acad. Sci. **20A**, 224 (1944).

TABLE I. Arsines.

Compound	χ_a	χ_m	Z	Z_R	χ_R	χ_{As}
$C_6H_5.AsH_2$ As found 47.72% As theory 48.68% Palmer and Adams[a]	0.518	79.71	76	43	57.95	21.76
$pH_3C.C_6H_4AsH_2$ As found 43.82% As theory 44.62% Palmer and Adams[a]	0.544	91.27	84	51	69.81	21.54
$(C_6H_5)_3.As$ As found 24.23% As theory 24.49% Pope and Turner[b]	0.580	177.40	156	123	156.27	21.13
$p(H_3C.C_6H_4)_3.As$ As found 21.45% As theory 21.54% Michaelis[c]	0.610	212.10	180	147	191.85	20.25
$p(H_3CO.C_6H_4)_3As$ As found 18.87% As theory 18.92% Michaelis and Weitz[d]	0.570	225.60	204	171	205.68	19.92
$p(H_5C_2O.C_6H_4)_3.As$ As found 17.56% As theory 17.11% Michaelis and Weitz[d]	0.596	261.00	228	195	241.26	19.74
					Mean value of As = 20.72	

[a] Palmer and Adams, J. Am. Chem. Soc. **44**, 1356 (1922).
[b] Pope and Turner, Trans. Chem. Soc. **117**, 1447 (1920).
[c] Michaelis, Ann. Chem. **320**, 301 (1902); **321**, 216 (1902).
[d] Michaelis and Weitz, Ber. deut. chem. Ges. **20**, 49 (1887).

sidered to represent the susceptibility of the As atom in combinations of type $RASH_2$ and R_3As. This value includes the bond effect due to C—As bond. The good agreement between the authors' and Pascal's values is remarkable, since, while Pascal deduced the values from compounds of widely different characters, the authors value has been deduced from arsines only. This, however, does not rule out the possibility that the values of χ_{As} deduced from different types of compounds may be different.

The values of χ_{As} deduced from different alkyl arsines are slightly different from each other. Irene Kadomtzeff[5] found that the values of χ_{Pb} and χ_{Sn} deduced from the susceptibilities of alkyl plumbanes and stannanes decrease progressively as the number of carbon atoms in the alkyl chain is increased. However, since the differences in the several values of χ_{As} are small and are not beyond the experimental error, the mean of the several values of χ_{As} as the susceptibility of the As atom in aryl arsines is justifiable. This

TABLE II. Arseno compounds.

Compound	χ_a	χ_m	Z	Z_R	χ_R	χ_{As}
$C_6H_5.As{:}As.C_6H_5$	0.476	144.50	148	82	104.18	20.16
$pH_3C.C_6H_5.As{:}AsC_6H_4.CH_3$ As found 21.92% As theory 22.58% La Coste and Michaelis;[a] Michaelis[b]	0.498	165.20	164	98	127.90	18.65
$[H_2N.C_5H_4.As{:}As.C_6H_4.NH_2]{:}2HCl$	0.504	205.00	200	134	167.24	18.80
$[H_2N(OH).C_6H_3.As{:}As.C_6H_3(OH)NH_2]2HCl{:}2H_2O$ As found 31.58% As theory 31.60% Kober,[c] Forneau[d]	0.510	242.16	...	...	...	...
Same as above —anhydrous	...	216.24	216	150	176.24	19.88
					Mean value of As = 19.37	

[a] La Coste and Michaelis, Ber. deut. chem. Ges. **11**, 1818 (1888).
[b] Reference c of Table I.
[c] Kober, J. Am. Chem. Soc. **41**, 442 (1919).
[d] Forneau, *Organic Medicaments and their Preparation*, (1925), p. 235.

[5] Kadomtzeff, Compt. rend. **226**, 407, 661 (1948).

TABLE III(a). Arsinic acids, R—As:O(OH)$_2$.

Compound	χ_a	χ_m	Z	Z_R	$Z_{R'}$	χ_R	$\chi_{As:O(OH)_2}$
$H_3C.As:O(OH)_2$	0.501	70.09	68	9	35	14.79	55.39
$H_5C_2.As:O(OH)_2$ As found 47.92% As theory 48.68% Quick and Adams[a]	0.531	81.72	76	17	43	26.65	55.07
$H_7C_3.As:O(OH)_2$ As found 45.03% As theory 44.62% Quick and Adams[a]	0.555	93.19	84	25	51	38.51	54.68
$C_6H_5.As:O(OH)_2$ As found 37.47% As theory 37.11% Palmer and Adams[b]	0.539	108.80	100	41	67	52.09	56.71
p-$CH_3.C_6H_4As:O(OH)_2$ As found 34.51% As theory 34.70% Palmer and Adams[b]	0.556	120.00	108	49	75	63.95	56.05
p-$HO.C_6H_4As:O(OH)_2$ As found 34.49% As theory 34.38% Bart[c]	0.522	113.80	108	49	75	56.70	57.10
$(OH)_2C_6H_2AsO(OH)_2$ As found 31.56% As theory 32.03% Baure[d]	0.500	116.90	116	57	83	61.31	55.59
p-$NH_2C_6H_4.As:O(OH)_2$	0.540	117.10	108	49	75	60.59	56.41
[p-$NH_2C_6H_4As:O(OH)_2$].HCl	0.552	139.80	126	67	93	83.63	56.17
p-$NC.C_6H_4.As:O(OH)_2$	0.510	115.70	112	53	79	59.96	55.74

[a] Quick and Adams, J. Am. Chem. Soc. **44**, 809 (1922).
[b] Reference a of Table I.
[c] Bart, Ann. Chem. **429**, 91 (1922).
[d] Bauer, Ber. deut. chem. Ges. **48**, 509 (1915).

TABLE III(b). Disubstituted arsinic acid $R_2As:O(OH)_2$.

Compound	χ_a	χ_m	Z	Z_R	$Z_{R'}$	χ_R	$\chi_{As:O(OH)}$
$(CH_3)_2.As:O(OH)$	0.572	78.70	...	...	...	29.58	49.12

TABLE III(c). Triarsine dihydroxide $R_3As:(OH)_2$.

							$\chi_{As(OH)_2}$
$(C_6H_5)_3As:(OH)_2$ As found 21.69% As theory 22.04% Phillip[a]	0.628	213.50	...	...	...	156.27	57.23

[a] Phillip, Ber. deut. chem. Ges. **19**, 1032 (1886).

value is nearly the same as found by Honda[6] for As element.

(ii) χ_{As} *from Arseno Compounds*

The values of χ_{As} have also been calculated by deducting the values of χ_R, calculated as in (i) from the values of χ_m of different arseno compounds. The values of χ_R and χ_{As} are given in columns 6 and 7 of Table II.

[6] Honda, Ann. Physik **32**, 1027 (1910).

Since the several values of χ_{As} are nearly equal to each other, their mean value, 19.36, may be taken to be the susceptibility of the As atom in these compounds. It appears that the diamagnetism of As in arseno compounds is somewhat less than that in arsines. This is probably due to the fact that in arseno compounds two atoms of As are linked by a double bond whereby the covalent radius of As is decreased, and hence the value of χ_{As} is somewhat depressed. The difference (2.72) between

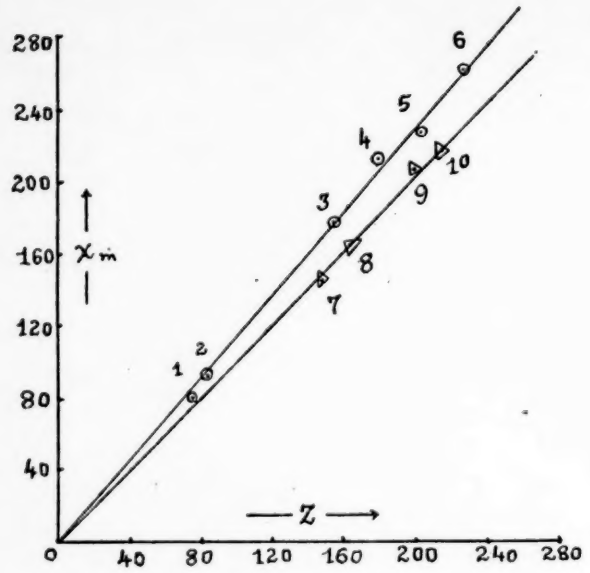

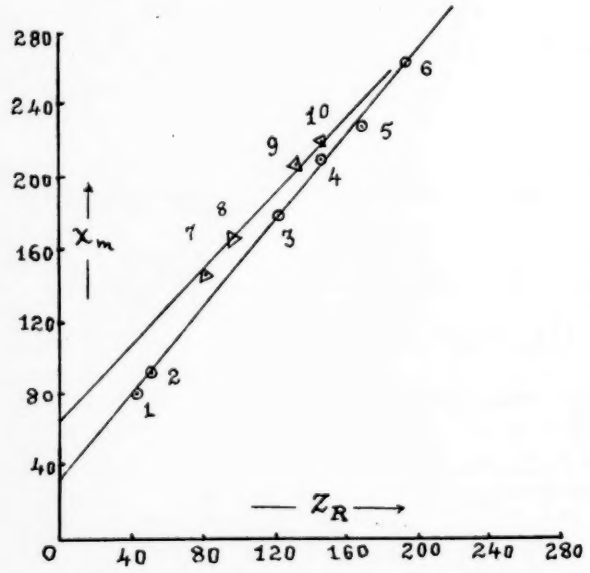

FIG. 1 (above). χ_m plotted against Z for several salts of As, Sb, and Bi. For Figs. 1 and 2: χ_m plotted against Z and Z_R for arsines and arseno compounds. 1-Phenyl arsine, 2-*P*-tolyl arsine, 3-triphenyl arsine, 4-tri-*P*-tolyl arsine, 5-tri-*P*-anisyl arsine, 6-tri-*P*-phenytyl arsine. 7-Arseno benzene, 8-arseno-*P*-toluene, 9-4:4′-diamino-arseno benzene-dihydrochloride, 10-3:3′-diamino-4:4′-dihydroxy arseno benzene dihydrochloride.

FIG. 2 (below). χ_m plotted against Z for the halides of As, Sb, and Bi.

the values of $\chi_{As:As}$ and χ_{2As} deduced from arseno compounds and arsines, respectively, would roughly constitute the magnitude of the depression due to As:As linkage.

(iii) χ_{As} *from Arsinic Acids*

For the purpose of this calculation the value of the susceptibility of the group $-As:O(OH)_2$ has been calculated by deducting the values of the susceptibility of the organic radical (χ_R), calculated as before, from the values of χ_m of these compounds. The values of χ_R and $\chi_{-As:O(OH)_2}$ are given in columns 7 and 8 of Table III(a). Since several values of $\chi_{-As:O(OH_2)}$ are nearly equal to one another, their mean value (55.89) may be taken to represent the susceptibility of the $-As:O(OH)_2$ group.

The values of the susceptibilities of the groups $>As:O(OH)$ and $\geqslant As(OH)_2$ have been similarly calculated from the molecular susceptibilities of their compounds and are given in Tables III(b) and III(c).

Since the valence of the As atom in $-As:O(OH)_2$, $As:O(OH)$, and $As(OH)_2$ groups is the same, the susceptibilities of .OH and :O in these groups have been calculated from the following equations based on the application of the law of additivity:

$$\chi_{-OH} = \chi_{-As:O(OH)_2} - \chi_{>As:O(OH)}$$

and

$$\chi_{:O} = \chi_{>As:O(OH)_2} \chi_{\geqslant As(OH)_2}.$$

They are found to be 6.77 and -1.34, respectively. The value for χ_{-OH} is in good agreement with that calculated from Pascal's constants for oxygen (in alcohols, ether) and hydrogen. The value for $\chi_{:O}$ is nearly the same as the paramagnetic value for oxygen in aldehydes and ketones. This observation is in agreement with that of Pascal,[1a] that $\chi_{:O}$ has a paramagnetic effect in combination with As.

The susceptibility of pentavalent As in arsinic acids has been calculated by subtracting the values for χ_{-OH} and $\chi_{:O}$ from the average value (55.89) of $\chi_{-As:O(OH)_2}$ and is found to be 43.69.

Since the susceptibilities of the $-As:O(OH)_2$, $>As:O(OH)$, and $\geqslant As(OH)_2$ groups have been deduced on the basis of the additivity law for homopolar compounds, these values should include a correction constant (λ) for the linkage of the As atom of these groups with the carbon atom of the organic radicals. The three values corresponding to these groups will therefore include the constants $-\lambda$, -2λ, and -3λ, respectively. Hence, the values of $\chi_{:O}$ and χ_{-OH} deduced before will include the correction constants 2λ and λ, respectively; and the value 43.69 deduced for χ_{As} will, therefore, include the correction constant of the magnitude 0.5λ. Since the exact value of λ is not known, it cannot be said that the value 43.69 is an absolutely correct value of the susceptibility of the pentavalent As atom.

2. Relation between χ_m and Z and Z_R in Arsines and Arseno-Compounds

The points obtained on plotting the values of χ_m against Z for the arsines and arseno-compounds (Fig. 1) lie on two different straight lines. This shows that the molecular susceptibility of both arsines and arseno-compounds increases proportionately with Z, that is, the magnetic behavior of arsines and arseno-compounds

considered as individual groups is similar but distinct from one another.

Since the two straight lines pass through the origin on extrapolation, their equation is of the form

$$\chi_m = C \cdot Z. \quad (1)$$

This equation is similar to that found by Ikenmeyer[7] in the case of halides of alkali and alkaline earth metals with the difference that the straight lines pass through the origin and thereby seem to fulfill the theoretical expectation that χ_m should be zero when Z is zero.

The values for C for the arsines and arseno-compounds are 1.1 and 1.0, respectively. The lower value of C for arseno-compounds indicates that the value of χ_{As} in these compounds is smaller than that in arsines.

Since Z is equal to $Z_R + Z_{As}$, where Z_{As} is the number of electrons in the As atom, the plots of χ_m against Z_R for arsines and arseno-compounds should also lie on straight lines. This is shown in Fig. 2. Their equations are of the form

$$\chi_m = C \cdot Z_R + p, \quad (2)$$

where C has the same value as in Eq. (1). According to the additivity law one obtains

$$\chi_m = \chi_R + \chi_{As}. \quad (3)$$

If χ_R follows Langevin's equation, that is, it is zero when Z_R is zero, then it follows from Eqs. (2) and (3) that

$$\chi_{As} = p. \quad (4)$$

The values of p, *viz.*, 34.0 and 65.0, read from Fig. 2 give the values of χ_{As} and $\chi_{As:As}$ in arsines and arseno-compounds, respectively. The values of χ_{As} in these compounds are given in Table IV along with authors'

TABLE IV.

χ_{As} from Fig. 2		Mean χ_{As} using Pascal's constants			
Arsines	Arseno-compounds	Arsines	Arseno-compounds	χ_{As} Slater	χ_{As} Honda
34.00	32.50	20.72	19.36	35.89	23.00

values deduced by using Pascal's constants, the theoretical value calculated for As atom according to Slater's[7] method and the value obtained by Honda[6] for the element.

It will be seen that the difference between the two values deduced from Fig. 2 is nearly the same as found by using Pascal's constants. Further, the values deduced from Fig. 2 approach Slater's theoretical value; they are, however, higher than the corresponding values deduced from Pascal's constants, by nearly the same amount.

[7] Slater, Proc. Leeds Phil. Lit. Soc., Sci. Sect. **1**, 484 (1929); Phys. Rev. **36**, 57 (1930).

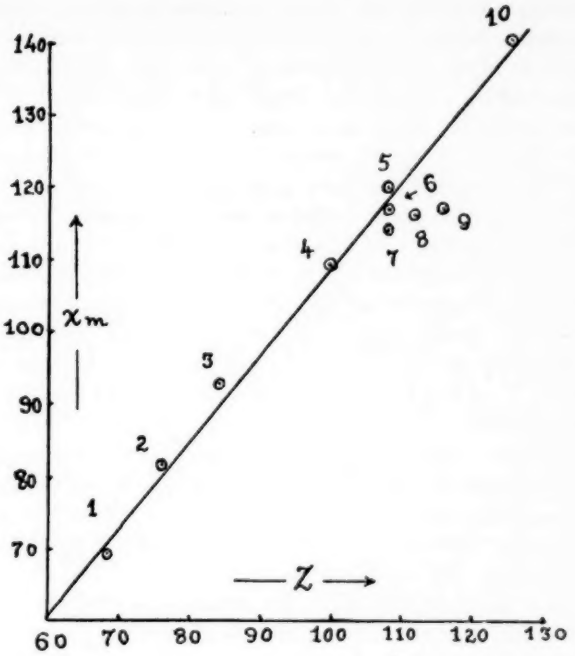

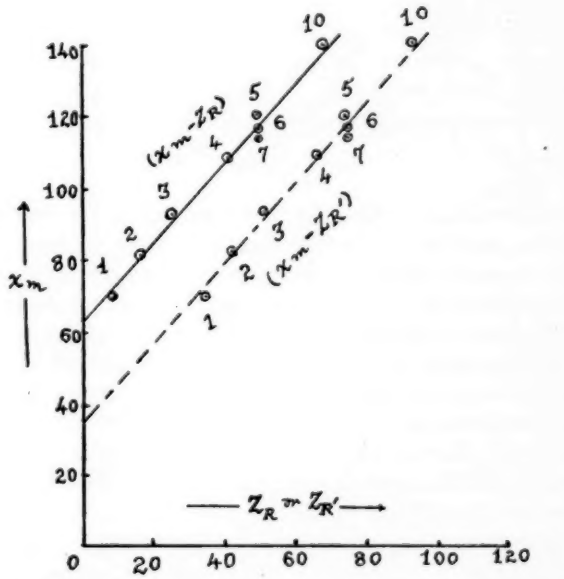

FIG. 3 (above). χ_m plotted against Z for the oxides, sulfides, and iodides of As, Sb, and Bi. For Figs. 3 and 4: χ_m plotted against Z, Z_R, and $Z_{R'}$ of arsinic acids. Arsinic acids: 1-methyl, 2-ethyl, 3-propyl, 4-phenyl, 5-*P*-tolyl, 6-*P*-amino phenyl, 7-*P*-hydroxylphenyl, 8-*P*-cyanophenyl, 9-2:4-dihydroxyphenyl, 10-hydrochloride of *P*-aminophenyl.

FIG. 4 (below). χ_m plotted against N for compounds containing the same anion.

3. Relation between χ_m and Z, and Z_R, Z_R', of Arsinic Acids

With the exception of the points for 2:4 dihydroxy phenyl and *p*-cyanophenyl arsinic acids the plots of χ_m against Z for the arsinic acids lie on a straight line (Fig. 3), showing that the magnetic behavior of a group of arsinic acids is similar. Further, the points

corresponding to the three electronic isomers *p*-tolyl, 4-aminophenyl, and 4-hydroxy phenyl arsinic acids are seen to obey the relation very well. This straight line also passes through the origin and therefore satisfies the condition that χ_m is zero when Z is zero. Since $Z=Z_R+Z_{-As:O(OH)_2}$, where $Z_{-As:O(OH)_2}$ is the number of electrons in the arsinic acid group, the relation between χ_m and χ_R will also be linear. The straight line (Fig. 4) representing this relation will be parallel to the χ_m-Z line shown in Fig. 3. If one follows the argument advanced in deducing Eq. (4), it will be seen that the intercept of the line in Fig. 4 on χ_m axis will be the susceptibility of the $-As:O(OH)_2$ group. This is found to be 63.50, the value obtained by using Pascal's constants being 55.89.

Further, since $Z=Z_{R'}+Z_{As}$, where $Z_{R'}$ is the number of electrons in atoms other than As in the arsinic acid (see column 6, Table III), the relation between χ_m and $Z_{R'}$ would also be linear. This straight line (shown by dotted line in Fig. 4) is also parallel to the χ_m-Z line (Fig. 3). According to the assumption made before, the intercept (36.5) of the line $\chi_m-Z_{R'}$ on the χ_m axis gives the susceptibility of As. Again, this value agrees well with Slater's theoretical value.

The authors are very grateful to Dr. C. R. Kanekar for his assistance throughout this work and to Dr. T. N. Ghosh and Dr. K. A. Hamied for supplying some organo-metallic compounds of arsenic.

SUMMARY

The susceptibility of As in arsines of type $R-As-H_2$, R_3As, and in arseno-compounds of type R.As:As.R has been evaluated by subtracting from the molecular susceptibilities (χ_m) of a number of such compounds, the susceptibilities of the organic radicals (χ_R) calculated by using Pascal's constants. The values 20.72 and 19.36 obtained from arsines and arseno-compounds are in good agreement with the values found for the As element by Honda, but are considerably smaller than the value (35.89) calculated theoretically for the As atom according to Slater's method.

The susceptibilities of several arsinic acids R.As:$O(OH)_2$, a disubstituted arsinic acid R_2.As:O(OH), and a triarsine dihydroxide $R_3.As(OH)_2$ were used in the first instance to calculate the susceptibilities of the groups $-As:O(OH)_2$, >As:O(OH), and ⩾$As(OH)_2$ by using Pascal's constants for the organic radical R and secondly to evaluate the susceptibilities of the groups :O and −OH attached to As in these acids. Using these values, the susceptibility of As in arsinic acids has been found to be 43.69, which is far different from the value found for As in arsines and arseno-compounds.

The plots of χ_m against Z, the total number of electrons in the molecule of arsines and arseno-compounds lie on two different straight lines, which, on extrapolation, pass through the origin. This indicates that (i) the magnetic behavior of arsines and arseno-compounds, considered in individual groups is similar, (ii) the magnetic behavior of the arseno-compounds is different from that of the arsines, and that (iii) the linear relation $\chi_m=C.Z$, which is similar to Ikenmeyer's relation, satisfies the theoretical expectation that χ_m should be zero when Z is zero. The plots of χ_m against χ_R, the number of electrons in the organic radical, lie on a straight line parallel to the χ_m-Z line. The equation of this straight line has been used to evaluate the susceptibility of As in these compounds. The value of χ_{As} deduced in this manner is seen to be less in arseno-compounds (32.5) than in arsines (34.0), the difference between the two values being nearly the same as in the case of values of χ_{As} deduced by using Pascal's constants. The values of χ_{As} obtained from the graphs agree closely with Slater's value (35.89) for the susceptibility of the As atom.

The plots of χ_m against Z for the arsinic acids also lie on a straight line, passing through the origin. This linear relation has been extended to evaluate the susceptibilities of the $-As:O(OH)_2$ group and As in such compounds, the values being 63.5 and 36.5, respectively. The value (36.5) deduced for χ_{As} is again found to be in close agreement with Slater's theoretical value.

The Effect of Grinding on Particles

BENJAMIN C. BRADSHAW
Signal Corps Engineering Laboratories, Fort Monmouth, New Jersey
(Received May 2, 1951)

Although much experimental work has been done on grinding, many well-known facts concerning this process and its effect on particles remain unexplained. The writer postulates that the well-known limiting distribution of particle sizes, which results from long-continued grinding, is dynamic rather than static.

THEORY

IT is known empirically that if a material is ground for an indefinite period there occurs a time after which further grinding produces no change in the particle size distribution. This means that the ultimate, i.e., complete reduction to molecular or atomic dimensions, is not achieved by grinding no matter how prolonged. Either of the following two hypotheses may explain this:

1. After a certain time no particle of any size breaks.
2. Particles of all sizes break, but some particles, probably the smallest, either unite with one another or with larger particles as rapidly as they are formed and thus produce a dynamic equilibrium.

The first hypothesis does not appear probable, because it would be contrary to all experience and theory if a large number of particles could be rubbed, swirled, pressed, and in many cases submitted to a form of pounding such as results from the collision of the balls in a ball mill, without many of them being broken.[1]

DISCUSSION

That the relatively small particles disappear by union with one another or with larger particles is probable; it remains but to discover mechanisms applicable to the phenomenon. Some observations are described which furnished the basis for an attack on this problem.

When samples of nickel powder sprinkled on a Parlodion film were examined in an electron microscope,* some very small irregularly shaped particles of nickel were seen to jump and be converted simultaneously into cubes of about 100A on edge. The sharp points on large particles were also observed to disappear instantaneously. Since the electron beam was the only likely source of energy for this transformation, the hypothesis was made that the change was caused by the absorption of one or more electrons. In order to test this hypothesis, the order of magnitude of the probable time necessary for a particle 100A on edge to absorb an electron was calculated. The energy and momentum of both the electron and the particle were also calculated, and the energy found for the electron was compared with that necessary to heat the nickel cube 100A on edge to a high temperature.

When the absorption coefficient $\alpha=4\times10^2 D$ for $\beta=0.45$† was used and the order of magnitude of the number of electrons which would strike a cube 100A on edge was estimated, it was found that one electron should be absorbed at approximately two-minute intervals. This time is short enough so that one can assume that the energy needed to transform the irregular particle to the cube was furnished by the absorption of a single electron provided the momentum of the particle and the electron were of the same order of magnitude, and if one electron had the energy necessary to heat the particle to a high temperature. It was estimated from visual observation of lateral motion that the duration of the jump of the particle was about 0.01 second. Assuming this and that the volume of the particle was 10^{-18} cm^3 and its density 7, it was calculated that the nickel particle acquired a kinetic energy of the order of 10^{-16} erg and a momentum of 10^{-17} g-cm per second. The kinetic energy of the particle is negligible with respect to that of the electron which is of the order of 10^{-7} erg. However, the momentum of the particle was about that of the electron whose momentum was 10^{-17} g-cm per second.‡ Such close agreement between the momentum of the electron and particle can only be regarded as fortuitous (a factor of 10 or 100 between them would not have been surprising) when it is remembered how crude are the estimates of both the size of the particles and the time during which they remained above the Parlodion film. It must also be remembered that a particle of this approximate size would be repelled to a significant extent by the film, if, as is probable, it had a similar charge. Assuming that the nickel particles had a volume of 10^{-18} cm^3 and a specific heat equal to that of bulk nickel, it was found that the absorption of one electron of 50,000 volts would supply enough energy to heat this particle to a temperature greater than 1600°C. Thus, the momentum is conserved, and the energy has been shown to be both present and available. The

[1] Research on the theory of fine grinding, Trans. British Ceram. Soc. 26–45 (1926–1927).

* The electron microscope used a beam of electrons which had passed through a potential drop of 5×10^4 volts.

† Landolt-Börnstein, *Physakalisch-Chemische Taballen*, 5. Auflage, 2 Band, p. 890, gives the value of α as 4×10^2 cm^2 g^{-1} for $\beta=0.45$. However, the statement on p. 428, Sec. C, paragraph 2 of 1 Erganzungsband in this connection may cast some doubt on the exact figure.

‡ Calculations of the momentum of the electron were made from its known kinetic energy (relativity corrections included).

hypothesis that the energy needed to change particles of nickel powder of about 10^{-18} cm^3 from irregular masses to what appeared to be perfect cubes was furnished by the absorption of a single electron has been shown to be very probable. The disappearance of sharp points on larger particles may also be explained by the same hypothesis.

Our second hypothesis states that particles unite as well as break in a grinding machine. One mechanism for their union is as follows: electrostatic charges build up until they are discharged in the form of sparks or corona. Discharge occurs between two portions of the interior of the grinding machine, thus furnishing the energy necessary to give the molecules of the particles at the point of discharge high energy. It is believed that a particle in this high energy state, consisting of a few thousand atoms, and in contact with a much larger particle of the same material, would unite with it to form a single larger particle. However, this mechanism is not possible in a conducting system and, moreover, is inadequate to account for the amount of fine powder transformed into coarser powder.

The work of Bowden[2] and his students suggested another mechanism by which small particles might be united to form larger ones, namely, welding due to frictional energy. These authors found that if two dissimilar metals were slid over one another and if these metals were used as thermocouples, the temperature in the plane of sliding was, in most cases, that of the melting point of the lower melting metal. This method of measuring temperature is questionable. These workers[3] found further that liquid and gelatinous explosives may be exploded by an impact of 20 g-cm if minute air bubbles are present but that an impact of 10^5 to 10^6 g-cm are necessary to cause this explosion if all bubbles are removed. The explanation which is given is that the gas bubbles are heated by adiabatic compression and hence initiate the reaction. It was further found[4] that if grit were added to the explosive, "P.E.N.T," and this were rubbed, then an explosion was generated if the melting point of the grit were above 500°C. However, very few explosions were generated if the melting point of the grit were 500°C or less.

Hot spots were shown by flashes of light if a metal slider, the melting point of which was above 570°C, were slid over a glass plate. If the melting point were lower, no flashes were seen. The addition of a lubricant such as glycerine and water increased the speed of sliding necessary for the appearance of these flashes but did not cause them to disappear. It was further shown that the hardness of the grit was of no importance. Bowden and Hughes[5] showed that when lead, Woods-metal, and gallium were rubbed with filter paper or camphor, the mass of metal lost was greater the lower the melting point; the mass of metal lost showed no relation to the hardness of the metal.

This evidence tends to confirm the results of the thermocouple measurements which showed that either a high temperature or else a temperature equal to the melting point of the lower melting metal was reached when two metals were slid over each other.

Bowden and Moore[6] showed that if a copper rod were slid over a piece of milled steel, fragments of copper were welded to the steel. This welding took place even when the surfaces were lubricated. J. N. Gregory[7] confirms this. Bowden and Tabor[8] showed that the real area of contact between two surfaces which are pressed together is very small. It is the opinion of these authors, however, that welding takes place between those small areas which do come into contact due to the very high pressure (equal to that of plastic flow of the substance in question) at these points.

In a grinding machine of any type there is a continual rubbing together of all surfaces, specifically, the surfaces of the grinder and the material ground, and the surfaces of each of the particles composing the material. If some of the particles of the material being ground are as small as 100A on edge, then very often the pressure between these and much larger particles will be great and accompanied by sliding motion. High points are not apt to exist on particles having an area of the order of 10^4 A^2, and, therefore, their whole surfaces will make contact. In view of the work of Bowden and his students, it appears almost certain that many of these contacts, especially when accompanied by rubbing, will result in the welding of the small particle on to the larger, thus removing the smaller particles from the system. When the small particles disappear as rapidly as they are produced, a kind of dynamic equilibrium will have been established and further grinding will be without effect on the state of subdivision of the material. There is no reason for restricting the process of union to that in which the finest particles must necessarily play a part. It does seem, however, that it is more probable that a stable union will take place between a large and minute particle than that it will between two large particles, since, from the work of Bowden and his associates, the area of real welding appears to be nearer that of a particle 100A on edge than that of a particle of a micron or two on edge.

CONCLUSIONS AND EXPERIMENTAL VERIFICATION

The combination of theory, observation, and experiment leads one to the conclusion that particle size increases as well as decreases on grinding. In order to test this conclusion further, the following experiment

[2] F. P. Bowden *et al.*, Proc. Roy. Soc. (London) **A169**, 371 (1939).
[3] F. P. Bowden, Proc. Roy. Soc. (London) **A188**, 291 (1947).
[4] F. P. Bowden, Nature **162**, 654 (1948).
[5] F. P. Bowden and T. P. Hughes, Proc. Phil. Soc. (London) **A160**, 575 (1937).
[6] F. P. Bowden and A. J. W. Moore, Nature **155**, 451 (1945).
[7] J. N. Gregory, Nature **157**, 443 (1946).
[8] F. P. Bowden and D. Tabor, Proc. Roy. Soc. (London) **A169**, 391 (1939).

was carried out. A sample of white blasting sand was washed several times with water, heated with cleaning solution, rinsed many times with distilled water, and ground under water for twenty-four hours, using a mechanically operated mullite mortar and pestle. The suspension thus produced was poured into a salt mouth bottle, diluted with water, thoroughly shaken, and allowed to stand for twenty minutes, after which time the coarser particles settled at the bottom of the bottle. The liquid, carrying the finer particles in suspension, was then drawn off and the residue discarded. This suspension was then dried and heated to 150°C for twelve hours, and finally ground dry in the original grinder for twenty-four hours. The result was that the texture had changed from that of a very fluffy powder to a rather granular structure and the apparent volume had decreased considerably. The powder was then triturated with water, diluted, and thoroughly stirred. At least three-fourths of the material fell out of the suspension within the first two minutes, and when ground under a spatula felt much more gritty than the discarded residue from the wet grinding. There can be no doubt that particle size growth had occurred during the dry grinding. The conclusion that the particles increase as well as decrease in size during grinding is thus confirmed.

THE JOURNAL OF CHEMICAL PHYSICS VOLUME 19, NUMBER 8 AUGUST, 1951

Concerning the Temperature Coefficient of the emf of Reversible Galvanic Cells Operated at Variable Concentration

JAMES C. M. LI
Department of Chemistry and Chemical Engineering, University of Washington, Seattle, Washington
(Received May 14, 1951)

The usual form of the Gibbs-Helmholtz equation such as $d\Delta F/dT=-\Delta S$ is limited in its application to reversible galvanic cells where all variables except temperature, which can change the emf of the cell, keep unchanged when temperature varies. For cells where concentration changes simultaneously with temperature, a form including concentration terms should be used instead. Barieau's idea concerning the confusion in literature is discussed. His "correct reaction" is explained and a method for writing this reaction is evaluated in general. It is found that his idea is only useful in certain cases.

THE problem concerning the application of the Gibbs-Helmholtz equation to reversible galvanic cells has been discussed recently by Barieau.[1] His main idea is that the Gibbs-Helmholtz equation of the form:

$$d\Delta F/dT=-\Delta S \tag{1}$$

should be directly applicable to any reversible galvanic cell. From this idea, and the fact that a number of reactions of the same ΔF but different ΔS usually can be assigned to a given cell, he concluded that the confusion over the application of that equation to cells with variable concentration had resulted from the failure to write correct cell reactions; and based on this conclusion, he found a general principle in writing the correct reaction for a cell.

Since Eq. (1) has originated from the fundamental form $dF/dT=-S$, which is derived for systems with temperature as the only independent variable, it is obvious that Eq. (1) is not applicable to any reversible galvanic cell operated at variable concentration, as pointed out by Brickwedde and Brickwedde.[2] For systems with other variables such as pressure, concentration, electric and magnetic fields, etc., the free energy of the system or of any component in the system will be a function of all the possible variables: $F=F(T, P, c_1, c_2, \cdots, c_n, X, H, \cdots)$. Let us restrict ourselves to the case where only temperature and concentration are variables; the change of free energy with temperature is then:

$$\frac{dF}{dT}=-S+\sum_{i=1}^{n}\left(\frac{\partial F}{\partial c_i}\right)_{T,c'}\frac{dc_i}{dT}.$$

When this equation is applied to reversible galvanic cells, we have:

$$\frac{d\Delta F}{dT}=-\Delta S+\sum_{i=1}^{n}\left(\frac{\partial \Delta F}{\partial c_i}\right)_{T,c'}\frac{dc_i}{dT}, \tag{2}$$

where n is the number of independent concentration variables and c' means $c_1, c_2, \cdots, c_n$ except c_i. Therefore for cells operated at variable concentration, Eq. (2) is the one of general applicability. If a number of reactions can be assigned to a given cell, Eq. (2) is applicable to any one of them and hence all of them can be considered correct. Among those reactions, however, it is possible to find one satisfying the following:

$$\sum_{i=1}^{n}\left(\frac{\partial \Delta F}{\partial c_i}\right)_{T,c'}\frac{dc_i}{dT}=0 \tag{3}$$

and then also satisfying (1). This is why Barieau can conclude that only one of the reactions can be considered correct. Actually the confusion existing in the literature is the result of the misuse of Eq. (1) rather than the failure to write a correct cell reaction defined by (3).

[1] R. E. Barieau, J. Am. Chem. Soc. **72**, 4023 (1950).
[2] F. G. Brickwedde and L. H. Brickwedde, Phys. Rev. [II] **60**, 172 (1941).

Barieau's idea could be useful if for any cell there was a simple "correct" reaction satisfying (3) and easily obtainable by inspection of the cell. It is, however, not the case. The principle given by Barieau for writing "correct" reactions is limited in its use to certain cases only. In general, if a cell involves n independent concentration variables, $n+1$ independent reactions (any one of them cannot be written by linear combination through others) can be written for the cell, because, for each concentration variable, there is a temperature-concentration relationship in addition to the fundamental cell reaction. Suppose ΔF_1, ΔF_2, $\cdots$, ΔF_{n+1} are those reactions. It is possible to find a combined reaction ΔF^* satisfying (3),

$$\Delta F^* = \sum_{j=1}^{n+1} A_j \Delta F_j,$$

where A's can be functions of concentration and temperature, and are found mathematically to be $A_j = D_j/D$ with D in the form:

$$D = \begin{vmatrix} 1 & 1 & \cdot & \cdot & \cdot & 1 \\ \dfrac{\partial \Delta F_1}{\partial c_1} & \dfrac{\partial \Delta F_2}{\partial c_1} & & & & \dfrac{\partial \Delta F_{n+1}}{\partial c_1} \\ \dfrac{\partial \Delta F_1}{\partial c_2} & \dfrac{\partial \Delta F_2}{\partial c_2} & & & & \dfrac{\partial \Delta F_{n+1}}{\partial c_2} \\ \cdot & \cdot & & & & \cdot \\ \cdot & \cdot & & & & \cdot \\ \cdot & \cdot & & & & \cdot \\ \dfrac{\partial \Delta F_1}{\partial c_n} & \dfrac{\partial \Delta F_2}{\partial c_n} & & & & \dfrac{\partial \Delta F_{n+1}}{\partial c_n} \end{vmatrix}$$

and D_j identical with D except in the jth column where all $(\partial \Delta F_j/\partial c_i)$'s $i=1, 2, \cdots, n$ are replaced by zero. Applying this method to any cell mentioned in Barieau's paper, one can obtain a reaction satisfying (3) or (1) and identical with Barieau's result. But the simple form of A's happened only in these cases. As an example, for cells of the following type:

$$H_2(g)\,|\,H_2SO_4(m) \text{ saturated with } CuSO_4 \cdot 5H_2O(s)\,|\,Cu(s),$$

where m is the molality of H_2SO_4 which is independent of temperature, the "correct" reaction is found to be:

$$H_2(g) + \frac{x+5y}{1+5y}\,CuSO_4 \text{ (in solution)} + \frac{1-x}{1+5y}\,CuSO_4 \cdot 5H_2O(s) = H_2SO_4 \text{ (in solution)} + \frac{5-5x}{1+5y}\,H_2O \text{ (in solution)} + Cu(s)$$

where $x = (\partial \bar{F}_{H_2SO_4}/\partial \bar{F}_{CuSO_4})_T$, $y = (\partial \bar{F}_{H_2O}/\partial \bar{F}_{CuSO_4})_T$. This reaction can no longer be written from Barieau's principle and seems less useful because of the complicated form of A's. It is also hard to realize that this reaction should be more correct than the following one:

$$H_2(g) + CuSO_4 \text{ (in solution)} = H_2SO_4 \text{ (in solution)} + Cu(s).$$

So Barieau's idea is only useful for certain types of cells.

Notice

Preliminary Announcement of Ninth Annual Pittsburgh Diffraction Conference

THE Ninth Annual Pittsburgh Diffraction Conference will be held at Mellon Institute, Pittsburgh 13, Pennsylvania on November 29 and 30, 1951. Sessions are tentatively being arranged on *Instrumentation and Methods*, and *Metals and Alloys*. Papers are solicited on these and related subjects, and will be considered in the order in which they are received. Titles should be sent to the Program Chairman, Mr. R. W. Turner, Carnegie Institute of Technology, Pittsburgh 13, Pennsylvania, before September 1.

The Conference will also include a symposium of invited papers on the subject of *Diffraction and Thermomagnetic Studies of Reactions of Metastable Carbides of Iron.*

For further information, and for a copy of the preliminary program when available, write to Mr. C. W. Cline, Aluminum Research Laboratories, P. O. Box 772, New Kensington, Pennsylvania.

Letters to the Editor

THIS section will accept reports of new work, provided these are terse and contain few figures, and especially few half-tone cuts. The Editorial Board will not hold itself responsible for opinions expressed by the correspondents. Contributions to this section should not exceed 600 words in length and must reach the office of the Managing Editor not later than the 15th of the month preceding that of the issue in which the letter is to appear. No proof will be sent to the authors.

Phase Transition in Beriumdicalcium-Propionate

SYÛZÔ SEKI, MASANOBU MOMOTANI, AND KAZUMI NAKATSU
Department of Chemistry, Faculty of Science, Osaka University, Osaka, Japan
(Received June 14, 1951)

IT has recently been recognized that the thermal motion as well as mutual interaction of molecules having methyl groups outside exhibit some interesting behavior in the solid state; for instance, in the cases of $C(SCH_3)_4$,[1] $Pb(C_2H_5)_4$,[2] $Sn(C_2H_5)_4$,[2]

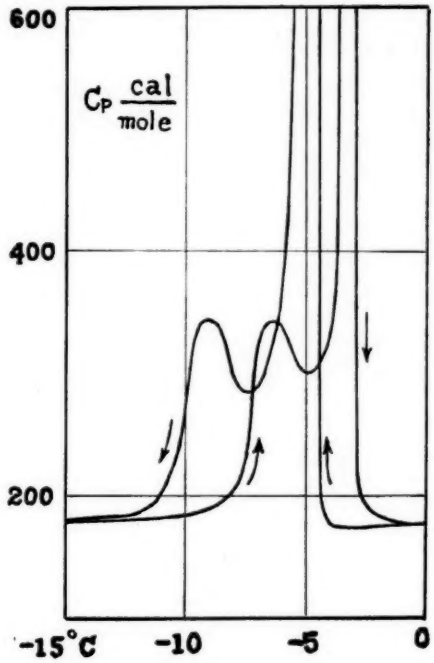

FIG. 1.

$C_2(CH_3)_6$,[3] $Be_4O(CH_3CO_2)_6$,[4] $C_6(CH_3)_6$,[5] etc. In view of these facts, we have undertaken to study the possibility of phase transition of the present material as one of a series of our investigation on the rotational phase transition. According to the results of x-ray crystal analysis of the cubic modification of this material carried out independently by Nitta and Watanabé[6] and by Biefeld and Harris[7] the methyl group is to be looked upon as making rotation, partial or complete, about the C—C axis so as to regain the diagonal character of the propionic radical to account for and fulfill the required symmetry properties of the crystal statistically. Hence, it may be expected there might occur a phase transition which is to be attributed to the stopping of the rotational motion of the methyl group as the temperature goes lower. For this purpose we have made preliminary differential thermal analysis and found actually the existence of the phase transition at about −6°C.

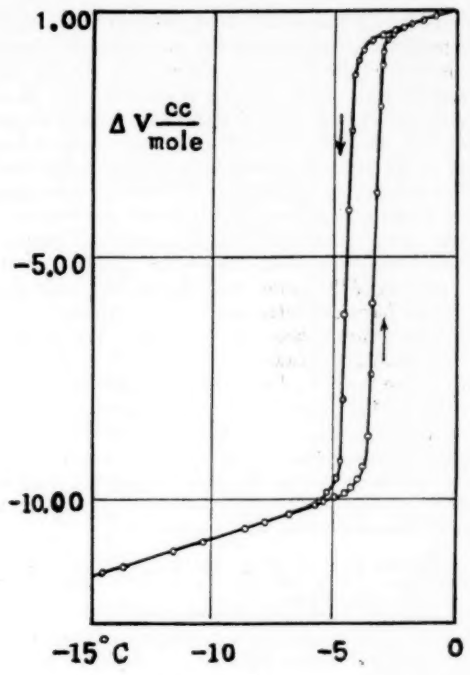

FIG. 2.

To investigate further in detail this phase transition, we then measured the specific heats in the vicinity of this temperature in heating and cooling directions by the conduction calorimeter. As shown in Fig. 1, two peaks of anomalous specific heat were discovered, suggesting that the phase transition takes place in two steps. Such an anomaly of specific heats seems to be rare for pure crystals. Furthermore, by our dilatometric study it was found that the high temperature side (HTS) sharp transition is associated with an appreciable volume change, while the low temperature side (LTS) Schottky-type anomaly does not accompany any volume change (see Fig. 2). To elucidate further

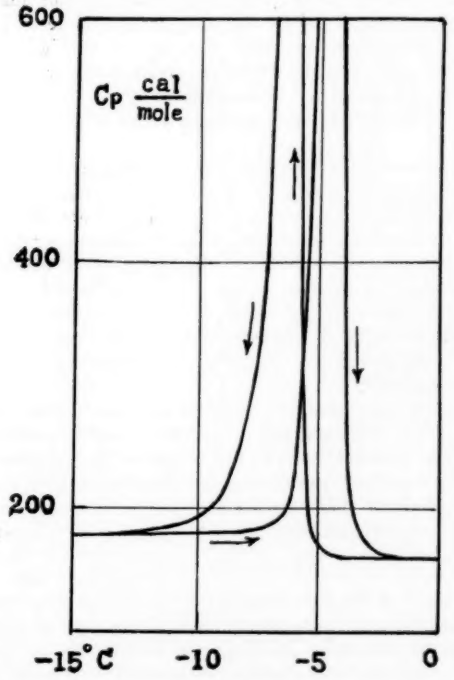

FIG. 3.

the nature of the LTS anomaly which seems to be correlated with a sort of pre-transition phenomenon, we examined the effect of the introduction of the Pb ion in place of the Ba ion, using the cubic mixed crystals of (Ba, Pb) $Ca_2(C_2H_5CO_2)_6$. As the amount of Pb ion increases, the heat of transition of the LTS anomaly diminishes and the peak becomes more sharp, with gradual displacement of its maximum to a higher temperature until it is absorbed completely to the HTS transition when the content of the Pb ion amounts to about 8 mole percent (see Fig. 3).

The pure crystal of $BaCa_2(C_2H_5CO_2)_6$ can form a cubic mixed crystal with $PbCa_2(C_2H_5CO_2)_6$ up to the composition of about 14.5 mole percent of the latter, and, beyond 44.4 mole percent of Pb-salt, it can form the tetragonal mixed crystal, while at any concentrations between these two limits they are unable to mix each other. These circumstances may be said to have some resemblance to the isothermal order-disorder phenomenon recently found by Grenall.[8] It is to be noted that Mandlsberg and Staveley[9] have investigated recently the effect of mixed crystal formation for clarifying the mechanism of phase transition similarly as we do in the present investigations. We are now studying more in detail the transition of the present material, of which the results and the discussion of the mechanism will be given later.

[1] H. J. Backer and W. G. Pendrock, Rec. trav. chim. **61**, 533 (1943).
[2] Staveley, Pagat, Goalby, and Warren, J. Chem. Soc. 2290 (1950).
[3] Seyer, Bennett, and Williams, J. Am. Chem. Soc. **71**, 3447 (1949).
[4] T. Watanabé and Y. Saito, Nature **163**, 225 (1949); Seki, Momotani, and Chihara, *ibid.* **163**, 226 (1949).
[5] S. Seki and H. Chihara, Sci. Pap. Osaka Univ. **1**, 1 (1950).
[6] I. Nitta and T. Watanabé, Sci. Papers Inst. Phys. Chem. Research (Tokyo) **26**, 164 (1935).
[7] L. P. Biefeld and P. M. Harris, J. Am. Chem. Soc. **57**, 396 (1935).
[8] A. Grenall, J. Chem. Phys. **17**, 1036 (1949).
[9] C. J. Mandlsberg and L. A. K. Staveley, J. Chem. Soc. 2736 (1950).

Note on Surface Tension and the Theory of Holes

ROBERT L. CHOATE AND LOUIS H. LUND
Missouri School of Mines and Metallurgy, Rolla, Missouri
(Received June 14, 1951)

IN a recent Letter to the Editor, Mukherjee[1] has considered the fusion process whereby the increase in volume at the fusion temperature is attributed to the formation of additional holes, the number being equal to the increase in volume at fusion divided by the volume per hole. Considering the holes to be of atomic size and using the formula, involving the surface tension, for the energy associated with the formation of a hole of macroscopic size, he is able to arrive at reasonable values of the specific heat.

It is interesting to note that the problem, in a sense, may be inverted and that the notion of a hole as corresponding to free volume per atom, or molecule, may be used to arrive at a knowledge of the surface tension over a fairly wide temperature range. If one imagines a spherical hole or cavity created in the liquid for the occupancy of an atom center, a spherical region of radius at least $\sigma+R$, where σ is the radius of the free volume and R is the atomic radius, must be made available in the liquid. The cavity, however, which may be viewed as unoccupied, is the spherical region of radius σ.

The energy, averaged over the radii, associated with the formation of such a spherical hole of radius σ is $\frac{1}{2}kT$, where k is the Boltzmann constant and T the absolute temperature.[2] If we imagine the surface tension associated with the hole to be that corresponding to that operative at a macroscopic surface, γ, modified by an appropriate constant factor β, we may write

$$\tfrac{1}{2}kT=4\pi\sigma^2\beta\gamma \quad (\beta<1). \tag{1}$$

The radius of the free volume may be found in several ways, but its approximate temperature dependence may be found by a fitting of the theoretical liquid atomic distribution of wall[3] to the experimental liquid distribution functions. This was done for the experimental distribution curves of liquid mercury,[4] which are available over a temperature range from −38°C to 200°C, and the temperature dependence of σ found to be given by

$$\sigma=97\times10^{-12}T^{0.62},$$

where σ is in centimeters, and T is the absolute temperature. This value of σ may be substituted in Eq. (1), giving for the surface tension

$$\gamma=582/\beta T^{0.24}. \tag{2}$$

The fraction $1/\beta$ may be found by substituting observed values[5] of the surface tension of mercury at absolute temperature T into Eq. (2). This was done for 8 different values of surface tension, and the results of the calculation are shown in Table I. It may be noted that the values of $1/\beta$ are unusually consistent. In Fig. 1 are shown experimental values of γ along with γ as calculated from Eq. (2), using an average $1/\beta$. The theoretical curve fits the experimental curve very well, and it is not surprising in view of its formulation that it predicts a nonvanishing γ at the critical temperature. However, the notation of definite trapping of the atoms in the liquid in spherical cells could be considered very unlikely at the critical temperature.

TABLE I. Values of surface tension factor $1/\beta$.

T°C	Observed surface tension dynes/cm	$1/\beta$
0*	480.3	3.15
30*	474.2	3.20
40*	471.3	3.20
60*	467.1	3.21
155	441.0	3.22
195	434.0	3.24
200	436.0	3.27
354	394.0	3.16
	Average	3.21

* Values of surface tension obtained by Harkness and Ewing, reference 5. Other values obtained by Hogness, reference 5.

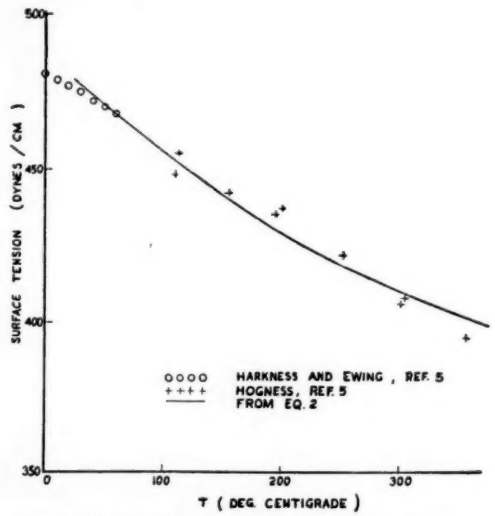

FIG. 1. Surface tension calculated from free volume.

Although there does not appear to be a way, at present, to calculate accurately the energy associated with the formation of a hole of the size contemplated here, it would appear from the preceding that Eq. (1) may be considered at least phenomenologically correct and thus be of use in calculation of surface tension.

[1] N. R. Mukherjee, J. Chem. Phys. **19**, 502 (1951).
[2] J. Frenkel, *Kinetic Theory of Liquids* (Clarendon Press, Oxford, 1946), p. 179.
[3] C. N. Wall, Phys. Rev. **54**, 1062 (1938).
[4] J. A. Campbell and J. H. Hildebrand, J. Chem. Phys. **11**, 330 (1943).
[5] W. D. Harkness and W. W. Ewing, J. Am. Chem. Soc. **42**, 2539 (1920); T. R. Hogness, *ibid.* **43**, 1621 (1921).

The Heat Capacity of Multimolecular Layers of Adsorbed Argon

J. A. MORRISON AND L. E. DRAIN*
Division of Chemistry, National Research Laboratories, Ottawa, Canada
(Received June 1, 1951)

MEASUREMENTS of the heat capacity of argon adsorbed on rutile at low surface coverages have been reported.[1] These measurements have now been extended to the region of multimolecular adsorption, where one may expect the properties of the adsorbed argon to approach those of the bulk substance. Of particular interest is the heat capacity of the adsorbed argon near the normal melting point (83.8°K). The results of measurements at concentrations corresponding to 1.6, 2.9, 4.0, and 4.6 V_m are shown in Fig. 1. The value of V_m was determined from a B.E.T. plot[2] of the adsorption data and found to be 755 cm³ at S.T.P. (for approximately 39 g of TiO_2 in the calorimeter). The calorimeter used for the work has been described.[3] The appropriate corrections[1] for desorption and for heat of compression in the calorimeter have been made. Calorimetrically determined heats of adsorption were employed for calculation of the desorption corrections. Within the limit of the experiments the heat capacity appears to be a continuous function of the temperature. For the measurements at 4.6 V_m, temperature increments as small as 0.3° were used.

The heat capacity maxima are interpreted as indicating rearrangement in the adsorbed film equivalent to fusion in the bulk substance. As the amount adsorbed increases, the peak in the heat capacity becomes larger rapidly and occurs at higher temperatures. It is reasonable to expect a lowering of the melting point in an adsorbed phase because distortion of the normal lattice as a result of the influence of the structure of the solid adsorbent would make solidification more difficult. Spreading of the effect over a small temperature interval might also be expected because of the small thickness of the adsorbed films.

Frederikse[4] has measured the heat capacity of helium adsorbed on jeweller's rouge and has shown that the λ-point appears when the adsorbed film is 5 to 6 layers thick. However, Mastrangelo[5] has pointed out that some uncertainty exists about the evaluation of the number of adsorbed layers in Frederikse's work, the first four layers being actually one layer according to the B.E.T. criterion for monolayer capacity. In the present case of adsorbed argon, the onset of bulk properties occurs between 1.6 and 2.9 V_m.

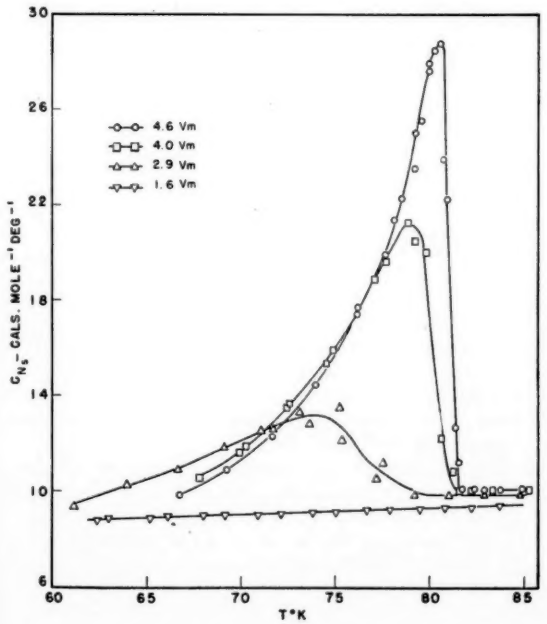

FIG. 1. The molar heat capacity of adsorbed argon. (C_{N_s}—heat capacity at constant amount adsorbed.)

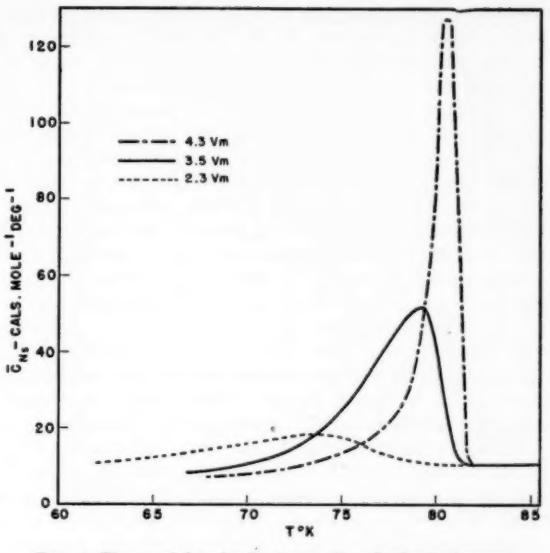

FIG. 2. The partial molar heat capacity of adsorbed argon.

Mastrangelo has also suggested that the shift in the λ-point of adsorbed helium is the result of compression on the surface. It seems unlikely that such an interpretation can be given for the shift in the heat capacity maxima in Fig. 1 because the effect of increased pressure would be to raise the melting point of argon.

The partial molar heat capacities of the adsorbed argon have been calculated from the data of Fig. 1, and the results are shown in Fig. 2. The accuracy of the molar heat capacities is not sufficient to permit a very precise calculation, but it is of interest to note that for 4.3 V_m the integral

$$\int_{65}^{83}(\bar{C}_{N_s}-C_{p_{\text{solid}}})dT$$

gives approximately the heat of fusion of argon (280 cal mole^{-1}).

* National Research Laboratories Postdoctorate Research Fellow.
[1] Morrison, Los, and Drain, Trans. Faraday Soc. (to be published).
[2] Brunauer, Emmett, and Teller, J. Am. Chem. Soc. **60**, 309 (1938).
[3] J. A. Morrison and J. M. Los, Faraday Soc. Disc., No. 8, 321 (1950).
[4] H. P. R. Frederikse, Physica **15**, 860 (1949).
[5] S. V. R. Mastrangelo, J. Chem. Phys. **18**, 896 (1950).

Microwave Spectrum and Dipole Moment of Methyl Mercaptan

T. M. SHAW AND J. J. WINDLE
Western Regional Research Laboratory, Albany, California*
(Received June 4, 1951)

THE microwave spectrum of methyl mercaptan has been studied in the 23,000- to 29,000-megacycle-per-second (Mc) region. The spectrometer used is of the Hughes-Wilson[1] type. Calibrations made on lines of known intensity[2] show the sensitivity of the spectrometer to be adequate to detect lines with absorption coefficients of about 10^{-8} cm^{-1}. Spectra were observed with the absorption cell at room temperature (~25°C) and at dry-ice temperature (−78°C).

Approximately fifty lines were found for methyl mercaptan between 23,000 and 29,000 Mc. The most intense line occurs at 25,291±1 Mc, and the observed temperature dependence of the intensity indicates that the line arises from a rotational transition of molecules in the ground vibrational state. This line and about twenty others which lie in the region between 23,000 and 25,700 Mc agree in frequency with lines recently measured by Hurd and Hershberger.[3]

Calculations of the rotational constants for methyl mercaptan were made on the assumption that the molecule can be represented as a freely rotating symmetrical top attached to a rigid frame.[4]

The results of the calculations and the observed Stark behavior show that the line observed at 25,291 Mc may be assigned to the $0_0 \rightarrow 1_{-1}$ transition of $CH_3S^{32}H$. The structural constants used in the calculation are $r(C-H)=1.10A$, $\angle HCH=109°28'$, $r(C-S)=1.815A$, $r(S-H)=1.34A$, $\angle CSH=100°$. These values are consistent with presently accepted values for methyl mercaptan or related compounds.[5] As might be expected, the theoretical frequency for the $0_0 \rightarrow 1_{-1}$ transition depends strongly on the value assumed for the C−S bond length. Thus the molecular parameters assumed for methyl mercaptan by Russell, Osborne, and Yost[4] in their thermodynamic investigations differ significantly from those given above only in the C−S distance (1.83A) and lead to an expectation of a strong line for the $0_0 \rightarrow 1_{-1}$ transition at 24,600 Mc.[3] Lines found near this frequency in the present study, however, are substantially weaker than the line at 25,291 Mc. The adoption of the same bond lengths and angles used to characterize the $0_0 \rightarrow 1_{-1}$ line for $CH_3S^{32}H$ give 24,840 Mc as the theoretical frequency for the $0_0 \rightarrow 1_{-1}$ line for $CH_3S^{34}H$. A line with the correct Stark behavior and approximately the correct intensity relative to that of the S^{32} line has been found at 24,880±10 Mc.

Measurements of the Stark effect splitting of the $0_0 \rightarrow 1_{-1}$ line at 25,291 Mc yields a value of 1.26±0.05 Debye units for the component of the dipole moment along the axis of least moment of inertia. The dipole moment of methyl mercaptan does not appear to have been determined previously, but the value found above may be compared with a value of 1.22 Debye units estimated from measured values of the moment for methyl sulfide and hydrogen sulfide.[6] For this calculation the sulfur valency angle was taken equal to 100° and the calculated value of the dipole moment of the methyl mercaptan molecule is 1.41 Debye units.

Further work is in progress, and a detailed account will be submitted to this Journal.

* Bureau of Agricultural and Industrial Chemistry, Agricultural Research Administration, U. S. Department of Agriculture.

[1] R. H. Hughes and E. B. Wilson, Phys. Rev. **71**, 562 (1947).
[2] P. Kisliuk and C. H. Townes, J. Research Natl. Bur. Standards **44**, 611 (1950).
[3] F. K. Hurd and W. D. Hershberger, Phys. Rev. **82**, 95 (1951).
[4] Russell, Osborne, and Yost, J. Am. Chem. Soc. **64**, 165 (1942).
[5] H. W. Thompson and C. H. Miller, Trans. Faraday Soc. **46**, 22 (1950). Gordy, Simmons, and Smith, Phys. Rev. **74**, 243 (1948). P. W. Allen and L. E. Sutton, Acta Cryst. **3**, 46 (1950).
[6] E. C. E. Hunter and J. R. Partington, J. Chem. Soc. 2812 (1932).

Spectroscopic Evidence of the Dimerization of NO in the Gaseous State

L. D'Or, A. de Lattre, and P. Tarte
Université de Liége, Centre d'analyse spectrale moléculaire, Liége, Belgium
(Received May 28, 1951)

THE dimerization of nitric oxide in the condensed (liquid and solid) state already made obvious by magnetic measurements was definitively proved by Raman and infrared spectroscopy in a recent paper by Smith, Keller, and Johnston.[1]

On the other hand, it has been found by Vodar,[2] and confirmed by Bernstein and Herzberg,[3] that liquid NO exhibits a very strong continuous absorption throughout the ultraviolet; this absorption is very probably the result of N_2O_2 molecules.

Dimerization of NO in the gaseous state is substantiated by the data of Eucken and D'Or[4] on the second virial coefficient of NO at low temperatures.

If dimerization of NO occurs in the gaseous state, one expects to find a continuous absorption in the ultraviolet region of the spectrum.

Such an absorption has indeed been found[3] below 2600A with a path length of 30 meters of gaseous NO at a pressure of 700 mm of Hg; but unfortunately, a slight quantity of HNO_2 was present as an impurity, and it was not possible to decide if the continuous absorption was the result of HNO_2, of N_2O_3, or of N_2O_2 molecules.

It is to be expected that dimer molecules are more abundant at low temperatures; and, accordingly, we have taken the ultraviolet spectrum of gaseous nitric oxide between −180° and +20°C.

The absorption cell was a quartz tube one meter long, surrounded by a roughly thermally insulated jacket. Series of spectra were taken on the same plate in the following manner:

(1) The tube is filled, at room temperature, with pure gaseous NO at a pressure of 700 mm Hg; and a first spectrum is taken.

(2) Liquid air is poured into the jacket: the pressure decreases rapidly, owing to the condensation of NO on the walls of the tube. A second spectrum is taken when the pressure has reached a value of 1.5–2 mm Hg.

(3) The temperature is allowed to rise gently, a series of spectra being taken during this time. These spectra are characterized by the following important features:

(a) The rising of temperature is first accompanied by the development of a more and more intense continuous absorption, which is overlapping the bands of NO. The most intense absorption is found in the spectra taken at a temperature very close to the boiling point of NO. *These spectra correspond to the lowest temperature consistent with the maximum number of molecules; the fact that they just show the most intense absorption is very significant.*

(b) A further rise of temperature above the boiling point of NO is accompanied by the regress of the continuous absorption.

The last spectrum was taken after returning to room temperature: it does not differ in any way from the first spectrum; consequently, *the substance responsible for the continuous absorption appears at lower temperatures and disappears at higher temperatures by a completely reversible process.*

(c) The spectra taken in a convenient range of temperatures and pressures exhibit, between 2360 and 2320A, a very weak system of diffuse bands. Maxima of absorption were found at 2353, 2345, 2338, and 2330A (42.486, 42.631, 42.758, 42.905 cm^{-1}).

These measurements give only rough values, owing to the weakness and diffuseness of the bands, but they suggest a frequency interval of the order of 140 cm^{-1}. *This low value is to be compared with the frequency 167 cm^{-1} found in the Raman spectrum of liquid* NO, *and which is undoubtedly a fundamental frequency of the dimer* N_2O_2.

The interpretation of these results by the existence of dimer molecules N_2O_2 in gaseous nitric oxide is almost obvious. Further experiments with a more refined apparatus are now in course with the purpose of measuring the bands with accuracy.

We wish to thank the FNRS and the CNBCPM for financial support given us for this work.

[1] Smith, Keller, and Johnston, J. Chem. Phys. **19**, 189–192 (1951).
[2] B. Vodar, Compt. rend. **204**, 1467 (1937).
[3] H. J. Bernstein and J. H. Herzberg, J. Chem. Phys. **15**, 77 (1947).
[4] Eucken and D'Or, Nachr. Ges. Wiss. Göttingen. F. **III** (17), 107 (1932).

Rotational Isomerism in Nitrous Acid and Alkyl Nitrites

L. D'Or and P. Tarte
Centre d'Analyse Spectral Moléculaire de l'Université de Liége, Liége, Belgium
(Received May 28, 1951)

AT the present time, very little information is available on the vibrational spectra of alkyl nitrites. Kohlrausch[1] found (among numerous other lines) two strong Raman shifts, which are common to the nitrites studied: 1660 and 600 cm^{-1}. Lenormant and Clément[2] published a few infrared data, which cover only the small region 5–8μ.

We have taken the infrared spectra of a number of nitrites in the gaseous state between 2 and 23μ. All the spectra exhibit a very strong absorption in the three regions 1660, 800, and 600 cm^{-1}. These bands are attributed to the three fundamental frequencies of the O−N=O group (N=O stretching, N−O stretching, and O−N=O bending vibrations, respectively).

Much more important is the fact that all the nitrites studied show not one, but two, bands at 1650 and 600 cm^{-1}; moreover, the first nitrites (methyl, ethyl, propyl) exhibit also two bands

at 800 cm^{-1}; and in the most simple one, namely, methyl nitrite, all the bands appear to be double.

An attractive explanation of these facts would be the existence of two forms of the nitrite molecule, such as

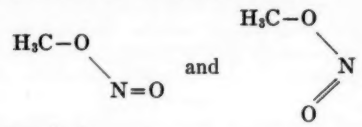

(rotational isomerism).

The temperature dependence of the intensity of the bands was studied in gaseous methyl nitrite. A temperature dependence was found for the following pairs of bands (which, in fact, represents all the bands between 6 and 15μ) (*i* represents an increase, *d* a decrease of the intensity of the band when the temperature is lowered):

1680 (*d*)–1625 (*i*); 1445 (*i*)–1375 (*d*); 1197 (*i*)–1131 (*d*);
1045 (*d*)–993 (*i*); 844 (*i*)–814 (*d*).

The same temperature dependence has been found in a number of harmonic or combination bands between 3 and 6μ.

Such a result supports strongly the hypothesis of rotational isomerism.

The nitrous acid itself HONO has been studied in the gaseous state, and the following pairs of bands have been observed (some of the frequencies reported here are not very accurate, owing to the overlapping of intense N_2O_3 bands):

3590–3425, 1700–1640, 1370–1267, 855–793, 598–525 cm^{-1}.

It is easy to recognize the 3 characteristic frequencies of alkyl nitrites (1700, 800, and 600 cm^{-1}), which once more appear to be double.

The remaining pairs (3590–3425 and 1370–1267 cm^{-1}) are undoubtedly the OH stretching and bending frequencies, because they are shifted at 2658–2537 and 1086–1015 cm^{-1}, respectively, in the deuterated compound DONO.

The presence of two OH bands is not the result of intermolecular association because the nitrous acid has been studied in the gaseous state at low pressures (a few mm Hg); moreover, the relative intensity of the bands has been found to be independent of the pressure.

Consequently, intramolecular association seems to be the true explanation, and the two forms of the nitrous acid molecule can be written

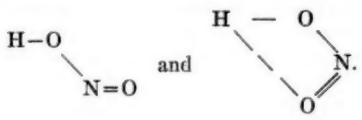

Further experiments are in course and detailed results will be published in the near future.

We wish to thank the FNRS for financial support given us for this work.

[1] K. Kohlrausch and co-workers, Monatsh. **58**, 428 (1931); *ibid.* **61**, 397 (1932).
[2] H. Lenormant and P. Clément, Bull. soc. chim. France, 559 (1946).

Fast Electrode Reactions

J. G. Barredo
Jones Laboratory, University of Chicago, Chicago, Illinois
(Received May 29, 1951)

In order to arrive at an explanation of the phenomena that occur at electrode-solution interfaces, the variation of current with time has been recorded over time intervals of the order of 4×10^{-3} to 1×10^{-4} second with platinum and mercury electrodes immersed in a solution of 0.00488 *M* potassium permanganate and 0.1 *N* sodium hydroxide and in other aqueous solutions. The experimental data thus obtained are satisfactorily described by Eq. (1),

$$d(N/\Sigma)/dt=(K/K_1)(N/\Sigma)^{\alpha}t^{-\frac{1}{2}}, \tag{1}$$

in which N is the number of potentially reactive particles, Σ is the value of the active surface of the electrode, t is the time, α is the number of particles participating in the elemental reaction at the electrode, and K and K_1 are constants. (Experimentally the factor K/K_1 has been found constant within 0.2 percent.)

Deduction of Eq. (1) is based in part on the demonstration of phenomenon most plausibly interpreted as the formation of a region of film around the electrode. The velocity of its formation may be indicated by Eq. (2),

$$dl/dt=K_1(1/l), \tag{2}$$

in which l can be considered as thickness. The phenomenon described is demonstrated by applying, to an electrode immersed in an aqueous solution, a constant negative potential for a sufficient length of time to attain a steady state of the current. In terms of the interpretation proposed, this is equivalent to the reduction of the l of Eq. (2) to a minimum. The applied potential is then discontinued, and, after a measured interval of time, the variation of current with time in the cell comprising the half-cell under examination and a standard calomel or silver-silver chloride half-cell is recorded with the aid of an oscillograph. Up to a limit approached asymptotically, the longer the time period intervening between discontinuation of applied potential and the oscillograph recording, the greater is the initial current recorded by the oscillograph. In the specific case of the solution of potassium permanganate, above mentioned, when the applied potential was 0.9 volt, the interval necessary to approximate the maximum initial current was thirty-eight minutes. Other electrodes in this and other solutions have given comparable results. The degree of reproducibility of the data obtained may be judged by the fact that a duplicate oscillograph recording on a single film is indistinguishable from a single recording. Whether the initial current has its maximum or some lesser value, it gradually decreases to the same constant value. This constant value is interpreted as coincident with a steady state in which the rate of formation of the electrode film is equal to the rate of destruction of the film through the elemental electrode reaction. It is an important fact that for different aqueous solutions the value of the exponent α corresponding to the order of the electrode reaction is equal to 2 ± 0.01.

When the steady state of the system is attained, Eq. (1) and Faraday's law, $I=NF$, are both valid, whence it may be deduced that

$$I=K_2(I^nF^n\Sigma^{n-1})t^{-\frac{1}{2}}. \tag{3}$$

On this basis it is possible to derive a generalized concept of active electrode surface,[1] defined by Eq. (4),

$$\Sigma=K_2^{-n+1}I^{n/n-1}t^{-\frac{1}{2}(n-1)}F^{n/-n+1}, \tag{4}$$

which embraces as a special case the geometrical concept of surface when all points of the surface are equally active. By substituting in Eq. (1) the value of Nd derived from the equation,

$$V=RT/nF\ln(N/N_o), \tag{5}$$

it is possible to derive Eq. (6), which facilitates comparison of the new theory proposed with the classical equations

$$i=K_3e^{\alpha(VnF/RT)}t^{-\frac{1}{2}}. \tag{6}$$

Equation (1) therefore may be regarded as the statement of a law more general than Ohm's, which is valid from the very instant that the passage of current is initiated, but which reduces to Ohm's law when the steady state is attained. As yet the validity of this expression has been demonstrated experimentally only for reactions at electrode-solution interfaces. It is believed, however, to be applicable also to electrode-gas interfaces.

The method here outlined may be employed in determinations of the apparent energies of activation involved in the release of respective isotopes of hydrogen over electrodes, and to a study

of conditions affecting the separation factors. A detailed description of the method (which is called chronopolarography because it is essentially the study of polarization as a function of time) will appear in a subsequent communication. In conclusion, if Eq. (1) holds for the electrolytic separation of hydrogen, then Tafel's equation,[2] namely,

$$\ln i = \text{const} + \alpha VF/RT \tag{7}$$

cannot yield the value of 2 for α. In fact, it is found experimentally that α has values commonly between 0.50 and 0.25.[3] Thus upon comparison of Eqs. (1) and (7) we see that the reason that the coefficient of Tafel's equation for the overvoltage of hydrogen cannot be equal to 2 as expected, is due to the fact that his equation does not take into account the rate-determining formation of film at the electrode.

[1] This concept has been proposed and discussed in a paper presented by the author before the American Physical Society, in Washington, D. C., April, 1951. Phys. Rev. **83**, 243(A) (1951).
[2] Eyring, Marker, and Kwoh, J. Phys. and Colloid. Chem. **53**, 1453 (1949). Tafel, Z. physik. Chem. **50**, 641 (1905).
[3] For a review of classical theories established in order to explain these "irregular" values consult Benneth and Thompson, J. Phys. Chem. **20**, 216 (1916). Modern theories are reviewed by Bockris, Chem. Revs. **43**, 525 (1948).

Contact Angles and Surface Tensions in Liquid/Solid Systems

G. A. H. Elton
Chemistry Department, Battersea Polytechnic, London, England
(Received May 21, 1951)

THE contact angle of a liquid against a solid can be expressed in terms of three surface tensions, using the well-known equation

$$\cos\theta = (\gamma_{SA} - \gamma_{SL})/\gamma_{LA},$$

where γ_{SA} is the surface tension of the solid, γ_{LA} is the surface tension of the liquid, and γ_{SL} is the interfacial tension at the solid/liquid interface. The contact angle may have various values in a given system depending on the degree of mutual saturation of liquid and solid, but should show one characteristic equilibrium angle corresponding to the surface tensions of the fully saturated phases.

In practice, contact angles cannot be predicted, as no adequate method exists for the measurement of either γ_{SA} or γ_{SL}. It is, however, of interest to note that for the case of two mutually saturated liquids, the interfacial tension may very often be expressed in terms of the individual surface tensions by the use of Antonoff's rule,[1] which states that the interfacial tension between two mutually saturated liquids is equal to the difference between the individual surface tensions of the saturated liquids. Experimental tests[2] indicate that this rule works fairly well for the majority of liquid pairs, although some exceptions have been noted.[3] It may well be legitimate to assume that this rule will work equally well for a solid/liquid interface, in which case we have

$$\gamma_{SL} = |\gamma_{LA} - \gamma_{SA}|, \tag{2}$$

the surface tensions here referring to mutually saturated phases. If we now combine Eqs. (1) and (2), we obtain, for $\gamma_{LA} > \gamma_{SA}$,

$$\gamma_{SA} = \tfrac{1}{2}\gamma_{LA}(1+\cos\theta) \tag{3}$$

or, if $\gamma_{LA} < \gamma_{SA}$,

$$\gamma_{LA}(1-\cos\theta) = 0, \quad \text{i.e.,} \quad \theta = 0. \tag{4}$$

Equation (4) leads to the conclusion that if the surface tension of the liquid is less than that of the solid, it will wet completely, while if the surface tension of the liquid is greater than that of the solid, a finite angle will be obtained, from which, using Eq. (3), the surface tension of the solid can be calculated.

The theoretical basis of Antonoff's rule is not sufficiently well understood to put this forward as yet as a reliable method of determining the surface tension of a solid, but it may be of interest to quote the following experimental results obtained using solid paraffin wax and three hydroxylic liquids, *viz.*, water, glycerol, and ethylene glycol, all of which are almost insoluble in paraffin wax. A plate coated with the wax was immersed for some hours at room temperature in the liquid to be studied, in presence of excess wax to insure mutual saturation, and the equilibrium contact angle of an air bubble placed in the liquid against the solid determined photographically. Surface tensions of the saturated liquids were determined by the pendant drop method.[4] Results are shown in Table I.

Table I.

Liquid	γ_{LA} dynes/cm	$\theta°$	$(1+\cos\theta)$
Water	72.9	105	27.0
Glycerol	63.9	98.5	27.2
Ethylene glycol	47.5	81.5	27.3

The figures in the final column of Table I would on this argument correspond with the surface tension of the saturated solid. We may note that the figures agree well among themselves, and are of similar magnitude to the surface tensions of liquid hydrocarbons at room temperature, e.g., benzene 28.9 dynes/cm at 20°C, *n*-octone 21.8 at 20°C.[5]

[1] G. N. Antonoff, J. chim. phys. **5**, 372 (1907).
[2] For example, W. C. Reynolds, J. Chem. Soc. **119**, 466 (1921); Bartell, Case, and Brown, J. Am. Chem. Soc. **55**, 2769 (1933).
[3] For example, E. G. Carter and D. C. Jones, Trans. Faraday Soc. **30**, 1027 (1934).
[4] Andreas, Hauser, and Tucker, J. Phys. Chem. **42**, 1001 (1938).
[5] *Handbook of Chemistry and Physics* (Chemical Rubber Publishing Company, Cleveland, Ohio, 1950–1951), thirty-second edition.

Isotopic Exchange between Metal Ions of Different Valency

Joseph Weiss
University of Durham, King's College, Newcastle upon Tyne, England
(Received May 28, 1951)

IN recent years a number of isotope exchange reactions have been studied with metal ions in different states of valency.[1] Although it has been recognized that a direct electron transfer between relatively highly charged ions of the same sign according to: (M, ^iM, metal and metal isotope, respectively),

$$^iM^{+n} + M^{+(n+1)} \rightleftarrows {}^iM^{+(n+1)} + M^{+n} \tag{A}$$

is highly improbable,[2] the actual mechanism of these exchange processes has remained rather obscure and no satisfactory explanation has been advanced, why many of these exchange processes proceed with considerable speed in aqueous solutions at ordinary temperatures.

It has been suggested recently,[2] that these exchange reactions are due to the operation of *reversible* oxidation-reduction processes. In homogeneous aqueous systems the water molecule itself, or its ions (OH^-, H^+), may give rise to a reversible redox system with the metal ions according to one of the following mechanisms:

Mechanism I

$$\mathfrak{M}^{+n} + H_2O \rightarrow \mathfrak{M}^{+(n+1)} + OH^- + H, \tag{1a}$$

$$\mathfrak{M}^{+n(n+1)} + H \rightarrow \mathfrak{M}^{+n} + H^+. \tag{1b}$$

Mechanism II

$$M^{+n} + OH^- \rightarrow M^{+(n-1)} + OH, \tag{2a}$$

$$M^{+(n-1)} + OH \rightarrow M^{+n} + OH^-. \tag{2b}$$

In general, with a substance, X, any reversible oxidation-reduction process:

$$M^{+n} + X \rightleftarrows M^{+(n+1)} + X^- \tag{B}$$

may lead to exchange. This can proceed either as a thermal or as a photochemically induced electron transfer process if the redox potentials of the systems (X/X^-) and ($M^{+n}/M^{+(n+1)}$) are suitably matched. X can be either an anion (e.g., Cl^-, Br^-, I^-, etc.) or an uncharged particle. Among the latter, the case of molecular oxygen is of particular interest, as atmospheric oxygen is normally present in aqueous solutions. The mechanism of this reaction

can be described by the following equations:

$$M^{+n}+O_2 \rightarrow M^{+(n+1)}+O_2^-, \quad (3a)$$

$$M^{+(n+1)}+O_2^- \rightarrow M^{+n}+O_2, \quad (3b)$$

with the intermediate formation of the O_2^--ion, i.e., the anion of the HO_2-radical.

As pointed out above, the operation of any particular mechanism will depend on the redox potentials of the systems under consideration.

In Table I some possible exchange mechanisms are indicated for a few ionic systems.

TABLE I.

System	Redox potential ev	Possible exchange mechanism: In aqueous solutions (absence of O_2)	Possible exchange mechanism: In the presence of O_2
Cr^{2+}/Cr^{3+}	−0.41	Mech. I	rapid autoxidation (no exchange)
Ti^{2+}/Ti^{3+}	−0.37	Mech. I	
V^{2+}/V^{3+}	−0.20	Mech. I	
Cu^{+}/Cu^{2+}	+0.17	no exchange	rapid exchange
$FeCy_6^{4-}/FeCy_6^{3-}$	+0.49	no exchange	rapid exchange
Fe^{2+}/Fe^{3+}	+0.77	no exchange	rapid exchange
Mn^{2+}/Mn^{3+}	+1.51	(Mech. II)	rapid exchange
Ce^{3+}/Ce^{4+}	+1.61	(Mech. II)	rapid exchange
Co^{2+}/Co^{3+}	+1.84	Mech. II	...

The elementary reactions of the exchange processes discussed above represent at the same time primary steps in the mechanism of the (irreversible) chemical reactions between the metal ions with water or with molecular oxygen, i.e., reactions (1a) and (1b) occur in the decomposition of water by strongly electronegative ions leading to the formation of molecular hydrogen, reactions (2a) and (2b) in the interaction between water and electropositive ions leading to the formation of oxygen, and reactions (3a) and (3b) in the autoxidation of metal ions (e.g., Fe^{2+}) in aqueous solutions. This has been discussed in earlier publications.[3,4]

However, exchange is only to be expected in those cases where the *net* rate of the irreversible chemical process is low, as for the exchange process the predominance of the *reversible* steps (1b), (2b), and (3b) is essential, which, on the other hand means a retarded chemical change. In any case a very rapid irreversible chemical reaction of M^{+n} to $M^{+(n+1)}$, makes a study of the exchange process impossible.

The rate of exchange itself is simply given by the rate of the corresponding forward reactions (e.g., (1a), (2a), and (3a).

A full discussion will be given elsewhere.

[1] See M. Haissinsky, J. chim. phys. **47**, 957 (1950).
[2] See C. D. Coryell, J. chim. phys. **45**, 231 (1948).
[3] J. Weiss, Réunion de la Société de Chimie Physique, Paris (May, 1951).
[4] See J. Weiss, Naturwiss **23**, 64 (1935); Ann. Reports Chem. Soc. (London) **44**, 60 (1948).

Erratum: The Intensities of Several of the Infra-Red Absorption Bands of Cyanogen and Cyanogen Chloride

[J. Chem. Phys. **18**, 1316 (1950)]

EUGENE R. NIXON AND PAUL C. CROSS
Metcalf Research Laboratory, Brown University, Providence, Rhode Island

IT has been called to our attention by Dr. David Z. Robinson that in the discussion of the dipole moment derivatives in ClCN there is an incorrect conclusion regarding the signs of the derivatives. Our assumption regarding the directions of the CN and CCl bond moments would obviously give the two-bond moment derivatives opposite signs, a CN stretch increasing and a CCl stretch decreasing the magnitude of the molecular moment. The lower set of values in Table II, rather than the upper set, would thus be applicable. We wish to thank Dr. Robinson for pointing out this discrepancy.

The Anomalous First Layer of Adsorbed Helium and a Modified B.E.T. Theory*

J. G. ASTON AND S. V. R. MASTRANGELO†
The Pennsylvania State College, State College, Pennsylvania
(Received March 30, 1951)

THE first completed B.E.T. "monolayer"[1] has an anomalous density.[2–4] We have assumed that this is composed of more than one layer with thermal properties and density of packing in layers analogous to the bulk solid in equilibrium with liquid helium at the temperature of the isotherm measurements. Table I lists

TABLE I.

Study	Average temperature T°K	$V_m \frac{cc}{m^2}$ at S.T.P.	$V_m' \frac{cc}{m^2}$ at S.T.P.	$\frac{V_m}{V_m'}$
Helium on jeweler's rouge[a]	1.60	0.92	0.318	2.90
Helium on glass[b]	1.622	0.98	0.318	3.06
Helium on steel[a]	2.31	1.035	0.34	3.05
Helium on TiO_2[c]	2.41	using Eq. (2)		2.00
Helium on glass[b]	4.218	0.366	0.365	1.00
Hydrogen on glass[d]	8.62	0.574	0.287	2.00
Hydrogen on glass[d]	17.07	0.305	0.305	1.00

[a] Reference 2.
[b] W. H. Keesom and J. Schweers, Physica **8**, 1020, 1032 (1941).
[c] Reference 6.
[d] Reference 5.

the results obtained when V_m, calculated by the ordinary B.E.T. theory, is divided by the quantity, V_m', which is the material, in cc/m² at S.T.P., in one layer, having a density of packing equivalent to the solid density as obtained from the solid-liquid equilibrium line for helium at the temperature of the isotherm. The last two lines of Table I show similar calculations for hydrogen on glass.[5] Except at 4.2°K in all cases the first layers of helium are multiple if these assumptions are correct. The 17.07°K isotherm for hydrogen yields a B.E.T. monolayer with solid packing, while the 8.62°K isotherm yields two layers, each with solid packing in the B.E.T. "monolayer." The 20.32°K isotherm yields a B.E.T. monolayer with ordinary liquid spacing.

The pressure required to solidify liquid helium increases from about 30 to 140 atmos on going from 2 to 4.2°K, and we assume that the solid layers melt when the pressure required to solidify them is larger than the effective "system pressure"‡ (analogous to the pressure inside a small drop).

If this assumption is correct, there should be transitions analogous to melting on going from 2 to 4°K at constant coverage, one when the third (uppermost) layer is continually melting, one when the second layer is melting, and one when the first (innermost) layer is melting. When the outer layer is completely liquid and the layer below starts to liquefy, the completely liquid layer becomes the second "B.E.T. layer."

A simple modification of the B.E.T. energy assumptions will explain the first "multilayer." For simplicity, for three such high energy layers it is assumed that $E_1=E_2=E_3>E_4=E_5=\cdots E_n=E_L$. Using all other B.E.T. assumptions, one obtains Eq. (1) after neglecting small terms

$$(1/3CV_{m_3})+[(C-1)/3CV_{m_3}]X=(X-\tfrac{2}{3}X^2+2/C)/(1-X)V \quad (1)$$

when $X>0.05$, or Eq. (2) for the case of two high energy layers:

$$(1/2CV_{m_2})+[(C-1)/2CV_{m_2}]X=(X-\tfrac{1}{2}X^2+1/C)/(1-X)V. \quad (2)$$

Equation (3) is the ordinary B.E.T. equation written in the slope-intercept form:

$$(1/CV_{m_1})+[(C-1)/CV_{m_1}]X=X/(1-X)V. \quad (3)$$

When X is small and C is large, the numerator on the right-hand side of Eqs. (1) and (2) reduces to X and a straight line is obtained by plotting the ordinary B.E.T. coordinates, i.e., $X/(1-X)V$ *versus* X. Since C is large, the following relations may be derived

from Eqs. (3), (2), and (1), respectively:

$$(C-1)/CV_{m1} \simeq 1/V_{m1} = K, \quad (4)$$
$$(C-1)/2CV_{m2} \simeq 1/2V_{m2} = K, \quad (5)$$
$$(C-1)/3CV_{m3} \simeq 1/3V_{m3} = K, \quad (6)$$

where K is the slope of the line obtained by plotting the ordinary B.E.T. coordinates. Obviously then, one obtains

$$V_{m1} = 1/K = V_m/1, \quad (7)$$
$$V_{m2} = 1/2K = V_m/2, \quad (8)$$
$$V_{m3} = 1/3K = V_m/3, \quad (9)$$

where V_m is the anomalous density of the first B.E.T. "monolayer" in column 3 of Table I and Vm_1, Vm_2, and Vm_3 correspond to V_m' in column 4 of Table I.

Equation (2) was used to plot our data[6] for helium on TiO_2 at 2.41°K. A straight line was obtained up to $X=0.5$ when the term in X^2 is included and to only $X=0.25$ when X^2 is neglected. The value of $V_{m2}=V_m'$ obtained when X^2 is included is 0.34 cc/m² at S.T.P. This is exactly the value calculated for one layer having ordinary solid packing at 2.41°K. Since neither Eq. (1) nor Eq. (3) yields good linear plots and since Eq. (3) yields a value of V_m between 0.62 and 0.66 cc/m² at S.T.P., depending on what region of the curve is selected, we concluded that our B.E.T. "monolayer" contains two ordinary layers as given in Table I.

A discussion of the energy assumptions and derivation of Eqs. (1) and (2) with experimental evidence from isotherm data for the form of these equations will appear soon in another publication. Eleven adsorption isotherms have recently been obtained for helium on rutile (230 m²/g) from 1.9 to 4.2°K with varying slopes for Eq. (2) that show melting of the second layer to occur between 2.6 and 3.4°K.

* This research was carried out under Contract N6ONR, Task Order X, of the ONR.

† Post-Doctoral Fellow, 1950–1951.

[1] Brunauer, Emmett, and Teller, J. Am. Chem. Soc. **60**, 309 (1938).
[2] H. P. R. Frederikse and C. J. Gorter, Physica **16**, 402 (1950).
[3] W. Band, Phys. Rev. **76**, 441 (1949).
[4] S. V. R. Mastrangelo, J. Chem. Phys. **18**, 896 (1950).
[5] W. H. Keesom and J. Schweers, Physica **8**, 1007 (1941).

‡ If a drop of a pure liquid or solid is small, the vapor pressure is increased and the free energy decreased. However, the free energy is uniform throughout the drop. The free energy decrease inside the drop is due to the fact that the pressure inside the drop is increased according to the relation between the pressure inside the sphere and the tension along the shell ($P=2\gamma/r$).

If the early adsorption on a solid is multilayer, in patches, this effect occurs in each patch. As the surface gets more completely covered, surface tension may pull the drop down to one or more complete layers (analogous to wetting). At this point the film is now under a pressure called the spreading pressure. In this process the pressure inside the drop may vary continuously and become equal to the conventional spreading pressure divided by the film thickness. This pressure is called the "system pressure."

[6] J. G. Aston and S. V. R. Mastrangelo, J. Chem. Phys., to be published.

Force Constants, Frequency Assignments, and Thermodynamic Properties of Ozone

MORTON J. KLEIN
Department of Chemistry
AND
FORREST F. CLEVELAND AND ARNOLD G. MEISTER
Spectroscopy Laboratory, Department of Physics, Illinois Institute of Technology, Chicago, Illinois

(Received April 18, 1951)

ANHARMONICITY relations are very useful in checking the reliability of vibrational frequency assignments. For example, assuming that no accidental degeneracies are present, the vibrational term values of a nonlinear triatomic molecule can be written as[1]

$$G(v_1, v_2, v_3) = G_0 + \omega_1(v_1+\tfrac{1}{2}) + \omega_2(v_2+\tfrac{1}{2}) + \omega_3(v_3+\tfrac{1}{2}) + G_{11}(v_1+\tfrac{1}{2})^2 + G_{22}(v_2+\tfrac{1}{2})^2 + G_{33}(v_3+\tfrac{1}{2})^2 + G_{12}(v_1+\tfrac{1}{2})(v_2+\tfrac{1}{2}) + G_{13}(v_1+\tfrac{1}{2})(v_3+\tfrac{1}{2}) + G_{23}(v_2+\tfrac{1}{2})(v_3+\tfrac{1}{2}),$$

where v_1, v_2, and v_3 are the vibrational quantum numbers and ω_i, G_{ij}, and G_0 are constants. From this expression, the relation

$$(mv_1+rv_2+sv_3) - m(v_1) - r(v_2) - s(v_3) = m(m-1)G_{11} + r(r-1)G_{22} + s(s-1)G_{33} + mrG_{12} + msG_{13} + rsG_{23}$$

is obtained; $(mv_1+rv_2+sv_3)$ is the observed wave number of the overtone or summation band, (v_1), (v_2), and (v_3) are the observed wave numbers of the fundamentals, and m, r, and s are vibrational quantum numbers for excited states. For a binary summation band, one of the constants m, r, s is zero; for an overtone, two of them are zero.

Applying this relation to Wilson and Badger's assignments[2] for ozone, one obtains:

$$\text{from } (v_2+v_3) = 1740 \text{ cm}^{-1},\ G_{23} = -8 \text{ cm}^{-1}; \quad (1)$$
$$\text{from } (v_1+v_3) = 2105 \text{ cm}^{-1},\ G_{13} = -48 \text{ cm}^{-1}; \quad (2)$$
$$\text{from } (v_2+2v_3) = 2800 \text{ cm}^{-1},\ G_{33}+G_{23} = 4.5 \text{ cm}^{-1}; \quad (3)$$
$$\text{and from } (3v_3) = 3050 \text{ cm}^{-1},\ G_{33} = -13.1 \text{ cm}^{-1}. \quad (4)$$

Relation (3) is inconsistent with (1) and (4), since the value of $G_{33}+G_{23}$ from (3) is +4.5 cm⁻¹, but from (1) and (4) it is −21.1 cm⁻¹. This inconsistency can be removed by assigning the 2800 cm⁻¹ band as $(v_1+v_2+v_3)$; this gives $G_{12}+G_{23}+G_{13} = -58$ cm⁻¹, which with (1) and (2) yields $G_{12} = -2$ cm⁻¹. In fact, Badger[3] points out that this assignment was made also by Wilson[4] immediately after their original note[2] was published.

Using the Wilson and Badger[2] values for the fundamentals, the electron diffraction values[5] of 127° and 1.26A for the equilibrium interbond angle α and bond distance d, and the potential energy expression

$$2V = f_d[(\Delta d_1)^2 + (\Delta d_2)^2] + d^2 f_\alpha (\Delta\alpha)^2 + 2f_{dd}(\Delta d_1)(\Delta d_2) + 2d f_{d\alpha}(\Delta\alpha)(\Delta d_1 + \Delta d_2),$$

the force constants obtained for ozone by the Wilson FG matrix method[6] are those given in Table I. Since there are 4 force constants, but only 3 fundamental frequencies, a unique set could not be obtained; hence several sets were calculated for a reasonable range of values for f_{dd}/f_d. The first and last two sets seem unsatisfactory because of the unusually large values of f_α and f_{dd}, respectively. The set with $f_{d\alpha}=0$ seems as good as any, so the three constant potential function for ozone appears to be a good approximation.

The sets of force constants obtained as the second root of the quadratic equation did not appear as reasonable as those given in Table I. Also, the sets of force constants calculated for the discarded 39° model, and for the Gutowsky and Petersen assignment[7] (for both 39° and 127°), were unsatisfactory. This represents some additional evidence against the 39° model, and against the assignment of Gutowsky and Petersen. This evidence is probably unnecessary, for Badger and Wilson[2] have given convincing arguments against the assignment of Gutowsky and Petersen, and the observed band types seem to establish the 127° model.

Using the fundamentals (705, 1043, 1110 cm⁻¹) given by Wilson and Badger[2] and the moments of inertia calculated by Simpson,[8] the calculated thermodynamic properties given in Table II were obtained. A rigid rotator, harmonic oscillator approximation was used and isotope and nuclear spin effects were neglected. The

TABLE I. Force constants for the ozone molecule (millidynes/angstrom; $d=1.26$A, $\alpha=127°$).

f_{dd}/f_d	f_d	f_α	f_{dd}	$f_{d\alpha}$
0.02[a]	4.02_{04}	2.31_{82}	0.080_4	0.470_{20}
0.05	4.14_{74}	2.10_{75}	0.207_{37}	0.238_{33}
0.10	4.37_{78}	1.88_{47}	0.437_{78}	0.0770_{76}
0.15	4.63_{53}	1.70_{04}	0.695_{30}	0.00210
0.1513	4.64_{25}	1.69_6	0.702_5	0
0.20	4.92_{50}	1.53_{38}	0.985_{00}	−0.0157
0.25	5.25_{33}	1.38_{08}	1.31_{33}	0.0221_0
0.43[a]	6.91_{22}	1.19_{33}	2.97_{22}	1.16_{85}

[a] If f_{dd}/f_d is less than 0.02 or greater than 0.43, imaginary values of $f_{d\alpha}$ and f_α are obtained.

TABLE II. Heat content, free energy, entropy, and heat capacity of ozone (O_3) for the ideal gaseous state at 1 atmos pressure (cal deg^{-0} mole^{-0}).

	$(H^0-H_0^0)/T$		$-(F^0-H_0^0)/T$		S^0		C_p^0	
T(°K)	Total[a]	Vib[b]	Total	Vib	Total	Vib	Total	Vib
100	7.95	0.00	39.76	0.00	47.70	0.00	7.95	0.01
200	8.02	0.08	45.28	0.01	53.30	0.09	8.38	0.43
298.16	8.30	0.35	48.53	0.09	56.82	0.44	9.37	1.42
300	8.30	0.36	48.58	0.09	56.88	0.45	9.39	1.44
400	8.71	0.76	51.02	0.25	59.73	1.01	10.44	2.49
500	9.14	1.19	53.01	0.47	62.15	1.66	11.26	3.32
600	9.55	1.60	54.71	0.72	64.26	2.32	11.87	3.92
700	9.91	1.97	56.21	0.99	66.12	2.96	12.30	4.36
800	10.23	2.29	57.56	1.28	67.79	3.57	12.62	4.68
900	10.51	2.57	58.78	1.56	69.29	4.13	12.86	4.91
1000	10.75	2.81	59.90[c]	1.85	70.65[c]	4.66	13.04	5.09

[a] Total = translational + rotational + vibrational contributions.
[b] Vib = vibrational contribution; this is listed separately to facilitate corrections if better values of the fundamentals should be reported later.
[c] If a better value of the product ABC of the 3 principal moments of inertia becomes available, the values in the table may easily be corrected by subtracting **8.65** from each of the values under "Total" for F and S, then adding **2.287** log ABC. Thus, if ABC were 7257.4 Awu A^3 (which is 20 percent greater than the present value), each of the F and S values would be 0.18 greater than those listed under "Total" in the table. The values for H and C_p do not depend on ABC, and thus would require no change.

value used for the product ABC of the 3 principal moments of inertia was (73.16) (67.56) (5.60) 10^{-120} g^{3}cm^6 = (44.064) (40.691) (3.373) Awu^3 A^6 = 6047.8 Awu^3 A^6 (2.287 log6047.8 = 8.65; see footnote c in Table II).

[1] H. H. Nielsen, Phys. Rev. **60**, 794 (1941).
[2] M. K. Wilson and R. M. Badger, J. Chem. Phys. **16**, 741 (1948); R. M. Badger and M. K. Wilson, J. Chem. Phys. **18**, 998 (1950).
[3] R. M. Badger, private communication, April 24, 1951.
[4] M. K. Wilson, thesis, California Institute of Technology, 1948.
[5] W. Shand, Jr., and R. A. Spurr, J. Am. Chem. Soc. **65**, 179 (1943).
[6] E. B. Wilson, Jr., J. Chem. Phys. **7**, 1047 (1939); **9**, 76 (1941).
[7] H. S. Gutowsky and E. M. Petersen, J. Chem. Phys. **18**, 564 (1950).
[8] D. M. Simpson, J. Chem. Phys. **15**, 846 (1947).

Proton Magnetic Resonance Absorption in Hydrogen Perchlorate Monohydrate and the Structure of Oxonium Ion

YOSHINOBU KAKIUCHI, HISAO SHONO, AND HACHIRO KOMATSU
Institute of Science and Technology, University of Tokyo, Meguro-ku, Tokyo
AND
KUNIHIKO KIGOSHI
Gakushuin University, Toshima-ku, Tokyo

(Received June 9, 1951)

THE formation of oxonium ion OH_3^+ in water was often assumed in explaining the abnormal conductivity of protons through water.[1,2] Its first and the most concrete experimental evidence would be the fact that the structure of the hydrogen perchlorate monohydrate crystal as revealed from x-ray studies is isomorphous to that of ammonium perchlorate. Since the latter is known to have an ionic structure $NH_4^+ClO_4^-$, Volmer[3] has concluded that the structure of the former is $OH_3^+ClO_4^-$. The above discussion, however, is still an indirect one, because the x-ray diffraction method is, in itself, incapable of determining the position of hydrogen atoms.

The recent development of the method of nuclear magnetic resonance absorption enabled us to determine the relative distance of protons in crystals, for instance, protons in various organic molecules[4] as well as the water of crystallization[5] in certain crystals. The shape of the proton resonance absorption line for powdered crystal is known to resemble the humps of the camel for two proton systems[5] and a shouldered peak for three-proton systems.[4] Therefore, if we observe the proton resonance absorption by $HClO_4 \cdot H_2O$ polycrystal, and determine to which of these two types the shape of the line belongs, it may become at once clear whether the water remains as the water of crystallization or exists in the form of oxonium ion in the crystal.

The shape of the proton resonance absorption line of the above-mentioned substance was observed according to the auto-

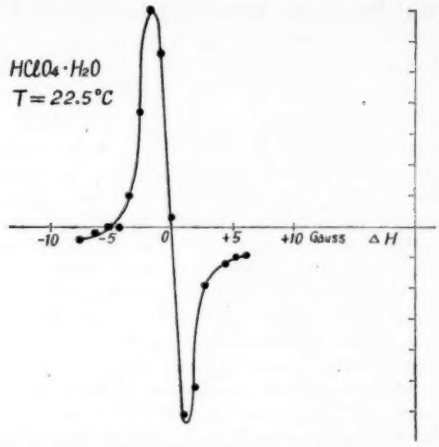

FIG. 1. The derivative of the absorption curve for $HClO_4 \cdot H_2O$ at high temperature.

dyne method through a narrow band amplifier with a phase sensitive detector.[6] The magnetic field was always kept constant, and its magnitude was roughly 3500 gauss. The frequency was varied through the resonance frequency. The depth of the modulation was made so small that the deflection of the galvanometer corresponds to the derivative of the absorption curve.

The result of the experiment at the room temperature is shown in Fig. 1, which corresponds to a simple bell-shaped line, contrary to our prediction. The width of the line is also too small to be interpreted as resulting from two- or three-proton systems. As the temperature was lowered, however, the width of the line increased abruptly at about −130°C, and the shape of the line becomes a typical three-proton type as shown in Fig. 2.

The above results may be interpreted as follows: namely, the oxonium ion *does exist* in $HClO_4 \cdot H_2O$ crystal, and at sufficiently low temperatures its orientation is well fixed. Above −130°C, however, the ion begins to *rotate*, and the width of the line is much reduced, as was often pointed out in case of certain ammonium salts and long chain compounds.[7-9]

The rough estimation of the H−H distance from experiment

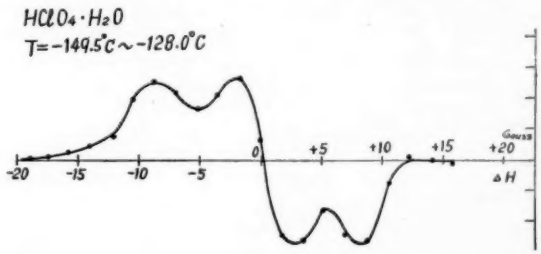

FIG. 2. The derivative of the absorption curve for $HClO_4 \cdot H_2O$ at low temperature.

amounts to 1.58A in accordance with the calculated value, assuming pyramidal structure of the ion and O−H distance 0.98A and O−H−O bond angle 110°C.

The more detailed report will be sent to the *Journal of the Physical Society of Japan*. The authors wish to express their sincere thanks to Professor H. Kumagai for putting his magnet at their disposal.

[1] Hückel, Z. Elektrochem. **34**, 546 (1928).
[2] J. D. Bernal and R. M. Fowler, J. Chem. Phys. **1**, 515 (1933).
[3] Volmer, Ann. Chem. **440**, 200 (1924).
[4] Gutowsky, Kistiakowsky, Pake, and Purcell, J. Chem. Phys. **17**, 972 (1949).
[5] G. E. Pake, J. Chem. Phys. **16**, 327 (1948).
[6] Thomas, Driscoll, and Hipple, J. Research Natl. Bur. Standards **44**, 569 (1950).
[7] H. S. Gutowsky and G. E. Pake, J. Chem. Phys. **16**, 1164 (1948).
[8] E. R. Andrew, J. Chem. Phys. **18**, 607 (1950).
[9] H. S. Gutowsky and G. E. Pake, J. Chem. Phys. **18**, 162 (1950).

Empirical Relations Involving Ionization Potentials

J. P. TEEGAN AND A. D. WALSH
Chemistry Department, The University of Leeds, Leeds, England
(Received May 14, 1951)

THE far ultraviolet spectra of H_2O, H_2S, H_2Se, and H_2Te contain extensive Rydberg series, from which the first ionization potentials of these molecules can be obtained with a likely error of only a few parts of ten thousand.[1] The first ionization potential refers in each case to the removal of an electron from the "$p\pi$" (b_1) lone pair orbital on the central atom. It has already been noted that if these accurate ionization potentials (I) are plotted against the first ionization potentials of the corresponding inert gases (e.g., I(H_2O) *versus* I(Ne))—which are also known with great accuracy and which refer to removal of an np electron—a remarkably linear plot is obtained (Fig. 3 of reference 1). If, with the same abscissa, the corresponding ionization potentials of the halogen acids* are plotted as ordinate, a tolerably good linear plot is also obtained. In what follows, all plots refer to I(Ne, A, ···) as abscissa. The slope decreases from the plot of I(Ne, A, ···) (necessarily linear and of 45° slope if the scales of the axes are the same to that of I(HF, HCl, ···) to that of I(H_2O, H_2S, ···).

The molecules H_2O, H_2S, ··· and HF, HCl, ··· are *iso*electronic with the inert gases. HF and H_2O may be thought of as produced by partially pulling out of the nucleus of a neon atom one and two protons, respectively. If a proton were completely removed from the Ne nucleus, the ion F^- would be produced. A plot of the first ionization potentials of the ions F^-, Cl^-, Br^-, I^- (i.e., the electron affinities of gaseous F, Cl, Br, I) yields, on the scale used in Fig. 1, a roughly linear plot of very small slope. The data have been taken from Latimer.[2] If two protons were completely removed from the Ne nucleus, the ion O^{--} would be produced. The ionization potentials of the ions Se^{--} and Te^{--} are not known. If, however, the values given by Latimer for O^{--} and S^{--} are plotted, it is of interest to note that the slope of the line joining the two points is negative.

If a proton were *added* to the Ne nucleus, the ion Na^+ would be produced. A plot of the first ionization potentials of the ions Na^+, K^+, ··· (i.e., the second ionization potentials of Na, K, ···) gives a roughly straight line of slope considerably greater than any of the above plots. If two protons were added to the Ne nucleus, the ion Mg^{++} would be produced. The line joining points representing the third ionization potentials of Mg and Ca (data for Sr and Ba are lacking) has an even greater slope than that of the plot for Na^+, K^+, ···.

These relations are indicative of underlying regularities and may be important in gaining a clearer understanding of the electronic structures of *iso*electronic atoms and molecules or in predicting ionization potentials not yet measured. The straight lines of Fig. 1 do not all pass through the same point, but (neglecting the plots for the hydrides) the successive points of intersection of adjacent lines lie on a smooth curve. The slope of the lines increases with increasing positive charge on the atom. The latter fact is brought out more clearly in Fig. 2. The plot of the slope *versus* charge on the atom is smooth and enables the effective charge on, e.g., the halogen atom of the halogen acids to be obtained by measuring the slope of the appropriate plot in Fig. 1. The effective charge turns out to be 0.4e. For the group VI hydrides, it is 0.7e. A remarkable constancy of structure in either the group VI or group VII hydrides seems evident. For example, each halogen acid appears to adjust its electronic arrangement so that the effective charge on the halogen atom is 0.4 of an electron, irrespective of whether we are speaking of HF, HCl, HBr, or HI.†

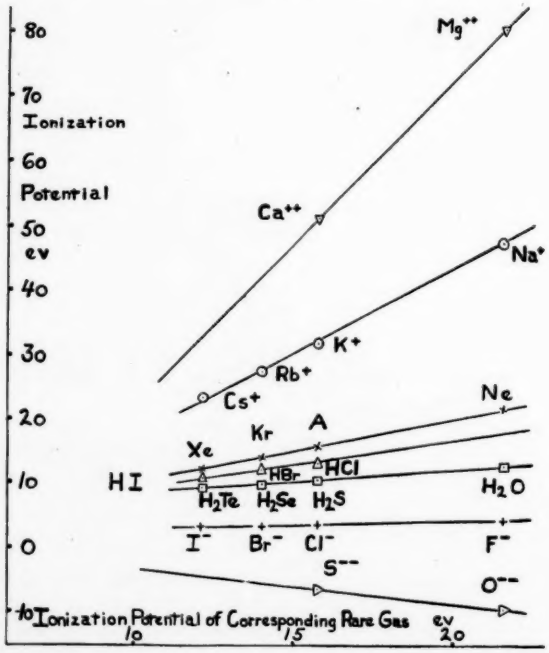

FIG. 1. Ionization potentials of some atoms and molecules plotted against the first ionization potential of the corresponding inert gases.

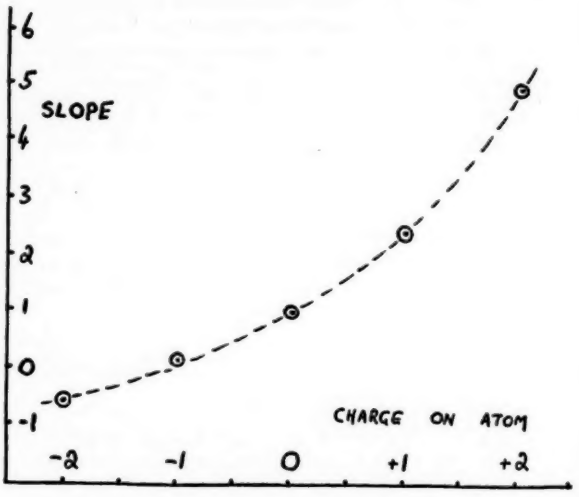

FIG. 2. Dependence of the slopes of the lines of Fig. 1 on the change of the atom.

[1] Price, Teegan, and Walsh, Proc. Roy. Soc. (London) **A201**, 600 (1950).
* The data for the halogen acids are less accurately known and are somewhat complicated by the doublet splitting of the ground states of the molecular ions.
[2] W. N. Latimer, *Oxidation Potentials* (Prentice-Hall, Inc., New York, 1938).
† In view of the complexity of total molecular dipole moments, this does *not* imply that the measured diipole moments of the halogen acids should be directly proportional to the intermolecular distances.

The Heat of Dissociation of Fluorine

RUSSELL N. DOESCHER
Jet Propulsion Laboratory, California Institute of Technology, Pasadena, California*
(Received June 22, 1951)

THERE has been considerable interest in the heat of dissociation of fluorine since Schmitz and Schumacher[1] obtained the unexpectedly low value 33.4 or 30.6 kcal/mole. The desirability of a direct method of measurement is clearly indicated, but the difficult problem presented by the reaction between the fluorine and the containing vessel at elevated temperatures required solution. Equilibrium pressure measurements have been completed at this laboratory, in which this problem was solved by a combination of two conditions, (1) the use of a nickel vessel coated step-

wise by heating in contact with fluorine at temperatures up to 850°C and (2) the use of a differentially applied manometer containing Fluorolube Standard.[2] This latter technique made it possible to carry out the measurements in the comparatively low temperature range 759 to 1115°K.

The method consisted essentially in a direct comparison of the pressure variation with temperature of a quantity of fluorine with that of a quantity of nitrogen. Twenty-four determinations of the equilibrium constant were made, and Fig. 1 shows $\ln K$ as a function of $1/T$. The line, established by the method of least squares, has the slope $-(19.0\pm0.2)10^3$ deg. The limits of error stated are the probable error due to random errors in $\ln K$. This slope gives $\Delta H = 37.7\pm0.4$ kcal/mole as the mean heat of dissociation in the temperature range of the experiments for the reaction $F_2(g)\rightarrow 2F(g)$. The value of $\ln K$ at 1000°K obtained from the line, -4.5, together with the standard entropy values[3] for F_2 and 2F at 1000°K, 58.62 and 88.58 cal/deg, respectively, results in $\Delta H = 38.9$ kcal/mole.

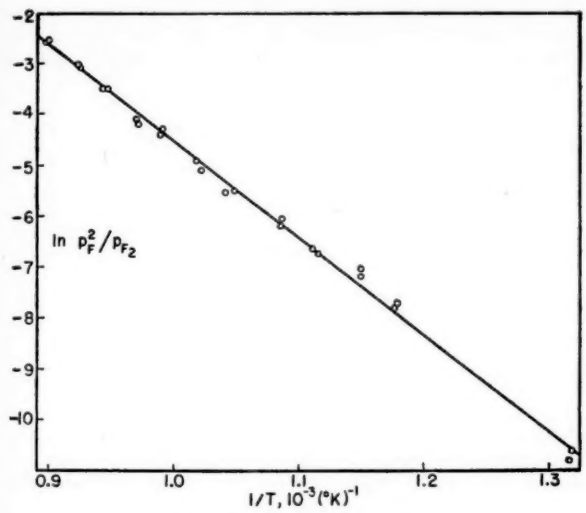

FIG. 1. Dissociation of fluorine.

It is planned to describe the apparatus, experimental procedure, and method of treating the results in a paper to be submitted later.

* This letter summarizes the results of one phase of research carried out at this laboratory, under Contract No. DA-04-495-ORD 18, sponsored by the U. S. Army Ordnance Department.

[1] H. Schmitz and H. J. Schumacher, Z. Naturforsch. **2a**, 359 (1947). See also A. L. Wahrhaftig, J. Chem. Phys. **10**, 248 (1942), and Evans, Warhurst, and Whittle, J. Chem. Soc. (London) 1524 (1950).

[2] Product of Hooker Electrochemical Company.

[3] Unpublished data calculated by Cole, Farber, and Doescher of this laboratory.

Determination of the Two-Dipole Moment Components in Nitrosyl Fluoride*†

DALE W. MAGNUSON
K-25 Laboratories, Carbide and Carbon Chemicals Company, Oak Ridge, Tennessee

(Received June 25, 1951)

THE dipole moment components along the least and intermediate principal inertial axes, μ_a and μ_b, have been determined for nitrosyl fluoride by means of the Stark effect in pure rotational transitions. These were $\mu_a = 1.70$ and $\mu_b = 0.62$ Debye units, which together give $\mu = 1.81$ Debye units. These were calculated using the perturbation theory of Golden and Wilson[1] and the tabulated line strengths of Cross, Hainer, and King.[2] The reciprocal moments of inertia, A, B, and C were determined from the microwave spectra.[3] Preliminary calculations of the molecular configuration of nitrosyl fluoride, using in addition microwave data on $N^{15}OF$, are N−F=1.52A, N−O=1.13A, and ∠ONF =110°. The Stark effect was measured for the 0_0-1_{-1} line and two components of the $3_{-2}-3_{-1}$ line. This provided an internal check on the experimental data.

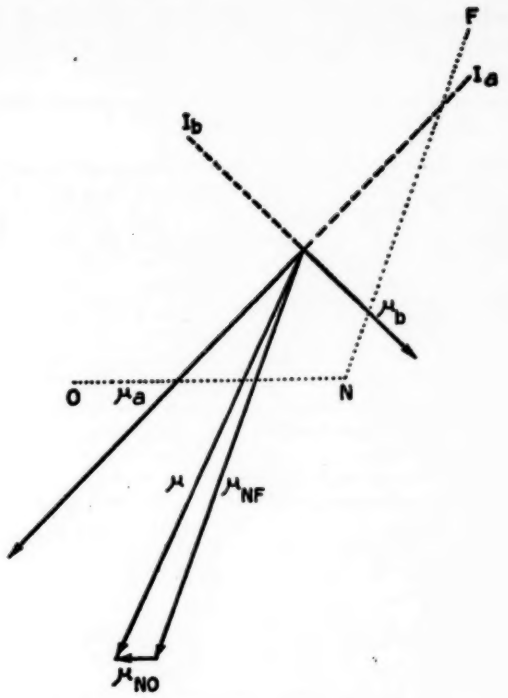

FIG. 1. Dipole moment components of nitrosyl fluoride.

There are four possible orientations of the dipole moment μ because the sign of the components is not determined. In the four cases, one calculates the following for the dipole moment components along the bonds: (a) $\mu_{NF}=1.75$, $\mu_{NO}=-0.17$; (b) $\mu_{NF}=0.81$, $\mu_{NO}=-0.96$; (c) $\mu_{NF}=-1.75$, $\mu_{NO}=+0.17$; (d) $\mu_{NF}=-0.81$, $\mu_{NO}=+0.96$. However, the large electronegativity difference between nitrogen and fluorine makes only one of these reasonable, i.e., case (a), where $\mu_{NF}=1.75$ and $\mu_{NO}=-0.17$. The configuration of the molecule and the orientation of the dipole moment are shown in Fig. 1. The origin of the total dipole moment, μ, represents the center of mass.

It is to be noted that the direction of μ_{NO} is opposite in sign to that which one would determine from differences in electronegativity. The magnitude of the moment in nitric oxide is 0.17 Debye unit.[4] The dipole moment of the N−F bond in nitrogen trifluoride is found to be 0.18 Debye unit when calculated from the dipole moment of 0.23 Debye unit[5] and the ∠FNF of 102°9, determined by Sheridan and Gordy.[6] Remeasurement of the dipole moment of nitrogen trifluoride may eliminate this discrepancy. The abnormal length of the N−F bond in nitrosyl fluoride may explain the large moment of this bond in this molecule.

* This document is based on work performed for the AEC by Carbide and Carbon Chemicals Company, UCC, at Oak Ridge, Tennessee.

† These results are included in a doctoral thesis being submitted to the Department of Physics, University of Tennessee.

[1] S. Golden and E. B. Wilson, Jr., J. Chem. Phys. **16**, 559 (1948).

[2] Cross, Hainer, and King, J. Chem. Phys. **12**, 210 (1944).

[3] These values were given by the author at the Southeastern Section, American Physical Society Meeting in Chattanooga, Tennessee, April 5, 1951. [See Phys. Rev. **83**, 485(A) (1951).]

[4] Watson, Gunda Rao, and Ramaswamy, Proc. Roy. Soc. (London) **A143**, 558 (1934).

[5] Watson, Kane, and Ramaswamy, Proc. Roy. Soc. (London) **A156**, 130 (1936).

[6] J. Sheridan and W. Gordy, Phys. Rev. **79**, 513 (1950).

Re-Examination of the Infrared Spectra of the Monodeutero Toluenes: A Method of Analysis

GEORGE VAN DYKE TIERS*
Jones Chemical Laboratory, University of Chicago, Chicago, Illinois
(Received June 20, 1951)

THE infrared spectra of the monodeutero toluenes have been investigated from 2 to 16 microns by Turkevich *et al*,[1] who failed to find a band characteristic of undeuterated toluene. In addition, the bands recommended by these authors for differentiating the ring monodeutero toluenes are weak in regions of strong absorption, and consequently unsuited for precise work.

Since a quantitative method of analysis would be of value for an isotopic study of orientation phenomena, the spectra of the ring monodeutero toluenes have been determined from 3 to 27 microns. Intense, characteristic absorptions for each isomer, and also for undeuterated toluene, have been found in the 13- to 17-micron region. Percent transmission is plotted *vs* wavelength in Fig. 1, for 3.17 percent by volume solutions of each compound in tetrachloro ethylene, with cell thickness 0.09 mm.

Satisfactory quantitative analyses of four-component mixtures have been performed, using the band at 13.73μ for estimation of toluene, and the bands at 15.85μ, 15.50μ, and 16.46μ for ortho, meta, and para deutero toluenes, respectively. Deviations from Beer's law are not serious. The measurements were made on a Perkin-Elmer model 12B spectrometer, equipped with KBr optics; the effective slit width was approximately 0.08 micron. Details of the technique will be described elsewhere.

The deutero toluenes were prepared by a modification of the method of Weldon and Wilson,[2] and purified by distillation followed by adsorption fractionation.[3] Refractive indices were in each case lower by 0.0003 than that of undeuterated toluene, an effect previously noted,[4] and densities agreed within 0.0002 of the estimated values.[2] The 99.8 percent D_2O was obtained through the AEC.

Mass spectral analyses done by Dr. F. L. Mohler at the National Bureau of Standards give the following impurities in the deutero toluenes: ortho 1.5 percent C_7H_8, 0.2 percent $C_7H_6D_2$; meta 1.3 percent C_7H_8, 0.4 percent $C_7H_6D_2$; para 0.8 percent C_7H_8, 1.2 percent $C_7H_6D_2$.

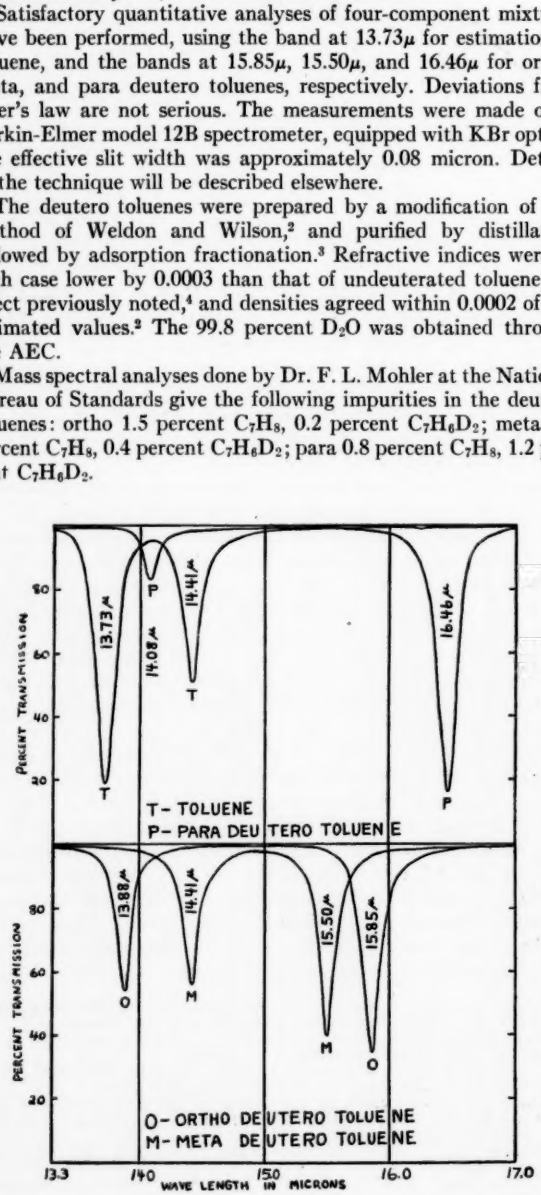

FIG. 1. Infrared spectra of toluene and of the monodeutero toluenes.

It is evident from these data that the previously reported spectra must be interpreted with caution. Not only did the samples contain considerable undeuterated toluene, but also the percent transmission values are erroneous, apparently because of failure of the double-beam instrument properly to define zero transmission. Since this error renders Beer's law useless even in a qualitative sense, it is serious, and should be considered in the interpretation of spectra from such instruments. This point does not appear to be widely recognized.

Thanks are due to Professor R. S. Mulliken of the Department of Physics for granting unlimited access to the infrared equipment, and to Professor G. W. Wheland, under whom the study of orientation in deuterium exchange processes is being actively pursued by this technique.

* Charles A. Coffin Fellow, 1950–1951.
[1] Turkevich, McKenzie, Friedman, and Spurr, J. Am. Chem. Soc. **71**, 4045 (1949).
[2] L. H. P. Weldon and C. L. Wilson, J. Chem. Soc. (London) **1946**, 235 (1946).
[3] Mair, Westhaver, and Rossini, Ind. Eng. Chem. **42**, 1279 (1950).
[4] Ingold, Raisin, and Wilson, J. Chem. Soc. (London) **1936**, 915 (1936).

A Novel Method for the Estimation of Very Low Pressures

ROBERT GOMER
Institute for the Study of Metals, University of Chicago, Chicago, Illinois
(Received June 22, 1951)

IN connection with other work on the field emission electron microscope of Müller[1] it was noticed that at pressures of the order of 10^{-7} mm of Hg fluctuations could be observed on the screen, of a size and frequency compatible with individual molecular impacts. The following method for the estimation of low pressures therefore suggested itself. Some phthalocynanine dye (zinc phthalocyanine in the present instance) is sublimed onto the tungsten tip of the microscope. (At the magnification employed an individual molecule of phthalocyanine appears as a four-leaf clover pattern with a spacing of about 6 mm between the centers of the bright spots.) Attention is now focused on any one molecule

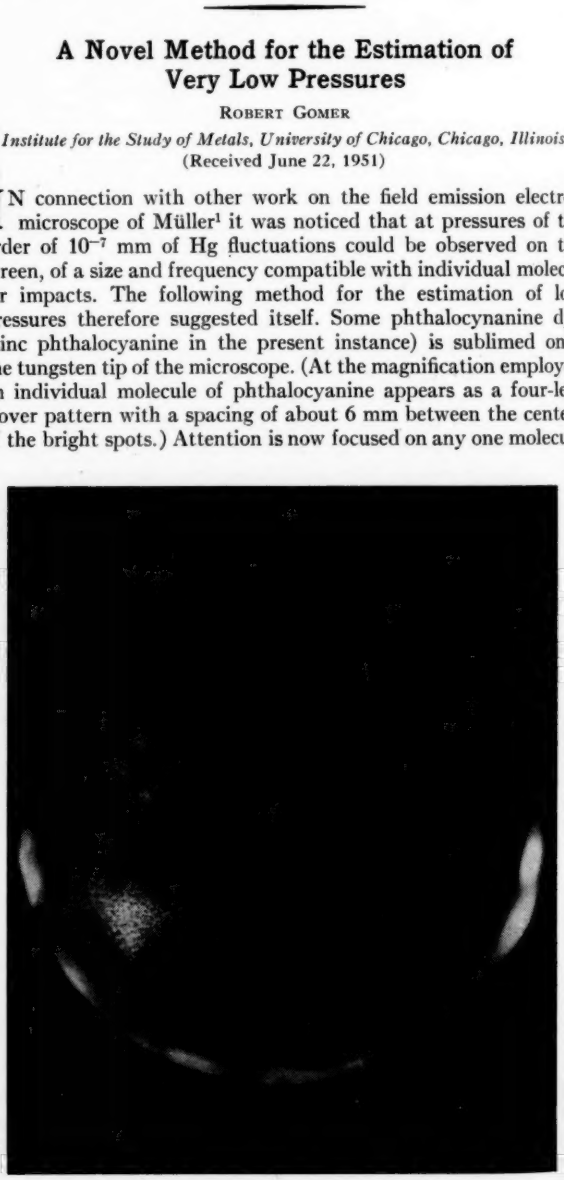

FIG. 1. Photograph of screen of microscope tube, showing images of three Zn phthalocyanine molecules.

TABLE I.

Time between impacts on a Pt molecule	Impacts on 1 cm² of screen per second
5 seconds	0.86
2	0.95
0.4	0.81
4	0.87 Average
3	
1	Calculated pressure 0.87×10^{-7}
0.9	(using area of Pt on screen
5	as $(0.8)^2=0.64$ cm²)
2	
1	
5	
2	
2	
5	
2.9 Average	

Impacts/sec: 0.35.

Calculated pressure (using $100A^{0.2}$ for area of molecule): 0.55×10^{-7} mm Mg.

Ion gauge reading: 1.2×10^{-7} mm Mg.

until some movement or fluctuation in brightness occurs. At this instant counting is started and the time noted until the molecule again undergoes some change, whether this be merely a momentary fluctuation in brightness, a rotation, or libration. The process is repeated several times and the average time noted. From this time and the calculated area of the phthalocyanine molecule the number of impacts per unit time per unit area may be calculated and hence the pressure in the tube. This scheme has the advantage that any arguments about the tip size (calculable from the voltage current relationship only for an assumed geometry and work function) or the nature of the image of a molecule are irrelevant, since the real area of the dye molecule is independent of whether one sees a diffraction pattern or a true molecular image (Fig.1). It is interesting to point out, however, that it is possible to count the number of impacts on a square cm of screen in a given time, and that the pressure calculated in this manner roughly agrees with that found by the above method if it is assumed that the phthalocyanine pattern is a true enlarged image. Evidence for the latter point is also found in the fact that the pattern size is independent of voltage, which means of electron wavelength. The size of a diffraction pattern should vary inversely with the square root of applied voltage. Table I illustrates the above points.

The author wishes to thank Dr. Samuel Isenberg of the Sampson Chemical and Pigment Corporation for a gift of ZnS phosphor and his most generous help and advice in the preparation of the fluorescent screens used. It is also a pleasure to acknowledge stimulating discussions with many members of the Division of Physical Sciences, notably Drs. J. R. Platt, C. S. Smith, and many others.

[1] E. W. Müller, Z. Physik **126**, 642 (1949) and earlier papers. See also Benjamin and Jenkins, Proc. Roy. Soc. (London) **180A**, 225 (1942).

Lack of Resonance Energy in Gaseous Carbonium Ions

J. L. FRANKLIN AND H. E. LUMPKIN
Technical and Research Divisions, Humble Oil and Refining Company, Baytown, Texas

(Received June 25, 1951)

WHEN it is possible to write two or more electronic structures of similar energy for a molecule, resonance theory predicts that the molecule is stabilized by resonance and that the energy of the molecule is less than would be expected from the energies of similar molecules that are not so stabilized. Thus, in the case of the allyl free radical and the allyl carbonium ion one can write the following principal resonance forms:

$$H_2C{=}C(H){-}CH_2 \leftrightarrow H_2C{-}C(H){=}CH_2,$$

$$H_2C{=}C(H){-}\overset{+}{C}H_2 \leftrightarrow H_2\overset{+}{C}{-}C(H){=}CH_2.$$

Similarly, several equivalent structures can be written for the benzyl radical and the benzyl ion. Thus one would expect the allyl and benzyl free radicals and ions to be stabilized by resonance and indeed to have approximately the same resonance energy.

Now if we compare the heat of a reaction yielding a resonance-stabilized structure with that of a similar reaction which gives no resonance hybrids, we can measure the resonance energy directly. Thus using the data of Roberts and Skinner[1] we find

$$CH_3{-}CH_2{-}CH_2Cl(g) \rightarrow CH_3{-}CH_2{-}\dot{C}H_2 + \dot{C}l - 77.4 \text{ kcal},$$

$$CH_2{=}CH{-}CH_2Cl(g) \rightarrow CH_2{=}CH{-}\dot{C}H_2 + \dot{C}l - 59.3 \text{ kcal}.$$

Since allyl chloride is not stabilized by resonance, the allyl free radical has a resonance energy of 18.1 kcal. Similarly, the benzyl radical is found to have a resonance energy of 18 kcal above that of the ring.

The appearance potentials of the ions formed from a series of similar molecules in a mass spectrometer would serve as a convenient measure of the resonance energies of the ions. Stevenson and Hipple[2] have measured the appearance potential of the *n*-propyl ion from the chloride. We have measured the appearance potential of the allyl and benzyl ions from the corresponding chlorides using a Westinghouse Type LV mass spectrometer similar to that used by Stevenson and Hipple and employing the vanishing current method of Mariner and Bleakney.[3] We have also measured the appearance potentials of the cyclohexyl dimethyl carbinyl ion and the phenyl dimethyl carbinyl ion from *t*-butyl cyclohexane and *t*-butyl benzene, respectively. Duplicate runs with two to four determinations for each run were made in all cases. Table I gives the results; the accuracy values shown are the statistical limits within which the true value will fall 90 percent of the time. It is apparent that the energy required to rupture similar bonds is the same regardless of whether or not the resulting carbonium ion is capable of resonance. One must conclude, therefore, that none of these ions is stabilized by resonance energy unless the small difference (0.17 volt) between the cyclohexyl- and phenyl-dimethyl carbinyl ions may be taken as significant. However, this difference is probably within the accuracy of the experiments.

TABLE I.

Compound	Ion	$AP\left(\frac{\text{electron}}{\text{volts}}\right)$	Work by
$CH_3{-}CH_2{-}CH_2Cl$	$CH_3{-}CH_2{-}\overset{+}{C}H_2$	11.1 ±0.3	Stevenson and Hipple
$CH_2{=}CH{-}CH_2Cl$	$CH_2{=}CH{-}\overset{+}{C}H_2$	11.09±0.11	Authors
$C_6H_5CH_2Cl$	$C_6H_5{-}\overset{+}{C}H_2$	11.13±0.12	Authors
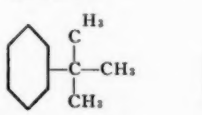	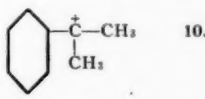	10.42±0.12	Authors
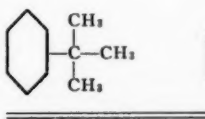	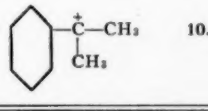	10.26±0.05	Authors

This result is confirmed qualitatively by the rates of displacement reactions of the allyl halides. Evans and Hamann[4] have shown that the rate of S_{N1} solvolysis of allyl chloride is about three times that of isopropyl chloride in formic acid. Hughes, Ingold, Martin, and Meigh[5] give the activation energy of S_{N1} solvolysis in 80 percent ethanol of isopropyl chloride and *n*-alkyl chlorides as 26.7 and 30 kcal, respectively. Although the data are not directly comparable, we may conclude then that the S_{N1} solvolysis of allyl chloride is about 10^3 times as great as the *n*-propyl chloride. The increased rate may be attributable to a possibly greater energy of solvation of the allyl ion. If the allyl or benzyl ion had a resonance energy of 18 kcal (equal to that of the radicals), the activation energy for their S_{N1} reaction would be reduced by this amount and their reaction rate would be about 10^{13} times as great as that of the *n*-alkyl halides. Thus, although chemical evidence points to the interchangeability of the resonance forms of the allyl ion, over-all rate data support the view that no resonance energy is involved.

It appears, then, that resonance energy results when there can be interaction between adjacent π-electrons (as in a conjugated system of double bonds) or between a free electron and an adjacent π-bond (as in the allyl and benzyl radicals), but that no energy results from interaction between a π-electron and a vacant orbital.

A more complete discussion of these results will be presented in the near future.

[1] Roberts and Skinner, Trans. Faraday Soc. **45**, 339 (1949).
[2] D. P. Stevenson and J. A. Hipple, J. Am. Chem. Soc. **64**, 2766 (1942).
[3] T. Mariner and W. Bleakney, Phys. Rev. **72**, 807 (1947).
[4] Evans and Hamann, Trans. Faraday Soc. **47**, 25 (1951).
[5] Hughes, Ingold, Martin, and Meigh, Nature **166**, 679 (1950).

20th Anniversary

of the

AMERICAN INSTITUTE OF PHYSICS

OCTOBER 23–27 HOTEL SHERMAN CHICAGO, ILLINOIS

A Joint Meeting of the American Institute of Physics and its Founder Societies

- **AMERICAN PHYSICAL SOCIETY (OCT. 25–27)**
- **OPTICAL SOCIETY OF AMERICA (OCT. 23–25)**
- **ACOUSTICAL SOCIETY OF AMERICA (OCT. 23–25)**
- **SOCIETY OF RHEOLOGY (OCT. 24–26)**
- **AMERICAN ASSOCIATION OF PHYSICS TEACHERS (OCT. 25–27)**

The American Crystallographic Association, an Affiliated Society of the American Institute of Physics, will participate in the Anniversary Meeting.

On Thursday, October 25, there will be an all-day symposium organized upon the theme "physics today", which will feature invited papers by:

ENRICO FERMI—The Nucleus
E. U. CONDON—The Atom
J. C. SLATER—The Solid State
HARVEY FLETCHER—Acoustics
EDWIN H. LAND—Optics
K. K. DARROW—Physics as Science and as Art

A JOINT BANQUET on Thursday evening, October 25, will have Senator Brien McMahon and K. T. Compton as guest speakers.

AN INDUSTRIAL EXHIBIT of scientific instruments and apparatus will provide manufacturers with an excellent opportunity to show their products to men who are responsible for many of the major scientific and technological advances of the past twenty years.

A PLACEMENT SERVICE for the benefit of employers and potential employees will be available during the meeting, and space in the Hotel Sherman will be reserved for this purpose.

Address inquiries to: The Secretary, American Institute of Physics, 57 East 55th Street, New York 22, New York